# Structural and kinetic study of rhodium complexes of N-aryl-N-nitrosohydroxylamines and related complexes

**J.A. Venter**

# Structural and kinetic study of rhodium complexes of N-aryl-N-nitrosohydroxylamines and related complexes

*A thesis submitted to meet the requirements for the degree of*

**Philosophiae Doctor**

*in the*

**Department of Chemistry**
**Faculty of Natural and Agricultural Sciences**

*at the*

**University of the Free State**

*by*

**Johan Andries Venter**

*Promotor*

**Prof. S.S. Basson**

*Co-promotor*

**Prof. W. Purcell**

December 2006

# Voorwoord

Hiermee wens ek my opregte dank en waardering uit te spreek teenoor Prof Steve Basson vir sy bekwame leiding met beide my M.Sc. en Ph.D. studies. Behalwe vir sy wye kennis van die vak het ek bewondering vir die aangename gesindheid waarmee hy met sy personeel en studente omgaan. Hy was altyd bereid om tyd vir my in te ruim, soos ook nou met die finalisering van hierdie tesis gedurende sy verloftyd. Sy invloed op my ontwikkeling reik so ver terug as die tyd toe ek as eerstejaarstudent in sy klas gesit het. Groot dank ook aan Walter Purcell, my medepromotor, vir sy insette en ondersteuning wat ook verder as Chemie strek. André Roodt het ’n belangrike bydrae, veral tot die kristallografiese ondersoeke gelewer waarvoor ek groot waardering het. Ander personeel by die Departement Chemie het ook op verskillende maniere ’n bydrae gelewer waarvoor ek my dank uitspreek. Veral Alet van Rooyen, Jeanet Conradie, Ina du Plessis en Michael Coetzee verdien vermelding.

’n Spesiale woord van dank aan my gesin, ouers, skoonouers, broer en suster vir hulle liefde, begrip, opoffering, aanmoediging en ondersteuning gedurende my studiejare. Ek waardeer dit baie, ook hulle insette met hierdie tesis. In besonder wil ek my ouers wat met hul opvoeding sedert my kinderjare die grondslag gelê het, asook Elizabeth, Gerhard en Ilse wat van ons huis ’n lewensoase maak en veral die laaste ruk baie moes opoffer, grootliks bedank. Pappa is klaar met die boek!

Met erkenning aan Koos du Plessis moet ek ook sê “wat ek is, is net genade, wat ek het is net geleen”. Die Here het voorsien. Aan Hom al die eer.

WAs helffen *FACKELN*, *LICHT* und *BRILLEN*,
Weil jedermann nach ſeinem Willen
In der *CHYMIA* ängſtlich ſucht,
Daſz ihm das *HERTZ* im Leibe pucht!
Er ſuchet zwvar die creutz und qver,
Alleine NICHTS das findet er,
Und ſetzte er auf alle *Brillen*,
Weil er nur thut nach ſeinem Willen,
So vvird er doch nicht treffen an
Die *WAHRHEIT*, ſo erfreuen kan,
Verſuchs, und lis das mit *VERSTAND*,
Und tapp nicht blindlings nach der *WAND*,
Gebrauch recht *FACKELN*, *LICHT* und *BRILLEN*,
So vvird *GOTT* deinen Wunſch erfüllen.

**Front page of a 1708 German alchemical work.[1] The poem says:**

What would torches, light and glasses help
while everyone is acting according to his own will,
and struggle anxiously with the Chemistry,
till his heart goes faint in his body.
He struggles from one extreme to the other
only to find nothing.
And if he relies on all the glasses
while acting according to his own will,
that way he will not find
the truth and be pleased.
Have faith and read it with intellect
and do not fumble blindly towards the wall.
Use torches, light and glasses the right way
and God will fulfil your wishes.

[1] Jackson, R., *The alchemists*, Weidenfeld & Nicolson, London (1997).

# Contents

# List of abbreviations

| | |
|---|---|
| COD | *cis*,*cis*-1,5-cyclooctadiene |
| Cy | cyclohexyl |
| $D_n$ | solvent donocity |
| DMF | N,N-dimethylformamide |
| DMSO | dimethylsulphoxide |
| Et | ethyl |
| Hacac | 2,4-pentanedione, acetylacetone |
| Hanmetha | 4-methoxy-N-methylbenzothiohydroxamate |
| Hba | 1-phenyl-1,3-butanedione, benzoylacetone |
| Hbpha | N-benzoyl-N-phenylhydroxylamine |
| Hbzaa | 3-benzyl-2,4-pentanedione, di-acetylbenzylmethane |
| Hcacsm | methyl(2-cyclohexylamino-1-cyclopentene-1-dithiocarboxylate) |
| Hcupf | N-phenyl-N-nitrosohydroxylamine, cupferron |
| Hdbbtu | N,N-dibenzyl-N'-benzoylthiourea |
| Hdbm | 1,3-diphenyl-1,3-propanedione, dibenzoylmethane |
| Hdmavk | dimethylaminovinylketone |
| Hdppe | $Ph_2PCH_2CH_2PPh_2$ |
| $HEt_2dtc$ | N,N-diethyldithiocarbamate |
| HEtmt | 1-(ethylthio)-maleonitrile-2-thiolate |
| Hfctfa | 1-ferrocenyl-4,4,4-trifluorobutane-1,3-dione, ferrocenoyltrifluoroacetone |
| Hhacsm | methyl(2-amino-1-cyclopentene-1-dithiocarboxylate) |
| Hhfaa | 1,1,1,5,5,5-hexafluoro-2,4-pentane, hexafluoroacetylacetone |
| Hhpt | 1-hydroxy-2-piridinethione |
| Hmacsm | methyl(2-methylamino-1-cyclopentene-1-dithiocarboxylate) |
| Hmnt | maleonitriledithiolate |
| Hneocupf | N-naphthyl-N-nitrosohydroxylamine, neocupferron |
| Hox | 8-hydroxyquinoline, oxine |
| Hpbtu | N-benzoyl-N-phenylthiourea |
| Hpic | 2-picolinic acid |
| Hquin | 2-carboxyquinoline |
| Hsacac | thioacetylacetone |
| Hsalnr | N-*o*-tolylsalicylaldimine |
| $HSpymMe_2$ | 4,6-dimethylpyrimidine-2-thiol |

## Abbreviations

| | |
|---|---|
| Hstsc | salicylaldehydethiosemicarbazose |
| Htfaa | 1,1,1-trifluoro-2,4-pentanedione, trifluoroacetylacetone |
| Htfba | 1,1,1-trifluoro-4-phenyl-2,4-butanedione, trifluorobenzoylacetone |
| Htfdma | 1,1,1-trifluoro-5-methyl-2,4-hexanedione |
| Htfhd | 1,1,1-trifluoro-2,4-hexanedione |
| Htftma | 1,1,1-trifluoro-5,5-dimethyl-2,4-hexanedione |
| Htrop | tropolone |
| Htta | 2-thenoyltrifluoroacetone |
| IR | infrared spectroscopy |
| L,L′-Bid | mono anionic bidentate ligand |
| L | one of the two donor atoms of the bidentate ligand L,L′-Bid |
| L′ | the second donor atom of the bidentate ligand L,L′-Bid |
| Me | methyl |
| MeO | methoxy |
| MTBK | methyl tertiary butyl ketone |
| NMR | nuclear magnetic resonance spectrometry |
| PGM | platinum group metals |
| Ph | phenyl |
| Phen | 1,10-phenanthroline |
| $P(OPh)_3$ | triphenylphosphite |
| $PPh_3$ | triphenylphosphine |
| $PX_3$ | tertiary phosphine with substituents X |
| S | solvent |
| T | temperature |
| TBP | trigonal bipyramidal |
| THF | tetrahydrofurane |
| Tol | tolyl |
| UV | ultraviolet spectroscopy |
| $\varepsilon$ | dielectric constant |
| $\theta$ | Tolman cone angle of tertiary phosphine |
| $\upsilon_{CO}$ | infrared stretching frequency of carbonyl |

# 1 Introduction

## 1.1 Strategic rhodium and the historical development of organometallic chemistry

The story of rhodium began in 1803 when both rhodium and iridium were discovered in the black residue left after crude platinum had been dissolved in aqua regia. William Hyde Wollaston discovered rhodium naming it after the Greek word ῥόδον (*rhodon*) for "rose" because of the rose-colour commonly found in aqueous solutions of its salts.[1] The discovery itself is formally dated 24th June 1804 when Wollaston read his paper, "On a new Metal, found in Crude Platina", as published in 1804 in Nicholson's "Journal of Natural Philosophy, Chemistry and the Arts", before the Royal Society.[2,3] For his study Wollaston used 1000 grains of crude platinum and obtained as the pure salt about 4 grains, that is less than 0.5 g of rhodium. His extraordinary skill has to be admired, since this quantity was for him enough to determine the main properties of the element. Rhodium and iridium, like ruthenium and osmium are still obtained by procedures designed to separate silver, gold and all the platinum metals.[4,5] After Pt, Pd and Au have been dissolved in aqua regia and Ag removed as its soluble nitrate, the residue is worked for Ru, Os, Ir and Rh. Rhodium is not extractable by any commercially available reagent and has to stay untill the final raffinate when it is separated from the iridium solvent extraction residue by fusing with $NaHSO_4$ and leaching with water, which dissolves Rh as $Rh_2(SO_4)_3$. Treatment with NaOH precipitates $Rh(OH)_3$ which is dissolved in HCl to yield a solution of $H_3[RhCl_6]$. $NaNO_2$ is firstly added and then $NH_4Cl$ to precipitate $(NH_4)_3[Rh(NO_2)_6]$

[1] Greenwood, N.N. and Earnshaw, A., *Chemistry of the elements*, Pergamon Press, Oxford (1984).

[2] Wollaston, W.H., *Philos. Trans. R. Soc. London*, **94**, 419 (1804).

[3] Kipnis, A., *Rhodium Ex.*, **1**, 31 (1993).

[4] Griffith, W.P., *The Chemistry of the Rare Platinum Metals (Os, Ru, Ir and Rh)*, Interscience, London (1967).

[5] Thompson, D., *Insights into speciality Inorganic Chemicals*, The Royal Society of Chemistry, Cambridge (1995).

which, after digestion in HCl, dissolves as $(NH_4)_3[RhCl_6]$. The solution is evaporated and then ignited in $H_2$ to complete the extraction of rhodium metal.[1]

The metals Rh, Ru, Os, Ir, Pd and Pt, all of them belonging to Group VIIIb of the periodic table, are often grouped together as the platinum metals and they, together with silver and gold, are known as the noble metals on account of their chemical inertness in the elemental state.[6] Of these, rhodium is one of the least abundant and consequently the most expensive platinum group metal (PGM). Rhodium and ruthenium comprise only 0.0001 ppm of the eath's crust, compared to the 0.001 ppm abundance of iridium, the 0.005 ppm of osmium, 0.015 ppm of palladium and 0.01 ppm of platinum. To put these figures into perspective, the abundance of silver is 0.08 ppm, gold is 0.004 ppm and cobalt 29 ppm.[1] In 2003, the total world production of rhodium was 20.4 ton of which South Africa produced a strategically significant 75.7% and Russia 19.4%.[7] Owing to its small market size (less than one-tenth the size of the platinum market) rhodium supply/demand imbalances can have a dramatic effect on prices. In 1989/1990 a rhodium supply shortfall caused prices to skyrocket to nearly seven times their previous values, only to get back in balance a year later. Again in 2003 the price dropped to $500 per oz from over $2000 per oz in 2001. Increased demand caused a steady rise from 2003 to a high of $3430 per oz in early 2006 (Figure 1.1). Currently, the rhodium price is $5765 per oz, platinum $1117 per oz, palladium $322 per oz, while gold trade at $619 per oz (prices as on 22 December 2006).

Rhodium, a silvery-white metallic element, is highly resistant to corrosion and is extremely reflective. It is therefore used as a finish for jewellery, mirrors and search lights. Electrical connections also benefit from its properties. Rhodium is furthermore used as an alloying agent to harden platinum and palladium for use in furnace windings, thermocouple elements, bushings for glass-fibre production, electrodes for aircraft turbine engines and laboratory crucibles. Complexes of rhodium also have medical applications. [Rh(acac)(cod)], 2,4-pentanedionato-$\eta^4$-cycloocta-1,5-diene-

[6] Parish, R.V., *The metallic elements*, Longman, London (1977).

[7] Platinum 2004, Johnson Matthey Public Limited Company (2004).

rhodium(I), in particular, showed antineoplastic activity comparable with that of cisplatin, *cis*-dichlorodiammineplatinum(II), towards Ehrlich ascite carcinomas. However, histological damage, in contrast to what was found for cisplatin, was virtually absent.[8] From a consumption point of view, the highest demand for rhodium is in the autocatalyst industry, using 18.8 ton per year, including 3.5 ton obtained from recycling (2003 value[7]). Autocatalysts consume on average about 90% of annual new rhodium production. The growing environmental concern as well as more strict emission regulations in Europe, Japan and the USA led to a steep increase in the use of autocatalysts (Figure 1.2).

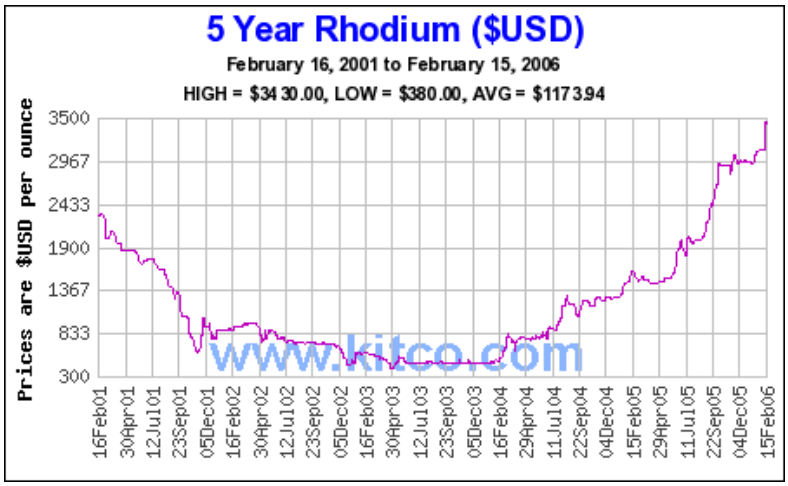


**Figure 1.1** Rhodium prices the past five years[9]

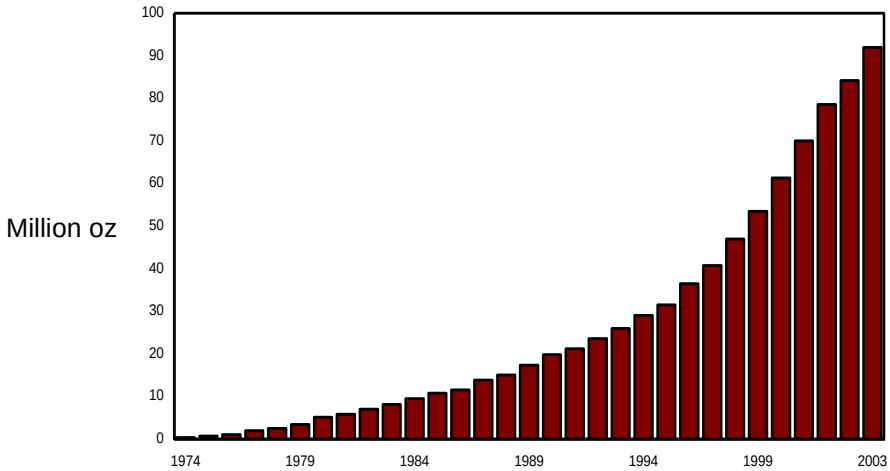


**Figure 1.2** Automotive industry purchases of PGMs for the period 1974 to 2003.[7]

[8] Giraldi, T., Sava, G., Bertoli, G., Mestroni, G. and Zassinovich, G., *Cancer Res*., **37**, 2662 (1977).

[9] www.kitco.com

Rhodium is a particularly effective catalyst for the conversion of $NO_x$ (mainly NO and $NO_2$) to harmless nitrogen with little or no ammonia formation[10] and consequently auto makers have increased average rhodium loading levels in autocatalysts. This is cost-effective as rhodium is used in much smaller proportions than platinum and palladium and a small rise in the rhodium content can help to maintain emissions conversion rates when platinum or palladium loadings are reduced. Johnson Matthey, one of the largest suppliers of PGMs and autocatalysts, claimed to have produced over 450 million autocatalysts since 1974 which have converted more than 4 billion tonnes of pollutants into harmless gases. In 1960 a car would typically pump out over 100 gram of CO, $NO_x$ and hydrocarbons for every mile driven. Today, a new car bought in the USA, Japan or Western Europe will only emit around 2 gram of these pollutants per mile.[7]

The second largest demand for rhodium, consuming about 1 ton per year (2003 value[7]), is from the chemical industry where rhodium catalysts have been prominently represented among catalytic applications of transition-metal coordination and organometallic chemistry. Rhodium catalysts exhibit a scope and versatility that probably are unmatched by those of any other element.[11] Rhodium forms organometallic compounds in oxidation states ranging from (+4) to (−3), although by far the most common oxidation states are Rh(I) and Rh(III). The rhodium(I) state has a $d^8$ electron configuration and its organometallic complexes usually form either four-coordinate square-planar or five-coordinate trigonal bipyramidal structures. Two-electron oxidation to the octahedrally coordinated rhodium(III) state ($d^6$) is usually facile through oxidative addition reactions, although these reactions can be reversible in many cases, unlike the corresponding iridium chemistry where oxidative addition usually occurs irreversibly. The reversibility of such reactions connecting the Rh(I) and Rh(III) oxidation states is responsible for many of the catalytic organic transformations which are encountered in organorhodium chemistry.[12] Among the rhodium-catalysed reactions that have received significant attention are the

[10] Tailor, K.C., *Catal. Rev. -Sci. Eng*., **35**, 457 (1993).

[11] Halpern, J., *Chem. Eng. News*, **8 Sept**, 114 (2003).

[12] Hughes, R.P., *Comprehensive coordination chemistry*, Vol. 5, Edited by Wilkinson, G., p. 278, Pergamon Press, Oxford (1987).

hydrogenation of olefins, including the first commercial asymmetric catalytic process (synthesis[13] of L-DOPA, i.e. L-3,4-dihydroxyphenylalanine, for the treatment of Parkinson's disease), hydrogenation of arenes, hydroformylation of olefins, olefin-diene codimerisation as well as Monsanto's carbonylation of methanol to acetic acid. In the case of hydroformylation, rhodium carbonyls show an activity approximately a thousand times higher than that of cobalt, the second most active.[14] Through hydroformylation, using rhodium carbonyls, about 2.5 million tonnes of heavy organic synthesis products is obtained per year, along with fine organic syntheses generating various pharmaceutical products.

While most transition-metal-catalysed reactions proceed through combinations of steps such as substitution, oxidative addition, insertion of olefins into metal-hydrogen or of carbon monoxide into metal-alkyl bonds, rhodium-catalysed reactions are distinctive in that the relative rates of the successive steps and stabilities of the diverse reaction intermediates are often matched to a degree that enables all or most of them to be directly observed and characterised. This makes rhodium very much suitable to be used in a study where the aim is to gain more knowledge about reaction steps that are essential in the application of organometallic complexes in catalysis.

The modern phase of research on the coordination and catalytic chemistry of rhodium extends back about half a century and goes hand in hand with the remarkable renaissance of transition-metal coordination and organometallic chemistry during the intervening half century. That would not have been possible, was it not for the pioneering work of a number of well-known names in chemistry, amongst them a number of Nobel laureates like A. Werner (1913), K. Ziegler and G. Natta (1963), D. Crowfoot-Hodgkin (1964), E.O. Fischer and G. Wilkinson (1973) as well as Y. Chauvin, R.H. Grubbs and R.R. Schrock (2005). They all contributed to the importance of organometallic chemistry and established its relevance to other disciplines in chemistry.

[13] Knowles, W.S. and Sabacky, M.J., *Chem. Comm*., 1445 (1968); Knowles, W.S., *J. Chem. Ed.*, **63**, 222 (1986).

[14] Imyanitov, N.S., *Rhodium Ex.*, **10**, 4 (1995).

To highlight some of the important landmarks in organometallic chemistry[15,16] it is appropriate to start with the discovery of the first organotransition-metal compound, a platinum-olefin complex by the Danish pharmacist W.C. Zeise in 1827. Some[17] attribute the first place to L.C. Cadet de Gassicourt[18] who, in 1760, was working on secret inks in a Paris military pharmacy. For their preparation, he used cobalt minerals that contained arsenic. His unintentionally prepared "fuming liquid" was however only characterised by R.W. Bunsen[19,20] in 1837. Zeise's discovery of potassium trichloro(ethylene)platinate(II) monohydrate was about forty years prior to the proposal of the periodic table by A.D. Mendeleev in 1869. The compound, prepared and formulated by Zeise as $PtCl_2(C_2H_4)\cdot KCl\cdot H_2O$ was not to be understood or appreciated for more than a century. When the synthesis of the compound, which is now called Zeise's salt, was first reported[21] (in Latin at that time), Zeise was severely attacked and the formulation of the compound condemned as a fantasy by Justus Liebig, a celebrity regarded as the father of organic chemistry. Later analysis and structural determination[22] established the essential soundness of Zeise's formulation unequivocally. His discovery would play an important role in the development of bonding theory in both inorganic and organic chemistry.[23]

About forty years later, in 1868, M.P. Schützenberger[24] obtains the first metal carbonyl, a platinum-chloride complex, $[Pt(CO)Cl_2]_2$. In 1890 L. Mond[25] prepared the

[15] Yamamoto, A., *Organotransition Metal Chemistry*, John Wiley & Sons, New York (1986).

[16] Collman, J.P. and Hegedus, L.S., *Principles and applications of organotransition metal chemistry*, University Science Books, California (1980).

[17] Elschenbroich, C.and Salzer, A., *Organometallics – A concise introduction 2nd Ed*., VCH, Weinheim (1992).

[18] Cadet de Gassicourt, L.C., *Mem. Math. Phys*., **3**, 623 (1760).

[19] Bunsen, R.W., *Annalen*, **24**, 71 (1837); **31**, 175 (1837).

[20] Bunsen, R.W., *Ann. Phys.,* **40**, 219 (1837).

[21] Zeise, W.C., *Ann. Phys.*, **9**, 932 (1827).

[22] Ziegler, K., *Angew. Chem.*, **67**, 543 (1955); Ziegler, K., Holzkamp, E., Breil, H. and Martin, H., *Angew. Chem.*, **67**, 541 (1955).

[23] Kauffman, G.B., *Comprehensive coordination chemistry*, Vol. 1, Edited by Wilkinson, G.,Pergamon Press, Oxford (1987).

[24] Schützenberger, M.P., *Annalen*, **15**, 100 (1868).

[25] Mond, L., *J. Chem. Soc.*, **57**, 749 (1890).

first binary metal carbonyl, $Ni(CO)_4$, and his discovery led to a commercial process for refining nickel. Soon afterwards he and M. Berthelot discovered $Fe(CO)_5$ as well.[26] In 1893 A. Werner proposed octahedral and square-planar coordination compounds and was in 1913 awarded one of the early Nobel prizes for developing the basic concepts of coordination chemistry. In 1909 W.J. Pope synthesised the first σ-organotransition-metal compound, $(CH_3)_3PtI$. F. Hein[27] prepared polyphenylchromium compounds in 1919, which were subsequently known to be π-arene chromium complexes. T. Midgley and T.A. Boyd introduced tetraethyllead for use as an antiknock additive in petrol engines in 1922. The Fischer-Tropsch process[28], which is a topic of great current interest and used on a large scale, was discovered in 1925 by F. Fischer and H. Tropsch. The first compound containing a rhodium-carbon bond was synthesised by Manchot and König in the same year.[29] In 1931 W. Hieber prepared $Fe(CO)_4H_2$, the first transition-metal hydride complex. While investigating the Fischer-Tropsch reaction O. Roelen discovered the cobalt-catalysed oxo process[30] in 1938. The oxo hydroformylation reaction soon became the first truly viable, commercial, homogeneously catalysed process and is still practiced today. It greatly stimulated research in homogeneous catalysis and organometallic chemistry. W. Reppe[31] started his work on the transition-metal catalysed reactions of acetylenes in 1939 and within a year M. Iguchi discovered homogeneous catalytic hydrogenation of fumaric acid by rhodium complexes.[32] As a result of wartime disruption of chemical research, little appeared to happen between 1939 and 1951. In that year the nature of the metal-carbonyl bond, the prototype of π-backbonding, was proposed by L.E. Orgel, L. Pauling and H. Zeiss, while two groups, T.J. Kealy[33] and P. Pauson, and S.A. Miller[34] independently obtained the first

[26] Mond, L. and Langner, C., *J. Chem. Soc.*, **59**, 1090 (1891); Berthelot, M., *C.R. Acad. Sci.*, **112**, 1343 (1891).

[27] Hein, F., *Ber.*, **52**, 195 (1919).

[28] Fischer, F. and Tropsch, H., DRP 411416 (1922); DRP 484337 (1925).

[29] Manchot, W. and König, J., *Chem. Ber.*, **58B**, 2173 (1925).

[30] Roelen, O., DRP 849548 (1938); *Angew. Cem.*, **60**, 62 (1948).

[31] Reppe, W., *Neue Entwicklungen auf dem Gebiete der Chemie des Acetylens und des Kohlenoxyds*, Springer-Verlag (1949).

[32] Iguchi, M., *J. Chem. Soc. Japan*, **60**, 1287 (1939).

[33] Kealy, T.J. and Pauson, P.J., *Nature*, **168**, 1039 (1951).

sandwich complex, ferrocene. In 1955, G. Wilkinson[35] and his student F.A. Cotton[36] described the fluxional behaviour of some organometallic compounds. Such dynamic intramolecular rearrangements were intensely explored by inorganic chemists for the next twenty years. In the same year J. Halpern began to lay the foundation for understanding the mechanism of homogeneously catalysed hydrogenations. The catalytic polymerisation of olefins under low-pressure conditions, the Ziegler-Natta process[37,38] employing mixed metal catalysts, was an event of great technological significance which initiated large industrial research programs and was also announced in 1955. The first compound containing a rhodium-alkene bond, [Rh($\eta^5$-$C_5H_5$)( $\eta^4$-1,5-cod)], was reported by Chatt and Venanzi[39] in 1956. In 1959 an early example of an oxidative addition reaction was described by B.L. Shaw[40] and J. Chatt, although the scope and potential of this reaction class was not evident until Vaska's[41] discovery in 1962 of the chemically versatile iridium compound, *trans*-[IrCl(CO)($PPh_3$)$_2$], that bears his name. The first rhodium complex containing a monoalkene ligand [{RhCl(η-$C_2H_4$)$_2$}$_2$] was isolated by Cramer[42] in the same year. This discovery was followed in 1963 by the report of the first compound containing a rhodium-carbon σ-bond, when the five coordinate Rh(III) complex [RhBr(1-naphthyl)$_2$($PX_3$)$_2$] was synthesised by Chatt and Underhill.[43] In 1964 two seemingly unrelated events occurred when E.O. Fischer[44] prepared the first transition-metal carbene complex while R.L. Banks discovered catalytic olefin metathesis. We now believe carbene complexes are the active catalysts for olefin metathesis. The next year G. Wilkinson[45] reported that solutions of [RhCl($PPh_3$)$_3$] would homogeneously

[34] Miller, S.A., Tebboth, J.A. and Tremaine, J.F., *J. Chem. Soc.,* 632 (1952).

[35] Wilkinson, G. and Piper, T.S., *J. Inorg. Nucl. Chem*., **2**, 23 (1956).

[36] Cotton, F.A., *J. Organomet. Chem*., **100**, 29 (1975).

[37] Ziegler, K., *Adv. Organomet. Chem*., **6**, 1 (1968).

[38] Natta, G., *Scientific American*, **205**, 33 (1961).

[39] Chatt, J. and Venanzi, L.M., *Nature*, **177**, 852 (1956).

[40] Chatt, J. and Shaw, B.L., *J. Chem. Soc.,* 4020 (1959).

[41] Vaska, L. and Kiluzio, J.W., *J. Am. Chem. Soc*., **84**, 679 (1962).

[42] Cramer, R., *Inorg. Chem*., **1**, 722 (1962).

[43] Chatt, J. and Underhill, A.E., *J. Chem. Soc.,* 2088 (1963).

[44] Fischer, E.O. and Maasbol, A., *Angew. Chem., Int. Ed. Engl*., **3**, 580 (1964).

[45] Young, J.F., Osborn, J.A., Jardine, F.H. and Wilkinson, G., *Chem. Comm*., 131 (1965).

catalyse the hydrogenation of alkenes and alkynes. The same discovery was made nearly simultaneously by R.S. Coffey.[46] The Wilkinson hydrogenation catalyst proved to be one of the most practical organotransition-metal catalysts. The resultant industrial and academic interest in the synthesis and chemistry of compounds containing rhodium-carbon and rhodium-hydrogen bonds produced a rapid acceleration in the number of papers published per annum after 1965.[12]

By this time the discoveries were occurring at an ever-increasing pace. The events already mentioned, however, laid the foundation of a bright future for organometallic chemistry to follow. Organometallic chemistry probably would not have been that prominent today if it were not for its important industrial applications. The technical and commercial importance of organometallic compounds was especially recognised with the development of successful homogeneous catalysed industrial processes. Some of the best known processes[47,48,49,50] involving organometallic compounds are the hydrogenation of olefins utilising complexes of low-valent transition metals such as rhodium (e.g. Wilkinson's catalyst, $[RhCl(PPh_3)_3]$), the hydroformylation of olefins in the oxo process using rhodium or cobalt catalysts, the oxidation of olefins to aldehydes and ketones in the Wacker process, the polymerisation of propylene using the Ziegler-Natta catalyst (organoaluminium-titanium), olefin isomerisation using nickel catalysts, the cyclooligomerisation of acetylenes using Reppe's or Wilke's catalysts (nickel complexes) and the carbonylation of methanol using either a cobalt catalyst (old BASF process), a rhodium catalyst (Monsanto process) or an iridium catalyst (Cativa process[51,52]). Homogeneous catalysis is indeed the success story of

[46] Coffey, R.S., Imperial Chemical Industries, Brit. Pat. 1, 121, 642 (filed 1965).

[47] Halpern, J., *Inorg. Chim. Acta*, **50**, 11 (1981).

[48] Herrmann, W.A. and Cornils, B., *Angew. Chem. Int. Ed. Engl.*, **36**, 1048 (1997).

[49] Purcell, K.F. and Kotz, J.C., *Inorganic Chemistry*, W.B. Saunders Company, Philadelphia (1977).

[50] Cotton, F.A. and Wilkinson, G., *Advanced Inorganic Chemistry 5th Ed*, John Wiley & Sons, New York (1988).

[51] Howard, M.J., Sunley, G.J., Poole,A.D., Watt, R.J. and Sharma, B.K., *Stud. Surf. Sci. Catal*., **121**, 61 (1999).

[52] Haynes, A., Maitlis, P.M., Morris, G.E., Sunley, G.J., Adams, H., Badger, P.W., Bowers, C.M., Cook, D.B., Elliot,P.I.P., Ghaffar, T., Green, H. and Griffin, T.R., *J. Am. Chem. Soc*., **126**, 2847 (2004).

organometallic chemistry and proof of mutual stimulation and support since early days.

Further developments in industrial chemistry towards clean, low-temperature, low-pressure, and economic processes clearly depend on improved catalysts. Progress in theoretical inorganic chemistry, mainly in the ligand-field theory played a large role in catalyst research. Consequently more emphasis was laid on the composition and activity of a catalyst. Ligands of a complex that was identified as a catalyst was modified systematically to induce specific changes in both the composition of the final product and the rate of the catalysed reaction. That lead to a better understanding regarding variables such as electron density on the metal, orbital energies and sterical hindrance, all of which can influence the reaction. In the reactions where tertiary phosphine complexes of transition metals are used as catalysts, a dramatic change in the catalytic activity and selectivity can be obtained by minor modifications to the steric and/or electronic properties of the phosphorous bound substituents. Each of the processes mentioned in the preceding paragraph represents a combination of several of the fundamental reactions that transition metal complexes can undergo, such as oxidative addition, insertion, substitution and reductive elimination. One type of reaction that can always be identified in the mechanistic representation of these catalytic reactions is oxidative addition. It is thus important to study the role of such a step in the catalytic process as a whole. The extent to which the oxidative addition step is affected by, for instance, the electronic and steric modifications to the phosphine ligand, lead to more effective modelling of such catalysts. A better understanding of catalytic processes is primarily dependent on the study of these fundamental reactions that transition metal complexes undergo.

Most organic reactions catalysed by transition metals proceed by a series of consecutive steps of which at least one reactive intermediate has to contain a carbon-metal σ-bond. In this context, the oxidative addition of iodomethane to the rhodium(I) complex in the well-known industrial catalytic carbonylation of methanol to acetic acid can be regarded as the key step. This process, developed by Monsanto, is probably to date the most successful classical example of an industrial process

catalysed by a metal complex in solution.[53] Acetic acid is a major industrial chemical, involved in the manufacture of various products such as vinyl acetate, cellulose acetate, pharmaceuticals, dyes and pesticides.[54] In 1993, approximately 60% of the world production of acetic acid of 5.5 million tonnes per year was manufactured according to the Monsanto process.[55] In this process (Figure 1.3) iodomethane undergoes oxidative addition to the square-planar Rh(I) complex, $[Rh(CO)_2I_2]^-$, in a rate-determining step[56] yielding an octahedral Rh(III) complex, $[Rh(CO)_2I_3CH_3]^-$. Subsequent CO-insertion into the *cis* $CH_3$-Rh bond gives a five-coordinate acetyl complex, $[Rh(CO)I_3(COCH_3)]^-$, which forms the six-coordinate species $[Rh(CO)_2I_3(COCH_3)]^-$ after coordination of a CO molecule. This complex then undergoes reductive elimination of acetyl iodide and the initial Rh(I) catalyst is regenerated. The reaction of acetyl iodide with water forms the required acetic acid and HI wherein the latter reacts with a next molecule of methanol to form iodomethane and the cycle starts again. The mechanism was resolved over a period of more than two decades of extensive research, leading to confirmation by Maitlis *et. al.*[57] of the existence of the intermediate, $[Rh(CO)_2I_3CH_3]^-$, utilising FTIR and FTNMR spectroscopy.

Other square-planar $d^8$ complexes with electron-rich $d_{z^2}$ orbitals and a vacant coordination site available undergo readily oxidative addition with alkyl and aryl halides, similar to that shown in the Monsanto process. A wide range of factors influence this $CH_3I$ addition making the mechanistic elucidation and related investigation of the extent of these factors essential before a specific complex can be considered as a potential catalyst.

[53] Maitlis, P.M., Haynes, A., Sunley, G.J. and Howard, M.J., *J. Chem. Soc., Dalton Trans*., 2187 (1996).

[54] Lukehart, C.M., *Fundamental transition metal organometallic chemistry*, Brooks/Cole Publishing Company, Monterey, California (1985).

[55] Howard, M.J., Jones, M.D., Roberts, M.S. and Taylor, S.A., *Catal. Today*, **18**, 325 (1993).

[56] (a) Fulford, A., Hickey, C.E. and Maitlis, P.M. *J. Organomet. Chem.,* **398**, 311 (1990); (b) Hickey, C.E. and Maitlis, P.M. *J. Chem. Soc., Chem. Comm*., 1609 (1984).

[57] Haynes, A., Mann, B.E., Gullivier, D.J. Morris, G.E. and Maitlis, P.M., *J. Am. Chem. Soc*., **113**, 8567 (1991).

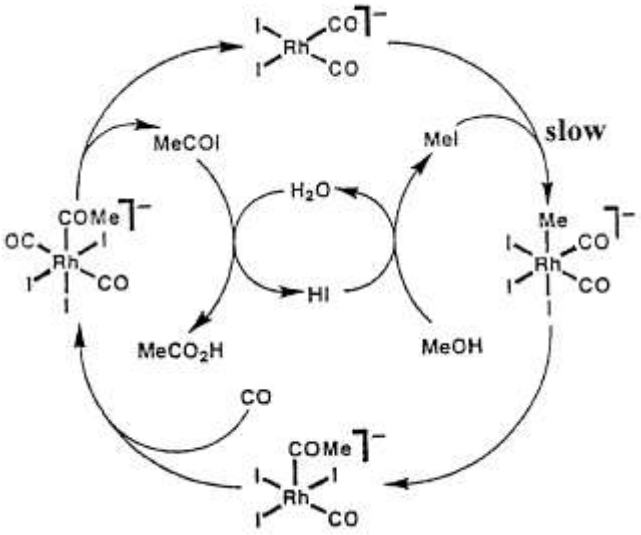


**Figure 1.3** Carbonylation of methanol in the Monsanto process.

## 1.2 Background and aim of this study

This study is related to the Monsanto process since two of the reaction steps in the catalytic cycle, oxidative addition and CO-insertion, were studied for the reaction between Rh(I) complexes and iodomethane. It is also a continuation of research on the rhodium complexes of the N-aryl-N-nitrosohydroxylamines, started with cupferron,[58,59] the ammonium salt of N-nitrosophenylhydroxylamine. As part of the preceding research, the structure of a Rh(I) phosphine complex, [Rh(cupf)(CO)($PPh_3$)], was solved crystallographically and showed the result of the substitution of one of the CO groups of [Rh(cupf)$(CO)_2$] by $PPh_3$. The relative *trans* influence of the cupferrate oxygen atoms could be compared with those results of similar formulated complexes, [Rh(LL')(CO)($PPh_3$)] (LL' = ligands such as β-diketones, thioacetylacetone, 8-hydroxyquinoline and 2-picolinic acid). The order of *trans* influence according to the Rh-P bond distances in the above complexes was found to be S > N > O.[60] According to the Rh-P distance for [Rh(cupf)(CO)($PPh_3$)],

[58] Basson, S.S., Leipoldt, J.G., Roodt, A. and Venter, J.A., *Inorg. Chim. Acta*, **118**, L45 (1986).

[59] Basson, S.S., Leipoldt, J.G., Roodt, A. and Venter, J.A., *Inorg. Chim. Acta*, **128**, 31 (1987).

[60] Graham, D.E., Lamprecht, G.J., Potgieter, I.M., Roodt, A. and Leipoldt, J.G., *Trans. Met. Chem*., 193 (1991).

the *trans* influence for the nitroso oxygen is comparable to those of the β-diketone ligands. In a kinetic study [Rh(cupf)(CO)($PPh_3$)] was used along with other [Rh(cupf)(CO)($PX_3$)] complexes [$PX_3$ = $PCy_3$, P(*o*-Tol)$_3$, $PPh_3$, $PPh_2C_6F_5$, P(*p*-$ClC_6H_4)_3$ and P(*p*-$MeOC_6H_4)_3$)] to react with iodomethane and Rh(III) alkyl products formed as a result of the oxidative addition. Addition was believed to take place with the $CH_3$ and I groups orientated in an unusual *cis* configuration in the final product, a Rh(III) alkyl complex.

Previous work done in our group also focussed on the mechanistic behaviour of the β-diketonato type bidentate ligands and analogues thereof in complexes of Rh(I) towards oxidative addition and CO-insertion.[61] Oxidative addition of iodomethane to such complexes showed results strongly in favour of an ionic $S_N2$ two-step operative mechanism. That implies a *trans* geometry of addition for the alkyl halide, as was observed in the case of [Rh(ox)(CO)($CH_3$)(I)($PPh_3$)].[62] A concerted three-centre *cis* addition with retention of configuration at the carbon atom of the alkyl halide is a well-known alternative operating for example exclusively in the case of homonuclear molecules like hydrogen and other unsymmetrical substrates like silanes. A clear-cut choice between these mechanistic types for a specific reaction is often difficult to make, but the net result for a number of variables during a kinetic study can serve as compelling evidence to exercise this choice. For this reason the N-aryl-N-nitrosohydroxylamines, like the cupferrate ligand, was chosen in a variation of the β-diketone formulated Rh(I) complexes. The cupferrate ligand offered a substantial smaller bite angle, which could favour an asymmetric concerted addition step during the oxidative addition of an alkyl halide. Apart from the structure of [Rh(cupf)(CO)($PPh_3$)], its oxidative addition product, [Rh(cupf)(CO)($CH_3$)(I)($PPh_3$)], gave suitable crystals for structure analysis. The ground state stereochemistry of these complexes, although not specific for establishing the mechanistic pathway, could aid the interpretation of the kinetic data for the oxidative addition reaction.

---

[61] (a) Basson, S.S., Leipoldt, J.G. and Nel, J.T., *Inorg. Chim. Acta*, **84**, 167 (1984); (b) Basson, S.S., Leipoldt, J.G., Roodt, A., Venter, J.A. and Van der Walt, T.J., *Inorg. Chim. Acta*, **119**, 35 (1986); (c) Steyn, G.J.J., Roodt, A. and Leipoldt, J.G., *Inorg. Chem*., **31**, 3477 (1992); (d) Smit, D.M.C., Basson, S.S. and Steynberg, E.C., *Rhodium Ex.*, **7-8**, 12 (1994); Roodt, A. and Steyn, G.J.J., *Resent Res. Devel. Inorg. Chem*., **2**, 1-23 (2000).

[62] Van Aswegen, K.G., Leipoldt, J.G., Potgieter, I.M., Lamprecht, G.J., Roodt, A. and Van Zyl, G.J., *Trans. Met. Chem*., **16**, 369 (1991).

Worldwide, the study of the N-aryl-N-nitrosohydroxylamines was limited to that of cupferron, with neocupferron almost unexploited. Cupferron, the best known member of the family, is commonly used on a large scale in industry as a metal chelator and as a polymerisation inhibitor. As a ligand, a number of cupferrate complexes are known (to be discussed in Chapter 4) but only one characterised neocupferrate complex, that of $[Co(neocupf)_2(H_2O)_2]$,[63] could be found in literature. Crystal structures of metal complexes of the N-aryl-N-nitrosohydroxylamines are expected to be good models for the binding mode of the nitroso group to metal ions. The N-nitroso compounds are known carcinogens[64] and in order to clarify their cytotoxicity, it is important to accumulate precise structural data concerning the interaction modes of these compounds. Furthermore the neocupferrate ligand offered the opportunity to vary the bidentate ligand in succession to the cupferrate study, as well as to reconfirm the unusual *cis* addition, with a possible similarity in the case of neocupferrate.

The bidentate ligands that were studied by our group mainly included monoanionic ligands with donor atom combinations O:O, O:S, N:S and N:O, while the size of the chelate ring was varied between five- and six-membered rings as well. It was found that these factors are important in terms of the reactivity of the transition metal complexes. The increase in the rate for the donor atoms of the bidentate ligand was found to be in the order O:O < O:S < N:O < N:S, while no meaningful correlation was found for the rate of acylation. In the case of $[Rh(Sacac)(CO)(PX_3)]$, oxidative addition of iodomethane has been found to follow second-order kinetics with only the acylrhodium(III) complex as product.[65] The reaction was proposed to proceed through an alkylrhodium(III) intermediate and two possible reaction routes via different transition states have been suggested. Compared to the cupferrate system it became clear that the reaction mechanism is influenced by the nature of the bidentate ligand.

[63] Tamaki, K. and Okabe, N., *Acta Cryst.*, **C54**, 195 (1998).

[64] Okabe, N., Tamaki, K., Suga, T. and Kohyama, Y., *Acta Cryst.*, **C51**, 1295 (1995).

[65] Leipoldt, J.G., Basson, S.S., and Botha, L.J., *Inorg. Chim. Acta*, **168**, 215 (1990).

Proceeding from what was given as background, the following goals were set for this study:

1. Obtain the crystal structure for [Rh(cupf)(CO)($CH_3$)(I)($PPh_3$)], the alkyl oxidative addition product, to confirm the stereochemical outcome in the solid state of that reaction.

2. Perform the kinetic study of the oxidative addition of iodomethane to [Rh(cupf)(CO)($PPh_3$)] under high pressure to obtain more information on the nature of the transition state.

3. With [Rh(cupf)(CO)($CH_3$)(I)($PX_3$)] as the starting complex, examine the effect of solvent on the rate of CO insertion. Resolve the nature of solvent participation using a series of methyl substituted tetrahydrofuranes among other solvents.

4. During the preparation of [Rh(cupf)(CO)($PPh_3$)] the effect of the addition of an excess $PPh_3$ was observed in IR spectra. Investigate and characterise this new complex.

5. The cone angles[66] for the phosphine ligands used in the study of the cupferrate system varied from 145° to 195°. Incorporate and investigate the effect of a phosphorous ligand like a bicyclic phosphite ester with a cone angle of only 101°.

6. Extend the study done on the cupferrate ligand to another N-aryl-N-nitrosohydroxylamine, the neocupferrate ligand:

   a) Synthesise and characterise a representative starting complex, the alkyl oxidative addition product as well as the subsequent acyl product, using X-ray crystallographic methods to accurately determine bonding distances, -modes and coordination geometry.

   b) Investigate the electronic and steric influence of different tertiary phosphines on the oxidative addition of iodomethane to [Rh(neocupf)(CO)($PX_3$)].

[66] Tolman, C.A., *Chem. Rev*. **77**, 313 (1977).

c) Study the reactivity of Rh(I) complexes in the above mentioned oxidative addition reaction with regard to solvent polarity and donicity effects and clear the nature of solvent participation in the reaction mechanism.

d) Determine the mechanism of the oxidative addition of iodomethane to the neocupferrate complexes.

e) An effort will be made to quantify the combined effect of the phosphine ligand and the bidentate ligand in a mathematical form, which can be compared with similar studies.

7. Study the kinetics and mechanism of the oxidative addition of iodomethane to [Rh(acac)(CO)($PX_3$)], where X = *p*-chlorophenyl, phenyl and *p*-methoxyphenyl. These phosphines have the same Tolman cone angle, but will influence the electron density on the rhodium atom differently due to variation in electronegativity of substituents on the phenyl rings.

8. Undertake a combined solvent-, temperature-, and pressure-dependence study of the oxidative addition of iodomethane to [Rh(Sacac)(CO)($PPh_3$)] in an attempt to further clarify the role of different donor atoms of the bidentate ligand on oxidative addition and to obtain a decisive answer regarding the two previously suggested transition state routes.

# 2 Fundamental aspects

## 2.1 Prominent ligands and their bonding characteristics

### 2.1.1 Introduction

In the +1 oxidation state rhodium is a $d^8$-specie capable of forming bonds with four monodentate ligands by overlap of a filled σ-orbital of each ligand with one of the four equivalent, unfilled $dsp^2$-hybrid orbitals of the metal to form 16-electron square planar complexes. A variety of neutral ligands such as carbon monoxide, substituted phosphines ($PX_3$), arsines, stibines, nitric oxide, and various molecules with delocalised π orbitals like ethylene, pyridine and 1,10-phenanthroline can be involved[1]. These ligands, also called π acid ligands, have except for their σ donating ability, also the ability to accept a significant amount of electron density from the metal centre into the empty π* orbitals of the ligand. This has a stabilising effect, since in many of these complexes, the metal atoms are in low positive, zero or even negative formal oxidation states. Stabilising of metals in low oxidation states is associated with the fact that these ligands have vacant π* orbitals in addition to lone-pair electrons. These vacant π* orbitals can accept electron density from filled metal orbitals to form π-bonds in addition to the σ bond that arises from the ligand donating a lone pair to the metal. Delocalisation of high electron density on the metal atom into the empty π* orbitals of the ligands can thus take place. The degree of transfer of electron density along the π-bond is variable. A π-bond stabilises the otherwise non-bonding d-electron pairs in order to make them less available for chemical reactions. As a consequence, strong π-acid ligands lower the reactivity of the metal with regard to oxidative addition reactions. The strength of a metal-ligand bond is determined in essence by the σ- and π-bond character of the ligand. In addition,

[1] Cotton, F.A. and Wilkinson, G., *Advanced Inorganic Chemistry 5th Ed*, John Wiley & Sons, New York (1988).

sterical factors play also a large role in the chemical behaviour of transition metal complexes.

### 2.1.2 The carbonyl ligand[1,2,3,4]

Schutzenberger was the first to recognise CO as a ligand in his preparation of $[Pt(CO)_2Cl_2]$.[5] The study of transition metal complexes containing carbon monoxide as ligand has since developed into an active field of research. Such complexes are frequent starting materials for the preparation of other compounds. Not only can CO be replaced by a wide variety of ligands, but any carbonyl group that remains in a complex usually stabilises the complex with respect to oxidation and/or thermal decomposition. Furthermore the carbonyl ligands can be used as a probe of the electronic and molecular structure of a compound by studying the frequency and intensity of the CO stretching modes in the infrared region. For these reasons, the study of the chemical and physical properties of metal carbonyls and their derivatives have been extensively pursued. Carbonyl ligands therefore serve well to explain the bonding characteristics of $\pi$ acid ligands.

A metal-carbonyl bond consists of two components, namely a filled $\sigma$ hybrid orbital of carbon which overlaps with an empty $dsp^2$ hybrid orbital of the metal to form a $\sigma$-bond, as well as $\pi$-bonds, formed from the overlap of filled metal d orbitals of $\pi$ symmetry with empty $\pi^*$ or anti-bonding orbitals of the carbonyl (Figure 2.1). This flow of electron density from the metal to the carbonyl, called $\pi$ back donation or back bonding, causes an increase in the effective nuclear charge, Z*, of the metal. It is an increase which eventually limits the degree of metal $t_{2g} \rightarrow \pi^*$ electron flow. Furthermore, the increase in Z* has the effect of causing a stronger ligand $\rightarrow$ metal $\sigma$ bond than usual because of the stronger attraction by the metal. As the delocalised electron density of the CO $\sigma$ orbital towards the metal increases, Z* decreases and

[2] Collman, J.P. and Hegedus,L.S., *Principles and applications of organotransition metal chemistry*, University Science Books, Mill Valley, California (1980).

[3] Abel, E.W., and Stone, F.G.A., *Quart. Rev*., **23**, 325 (1969).

[4] Purcell, K.F. and Kotz, J.C., *Inorganic Chemistry*, W.B. Saunders Company, Philadelphia (1977).

CO is getting more positive, which enlarge the acceptor strength of the π* orbital making further $t_{2g} \rightarrow \pi^*$ electron flow possible. The consequence of this two-way electron flow, known as a synergistic effect, is a mutual strengthening of the carbonyl to metal σ-bond and the metal to carbonyl π bonds, resulting in a metal-carbonyl bond stronger than the sum of the two types of bonds acting individually.[4]

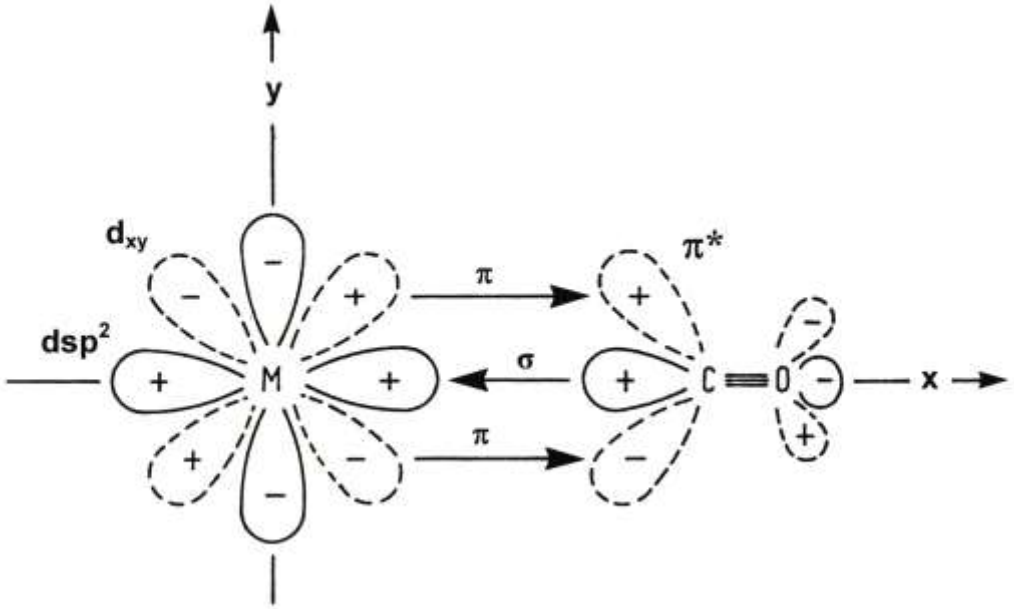


**Figure 2.1** Representation (in one plane) of the σ-bond and π back donation between metal d-orbitals and a CO molecule.

Due to the relative ease of observation and interpretation of carbonyl stretching modes of metal carbonyls, infrared spectroscopy is the single most useful physical method in the study of metal carbonyl compounds. Infrared data can be used to correlate changes in the metal-carbonyl bond, to follow the progress of reactions, to test for impurities and to gain information regarding the molecular structure. This can be done by studying the frequency, the number and relative intensities of observed bands. The CO stretching mode of the carbonyl ligand provides the most information on the electronic and molecular structure of a compound, since metal-carbon stretching modes occur in the same region as other vibrations, and allocations cannot easily be made. The appreciable amount of solvent related shifts of CO stretching frequencies is however a disadvantage.[6]

[5] Schutzenberger, P., *J. Chem. Soc.,* 1008 (1871).

[6] Beck,W. and Lottes, K., *Z. Naturforsch*, **19b**, 987 (1964).

A decrease in the stretching frequency of the CO bond with coordination to a metal and with increasing oxidation state of the metal give further evidence in favour of the model of back donation in metal carbonyl compounds. The experimental results[7] in Table 2.1 support the model extremely well. The CO stretching frequencies of the hexacarbonyls increase in the iso-electronic series from V to Cr to Mn, while the MC stretching frequencies decrease.

**Table 2.1** Infrared results for the iso-electronic series $[V(CO)_6]^-$, $[Cr(CO)_6]$, $[Mn(CO)_6]^+$. Stretching frequency values are given in $cm^{-1}$.

| | **$[V(CO)_6]^-$** | **$[Cr(CO)_6]$** | **$[Mn(CO)_6]^+$** |
|---|---|---|---|
| **M—C** | 460 | 441 | 416 |
| **C—O** | 1859 | 1981 | 2101 |

The stretching frequency of free CO is 2140 $cm^{-1}$ while the value for $[Cr(CO)_6]$ is only 1981 $cm^{-1}$. The explanation is that back donation fills the $\pi^*$-orbital and results in a weaker stretching frequency.[8] Substitution of CO by ligands with a low $\pi$-acceptor ability causes that remaining CO groups have to accommodate $d\pi$ electrons from the metal to a larger extent in order to prevent accumulation of negative charge on the metal atom. This causes a weaker CO bond. Allocation of bond order relies on the assumption that the valence of C remains constant in order that an increase in the MC bond order will cause a decrease of equal measure in the CO bond order. To illustrate this phenomenon the following two canonic forms can be presented:


Infrared intensities of the CO modes in transition metal carbonyl bonds are only determined by $\pi$-bonding effects.[9] In confirmation thereof the intensities of CO

[7] Cotton, F.A., *Inorg. Chem*., **3**, 702 (1964).

[8] Caulton, K.G. and Fenske, R.F., *Inorg. Chem*., **7**, 1273 (1968).

[9] Brown, T.L. and Darensbourg, D.J., *Inorg. Chem*., **6**, 971 (1967).

stretching modes decrease drastically for the iso-electronic series $[V(CO)_6]^-$, $[Cr(CO)_6]$ and $[Mn(CO)_6]^+$.

### 2.1.3 Trivalent phosphorous ligands

The ground state electron configuration of phosphorous, namely $[Ne]3s^23p^3$, is similar to that of nitrogen, $[He]2s^22p^3$, yet there is little in common in their chemical behaviour. One of the underlying reasons for this is the difference in the strength of the bonds they form with other elements. If phosphorous would use its 3p orbitals for bonding, then the non-bonding pair will reside in the 3s orbitals, which will be dispersed spherical symmetrical over a relatively large area. The lone pair electrons are therefore less available in $PH_3$ than in $NH_3$, as reflected in their basicity values. As the s-character of the bond increases, the p-character of the lone pair will increase, making it less dispersed and thus more readily available. A large bond angle of the phosphorous bound groups implicates a high percentage p-character of the donor electron pair, while a small bond angle is the result of a high percentage s-character. The nature of the phosphorous bound groups plays an equally important role in the behaviour of the lone pair than the bond angle. In the series $PH_3$, $MePH_2$, $Me_2PH$ and $Me_3P$, the increasing number of methyl groups results in a large increase in basicity, more than in the case of nitrogen. Basicity, expressed in terms of $pK_a$, depends on various factors, including the availability of the lone pair electrons.[10,11]

Trivalent phosphorous donor ligands, $PX_3$ (X = F, Cl, H, alkyl, aryl, etc.) played an important role in the development of coordination and organometal chemistry. They form complexes with almost all transition metals across a wide range of oxidation states (+IV to –I). The electron pair donor properties of phosphine ligands follow certain patterns. Trialkylphosphines form for example stronger metal-ligand bonds than triarylphosphines in the case where ligand basicity is the dominating effect.[12] However, ligand basicity fails to explain the unusual stability of phosphite and some

[10] Emsley, J. and Hall, D., *The chemistry of phosphorous*, Harper & Row Publishers, New York (1976).

[11] Streuli, C.A., *Anal. Chem*., **32**, 985 (1960).

[12] Tolman, C.A., *J. Am. Chem. Soc*., **92**, 2953 (1970).

$PX_3$ ligands (X = F, Cl).[13] Since the latter is often associated with metals in low oxidation states, the π-acceptor behaviour of phosphorous ligands, similar to that of carbon monoxide, is considered important. The idea of $PX_3$ acting as π-acids has been supported by many arguments. If the $PX_3$ ligands would have π-acceptor properties, the nature of the π-acceptor orbital would also be in question.

In order to explain the effective bonding ability of phosphine ligands, Chatt[14] suggested in 1950 that the donor σ-bond (lone pair donation), formed between the phosphine ligand and the metal, is strengthened by nd (metal) → 3d (phosphorous) π back donation from the metal to phosphorous (Figure 2.2). Accordingly, P(III) ligands are considered as belonging to a group of ligands called π-acids, which also include carbonyl, nitrosyl and isocyanide groups.

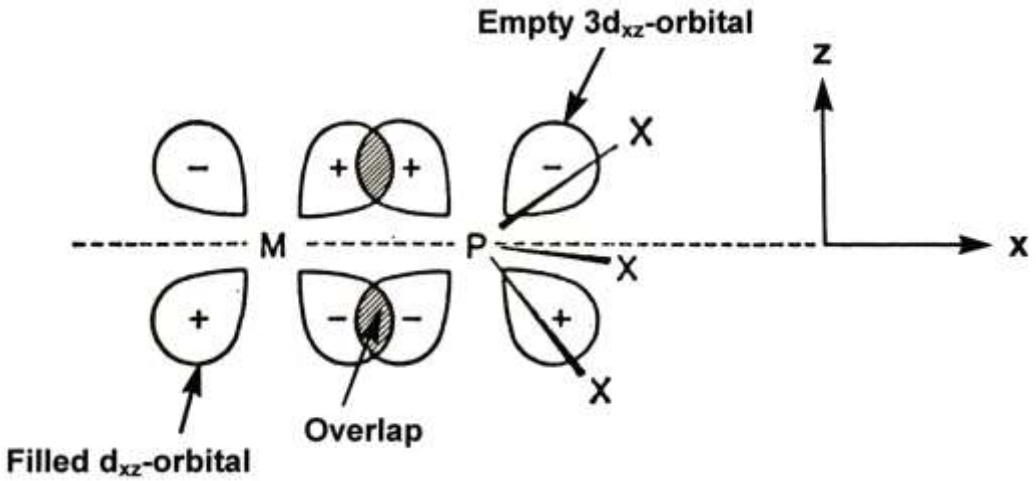


**Figure 2.2** Simplified presentation of the back donation from filled metal d-orbitals to an empty 3d-orbital of phosphorous in the $PX_3$ ligand. A similar overlap happens in the yz plane, where $d_{yz}$ orbitals are used. The σ-bond forms through the overlap of a filled $sp^3$ hybrid orbital of phosphorous with the empty metal $dsp^2$ hybrid orbital.

The 3d orbitals of phosphorous atoms are empty in the case of phosphines, but the extent to which they can effectively overlap with a filled metal d-orbital depends on the nature of the groups attached to phosphorous. As a ligand, $PF_3$ has a lot in

[13] Huheey, J.E., *Inorganic chemistry*, Harper & Row Publishers, New York (1972).

[14] Chatt, J., *Nature*, **165**, 637 (1950).

common with CO, since complexes are not formed with metals in high oxidation states, although low oxidation states are indeed stabilised. The Ni-P bond distance in $[Ni(PF_3)_4]$ is shorter by 10% compared to other Ni-P bonds, indicating a stronger metal-ligand interaction. There are also reasons to exclude P(III) ligands with weak electronegative atoms or groups as $\pi$-acceptors. According to the ligand field constriction theory,[10] only strongly electronegative atoms have the ability to constrict the 3d (phosphorous) orbitals sufficiently for $\pi$-bonding. Chlorine atoms and phenyl groups are less effective in this regard and have the tendency to reduce the $\sigma$-donor ability of phosphorous on a smaller scale than fluorine atoms. As a result there is an increased flow of electron density toward the metal atom in the M-P $\sigma$-bond while the metal compensates for the increased electron density by change transfer to $\pi^*$-orbitals of CO ligands, leading to a decrease in the carbonyl stretching frequency in complexes containing for example a M-CO bond *trans* to the M-P bond. The influence of ligands, like phosphines, with symmetric correct orbitals available for $\pi$-bonding, on such complexes is shown in Figure 2.3.[15] In carbonyl complexes where the CO stretching frequency, $\upsilon_{CO}$, depend on the extent of electron density flowing by retro-dative $\pi$-bonding from the metal to the antibonding $\pi^*$ orbital of CO, the bond between C and O weakens (and $\upsilon_{CO}$ decreases) as this electron flow increases. When electron density is withdrawn from the $\pi^*$(CO) by a $\pi$-acceptor in the *trans* position, $\upsilon_{CO}$ increases. The d$\pi$ orbitals of the metal act as a type of conductor for such electron flow.

Horrocks and Taylor[16] were amongst the first to use $\upsilon_{CO}$ as a measure of $\pi$-acceptance and established an order of ligands in terms of $\pi$-acceptance as follows: $CO>PF_3>PCl_3>P(OPh)_3>P(OMe)_3>PPh_3>PMe_3>PEt_3>P(piper)_3$.

[15] Henrici-Olivé, G. and Olivé, S., *Angew. Chem. Internat. Edit*., **10**, 105 (1971).

[16] Horrocks, W.D. and Taylor, R.C., *Inorg. Chem*., **2**, 723 (1963).

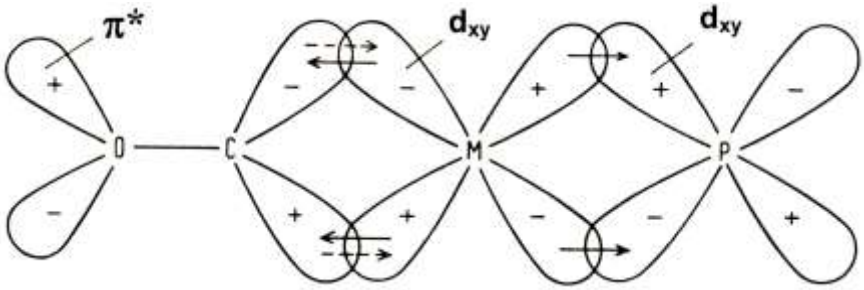


**Figure 2.3** Retrodative π-bonding between a metal and CO on the one hand and between the metal and phosphorous on the other. The π-bond towards CO is weakened by the presence of a π-accepting phosphine ligand (σ-bonds not shown).

Cotton[17] considered the differences in $\upsilon_{CO}$ as less reliable in comparison to changes in force constants. A simplified method known as the Cotton-Kraihanzel force field technique (CK) was used in their calculations. The result was a change in the order of π-acceptance, with the most important change that $PF_3$ was indicated as a better π-acceptor than CO, in fact 1,32 times better[18]. Later research[19,20] has shown that the metal-ligand π-bonds in $[Ni(PF_3)_4]$ were indeed stronger than those in $[Ni(CO)_4]$.

Other researchers demonstrated that π-bonding is not necessary to explain the properties of metal-phosphorous bonds in most of the complexes. Observations by Angelici[21] on *cis*-$[Mn(CO)_3L_2Br]$, where L also included amine ligands which are unable to undergo π-bonding, confirmed that certain tendencies in CO frequencies can be explained without making use of the π-bonding model. According to him the $pK_a$ of amines (pure σ-donors towards $H^+$) varies linearly with $\upsilon_{CO}$. This relationship is followed for $P(Bu^n)_3$ and $PEt_2Ph$, which leads to the conclusion that no π-bonding occurs in these complexes.

[17] Cotton, F.A. and Kraihanzel, C.S., *J. Am. Chem. Soc*., **84**, 4432 (1962).

[18] Cotton, F.A., *Inorg. Chem*., **3**, 702 (1964).

[19] Green, J.C., King, D.I. and Eland, J.H.D., *J. Chem. Soc., Chem. Commun.,* 1121 (1970).

[20] Yarbrough, L.W. and Hall, M.B., *Inorg. Chem*., **17**, 2269 (1978).

[21] Angelici, R.J., *J. Inorg. Nucl. Chem*., **28**, 2627 (1966).

Bigorne[22] plotted $B_1\upsilon_{CO}$ modes of $[Ni(CO_2(PX_3)_2]$ complexes (X = Me, Et, Ph, C≡CPh, $CF_3$ and F) against the Taft inductive constants ($\sigma^*$) of the phosphorous bound groups and obtained a linear relationship. He concluded that the $\pi$-electrons are not involved in the metal-phosphorous bond of any of these complexes. Tolman's research on $[Ni(CO)_3PX_3]$ complexes[12] covered a larger variety of phosporous ligands and a graph of these $A_1\ \upsilon_{CO}$ values against $\sigma^*$ is represented in Figure 2.4.

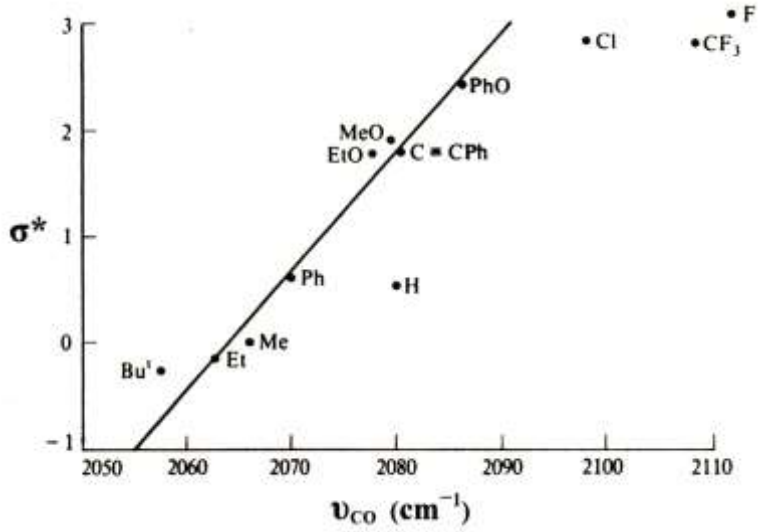


**Figure 2.4** A graph of carbonyl frequencies of $[Ni(CO)_3PX_3]$ against Taft inductive constants, $\sigma^*$. (X = H, Me, Et, $Bu^t$, Ph, OMe, OEt, Cl, $CF_3$, Oph, C≡CPh, F)

Aryl, alkyl, alkoxy and aryloxy phosphorous ligands show a linear relationship while $PF_3$, $PH_3$ and $P(CF_3)_3$ have a total contradictory behaviour. Tolman had however doubts whether the Taft $\sigma^*$ constants were relevant since they are related to inductive effects operating through carbon atoms and therefore not necessarily a measure of the inductive effects of phosphorous bound atoms and groups. Although Bigorne slightly overemphasised the $\pi$-argument, it served the purpose to demonstrate that not all P(III) ligands need a $\pi$-bond. Even though it can be argued that the 3d orbitals in phosphorous compounds are too dispersed to be involved in directed bonds[23], the $\pi$-acceptor ability of some phosphine ligands remain a reality. By means of photo-electron spectroscopy showing directly the removal of an electron from the $\pi$-system, proof was found that $\pi$-bonds exist indeed in $[Ni(PF_3)_4]$.[19] Further proof for $\pi$-bonding

[22] Bigorgne, M., *J. Inorg. Nucl. Chem.*, **26**, 107 (1964).

[23] Ball, E.E., Ratner, M.A. and Sabin, J.R., *Chem. Scr.*, **12**, 128 (1977).

with a ligand like $P(OPh)_3$ is found in an argument concerning bond distances. The more basic a ligand, the stronger the metal-phosphorous bond will be if the bond would be purely $\sigma$ in nature. On this basis, $PPh_3$ will be stronger bound compared to the less basic $P(OPh)_3$, and consequently a shorter M-$PPh_3$ bond distance than in the case of M-$P(OPh)_3$ can be expected[10]. The opposite is the case for Cr-$PPh_3$ and Cr-$P(OPh)_3$ bonds in identical environments,[24] which is proof of the larger electron density between Cr and P atoms in the case of the before mentioned complex. This situation can only occur if the metal allows the flow of electron density into a $\pi$-system.

In order to find a solution to the problem of assigning electronic effects to $\sigma$ and $\pi$ components, Graham[25] made use of force constants (k). He compared values of $[Mo(CO)_5(PX_3)]$ with these of $[Mo(CO)_5(NH_2C_6H_{11})]$, assuming that the cyclohexylamine in the latter complex does not have the ability for $\pi$-acceptance. His method makes use of $\Delta k(trans)$ and $\Delta k(cis)$, that is to say the change in the force constants for the CO bond *trans* and *cis* with regard to $PX_3$, compared to their values in the amine complex. The arbitrary equations

$$\Delta k(trans) = \Delta\sigma + 2\Delta\pi$$

and

$$\Delta k(cis) = \Delta\sigma + \Delta\pi$$

bring this change in relation to the change in the two types of bonds, $\Delta\sigma$ and $\Delta\pi$. Not much can be concluded from $\Delta\sigma$ values, but Graham believed that the $\Delta\pi$-values had accomplished a meaningful order of $\pi$-acceptor behaviour. This is a debatable point, because although he demonstrated that $PF_3$ is a better $\pi$-acceptor than CO, his comparative values of $PBu^t_3$ and $P(OPh)_3$ are in conflict with other evidence.[26] Graham based his calculations partly on the results of Darensbourg and Brown.[27]

[24] Plastas, H.J., Stewart, J.M. and Grim, S.O., *J. Am. Chem. Soc*., **91**, 4326 (1969).

[25] Graham, W.A., *Inorg. Chem*., **7**, 315 (1968).

[26] Pidcock, A., Transition metal complexes of P, As Sb and Bi ligands, McAuliffe, C.A. (Ed), Part I, Macmillan, London (1973).

[27] Darensbourg, D.J. and Brown, T.L., *Inorg. Chem*., **7**, 959 (1968).

Pidcock[26] summarised the situation by concluding that the bonding nature are clear with the following extremes: (1) metals with an oxidation number of II or higher form pure $\sigma$ bonds with organophosphines and (2) metals with an oxidation number of 0 or lower, form $\sigma$ and $\pi$-bonds with $PF_3$, $PCl_3$ and $P(OPh)_3$ ligands. The probability of the occurrence of a $\pi$-bond does not only depend on the phosphorous centre, but also on the metal. The interplay of these variables is shown diagramatically in Figure 2.5.

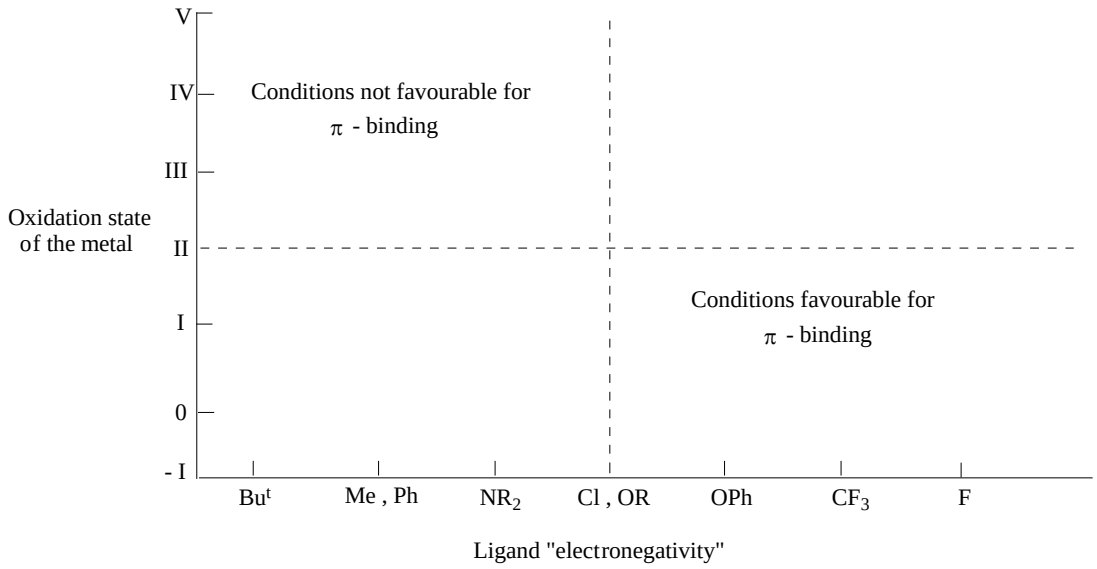


**Figure 2.5** Dependency of $\pi$-bonding on oxidation state of the metal and "electronegativity" of the phosphorous ligands.

Without electronegative phosphorous bound groups, the 3d orbitals will be very much dispersed, resulting in alkyl phosphines like $PBu^n_3$ not having the ability to undergo $\pi$-bonding.[10] In a similar way, $P(CH_3)_3$ does not show a $\pi$-acceptor tendency.[13,20,23] The dependency of the oxidation state of the metal has been demonstrated in a study of a series of complexes, $[CoBr_n(PMePh_2)_{4-n}]$, n = 0–2, where the oxidation state varied from Co(0) to Co(II).[28] Although the oxidation state of the metal is a more important factor, the choice of metal also has an influence even though it is more complicated to evaluate on a comparative basis. It has been demonstrated that for carbonyl complexes the $\pi$-donor ability is of the order W>Mo>Cr≥Ni.[29]

[28] La Mar, G.N., Sherman, E.O. and Fuchs, G.A., *J. Coord. Chem*., **1**, 289 (1971).

[29] Stelzer, O. and Schmutzler, *J. Chem. Soc.,* **A**, 2867 (1971).

The extent to which empty d-orbitals of phosphorous are defined is debatable though. Marynick[30] used molecular orbital calculations to demonstrate that π-accepting can be explained without taking d-orbitals into account. His research was based on a study of the *cis-trans* isomerisation energies of complexes like $[Cr(NH_3)_4(CO)_2]$ and $[Cr(PH_3)_4(CO)_2]$. It can be predicted on the basis of π-bonding arguments that the *cis*-isomer is more stable than the *trans*-isomer, because on the *cis*-configuration enables π-back donation to CO from all three filled $t_{2g}$-orbitals. In the argument it is assumed that $NH_3$ cannot act as π-acceptor. Calculations on *cis*- and *trans*- $[Cr(PH_3)_4(CO)_2]$, without taking into account the d-orbitals of phosphorous, indicate that the energy difference between the *cis*- and *trans*-isomers is very small. This is the result of stabilisation of all three $t_{2g}$-orbitals through π-back donation at both conformations. The phosphine ligands act therefore as π-acceptors, despite the fact that the d-orbitals were not taken into account.

Further evidence for the argument that other orbitals than d-orbitals were involved in back donation, was found through calculations on the complex $[Cr(NH_3)_5(PH_3)]$, once again without d-orbitals. It became clear from the calculations that the π-acceptor orbitals of phosphines have σ* symmetry with regard to the P-H bond axis. Involvement of σ*-orbitals in other organophosphorous systems was also discussed by Gray.[31]

In order to compare the relative importance of σ* and 3d-orbitals as π-acceptors, calculations were made on the complex $[NiNH_3)_3(PH_3)]$ with and without d-orbitals and phosphorous. There seemed to be a delocalisation of metal d-electrons to the phosphine hydrogens and phosphorous, but not to the ammine hydrogens or nitrogen. Calculations in the case where phosphorous d-orbitals were taken into account were showing only a small difference, leading to the conclusion that d-orbitals of phosphorous are relatively unimportant as far as back donation is concerned.

[30] Marynick, D.S., *J. Am. Chem. Soc*., **106**, 4064 (1984).

[31] Gray, G.A. and Albright, T.A., *J. Am. Chem. Soc*., **99**, 3243 (1977).

The theory that σ*-orbitals are responsible for π-acceptance can also explain the phenomenon that $PF_3$ is a better π-acceptor than $PH_3$. The general explanation is that the electronegative substituents decrease the energy of the d-orbitals of phosphorous, making them in this way more available as acceptors.[32] According to the theory of σ*-orbital involvement the reasons are the following: (a) highly polar bonds, for example P-F, have characteristically low-energy σ* orbitals and are therefore good π-acceptors. Likewise, the σ*-(P-H) orbital in $PH_3$ has a lower energy than the one in $NH_3$. (b) Considering that the σ-(P-F) bond is highly polar in the direction of F, as a matter of cause the σ*-orbital has to be highly polar in the direction of P, by which the σ*-metal-dπ-overlap is favoured.

The σ*-orbitals of phosphorous consist of 3s and 3p orbitals and can overlap more effectively with the 3d-orbitals of metals than for example the 2s and 2p orbitals used in the case of amines. A quantitative calculation of the π-acceptor ability of ligands, like $PF_3$, may in fact require d-orbitals to be included, but for a qualitative insight of π-back donation the d-orbitals of phosphorous are not required.

#### *2.1.3.1 Electronic and steric involvement of phosphorous ligands*

Substituent changes on phosphorous ligands can cause considerable changes in the behaviour of the free phosphine ligands, as well as to the transition metal complexes in question. Ligand steric and electronic effects play a key role in determining organometallic reactivity trends and catalytic properties.[33] Steric effects are equally important to electronic effects and can dominate in some cases. An electronic effect is the result of transmission via chemical bonds, whereas a steric effect develops as a result of non-bonding forces between parts of the molecule. The two phenomena are intimately related and it is difficult to distinguish at all times. Steric effects can have an important electronic result and vice versa. In this way, an increase in the angle between substituents will lower the percentage s-character of the lone pair

[32] Huheey, J.E., *Inorganic chemistry*, Harper & Row Publishers, New York (1983).

[33] Gonsalvi, L., Adams, H., Sunley, G.J., Ditzel, E. and Haynes, A., *J. Am. Chem. Soc*., **124**, 13597 (2002).

electrons of phosphorous.[34] On the contrary, a change in the electronegativity of the substituents on the phosphorous atom can affect bond distances and angles.[35]

#### *2.1.3.2 Electronic effects*

For almost forty years the Hammet equation[36] and Jaffé's extension thereof[37] have been used by researchers in the quest of a quantitative structure-reactivity relationship. According to this, log ($K_a/K^o$) $\alpha$ $\sigma_a$ ($K^o$ = ionisation constant of benzoic acid, $K_a$ = ionisation constant for the corresponding substituted benzoic acid and $\sigma_a$ = substituent constant of each *meta* and *para* substituent a). Unfortunately, a direct transfer of the results of organic systems to coordination compounds is not possible. Kabachnik[38,39] demonstrated however that the Hammet equation was applicable to a great variety of aryl and alkyl substituted phosphoric acids when the substituent constant, $\sigma^{ph}$, specifically for substituents bound to phosphorous was used. The substituent constant ($\sigma^{ph}$) is determined by applying the Hammet equation from measurements of the ionisation constants of organophosphoric acids in water and 50% aqueous alcohol. Hypophosphoric acid was used as reference standard with a substituent constant of zero. According to Kabachnik, this substituent constants would be applicable to all cases where the reaction would not require direct attack on the phosphorous atom. Both in metal complexes and organophosphoric acids the phosphorous atom is tetrahedrally bound and the electronic effect of the organic groups is transmitted through the phosphorous atom to the reactive centre of the molecule. Thompson and Sears[40] investigated the oxidative addition of Ir(I) complexes, containing a variety of steric equivalent phosphine ligands, with $CH_3I$ and obtained a linear relationship between the logarithms of the rate constants and the sum of the substituent constants, $\Sigma\sigma^{ph}$.

[34] Tolman, C.A., *Chem.Rev*., **77**, 313 (1977).

[35] Bent, H.A., *Chem.Rev*., **61**, 275 (1961).

[36] Hammet, L.P., *Chem.Rev*., **17**, 125 (1935).

[37] Jaffé, H.H., *Chem.Rev*., **53**, 191 (1953).

[38] Mastfyukova, T.A. and Kabachnik, M.I., *Russ. Chem. Rev. (Engl. Transl.)*, **38**, 795 (1969).

[39] Kabachnik, M.I., *Proc. Acad. Sci. USSR, Chem. Sect.,* **110**, 577 (1956).

[40] Thompson, W.H. and Sears, C.T., *Inorg. Chem*., **16**, 769 (1977).

Strohmeier[41] showed that phosphorous ligands could be fitted into an electronic series on account of the CO stretching frequencies of metal carbonyl phosphine complexes. Such a series is valid for a large variety of mono-substituted transition metal carbonyl complexes. In order to give expression to the electronic parameter, $\upsilon$, Tolman[12] studied a large number of $[Ni(CO)_3(PX_3)]$ complexes and deduced a relationship between the frequency of the $A_1$-carbonyl mode and the groups attached to phosphorous. By assigning to each group to each group a factor $\chi$, and taking $\chi_{Bu}{}^t$ as the zero value, the equation

$$A_1\ \upsilon_{CO}\ [Ni(CO)_3(PXYZ)]\ (cm^{-1}) = 2056.1 + \chi_x + \chi_y + \chi_z$$

can be used to calculate $\upsilon_{CO}$ for phosphines of which the value is unknown. In this way a $\upsilon$-value, for example for $PPh_2(C_6F_5)$ can be calculated which compares well with the observed value[34] of 2074.8 $cm^{-1}$:

$$\upsilon_{CO} = 2056.1 + (2 \times 4.3) + 11.2$$

$$= 2075.9\ cm^{-1}$$

where 4.3 represent the substituent contribution of Ph and 11.2 that of $C_6F_5$.

Tolman does not give an indication of the $\chi$-values related to $\pi$- or $\sigma$-effects, but does indicate a relationship with Kabachnik's[39] $\sigma$-constants. The values of $\chi$ and the proton basicities of phosphines correlate well with each other, as well as with inductive parameters for substituents on phosphorous. They can be derived from the ionisation constants of the acids $R_2POH$ in water. Although the correlation of carbonyl parameters with ligand proton basicity implicates that $\sigma$ donation by phosphorous increases the energy of the metal d$\pi$-electrons and promotes $\pi$-bonding to the carbonyl, Tolman noticed that the effect of substituents on the $\pi$-acid ability of the phosphines would lead to a similar order of metal d$\pi$-energies. There was insuficient information to separate the effects of a phosphorous-metal interaction with regard to $\sigma$- and $\pi$-bonds on the carbonyl frequencies.[12]

[41] Strohmeier, W. and Müller, F.J., *Chem. Ber.*, **100**, 2812 (1967).

Tolman's method to calculate υ is independent of the position of the ligands in relation to CO. The almost identical υ-values for P(*p*-Tol)$_3$ and P(*o*-Tol)$_3$ indicate that υ is indeed a measure of the electronic effect and is not influenced by steric factors.

#### *2.1.3.3 Steric effects*

The steric parameter, θ, came under discussion when the ability of phosphorous ligands to compete for coordination positions on Ni(0) could not be explained in terms of their electronic character.[42] For symmetrical ligands, with all three substituents on phosphorous the same, the steric parameter can be represented by the salient angle of a cylindrical cone, centred 2,28 Å from the centre of the P-atom and which forms a tangent with the Van der Waals radii of the outermost atoms in the model (Figure 2.6). For θ values larger than 180°, as indicated in Figure 2.7, trigonometric methods are used to obtain cone angles.[34]

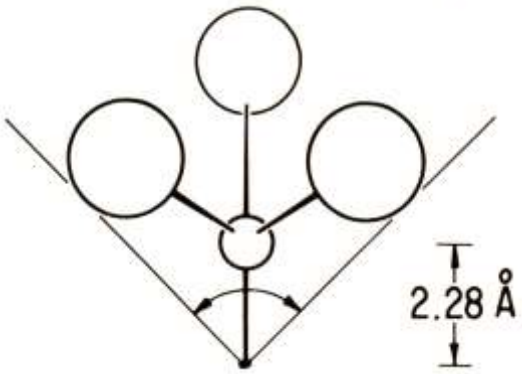


**Figure 2.6** Definition of the ligand cone angle.[34]

[42] Tolman, C.A., *J. Am. Chem. Soc.*, **92**, 2953 (1970).

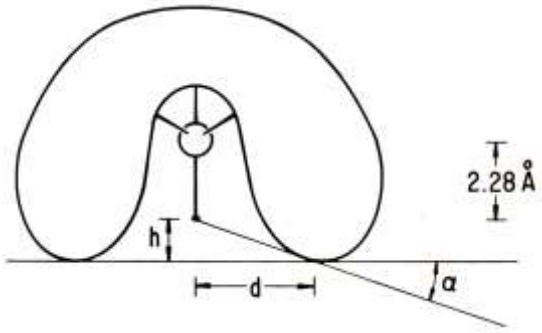


**Figure 2.7** Calculation of ligand cone angles larger than 180°.[34] Tan α = h/d, θ = 180 + 2α

In order to define an effective cone angle for an unsymmetrical ligand[43] $PX_1X_2X_3$, the following equation is used:

$$\theta = (2/3)\sum_{i=1}^{3}\theta_i / 2$$

The cone angles of symmetrical phosphine ligands[34] like $PPh_3$ (145°) and $PMe_3$ (118°) can be used by means of this equation to calculate a θ-value for $PPh_2Me$ for example:

$$\theta_{PPh_2Me} = 2/3(\frac{145}{2} + \frac{145}{2} + \frac{118}{2})$$

$$= 136°$$

Tolman used a model as shown in Figure 2.8 to keep the sum of the half angles as small as possible.

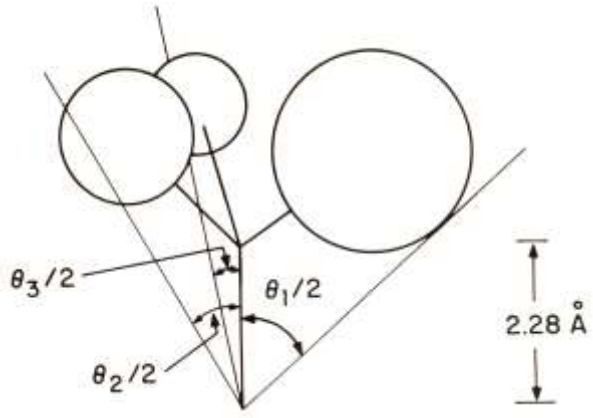


**Figure 2.8** Model for the calculation of ligand cone angles for unsymmetrical ligands.[34]

[43] Tolman, C.A., Seidel, W.C. and Gosser, L.W., *J. Am. Chem. Soc*., **96**, 53 (1974).

Criticism against the ligand cone angle method to determine the bulkiness of a phosphorous ligand is mainly aimed at the difference between measuring conditions and reality. The Ni-P bond distance varies from ligand to ligand and cannot be accepted as being constant. Ligands are not solid cones, making provision for slightly larger ligands to be accommodated if the overlap of "cones" of ligands is allowed. In the structure of for example $[Au(PPh_3)_3]^+$. three $PPh_3$-groups (with $\theta(PPh_3)$ = 145°) can be found in a plane.[44] There are different examples of calculating the steric bulk for specifically tertiary organophosphines,[45,46,47] and the review article by Minas de Pidade and co-workers[48] particularly describes aspects in great detail. For simplicity and since it is widely applied, the Tolman model[34] was chosen for the work described in this study.

An increase in the substituent size on the phosphorous atom in the $PX_3$ molecule leads to the following:[34]

(a) the XPX angles increase, as well as the angles between the $PX_3$ molecule and other ligands in the metal complex;

(b) M-P bond distances increase, as well as an increase from the metal to other ligands;

(c) smaller coordination numbers can be found;

(d) isomers with less steric crowding of ligands are favoured:

(e) increased rates of reaction for dissociative reactions and decreased rates of reaction for associative reactions are observed.

Cotton and Markwell[49] investigated the steric effect of phosphine ligands on the nucleophilic induced CO-insertion in metal-carbon bonds. For the reaction of

[44] Guggenberger, L.J., *J. Organomet. Chem*., **81**, 271 (1974).

[45] Roodt, A., Otto, S. and Steyl, G., *Coord. Chem. Rev*., **245**, 121 (2003).

[46] Ferguson, G., Roberts, P.J., Alyea, M. and Khan, M., *Inorg. Chem*., **17**, 2965 (1978).

[47] Grimmer, N. and Coville, N.J., *South Afr. J. Chem*., **54**, 50 (2001).

[48] Dias, P.B., Minas de Pidade, M.E. and Simoes, J.A.M., *Coord. Chem. Rev*., **135/136**, 737 (1994).

[49] Cotton, J.D. and Markwell, R.D., *Inorg. Chim. Acta*, **63**, 13 (1982).

[$\eta^5$-$C_5H_5$)(CO)(DMSO)Fe($COCH_2Cy$)] with various phosphine ligands in DMSO, a decrease in the rate constants with increased cone angles were found (Figure 2.9). Whereas the decrease for cone angles of 120 to 130° was gradual, it decreased drastically for larger cone angles, to such an extent that phosphines with very large cone angles (for example $PCy_3$, 170°) did not react noticeably. This behaviour is in accordance with the principle of a limited space in the region of the metal centre, with large intermolecular effects occurring when the size of the phosphine ligand and that of the available space become comparable.

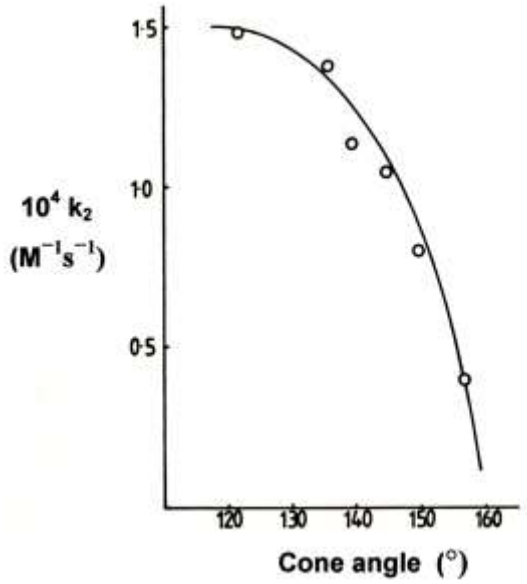


**Figure 2.9** Variation in the rate constant with phosphine cone angle for the reaction of [$\eta^5$-$C_5H_5$)(CO)(DMSO)Fe($COCH_2Cy$)] with tertiary phosphines in DMSO.[49]

A change in bonding as a result of increased ligand size has an influence on vibration spectra. Shaw[50] found an increase in $\upsilon_{Ir\text{-}M}$ with increased ligand size for a series of complexes of the form:

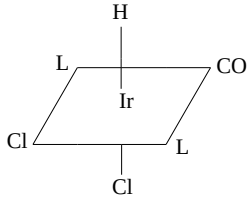


[50] Shaw, B.L., *J. Organomet. Chem*., **94**, 251 (1975).

Schoenberg and Anderson[51] used the relative intensities of symmetrical and asymmetrical carbonyl vibrations in $[PzB(Pz)_3Mn(CO)_2L]$ complexes to calculate the angles ($\alpha$) between the CO-groups. Larger ligands reduce $\alpha$. Steric effects can also modify the number of bands that can be perceived in the infrared spectrum. Cr, Mo and W complexes of the form $[M(CO)_5L]$ show a single E-carbonyl mode at approximately 1945 $cm^{-1}$, when L = P(*p*-Tol)$_3$ or P(*m*-Tol)$_3$. The band is however divided into a doublet, with a separation of about 10 $cm^{-1}$ when L = P(*o*-Tol)$_3$.[52]

#### *2.1.3.4 Separation of steric and electronic effects*

A large range of $\theta$ and $\upsilon$-values for phosphorous ligands is known.[34] Table 2.2 represents merely a summary.

**Table 2.2** Cone angles and electronic parameters for selected phosphine ligands.

| Phosphine ligand | $\theta$ (degrees) | $\upsilon_{CO}$ ($cm^{-1}$) |
|---|---|---|
| $P(Bu^t)_3$ | 182 | 2056.1 |
| $PCy_3$ | 170 | 2056.4 |
| $P(p\text{-}MeOC_6H_4)_3$ | 145 | 2066.1 |
| $P(o\text{-}Tol)_3$ | 194 | 2066.7 |
| $P(p\text{-}Tol)_3$ | 145 | 2066.7 |
| $PPh_2Me$ | 136 | 2067.0 |
| $PPh_3$ | 145 | 2068.9 |
| $P(p\text{-}ClC_6H_4)_3$ | 145 | 2072.8 |
| $PPh_2C_6F_5$ | 158 | 2074.8 |
| $P(OPh)_3$ | 128 | 2085.3 |
| $PF_3$ | 104 | 2110.8 |

Steric and electronic effects usually occur together and a measurable parameter, Z, also depends on both effects. The relationship can be represented in a graphical

[51] Schoenberg, A.R. and Anderson, W.P., *Inorg. Chem*., **13**, 465 (1974).

[52] Bowden, J.A. and Colton, R., *Aust. J. Chem*., **24**, 2471 (1971).

way[34] by plotting the electronic parameter against the steric parameter (steric-electronic map, Figure 2.10) and then by plotting Z as a vertical height on this two-dimensional map. Sufficient experimental determined Z-values will then form a plane in the three-dimensional space Figure 2.11) that can be defined by

$$Z = a\theta + b\upsilon + c \qquad 2.1$$

where a, b and c are constants for a specific plane.

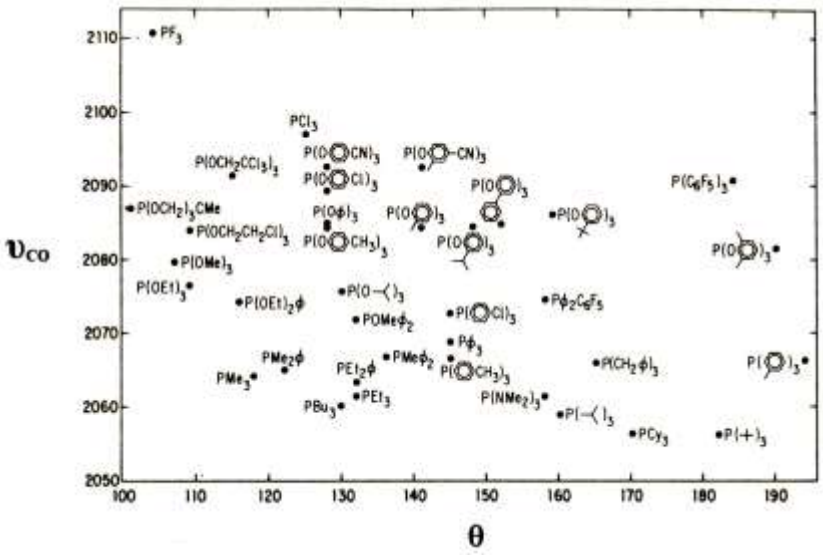


**Figure 2.10** Steric-electronic map of phosphorous ligands investigated by Tolman.[34]

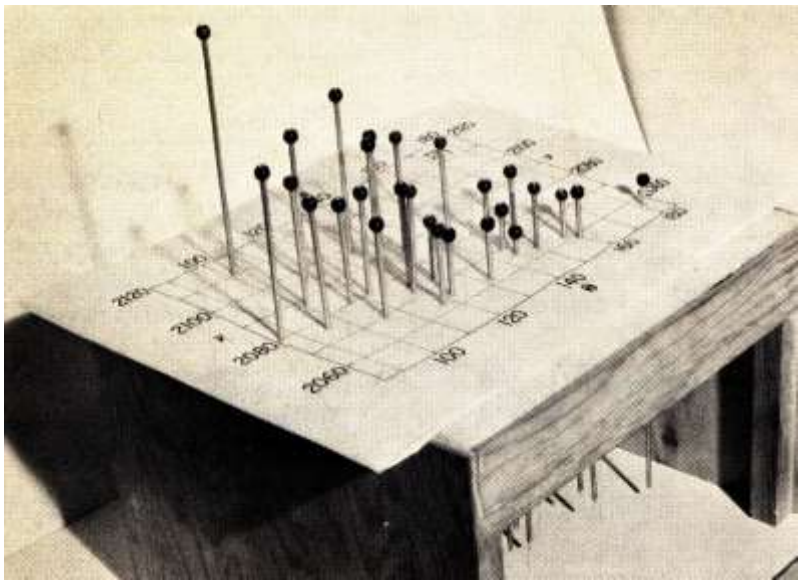

**Figure 2.11** Three dimensional representation of a measurable parameter (in this case the first ionisation potensials of the electron pair of a number of free phosphorous ligands, as determined by UV photo-electron spectroscopy), plotted against the steric and electronic parameters.[34]

Similar to the calculations of Swain and Lupton[53] in organic chemistry, regarding electronic field and resonance effects, the percentage of involvement of the steric and electronic effects can also be calculated separately. In this way it can be defined[34] that the percentage steric character equals 100[a/(a+b)], where a and b refer to the constants in equation 2.1. This information can be very useful in the selection of the best ligand for a specific system. The plane is only defined for a specific temperature, solvent and ratio of reactants.

More recent attempts to correlate electronic or steric effects with chemical and physical properties also found it necessary to dissect the overall effect into its steric and electronic components.[54] Drago[55] has established the ECW model, while papers by Giering, Prock and co-workers[56,57] and by Poë and co-workers[58,59,60] have reported methods to perform a quantitative analysis of ligand effects (QALE) of the stereo-electronic properties of ligands of the type $AR_3$, $Ar_nAr_{3-n}$ and $A(4{-}XC_6H_4)_3$. Application of QALE to rate data provides a means of ascertaining the relative importance of electronic and steric properties of the spectator ligands in governing the lability of the substrates. The way in which the size and the electron-releasing ability of the substituents on a phosphorous atom for example influences the spectroscopic properties of complexes could be obtained.[54] It is possible to analyse a large body of kinetic and physicochemical properties with the general equation[61]

$$\text{Property} = a(\chi) + b(\chi) + b'(\theta - \theta_{st})\lambda + c(E_{ar}) + d$$

[53] Swain, C.G. and Lupton, E.C., *J. Am. Chem. Soc*., **90**, 4328 (1968).

[54] Romeo, R. and Alibrandi, G., *Inorg. Chem*., **36**, 4822 (1997).

[55] Joerg, S., Drago, R.S. and Sales, S., *Organometallics*, **17**, 589 (1998).

[56] Lorsbach, B.A., Bennett, D.M., Prock, A. and Giering, W.P., *Organometallics*, **14**, 869 (1995).

[57] Lorsbach, B.A., Prock, A. and Giering, W.P., *Organometallics*, **14**, 1694 (1995).

[58] Chen, L. and Poë, A.J., *Coord. Chem. Rev*., **143**, 265 (1995).

[59] Farrar, D.H., Poë, A.J. and Zhang, Y., *J. Am. Chem. Soc*., **116**, 6252 (1994).

[60] Hudson, H.E. and Poë, A.J., *Organometallics*, **14**, 3238 (1995).

[61] Bartholomew, J., Fernandez, A.L., Lorsbach, B.A., Wilson, M.R., Prock, A. and Giering, W.P., *Organometallics*, **15**, 295 (1996).

where $\chi$ is an infrared parameter[62] that measures the σ-donicity of the ligand (the electron-donor ability decreases as $\chi$ increases), $\theta$ is Tolman's cone angle,[34] $\theta_{st}$ is the steric threshold, below which no steric effects are evident, λ is a switching function that equals 0 when $\theta < \theta_{st}$ and equals 1 when $\theta > \theta_{st}$ and $E_{ar}$ is the aryl-effect parameter[63], which depends on the number of pendent aryl groups of $Ar_nAr_{3-n}$ and $A(4-XC_6H_4)_3$ but is independent of any substituents on the aryl rings. a, b, b' and c are regression coefficients that measure the relative importance of electronic, steric and aryl factors in the process. The response of the property to $\chi$ is assumed to be linear over the entire range of ligands, while the response to the steric parameter $(\theta - \theta_{st})\lambda$ is not linear. However, the presence of so many variables makes the results from regression analysis questionable, especially in the detection of a meaningful value for the steric threshold.

### 2.1.4 *Cis*- and *trans*-influence of coordinated ligands

The coordination of one ligand to a metal atom influences the bond between the metal and each other ligand. This phenomenon can have a kinetic or thermodynamic nature[64] and it is known as the *trans/cis*-effect and the *trans/cis*-influence respectively.

Both the *cis*-effect[65,66] and the *cis*-influence[67] are similar, but smaller in magnitude than the corresponding *trans*-processes. The *trans*-effect that has to do with the excited state and consequently with the transition state of a reaction, can be defined as the effect of a coordinated ligand on the rate of substitution of ligands *trans* to it.[68] On the contrary, a *trans*-influence is a ground state phenomenon and can be defined

[62] Bartik, T., Himmler, T., Schulte, H.G. and Seevogel, K.J., *J. Organomet. Chem.,* **29**, 272 (1984).

[63] Wilson, M.R., Woska, D.C., Prock, A. and Giering, W.P., *Organometallics*, **12**, 1742 (1993).

[64] Appleton, T.G., Clark, H.C. and Manzer, L.E., *Coord. Chem. Rev*., **10**, 335 (1973).

[65] Basolo, F., Chatt, J., Gray, H.B., Pearson, R.G. and Shaw, B.L., *J. Chem. Soc.,* 2207 (1961).

[66] Zumdahl, S.S. and Drago, R.S., *J. Am. Chem. Soc*., **90**, 6669 (1968).

[67] Mason, R. and Meek, D.W., *Angew. Chem. Int. Ed. Engl.*, **17**, 183 (1978).

[68] Basolo, F. and Pearson, R.G., *Prog. Inorg. Chem*., **4**, 381 (1962).

as the extent to which a ligand weakens the bond *trans* to it in the equilibrium state.[69] This means that certain ligands are causing the substitution of ligands *trans* to themselves by weakening the bond of the *trans*-ligand.

Various theories have been suggested to explain the *trans*-influence. The polarisation theory of Grinberg[70] is the oldest theory, but it is still applicable. He considered the *trans*-influence as a pure electrostatic phenomenon. A strong dipole interaction between a ligand and the central metal atom will have the tendency to weaken the bond between the metal and the ligand *trans* to it. In a symmetrical complex, the bond dipole of the different ligands is identical and cancel each other out. Replacement of one of the ligands by a more polarising ligand will induce an additional uncompensated dipole in the metal, which will oppose the natural dipole of the ligand *trans* to the polarising ligand. A repulsive force causes the M-L bond to weaken Figure 2.12.

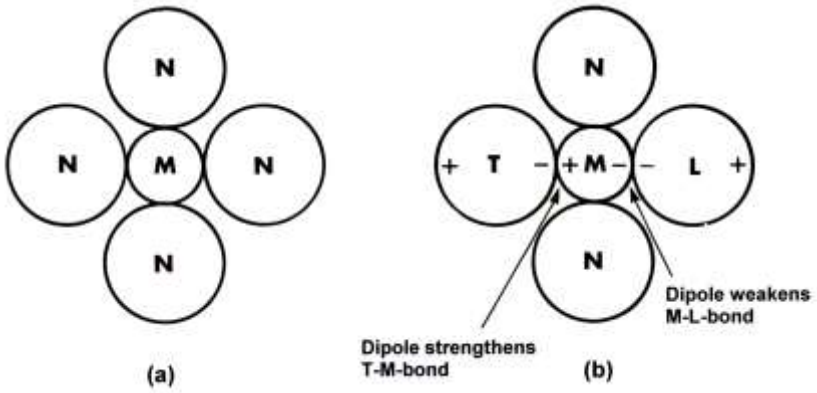


**Figure 2.12** The polarisation theory of Grinberg: (a) No *trans*-influence (b) *Trans*-influence: T = polarising ligand, L = ligand *trans* to polarising ligand

Langford and Gray[71] reformulated Grinberg's polarisation theory in terms of modern molecular orbital theory. According to this, ligands *trans* to each other compete for the p-orbital of the metal next to the T-M-L axis. A ligand competing more effectively can claim this p-orbital to weaken the *trans*-ligand bond. According to Mason and Meek,[67] the *trans*-influence on a particular ligand will be the largest when this ligand

[69] Pidcock, A., Richards, R.E. and Venanzi, L.M., *J. Chem. Soc.,* **A**., 1707 (1966).

[70] Grinberg, A.A., *Acta Physicochim. USSR*, **3**, 573 (1945).

[71] Langford, C.H. and Gray, H.B., *Ligand substitution processes*, Benjamin, New York (1965).

experiences maximum overlap with metal pσ-electrons. Stronger σ-bonding ligands ($H>Ph_3>CH_3>H_2S>Cl>NH_3>H_2O$) lower the electron density in the area of overlap of the particular atomic orbitals between the metal and all the other ligands and weaken these bonds. All the other metal-ligand bonds weaken with an increase of σ-donor strength of a specific ligand, although the *trans*-ligand is influenced most.[15]

The static π-bond theory is based on the competition of *trans*-ligands for the same metal d-orbitals.[10] Utilisation of these d-orbitals in a π-bond on one side of the metal will decrease their availability on the other side (Figure 2.13).

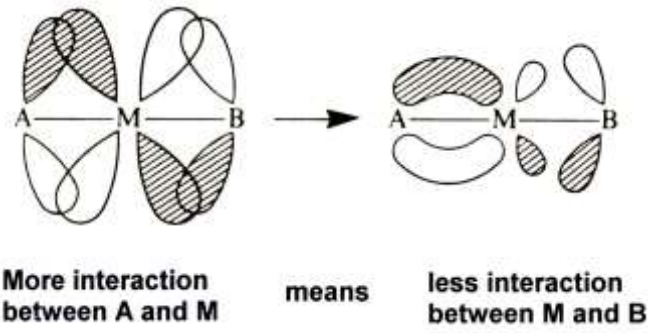


**Figure 2.13** Representation of the static π-bond theory

According to this, a good π-acceptor ligand has a strong *trans*-influence. There are two common d-orbitals for the *trans*-ligands of which one is found in the plane of the complex. It is only this one d-orbital which is common to the *cis* ligands. On this basis it can be expected that two π-acceptor ligands in a complex will adopt a *cis*-orientation in order that each ligand may have one of the two d-orbitals outside the plane to its own disposal. (The d-orbital in the plane is shared between the two ligands.) A *trans* orientation requires competition for both the in and out of the plane d-orbitals. This explains why the *cis*-$[PtCl_2(PR_3)_2]$ isomer is thermodynamically about 40 kJ $mol^{-1}$ more stable than the *trans*-isomer.[72,73]

[72] Chatt, J. and Wilkins, R.G., *J. Chem. Soc.,* 4300 (1952).

[73] Chatt, J. and Wilkins, R.G., *J. Chem. Soc.,* 525 (1956).

Force constant analysis led Graham[25] to the conclusion that the σ-donor ability of a ligand influences the stretching frequency of carbonyls *cis* and *trans* to it in almost the same way, while a π-bond between the ligand and metal has an effect twice as large on the CO *trans* to it compared to the *cis* CO groups. The reason for the difference between σ- and π-influence is that *trans*-ligands act through two metal dπ-symmetry orbitals, while *cis*-ligands only have one metal π-orbital available (Figure 2.14). The ability of the of the σ-system to act as carrier of the *trans*-influence is best demonstrated by nuclear magnetic resonance studies of $^{31}P$ in complexes like $[Pt(PBu^n_3)_3Cl]$ and $[Pt(PEt_3)_2MeCl]$.[74]

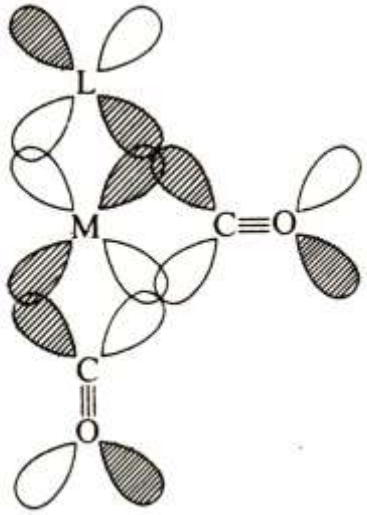


**Figure 2.14** Representation of the difference between the availability of orbitals for *cis*- and *trans*-ligands.

Mason and Randaccio[75] discussed the metal-ligand bonds in terms of centroids of densities of overlap, derived from orbitals, calculated on the basis of the maximum sum of integrals of overlap for metal hybrid orbitals with σ-orbitals of chloride and phosphine ligands. The method of maximum overlap has not yet been applied for other ligands and gives equal importance to overlap with the metal s-, p- and d-orbitals without involving orbital energies in the calculation. According to this, the *trans*-influence of phosphine ligands, compared to chloride, can be described as a rehybridisation of the metal orbitals in reaction to the form of the σ-orbital of

[74] Nixon, J.F. and Pidcock, A., *Ann. Rev. NMR Spectrosc*., **2**, 345 (1969).

[75] Mason, R. and Randaccio, L., *J. Chem. Soc.,* **A**., 1150 (1971).

phosphorous, with the effect that the covalence and specifically the s-character of the *trans*-bonds are reduced while the *cis*-bond remains relatively unchanged.

The *trans*-influence of ligands can be determined by means of techniques like structure determination by means of X-ray crystallography, infrared, NMR, photo-electron and Mössbauer spectroscopy.[76] Accurate information regarding the difference in bond distances of Pt-Cl bonds *trans* to different ligands was for example obtained by means of X-ray crystallography. In the case of the following compounds the *trans* Pt-Cl bond distances decreased from A to C.[77]

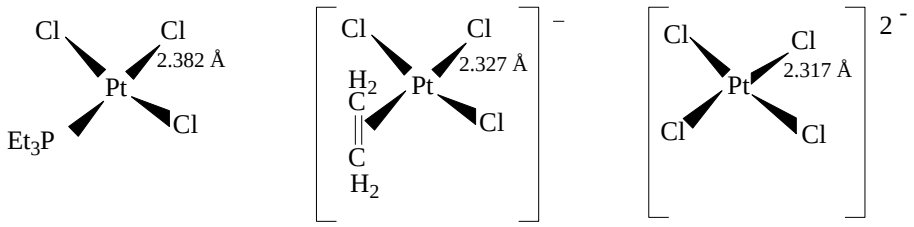


**A** **B** **C**

Based on more experimental data, the order of *trans*-influence for a number of selected ligands can be represented as follows:

$$\sigma\text{-R} \geq \text{Carbenes} \approx PR_3 \geq AsR_3 > CO \approx RNC \approx C{=}C \approx Cl^- \approx NH_3$$

### 2.1.5 *Trans*-influence of bidentate ligands

The fact that only one of the carbonyl groups in complexes of the type $[Rh(LL')(CO)_2]$ (where LL' is a mono anionic bidentate ligand with donor atoms L and L') can be substituted by certain neutral ligands, like triphenylphosphine,[78,79] can be used to determine the relative *trans*-influence of the bonding atoms, L and L' of bidentate

[76] Bancroft, G.M. and Butler, K.D., *J. Am. Chem. Soc*., **96**, 7203 (1974).

[77] Bushnell, G., Pidcock, A. and Smith, M.A.R., *J. Chem. Soc., Dalton Trans*., 572 (1975).

[78] Bonati, F. and Wilkinson, G., *J. Chem. Soc.,* 3156 (1964).

[79] Varshavskii, Y.S., Knyazeva, N.N., Cherkasova, T.G., Ivannikova, N.V. and Ionina, T.I., *Russ. J. Inorg. Chem*., **15**, 367 (1970).

ligands.[80] In this case the carbonyl group *trans* to the atom with the largest *trans*-influence is replaced by $PPh_3$:

$$[Rh(LL')(CO)_2] + PPh_3 \longrightarrow [Rh(LL')(CO)(PPh_3] + CO$$

The crystal structures of $[Rh(TTA)(CO)(PPh_3)]$[81] and $[Rh(BPHA)(CO)(PPh_3)]$[82] showed that the oxygen atom closest to the most electronegative substituent of the bidentate ligand has the smallest *trans*-influence. In both structures the carbonyl group *trans* to this oxygen was not replaced, rather the carbonyl group *trans* to the other oxygen atom with a larger *trans*-influence. Nitrogen has a larger *trans*-influence than the more electronegative oxygen atom. This can be seen in the crystal structures of $[Rh(oxine)(CO)(PPh_3)]$[83] and $[Rh(sal\text{-}NR)(CO)(PPh_3)]$,[84] where the carbonyl group *trans* to the nitrogen atom has been replaced. The structure of $[Rh(Sacac)(CO)(PPh_3)]$[85] indicates that the sulphur atom also has a larger *trans*-influence than the oxygen atom. Supplementary studies on bidentate ligands with S, N donor atoms[86,87,88] established the increasing order of the *trans*-influence of the donor atoms as O < N < S in complexes of the type $[Rh(LL')(CO)(PPh_3]$.

The weakening of the bond *trans* to the atom with the largest *trans*-influence is demonstrated in a number of crystal structure determinations and it supports the determination of the relative *trans*-influence of the coordinating atoms of bidentate ligands. The distances from Rh to the coordinating positions of COD (*cis*,*cis*-1,5-cyclooctadiene) were studied for example in the crystal structures of

[80] Graham, D.E., Lamprecht, G.J., Potgieter, I.M., Roodt, A. and Leipoldt, J.G., *Trans. Met. Chem*., **16**, 193 (1991).

[81] Leipoldt, J.G., Bok, L.D.C., Van Vollenhoven, J.S. and Pieterse, A.I., *J. Inorg. Nucl. Chem*., **40**, 61 (1978).

[82] Leipoldt, J.G. and Grobler, E.C., *Inorg. Chim. Acta*, **60**, 141 (1982).

[83] Leipoldt, J.G., Basson, S.S. and Dennis, C.R., *Inorg. Chim. Acta*, **50**, 121 (1981).

[84] Leipoldt, J.G., Basson, S.S., Grobler, E.C. and Roodt, A., *Inorg. Chim. Acta*, **99**, 13 (1985).

[85] Botha, L.J., Basson, S.S. and Leipoldt, J.G., *Inorg. Chim. Acta*, **126**, 25 (1987).

[86] Steyn, G.J.J., Ph.D. Thesis, Free State University, Bloemfontein, South Africa (1994).

[87] Steyn, G.J.J., Roodt, A., Poletaeva, I. and Varshavsky, Y.S., *J. Organomet. Chem.,* **536**, 197 (1997).

[88] Steyn, G.J.J., Roodt, A. and Leipoldt, J.G., *Inorg. Chem*., **31**, 3477 (1992).

[Rh(oxine)(COD)][89] and [Rh(TFBA)(COD)].[90] A definite lengthening in the average Rh-P bond lengths of different [Rh(LL')(CO)($PPh_3$] complexes was also observed.[85,86,87,88] The results confirmed earlier observations that the most electronegative atom (or in the case of β-diketone and other similar ligands, the oxygen atom closest to the strongest electron withdrawing group of the chelate ring) exerts the smallest *trans*-influence. It is in accordance with the polarisation theory[70] since the most electronegative group will be the least polarisable and a weaker σ-donor. The sulphur atom is the only atom capable of forming a strong π-bond with the rhodium atom (it is expected that a π-*trans* influence is greater than a σ-*trans* influence), while the nitrogen atom being less electronegative than an oxygen atom is the better σ-donor of the two thus having a larger σ-*trans* influence than the oxygen atom.[85]

Exceptions to this substitution pattern were found with the crystal structure determinations of [Rh(TFDMA)(CO)($PPh_3$)],[91] [Rh(TFHD)(CO)($PPh_3$)][92] and [Rh(TFTMA)(CO)($PPh_3$)].[93] The carbonyl group *trans* to the oxygen atom closest to the more electronegative $CF_3$-group was substituted by $PPh_3$. This products was formed as a result of predominantly steric control, and explained by considering the structure of the transition state during the course of the substitution reaction.[92] The CO-group displaced in this case is the result of the most stable trigonal bipyramidal transition state with the least steric repulsion.

The size of the chelate ring also has an influence on the trans influence of the donor atoms. This topic is discussed more elaborately in Chapter 4. Essentially, the smaller bite angle of a five-membered chelate ring (average about 79°) decreases the *trans*-influence of the donor atom in the ring, relative to the same donor atom in a six-membered chelate ring (average about 89°). The explanation lies in the effective

[89] Leipoldt, J.G. and Grobler, E.C., *Inorg. Chim. Acta*, **72**, 17 (1983).

[90] Leipoldt, J.G., Basson, S.S., Lamprecht, G.J., Bok, L.D.C. and Schlebusch, J.J.J., *Inorg. Chim. Acta*, **40**, 43 (1980).

[91] Leipoldt, J.G., Basson, S.S. and Nel, J.T., *Inorg. Chim. Acta*, **74**, 85 (1983).

[92] Steynberg, E.C., Lamprecht, G.J. and Leipoldt, J.G., *Inorg. Chim. Acta*, **133**, 33 (1987).

overlap of the relevant σ-orbitals of the bidentate ligand with the $dsp^2$-hybrid orbitals of the metal. A bite angle of 90° will allow for the most effective overlap, whereas any deviation from 90° will inhibit the electron donating power of the donor atom to the metal, decreasing its effective *trans*-influence. Although the ligand bite angle has been shown to be important,[94,95] the precise way in which the effect of the bite angle is transmitted to the active site of the metal complex is still a matter of some debate, with electronic and steric effects both contributing.[33,96]

## 2.2 Important reactions

### 2.2.1 Oxidative addition reactions

#### *2.2.1.1 Introduction*

Often, low-spin $d^8$- and $d^{10}$- complexes react with a covalent molecule in order to increase the size of their coordination sphere by means of so-called oxidative addition reactions. The prototype of this vast field of reactions was observed for the first time in 1962 by Vaska and DiLuzio,[97] when hydrogen was added to a square-planar iridium complex.

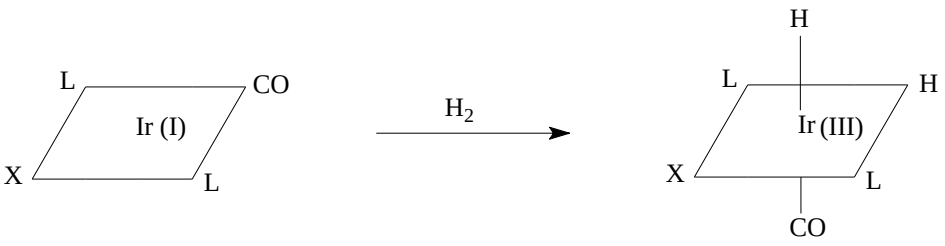


X = Cl, Br, I; L = $P(C_6H_5)_3$

During oxidative addition, the metal complex serves as both a Lewis acid and a base, the formal oxidation state of the central metal atom increases with two units, and two

[93] Leipoldt, J.G., Basson, S.S. and Potgieter, J.H., *Inorg. Chim. Acta*, **117**, L3 (1986).

[94] Casey, C.P. and Whiteker, G.T., *Isr. J. Chem*., **30**, 299 (1990).

[95] Dierkes, P.and Van Leewen, P.W.N.M., *J. Chem. Soc., Dalton Trans*., 1519 (1999).

[96] Casey, C.P., Paulsen, E.L., Beuttenmueller, E.W., Proft, B.R., Petrovich, L.M., Matter, B.A. and Powell, D.R., *J. Am. Chem. Soc*., **119**, 11817 (1997).

[97] Vaska, L. and DiLuzio, J.W., *J. Am. Chem. Soc*., **84**, 679 (1962).

new groups join the coordination sphere. Thus, a molecule is reduced when it joins the coordination sphere of a metal atom, and the metal atom itself is oxidised.

An oxidative addition reaction could be represented by the following equilibrium:[98]

$$L_nM^m + XY \rightleftharpoons L_nM^{m+2}(X)(Y)$$

where L is representative of the ligands; n, the number of ligands; M, the metal atom, and m, the oxidation state. The course of the reaction to the right is known as oxidative addition, and that to the left, reductive elimination. The position of equilibrium, *inter alia*, is determined by the type of metal and bound ligands, the type of added molecule XY, the bonds M-X and M-Y that are formed as well as the medium in which the reaction is executed.

#### *2.2.1.2 Requirements for oxidative addition*[98,99]

Before oxidative addition is possible, many prerequisites have to be fulfilled first. These can be summarised as follows: (a) There has to be a non-bonding electron density on the metal atom. (b) The availability of two vacant coordinating positions on the complex, as to make the formation of two new bonds possible with the joining ligands, X and Y. (c) The oxidation state of the metal atom has to be two units lower than the most stable oxidation state. In the process, the metal strives to attain 18-electron configuration. Examples of the way in which all of the above prerequisites can be met, are evident in the following reactions.

In order to establish a vacant coordination position, it becomes necessary at times for the complex to dissociate before the oxidative addition can occur. The complexes $[M(PPh_3)_4]$, with M = Ni(0), Pd(0), Pt(0), have $d^{10}$-electron configurations and are coordinatively saturated. Dissociation of phosphine ligands in solution yield three- and two-coordinated complexes that are coordinatively unsaturated, thus reactive with regard to oxidative addition.[99]

---

[98] Cotton, F.A. and Wilkinson, G., *Basic inorganic chemistry*, John Wiley & Sons, Inc., New York (1976).

[99] Stille, J.K. and Lau, K.S.Y., *Acc. Chem. Res*., **10**, 434 (1977).

Oxidative addition of coordinatively unsaturated square-planar, 16-electron $d^8$-complexes of, for example, Rh(I) and Ir(I), produces six-coordinate, 18-electron, $d^6$-complexes[100] of Rh(III) and Ir(III) (reaction 3.1).

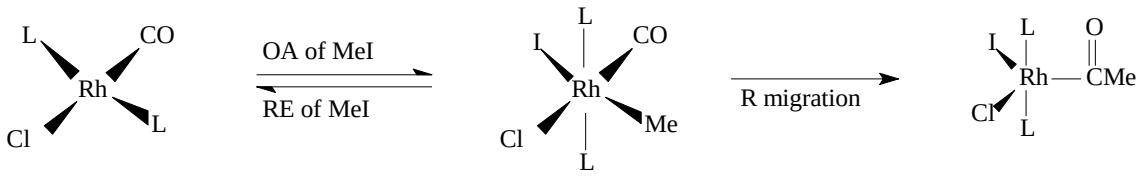


**3.1**

In most cases, loss of ligands of square-planar molecules does not take place before the occurrence of oxidative addition. This has been substantiated by Milstein and Stille[101] as well as Stieger and Kelm.[102] However, there are a few known cases where dissociation of L occurs, for example, during the oxidative addition of $H_2$ with $[RhClL_3]$[103] or $[IrX(CO)L_2]$.[104] The increased lability of rhodium compounds, or higher reaction temperatures in the case of iridium species, has been stated as reasons. Most probably, this ligand dissociation is catalysed through the solvent. Self-evidently, the solvated species, formed in this manner, undergo oxidative addition according to the same mechanism as usual, but only at different tempos.[103,105]

In the case of 18-electron penta-coordinated molecules, oxidative addition leads to a six-coordinated cationic complex. As such, this complex can exist, or can lead through nucleophilic substitution of a neutral ligand to species of greater stability.[106] (reaction 3.2)

[100] Douek, I.C. and Wilkinson, G., *J. Chem. Soc.,* **A***,* 2604 (1969).

[101] Milstein, D. and Stille, J.K., *J. Am. Chem. Soc*., **101**, 4992 (1979).

[102] Stieger, H. and Kelm, K., *J. Phys. Chem*., 290 (1973).

[103] Ohtani, Y., Fujimoto, M. and Yamagishi, A., *Bull. Chem. Soc. Japan*, **50**, 1453 (1977).

[104] Cross, R.J., *Chem. Soc. Rev*., **14**, 197 (1985).

[105] Mureinik, R.J., Weitzberg, M. and Blum, J., *Inorg. Chem*., **18**, 915 (1979).

[106] Collman, J.P. and Roper, W.R., *J. Am. Chem. Soc*., **88**, 3504 (1966).

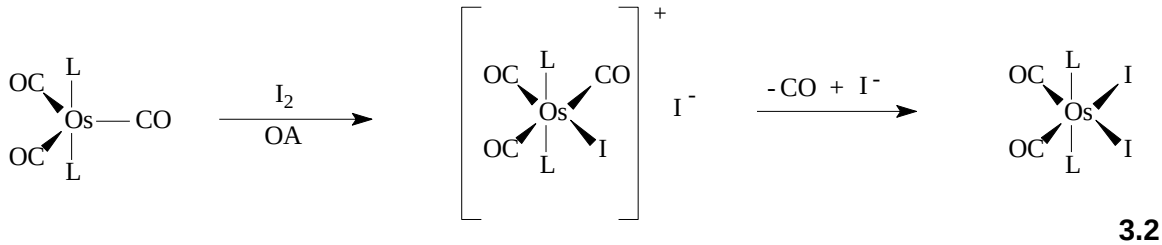


**3.2**

Before oxidative addition can occur, other suggested mechanisms require dissociation to reactive four-coordinate, 16-electron complexes.[107,108,109] Chen and Halpern[110] found that oxidative addition of $H_2$ to the five-coordinate 18-electron $d^8$-Ir(I)-complex, $[Ir(CO)(PMe_2Ph)_3Cl]$, progresses more rapidly than the corresponding reaction in which the four-coordinate complex $[Ir(CO)(PMe_2Ph)_2Cl]$ is used. This is in contrast to other five-coordinated $d^8$-complexes that are non-reactive to substrates like $H_2$. Thus, the expected behaviour of five-coordinate $d^8$-complexes is that of heightened reactivity. The reason for this is that they are inherently stronger Lewis bases than four-coordinate complexes should be.

#### *2.2.1.3 Stereochemistry of oxidative addition*

The stereochemistry of oxidative addition reactions was thoroughly studied in an effort to elucidate an understanding of the reaction mechanism and the structure of the transition state. To complicate the problem, the stereochemistry of the isolated product does not necessarily point to the addition method, the reason being that possible ligand exchange or rapid isomeric reactions may alter the conformation of the complex initially formed. Usually, the final product consists of the isomer or isomeric blend that is thermodynamically the most stable given the particular reaction conditions.[111]

[107] Harrod, J.F. and Smith, C.A., *Can. J. Chem*., **48**, 870 (1970).

[108] Church, M.J., Mays, M.J., Simpson, R.N.F. and Stefanini, F.P., *J. Chem. Soc.,* **A***,* 2909 (1970).

[109] Burnett, M.G. and Morrison, R.J., *J. Chem. Soc.,* **A***,* 2325 (1971).

[110] Chen, J. and Halpern, J., *J. Am. Chem. Soc*., **93**, 4939 (1971).

[111] Dickson, R.S., *Organometallic chemistry of rhodium and iridium*, Academic Press, London (1983).

In the case of the molecule XY, if addition take place without breaking the XY bond, the X- and Y- groups necessarily adopt a *cis*-configuration in the product. On the other hand, breaking the bond of the X-Y molecule opens the possibility that the stereochemistry of the product can have a *cis*- or *trans*-configuration. In general, non-polar compounds, like $H_2$, will lead to *cis*-addition, while polar compounds, such as alkyl halides, will add *trans* in most cases.[4]

The use of NMR- and infrared techniques has led to the disentanglement of the stereochemistry of the addition of methyl iodide to [Ir(Cl(CO)$L_2$]. Self-evident from the schematic representation (reaction 3.3), the formation of nine isomeric products is possible. There are six isomers in which the L-ligands are *cis* (only two isomers, 1 and 2, are indicated), and three isomers (3, 4 and 5) in which the L-ligands remain *trans*. However, addition of $CH_3Br$ or $CH_3I$ to [Ir(Cl(CO)$L_2$] (L = $PPh_2CH_3$ or $PPhMe_2$) in a benzene solution, only produces one isomer in each case.[112,113] This isomer is represented in structure 4. Thus, in these particular cases, stereospecific *trans*-addition has taken place.

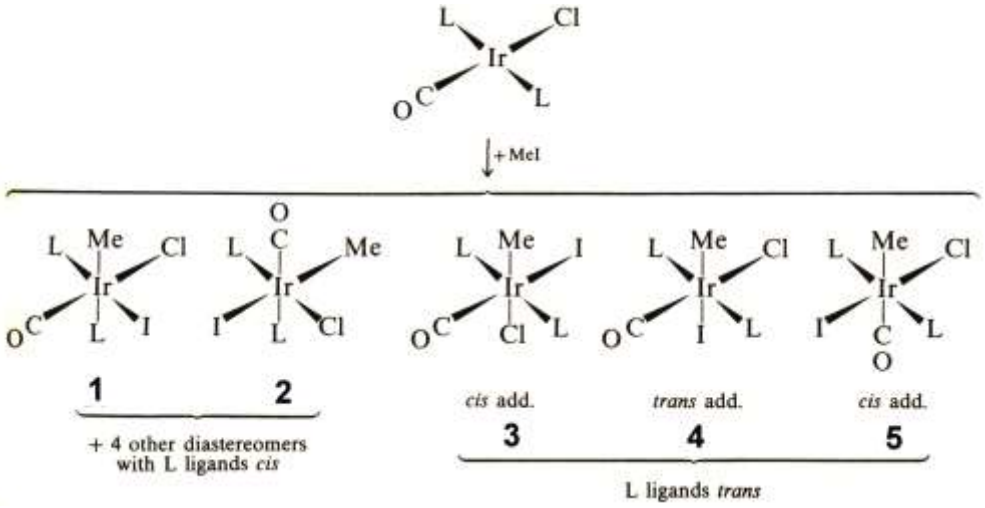


**3.3**

Since stereochemistry is dependent upon factors such as the solvent, temperature, and pressure, it may also vary in a specific reaction.[98] An evident example of the solvent's influence on the stereochemistry of an oxidative addition reaction, is the addition of $CH_3Br$ or $CH_3I$ to [IrCl(CO)$(PPhMe_2)_2$].

[112] Deeming, A.J. and Shaw, B.L., *J. Chem. Soc.,* **A**, 1128 (1969).

[113] Collman, J.P. and Sears, C.T., *Inorg. Chem.*, **7**, 27 (1968).

In contrast to the product formed in a benzene solution (reaction 3.3, structure 4), both *cis*- and *trans*- isomers (structures 3 and 4) are obtained in a methanol solution.[112] Addition of $CH_3Cl$ to *trans*-[IrBr(CO)($PPh_2Me$)$_2$] in a benzene medium produces the *trans*-product (reaction 3.4, structure 6). Refluxing the *trans*-product in a methanol-benzene mixture causes isomerisation to the *cis*-product[113] (structure 7).

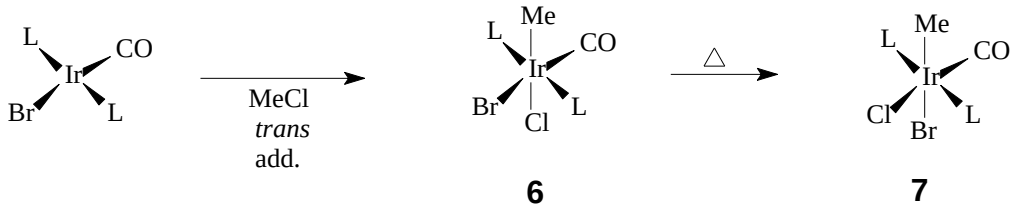


**6** **7** **3.4**

Thus, these results indicate that the stereochemistry of oxidative addition reactions is controlled, to a greater extent, by kinetic, rather than thermodynamic factors.

Another aspect of the stereochemistry of oxidative addition reactions is the regiochemistry of the metal-bound carbon atom during alkyl halide additions. Through establishment of the configuration at the carbon atom, before and after addition, insight into the nature of the transition state is gained.[4] Such a study has been conducted on reactions 3.5 and 3.6.[114]

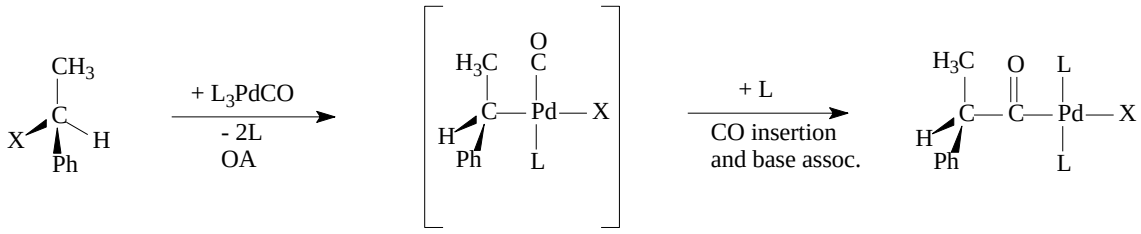


**3.5**

S -(-) R -(+) R - (+)

**8**

S-(−)-α-phenetyl bromide adds oxidatively to carbonyltris(triphenylphoshine)= palladium, in order to form, after an alkyl migration (with retention of configuration), compound 8, with inversion of configuration (reaction 3.5). Compound 8 can also be obtained through the reaction of the acyl halide of known configuration (compound 9), with [$Pd(PPh_3)_4$] (reaction 3.6). This is evidence of the inversion of configuration

[114] Lau, K.S.Y., Fries, R.W. and Stille, J.K., *J. Am. Chem. Soc*., **96**, 4983 (1974); *Ibid*., **96**, 5956 (1974).

that has occurred with the addition of Ph(Me)(Br)CH, as addition of compound 9 can only occur with retention of configuration.

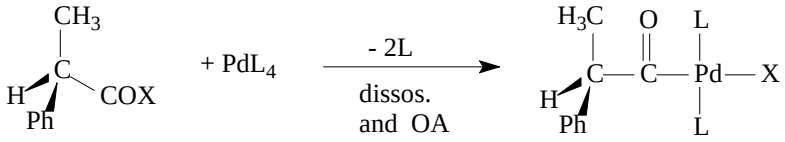


**3.6**

R - (-)

**9**

R - (+)

**8**

Various cases of racemisation have already been observed,[114,115] in addition to the above and other examples of configuration inversion. The mechanistic implications of these factors are discussed in the next paragraph.

#### *2.2.1.4 Mechanisms of oxidative addition*

The mechanisms whereby oxidative reactions proceed have been researched extensively. However, in certain cases, conclusions are debatable. The reason for this is that a delicate balance exists between certain mechanisms. Therefore, each case should be investigated thoroughly so as to ascertain the predominant mechanism. Factors like the formal charge of the complex, the nature of the metal, ligands and the addendum, as well as the experimental conditions (like the solvent, temperature, and the presence of impurities), determine the particular mechanism.

The possibility of migrations and geometrical change of the various five-coordinate intermediates indicates that great care should be taken when mechanistic conclusions are drawn from product geometries.[104]

Criteria used in determining the dominant mechanism, include: (a) stereochemistry, both at the metal and the addendum; (b) interpretation of polar- or radical intermediates; (c) rearrangement of radical intermediates; (d) formulation of the rate law and the nature of the activation parameters and (e) the effect of solvent polarity and radical scavengers on the rate.

[115] Lappert, M.F. and Lednor, P.W., *Adv. Organomet. Chem*., **14**, 345 (1976).

On the above basis, the following division can be used to summarise the representative mechanisms:

(1) Concerted one-step mechanism ;
(2) Two-step $S_N2$-type mechanism;
(3) Free radical mechanism; and
(4) Ionic mechanism.

Crossover between mechanisms causes the increase of the possible number of reaction pathways, that, in turn, impedes classification.

(1) Concerted one-step mechanism[104,111]

Concerted oxidative addition occurs when the reaction takes place under non-polar conditions and is typified by $H_2$-addition to Vaska's complex (structure 10, reaction 3.7).

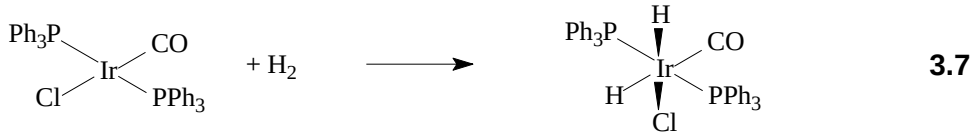


**10** **3.7**

Usually, the addendum is a homonuclear molecule or another molecule with little or no polarity, for example $H_2$, $O_2$, $Cl_2$, $C_2H_4$, etc. However, Stille and Lau[99] speculated about the involvement of a concerted mechanism during the addition of organic halides in particular, since it provides an alternative pathway that does not necessitate an ion-pair intermediate.

While the concerted *trans*-addition remains a symmetry-prohibited process,[116,117] *cis*-addition is permitted. Furthermore, the mechanism also leads to a *cis*-arrangement of added groups if no rearrangement has taken place. Essentially, the reaction course is an elecrophilic attack on the metal. Therefore, concerted oxidative addition

[116] Braterman, P.S. and Cross, R.J., *Chem. Soc. Rev*., **2**, 271 (1973).

[117] Pearson, R.G., *Symmetry rules for chemical reactions*, Wiley Interscience, New York (1976).

is referred to as such.[118,119] Usually, this type of reaction is described in terms of the overlap of filled $d_{xz}$- or $d_{yz}$-metal orbitals with a vacant σ*-antibonding orbital of the added molecule,[117] representing a cyclic transition state as represented in Figure 2.15.

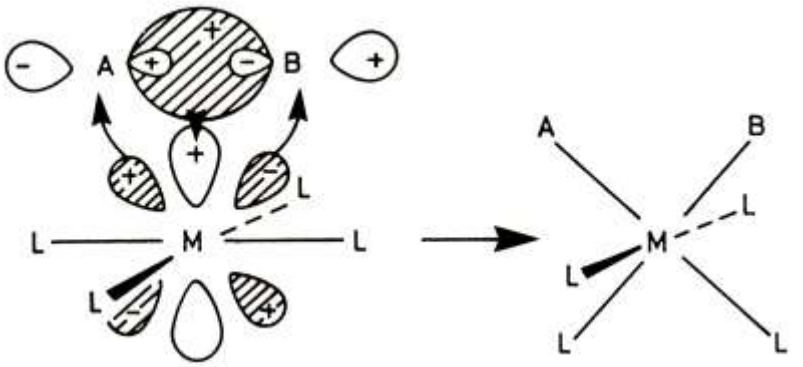


**Figure 2.15** Orbital overlap in the concerted *cis*-addition of a molecule AB.[117]

However, Saillard and Hoffmann[120] point to the fact that overlap of a filled σ-orbital of AB, with a vacant metal acceptor-orbital, also have to be involved. This overlap represents a charge transfer in another direction, that of AB to the metal. As a result of the coordinative unsaturation requirement, the initial flow of electron density from AB to M, may be of greater significance than the reverse. Both interactions impair the A-B bond, while M-A and M-B bonds are strengthened. According to this description, the starting phases of the concerted oxidative addition of for example $H_2$ to a square-planar molecule correspond to nucleophilic attack on the metal. Furthermore, stereospecific *cis*-addition of $H_2$ to [IrX(CO)(dppe)] is explicated with additional interaction of $\sigma(H_2)$ with $\pi^*(CO)$, thus pointing to the fact that the type of ligands of the complex also have a role to play.[121]

Stille and Lau[99] mention the stereochemistry involved with the concerted oxidative addition of organic halides. As seen from the reaction scheme 3.8, a trigonal-bipyramidal transition state is formed, despite the position of the C-X bond with regard to the tetrahedral planes.

---

[118] Collman, J.P. and Roper, W.R., *Adv. Organomet. Chem*., **14**, 345 (1976).

[119] Halpern, J., *Acc. Chem. Res*., **3**, 386 (1970).

[120] Saillard, J.Y. and Hoffmann, R., *J. Am. Chem. Soc*., **106**, 2006 (1984).

[121] Johnson, C.E. and Eisenberg, R., *J. Am. Chem. Soc*., **107**, 3148 (1985).

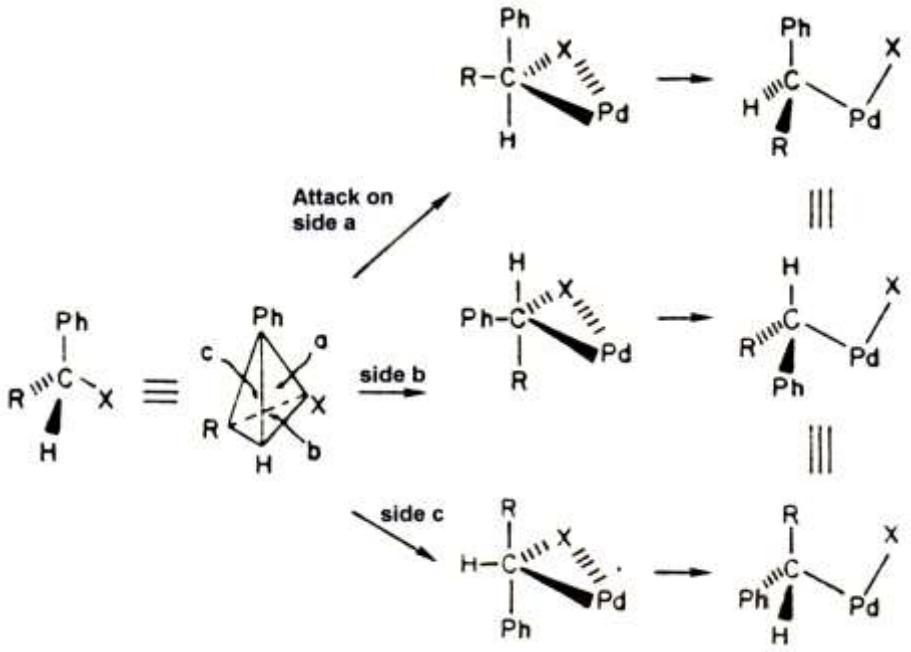


**3.8**

If the separation of C and X always occurs with the least movement of the equatorial group in the preferred direction (to Pd), the same enantiomer will be obtained every time, which will be the net effect of an inversion of configuration at the carbon atom. Because the Pd-C distance is larger than that of the C-X distance, the movement of the equatorial group to Pd will be the least obstructed pathway, at least in a transition state where the Pd-C bond formation and C-X bond breaking will proceed at the same rate.

Moreover, this mechanism explicates the loss of optical purity in the product and the racemisation of the reactants. Movement of the equatorial group in the opposite direction, i.e., away from Pd, produces the other enantiomer, causing a loss of optical purity. The degree of this loss, as a result of competitive movements, is expected to be independent from steric factors. Of greater significance is the measure of bond formation (of Pd-C) and breaking (of C-X) in the transition state, influencing the enantiomer distribution. Coinciding of the transition state with the products (i.e., well-formed Pd-C and Pd-X bonds and a long C-X bond) will favour movement of the equatorial group to X.

A pseudorotation of the trigonal bipyramid, followed by product formation or reductive elimination to reactants, is responsible for a reduction in optical output of the product,

as well as the observation that the recycled starter halide is partially a racemic blend. Although only speculative in nature, this mechanism is proposed for oxidative addition of both vinyl and aryl halides to the platinum group metals.[99]

(2) Two-step $S_N2$-type mechanism

Although it has been almost the only mechanism considered until about 1972[4], the two-step $S_N2$-mechanism is one of the most difficult mechanisms to analyse.[104] In contrast to the concerted one-step mechanism, in this mechanism there is involvement of an electrophilic attack on the metal atom.[99,117,118,119] As represented in Figure 2.16, the two-step mechanism can be applied to the addition of dipolar molecules such as $CH_3I$ and HCl.

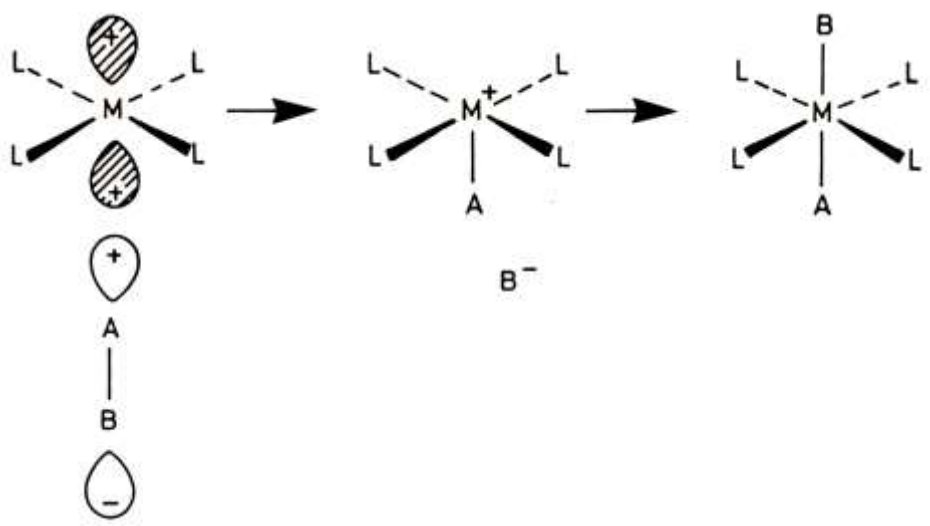


**Figure 2.16** Representation of the addition of dipolar molecules according to the two-step mechanism.

In this respect, square-planar molecules are differentiated from other systems through the donor orbital (probably the filled $d_{z^2}$) and the acceptor orbital ($p_z$) by virtue of having the same symmetry in relation to the incoming group in the direction of the z-axis.

The nature of the attack on the metal and the substantial polarity of the two- or three-centred transition state, can be concluded[4] from observations like the large negative values of activation entropies, the dependence of activation parameters on solvent polarity, the dependence of the rate on the nucleophilicity of the metal complex as

well as the fact that the first-order relationship is found for both reactants. The following reaction scheme[4] (3.9) gives an indication of the transition between a two- and three-centred transition state.

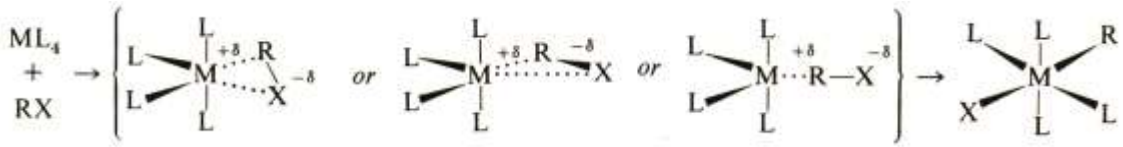

**3.9**

Oxidative addition via a two-centred transition state leads to stereochemical inversion[122] of configuration at the carbon centre of the alkyl group, as seen in many organic $S_N2$ processes. On the other hand, it can be expected that reactions via a three-centred transition state could lead to retention or inversion of configuration at carbon. This is dependent upon the degree by which the metal halogen bond is formed during the transition state.[123] Inversion of configuration is found in the oxidative addition of $[Pt(PPh_3)_3]$ with 8α-bromoethylquinoline,[124] while no stereospecifity was observed in the oxidative addition of $[Pd(PPh_3)_4]$ with $PhCH(Cl)CF_3$.[114,125] However, it is unclear as to whether racemisation occurrs during oxidative addition or whether the adduct undergoes racemisation, since various processes can lead to racemisation such as a reversible σ-π-rearrangement,[126,127] or α-elimination,[128,129] homolysis,[130] and intermolecular alkyl-transfer.[131,132] Free radical

[122] Labinger, J.A., Braus, R.J., Dolphin, D. and Osborn, J.A., *J. Chem. Soc., Chem. Comm*., 612 (2002).

[123] Ugo, R., Pasini, A., Fusi, A. and Cenini, S., *J. Am. Chem. Soc*., **94**, 7364 (1972).

[124] Sokolov, V.I., *Inorg. Chim. Acta*, **18**, L9 (1976).

[125] Stille, J.K., Hines, L.F., Fries, R.W., Wong, P.K., James, D.E. and Lau, K., *Adv. Chem. Ser*., **132**, 90 (1974).

[126] Stevens, R.R. and Shier, G.D., *J. Organomet. Chem.,* **21**, 495 (1970).

[127] Hancock, M., Levy, M.N. and Tsutsui, M., *Organomet. React*., **4**, 1 (1972).

[128] Cooper, N.J. and Green, M.l.H., *J. Chem. Soc., Chem. Comm*., 208, 761 (1974).

[129] Elmit, K., Green, M.L.H., Forder, R.A., Jefferson, I. and Prout, K., *J. Chem. Soc., Chem. Comm*., 747 (1974).

[130] Sneeden, R.P.A. and Zeiss, H.H., *J. Organomet. Chem.,* **22**, 713 (1970).

[131] Johnson, M.D., *Acc. Chem. Res*., **8**, 57 (1978).

[132] Van den Bergen, A., West, B.O., *J. Chem. Soc., Chem. Comm*., 52 (1971).

processes, often in competition with other mechanisms,[133] also lead to racemisation. The degree of involvement of the free radical processes, intrinsically or via exposure to oxygen,[134,135] can therefore impair the optical purity of a product of oxidative addition.

Furthermore, the stereochemistry at the metal centre cannot be differentiated, since the two-centred process is leading to the ionic pair $MR^+X^-$, which can disintegrate into either *cis*- or *trans*-adducts. It is understandable that the three-centred addition can also lead to *cis*- or *trans*-adducts, especially with coordinatively unsaturated metal-complexes.[136,137]

The use of other criteria to distinguish between two- and three-centred transition states seems problematic. The activation enthalpy- and activation entropy values for various oxidative addition reactions of *trans*-[IrCl(CO)$(PPh_3)_2$] has indicated for example that, only on the grounds of this correlation, a distinction cannot be made between a two- and three-centred transitional state.[138] The sensitivity of different addenda towards polar effects during oxidative addition was measured by variation of the donor properties of the triarylphosphine ligands, L = $(p\text{-}ZC_6H_4)_3P$, in [IrCl(CO)$L_2$].[123] In comparison to $O_2$ and $H_2$, the large variation in values between methyl iodide and benzyl chloride indicates that polar effects cannot be used to draw a distinction.[139]

The correspondence of the activating parameters (especially the large negative values of $\Delta S^*$) for $CH_3I$ and [IRX(CO)$(PPh_3)_2$][140] with those of the $S_N2$-reactions of alkyl halides with tertiary amines, have led to the idea that oxidative addition

[133] Pearson, R.G. and Figidore, P.E., *J. Am. Chem. Soc*., **102**, 1541 (1980).

[134] Labinger, J.A., Kramer, A.V. and Osborn, J.A., *J. Am. Chem. Soc*., **95**, 7908 (1973).

[135] Bradley, J.S., Connor, D.E., Dolphin, D., Labinger, J.A. and Osborn, J.A., *J. Am. Chem. Soc*., **94**, 4043 (1972).

[136] Lee, T.W. and Stoufer, R.C., *J. Am. Chem. Soc*., **97**, 195 (1975).

[137] Deeming, A.J., *Int. Rev. Sci., Inorg. Chem. Ser. Two*, **9**, 282 (1974).

[138] Burgess, J., Macker, M.J. and Kemmit, R.D.W., *J. Organomet. Chem.,* **72**, 121 (1974).

[139] Kochi, J.K., *Organometallic mechanisms and catalysis*, Academic Press, London (1978).

[140] Chock, P.B. and Halpern, J., *J. Am. Chem. Soc*., **88**, 3511 (1966).

reactions of organic halides and similar molecules occur via a nucleophilic attack on carbon. The reactions of alkyl halides and tertiary amines proceed via linear $S_N2$-displacements at carbon, so that a transition state, like structure 11, that is similar to the Menschutkin-reaction, could be acceptable to the $CH_3I$-addition.

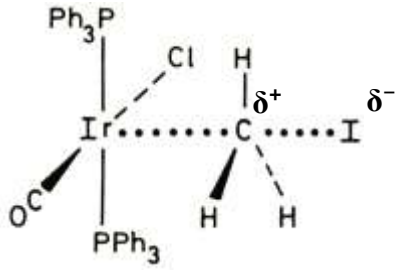


**11**

Later studies of related oxidative addition reactions have indicated that the significant solvent effect on the reaction rates was not in total agreement with the change in solvent polarity. For example, the substituted effect on the rate of addition of *para*-substituted benzyl halide does not agree with that of their reactions with pyridine.[123] The researchers have concluded that an asymmetrical transition state, like structure 12, is more probable than a linear geometry, thus explicating the large negative value of ΔS* and the solvent effect, through significant deviations of the iridium complexes from planarity. A greater measure of the Ir-C-bond formation in comparison to C-X-bond breaking, was needed to explain the observed electronic effects.

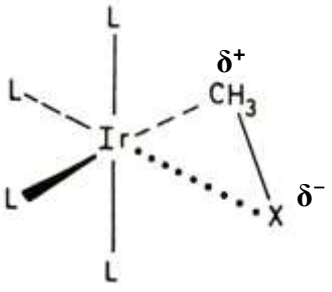


**12**

Measurements of the volume of activation of the addition of $CH_3I$ or $O_2$ to Vaska's complex in various solvents provide more information.[102] A rate determining, bond forming associative step correlates with the negative ΔV*-value. The $CH_3I$-values are not as large as those of the Menschutkin-reaction between $CH_3I$ and pyridine. The authors consider a linear transition state, like structure 11, to explain the results better than the simultaneous formation of two bonds, as seen in 12. According to the

researchers, an Ir- - -I- - -$CH_3$-bond formation would have correlated just as well with the data as in the case of Ir- - -$CH_3$- - -I. The presence of other anionic species in the reaction mixture during an oxidative addition reaction that proceeds according to the $S_N2$ two-step mechanism, leads, as expected, to the inclusion thereof in the product. Reaction scheme 3.10 serves as an example.[141]

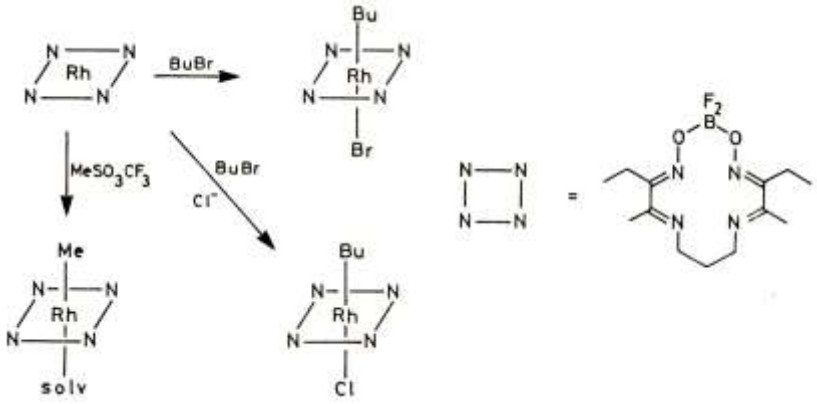


**3.10**

Oxidative addition of butyl bromide in the presence of $Cl^-$ leads to the formation of the chlororhodium complex. A later halogen interchange cannot be held accountable for this. Acetonitrile solvento species are formed as a product of methyl tosilate-reactions. In contrast to these reactions, the addition of $CH_3I$ to [Ir(SCN)(CO)$L_2$] (L = $PPh_3$ or $PMePh_2$) in the presence of an excess $SCN^-$ in dichloroethane, or to [IrCl(CO)$L_2$] in the presence of $Cl^-$, does not lead to the inclusion of free anions in the products.[142] Addition of $CH_3I$ to Vaska's complex in the presence of $^{131}I^-$ does not lead to the uptake of radioactive iodine,[143] although the geometry of these additions can be accepted as *trans.*[113] It is clear that intimate ionic pairs are retained throughout the reaction or that there is a one-step mechanism playing an active role. The order of the reaction is not of much use in determining the mechanism, since it cannot be used to distinguish between a two-step mechanism (in which the initial step is rate-determining) and concerted processes, or even compromises between the two.[104]

The possibility of nucleophilic catalysis in oxidative addition reactions both strengthens and weakens the $S_N2$-two-step pathway-argument.[104] During

[141] Collman, J.P. and MacLaury, M.R., *J. Am. Chem. Soc*., **96**, 3019 (1974).

[142] Pearson, R.G. and Muir, W.R., *J. Am. Chem. Soc*., **92**, 5519 (1970).

[143] Chock, P.B. and Halpern, J., *Proc. 10th Int. Conf. Coord. Chem*., 135 (1967).

nucleophilic catalysis, even through solvent coordination, the species attacked by the electrophile are an 18-electron, five-coordinated molecule, and not the 16-electron square-planar complex under discussion. Various examples of electrophilic attack on 18-electron species are known and the process is considered as well-established.[144,145,146] While certain examples of the $S_N2$-two-step pathway could be assigned to the 18-electron route, there are, however, many cases where this route is not possible. Some reactions proceed in non-polar solvents, in which a significant solvent interaction is unlikely. In other cases, neither change nor inclusion has been observed when potential catalytic anions were present. Because it can be expected that 18-electron species will undergo similar processes to those that 16-electron molecules will undergo,[133] the argument for electrophilic attack is strengthened, at least at some square-planar molecules. Examples include adducts of Vaska's complex and related molecules with $BF_3$ or $B(C_6F_5)_3$, which can be described in terms of an Ir→B coordinated bond.[147]

By establishing the electrophilic route of attack, the situation arises that square-planar molecules can undergo oxidative addition through nucleophilic attack, followed by an electrophilic attack, or vice versa.[104] Since electrophilic attack can happen at the metal atom, the ligand atom or the metal-ligand bond, it can be expected that migration of the attacking electrophile across this bond may happen in some cases. It could be difficult to prove, though a theoretical study has indicated that such migrations are indeed possible.[148]

The effect of structural change of alkyl halides also supports the $S_N2$-type transition state for oxidative addition. Concurring with organic substitution processes, a number of oxidative addition reactions[141,149,150] follow the classic pattern for the rate of $S_N2$-subsitution, namely methyl- > ethyl- > isopropyl halides and methyl iodide > -

[144] Deeming, A.J. and Shaw, B.L., *J. Chem. Soc.,* **A***,* 3356 (1970).

[145] Hart-Davis, A.J. and Graham, W.A.G., *Inorg. Chem*., **9**, 2658 (1970).

[146] Oliver, A.J. and Graham, W.A.G., *Inorg. Chem*., **9**, 243 (1970).

[147] Scott, R.N., Shriver, D.F. and Lehman, D., *Inorg. Chim. Acta*, **4**, 73 (1970).

[148] Ortiz, J.V., Havlas, Z. and Hoffmann, R., *Helv. Chim. Acta*, **67**, 1 (1984).

[149] Schrauzer, G.N. and Deutsch, E., *J. Am. Chem. Soc*., **91**, 3341 (1969).

[150] Hart-Davis, A.J. and Graham, W.A.G., *Inorg. Chem*., **10**, 1653 (1971).

bromide > -chloride.[139] The reactivity of a number of alkyl halides against cobalt(I)-complexes is in agreement with the values obtained in typical $S_N2$-reactions,[149] as seen in Figure 2.17. Similar reactivities of alkyl halides in oxidative addition reactions of tetracarbonylferrate(2−), $[Fe(CO)_4]^{2-}$ were found.[151]

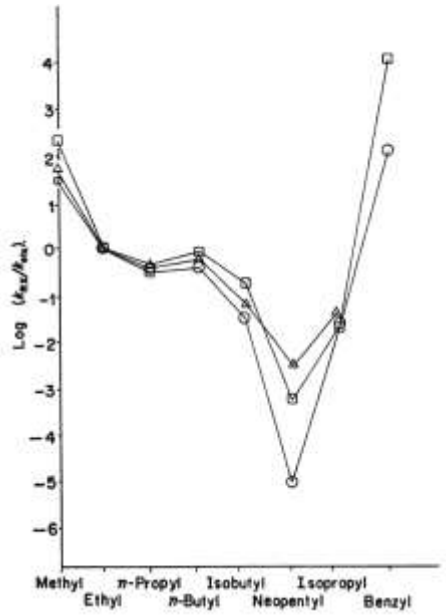


**Figure 2.17** Rate profile for $S_N2$-reactions on alkyl halide substrates: ○, average relative rate data for a variety of $S_N2$-reactions in different solvents at different temperatures; □, cobaloxime + RX; Δ, Vit. $B_{12}$ + RX.

Changes of the halide in the addendum, RX, have a relatively small influence,[123,138] but when R is an aryl, it was found that electron-withdrawing substitutes enhanced the rate.[101,105,152] This is also an indicator of electrophilic attack by carbon on the metal, while a three-centred transition state, like structure 12, can still be formed.[105] Oxidative addition of $CF_3I$ to $[RX(CO)(PPh_3)_2]$ does not occur, while $CH_3I$ added readily.[100] Inversion of polarity of the C-I bond could explain this and could have supported the $S_N2$-two-step mechanism as the general mechanism for organic halide addition. However, steric or other factors may also be involved.[104]

(3) Free radical-mechanism

[151] Collman, J.P., Finke, R.G., Cawse, J.N. and Brauman, J.I., *J. Am. Chem. Soc*., **99**, 2515 (1977).

[152] Blum, J., Weitzberg, M. and Mureinik, R.J., *J. Organomet. Chem.,* **122**, 261 (1976).

A comparative study of several oxidative addition processes indicates that free radical processes virtually are in competition with other routes.[133,153,154] Sometimes, it is difficult in practice to distinguish between $S_N2$-type two-step- and free radical mechanisms.[99,117] The distinction between two-equivalent and the successions of one-equivalent changes in oxidative addition becomes part of the bigger picture that is dealing with nucleophiles (or electrophiles) and electron-transfer processes respectively.[155] Both mechanisms are partially dependent upon the oxidation-reduction characteristics of the metal-complex. An important prerequisite for participation (or non-participation) of a free radical mechanism is that the X-Y bond breaking of the added molecule, XY, should occur first, before interaction with the metal centre.[1]

Theoretically, the free radical mechanism can be operative in two ways,[139] and is summarised as follows:

(a) Radical chain reaction (propagating succession)

$$RX + RM\bullet \longrightarrow RMX + R\bullet$$
$$R\bullet + M \longrightarrow RM\bullet \quad \text{etc.}$$

(b) Radical non-chain reaction (electron-transfer)

$$RX + M \longrightarrow [R\bullet MX\bullet]$$
$$[R\bullet MX\bullet] \longrightarrow RMX$$

The radical chain reaction has already been observed in oxidative addition reactions of Ir(I), Rh(I) and Pt(0) with alkyl halides,[139] and the two steps of the mechanism may be represented as follows:[2]

$$Q\bullet + L_nM(I) \longrightarrow L_nM(II)\text{-}Q$$
$$L_nM\text{-}Q + R\text{-}X \longrightarrow X\text{-}L_nM\text{-}Q + R\bullet \quad \text{(Initiation)}$$

$$R\bullet + L_nM(I) \longrightarrow R\text{-}L_nM(II)$$
$$R\text{-}L_nM(II) + R\text{-}X \longrightarrow R\text{-}L_nM(III)\text{-}X + R\bullet \quad \text{(Propagation)}$$

[153] Kramer, A.V. and Osborn, J.A., *J. Am. Chem. Soc*., **96**, 7832 (1974).

[154] Connor, J.A. and Riley, P.I., *J. Chem. Soc., Chem. Comm*., 634 (1976).

[155] Nugent, W.A. and Kochi, J.K., *J. Am. Chem. Soc*., **98**, 5979 (1976).

where Q is a radical source. Connor and Riley[154] supplied the first irrefutable proof of the formation of R• and a metal centre of intermediate valence.

Some properties are characteristic of radical chain reactions. For example, the reaction of $[IrCl(CO)(PMe_3)_2]$ with $PhCHFCH_2Br$ is initiated through radical sources like $O_2$ or benzoyl peroxide and inhibited by radical scavengers, like hydroquinone, galvinoxyl or duroquinone.[135] Sometimes, initiation reactions are also started by trace amounts of oxygen, paramagnetic impurities or light. Racemisation is observed with the addition of chiral $MeCHBrCO_2Et$ to the same Ir(I)-compound.[156] Of greater significance is that CIDNP (Chemically induced dynamic nucleus polarisation) is observed in NMR-spectra of a reaction mixture of $[Pt(PEt_3)_3]$ and isopropyl iodide.[153] This is an effect observed only in the presence of free radicals.

The following reaction scheme (3.11) is proposed for the reaction of $[PtL_3]$ with an alkyl halide:[4]

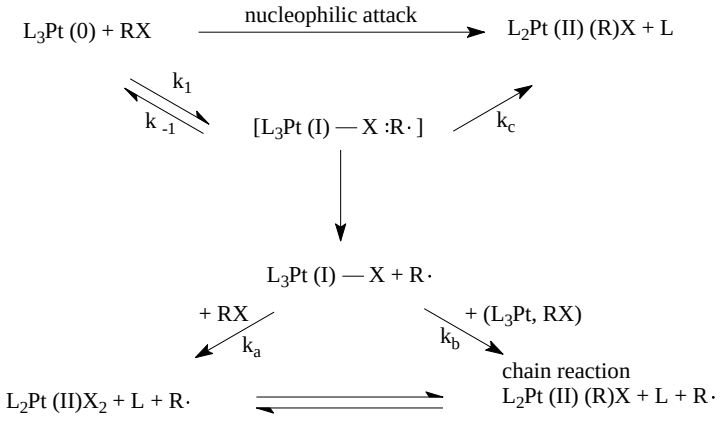


**3.11**

In addition to the nucleophilic attack of the metal complex on the alkyl halide, an alternative reaction pathway encompasses the withdrawal of a halide by the metal complex to form a radical pair, $L_3Pt(I)$-X:R•. This radical pair can decompose in order to produce the original product (the $k_c$-pathway) or it can separate independently to form $L_3Pt(I)$-X and R•. After this, the progress of the reaction depends mainly upon the reactivity of the alkyl halide. As a C-Br bond is stronger than a C-I bond, a chain mechanism ($k_b$-pathway) will dominate for isopropyl bromide, while $k_a$ and $k_b$ are comparable for isopropyl iodide.

[156] Kramer, A.V., Labinger, J.A., Bradley, J.S. and Osborn, J.A., *J. Am. Chem. Soc*., **96**, 7145 (1974).

Oxidative addition of reactive alkyl halides, like $CH_3I$, $CH_3OCH_2Cl$, benzyl chloride, etc., to $[IrCl(CO)(PMe_3)_2]$ is not affected by suppressants. Similarly, oxidative addition to the rhodium(I)-complex $[RhCl(CO)(PEt_3)_2]$ occurred only with reactive alkyl halides and the reaction was not affected by radical scavengers. Thus, oxidative addition under such circumstances[139] does not occur according to a radical chain reaction, but rather according to a non-chain reaction.

Initially, the formation of $[Br_2PtL_2]$ from $[PtL_3]$ and $Bu^nBr$ was attributed to a radical chain process, as the rate was accelerated by an azo-initiator. However, this mechanism cannot explain the reactions of other halides that are not influenced by radical scavengers. On these premises, Osborn and Kramer[153] proposed a non-chain reaction for the formation of dibromoplatinum(II) in which the following one-equivalent changes are involved:

$$RX + Pt \longrightarrow R\bullet + XPt(I) \qquad \textbf{3.12}$$
$$XPt(I) + RX \longrightarrow X_2Pt(II)L_2 + R\bullet$$

The direct interaction of alkyl halide and platinum(0) to form radicals in reaction 3.12, can be regarded as an electron-transfer process. The stepwise process of reaction 3.12 may be represented as follows:

$$RX + Pt \longrightarrow RX\bullet^- + Pt(I)$$
$$RX\bullet^- + Pt(I) \longrightarrow R\bullet + XPt(I) \qquad \textbf{3.13}$$

Disintegration of the radical pair, formed in 3.13, opens up an alternative pathway for oxidative addition. As seen in the following reaction scheme, the non-chain reaction produces radicals as intermediates and comprises successive one-equivalent changes.

$$RX + Pt \longrightarrow R\bullet + XPt(I)$$
$$R\bullet + XPt(I) \longrightarrow RPt(II)X \qquad \textbf{3.14}$$

Such a non-chain homolytic mechanism is specifically applicable to reactive alkyl halides where the oxidative addition is not suppressed by radical scavengers.[153] The

mechanism in scheme 3.14 has also been proposed independently by Lappert and Lednor.[157]

Both the chain- and non-chain reactions can be involved simultaneously and are dependent upon the reactivity and structure of the alkyl halides. Mainly, distinctions are based on the effect of radical scavengers and initiators.[139]

(4) Ionic mechanism

Coming very clearly to the fore is the effect of the solvent in determining the mechanism, distinguishing the ionic mechanism from the concerted mechanism occurring in the non-polar solvent where *cis*-addition is obtained. It is possible that a mixture of isomers in polar solvents may be obtained, as addition can be either *cis* or *trans.* The ionic mechanism causes the formation of a five-coordinated cationic complex as intermediate. It would seem from the square-pyramidal geometry of the intermediate that only *trans*-addition is possible, but rapid intramolecular rearrangement of the five-coordinated complex can easily produce the *cis*-product, so that the course of the reaction may be represented in the following manner (scheme 3.15):

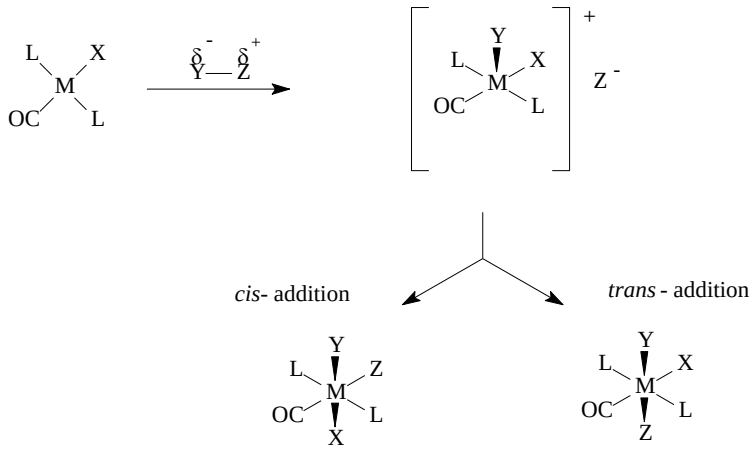


**3.15**

The route leading to *trans*-addition occurs more readily if the reaction occurs in a polar solvent like dimethylformamide, and when Y-Z is a substrate that can be ionised, like HCl.

[157] Lappert, M.F. and Lednor, P.W., *J. Chem. Soc., Chem. Comm*., 948 (1973).

#### *2.2.1.5 Factors influencing oxidative addition*

Various factors may influence the reaction rate and the reaction products. These include the metal, steric and electronic properties of the bound ligands and addendum as well as the reaction medium and the possibility of catalysis. The reason for this influence lies in the nucleophilic character of the metal-complex, and that any factor influencing the nucleophilicity of the metal, will determine the outcome of the reactions.[158,159]

(1) The metal

Coordinatively unsaturated complexes are more reactive than analogue saturated complexes. This is particularly evident in $d^{10}$ complexes of the $ML_4$-type, with M = Ni, Pd, Pt and L = $PR_3$. In such cases, $ML_2 > ML_3 > ML_4$.[2]

The nature of the metal also influences the reactivity, which is a reflection of the relative comfort with which a metal can be oxidised. Usually, it is impossible to draw comparisons between three members of a particular sub-group or between metals of neighbouring sub-groups. The problem with such comparisons is that there are so few complete isostructural complex series. Furthermore, comparisons are hampered by the characteristic tendency of $d^8$-complexes to become coordinatively unsaturated, as sub-groups are ascended or one moves to the left in group VIII. Thus, it is difficult to maintain the same degree of saturation in a series.

Although there are exceptions, the largest metals in the lowest oxidation states show the greatest tendency to undergo oxidative addition.[160] Schematically, these two tendencies may be represented as follows:

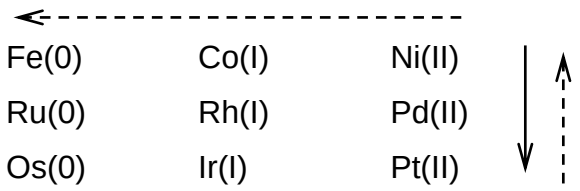


[158] Brown, C.K., Georgian, D. and Wilkinson, G., *J. Chem. Soc., Dalton Trans*., 929 (1973).

[159] Deeming, A.J. and Shaw, B.L., *J. Chem. Soc.,* **A**, 1802 (1969).

[160] Nyholm, R.S. and Vrieze, K., *J. Chem. Soc.,* 5337 (1965).

——— Tendency to undergo OA (Tendency for a $d^8$-complex to be oxidised to $d^6$).

- - - - - - - Tendency for $d^8$-complex to adopt five-coordinated geometry.

Usually, acidic characteristics are associated with transition metals with high oxidation states, while metals with low oxidation states act as Lewis bases. There are various indications that lighter metals in a given sub-group are less basic or nucleophilic than the heavier elements. For example, the Vaska complex reacts fully and irreversibly with $CH_3I$, while the reaction with the corresponding rhodium complex is reversible[161,162] (reaction 3.2). Vaska studied a complete iso-electronic series in the reaction of $[M(2{=}phos)_2]A$ with XY (2 = phos is *cis*-$(C_6H_5)_2PCHCHP(C_6H_5)_2$; A is Cl, I, $BF_4$ and XY is $O_2$, HCl, $H_2$, CO, $SO_2$).[163] He found an order of reactivity of Co > Ir > Rh, which represents a deviation from the expected results.

In contrast to this, the relative reaction rates of the oxidative addition of $[(\eta^5\text{-}C_5H_5)M(CO)PPh_3]$ with $CH_3I$ (reaction 3.16), are 1.0 for M = Co, 1.4 for M = Rh and about 8 for M = Ir.[145]

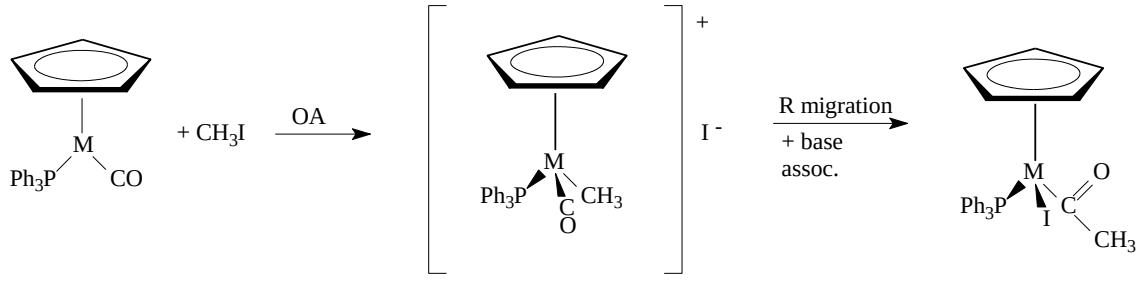


**3.16**

The Vaska complex reacts with $BF_3$, $BCl_3$ and $BBr_3$ to form an Ir-B bond in a 1:1-adduct (reaction 3.17).

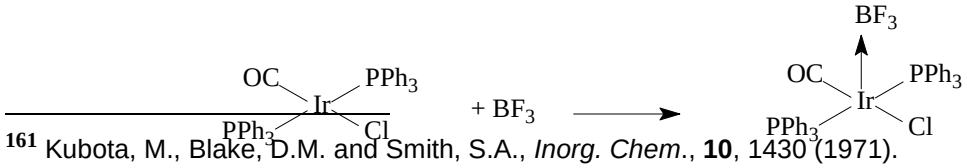


[161] Kubota, M., Blake, D.M. and Smith, S.A., *Inorg. Chem*., **10**, 1430 (1971).

[162] Kubota, M. and Blake, D.M., *J. Am. Chem. Soc*., **93**, 1368 (1971).

[163] Vaska, l., Chen, L. and Miller, W.V., *J. Am. Chem. Soc*., **93**, 6671 (1971).

**3.17**

In contrast to the above, the corresponding rhodium complex forms adducts only with $BCl_3$ and $BBr_3$, but not with $BF_3$. The order of acidic strength,[164,165] $BF_3 < BCl_3 < BBr_3$, implies that the iridium complex is a stronger bases than the corresponding rhodium complex.

As seen in Figure 2.18, coordinatively unsaturated, square-planar complexes, like those of Ir(I) and Rh(I), allow attack by both nucleophilic and electrophilic reactants on an orbital with σ-symmetry. This, in turn, leads to nucleophilic and electrophilic attacking mechanisms.

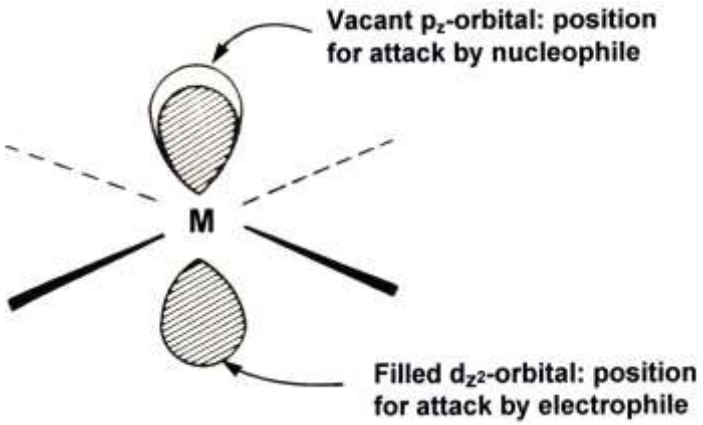


**Figure 2.18** Possible attack by nucleophilic and electrophilic reagents on an orbital of σ-symmetry.

(2) Bound ligands

Metal bound ligands exert a significant influence on the course of oxidative addition reactions. Any change in the metal complex causing an increase in electron density around the central metal atom and thus, an increase in the nucleophilicity of the metal atom will lead to an increased reactivity. Certain exceptions excluded,[163] the kinetics of oxidative addition is thus also a function of the σ- and π-bonding properties of the ligands.[4] Ligands with good σ-donor properties will increase the electron density on the central atom, and the increased nucleophilicity will cause a more rapid reaction rate. In contrast to this, a ligand with strong π-acceptor properties will lower

[164] Brown, D.G., Drago, R.S. and Bolles, T.F., *J. Am. Chem. Soc*., **90**, 5706 (1968).

[165] Shriver, D.F. and Swanson, B., *Inorg. Chem*., **10**, 1354 (1971).

the electron density on the central metal atom, resulting in a slower reaction. Added to the electronic effect, steric factors also play a role in determining the reaction rate and/or the stereochemistry of the product.

Carbonyl ligands, which are good π-acceptors, cause the nucleophilicity of the metal to decrease as a result of metal-to-carbonyl electron back donation (discussed in the first part of this chapter). There is a direct correlation between the electronegativity of halogen ligands and the tendency of the complex to undergo oxidative addition. According to Chock and Halpern[140] as well as Deeming and Shaw,[159] who have studied the effect of the halogen, X, in the complex *trans*-[IrX(CO)($PPh_3$)$_2$], the order of reactivity with regard to oxidative addition is I > Br > Cl.

Nakamoto[166] has investigated the influence of the change of substituents on β-diketones. The study of infrared spectra of acetylacetonates, and trifluoro- and hexafluoroacetylacetonates of nickel and copper, has led to the observation that successive displacement of methyl groups by trifluoromethyl groups causes an increase in the stretching frequencies of C—O and C—C and a reduction of the corresponding M—O stretching frequencies. This observation corresponds with the electronic bond-theory, stating that the strong negative inductive effect of a $CF_3$ group strengthens C—O and C—C but weakens the M—O bond.

A study conducted by Basson, Leipoldt and Nel[167] confirms this expected reduction in the nucleophilicity of the metal, with increasing electron withdrawing substituents on the β-diketone. These researchers have investigated the influence of different β-diketones on the reaction rate of the following oxidative addition reactions:

[Rh(β-diketone)(CO)($PPh_3$)] + $CH_3I$ ⟶ [Rh(β-diketone)(CO)($PPh_3$)($CH_3$)(I)]

The relative nucleophilicity of the β-diketone complexes that have been used, followed a reactivity order of: acac (1.0) > TFAA (0.24) ≈ TFDMAA (0.22) >> HFAA(0.02). This order corresponds with the increasing number of electronegative substituents on the β-diketone and thus, also with the decreasing order of $pK_a$-values

[166] Nakamoto, K., Morimoto, Y. and Martell, A.E., *J. Phys. Chem*., **66**, 346 (1962).

[167] Basson, S.S., Leipoldt, J.G. and Nel, J.T., *Inorg. Chim. Acta*, **84**, 167 (1984).

for the series of β-diketones. The carbonyl stretching frequencies, which are a linear function of the electron density on the metal, increased correspondingly to the decrease in the electron density on the metal.

According to Kubota[168] and associates, triphenylarsineiridium(I)-complexes react more rapidly with methyl iodide than the corresponding triphenylphosphine-complexes. When tertiary phosphine ligands are viewed in more detail, it is evident that changes in the phosphine ligand cause significant differences in the reactivity of complexes with regard to oxidative addition.[40,169,170] A series of *para*-substituted triphenylphosphine ligands should reveal the same steric effects. Therefore, a difference in reactivity may be attributed entirely to electronic factors. The reaction rate of the addition of methyl iodide to *trans*-[IrCl(CO){P(*p*-$ZC_6H_4)_3$}$_2$] increases in the order Z = Cl > H > Me > OMe, which represents the expected order of increasing donor ability of the ligands P(*p*-$ZC_6H_4)_3$.[123] Although the *para*-substituents are only bound indirectly to the iridium atom, for example through the π-electron density of the phenyl rings of the phosphine ligand, a significant difference in reaction rates has been observed. The activation entropies for the different reactions are almost constant. This serves as additional proof of a constant steric factor in the transition state. The researchers conclude that electronic effects as a result of phosphine ligands are of greater importance in reactions in which a significant localised charge transfer occurs in the transition state. In concurring, Vaska and Chen[171] found that there is a reasonably correlation between the electronic properties of *para*-substituted triphenylphosphine ligands, as measured by Hammet σ-constants, and reaction rates.

The order of Lewis basisity for aryl-, alkyl- and mixed aryl-alkylphosphines, may be summarised as follows:[145,159]

$$PPh_3 < P(Ph)_2CH_3 < P(Ph)(CH_3)_2 < P(CH_3)_3$$

[168] Kubota, M., Kiefer, G.W., Ishikawa, R.M. and Bencala, K.E., *Inorg. Chim. Acta*, **7**, 195 (1973).

[169] Miller, E.M. and Shaw, B.L., *J. Chem. Soc., Dalton Trans*., 480 (1974).

[170] Ingold, C.K., *Quart. Rev., Chem. Soc*., **11**, 1 (1957).

[171] Vaska, L. and Chen, L., *J. Chem. Soc., Chem. Comm*., 1080 (1971).

**Increase in Lewis basisity** ⟶

Increasing basisity of the phosphine ligand increases the nucleophilicity of the metal, thus promoting the tendency of the complex to undergo oxidative addition. In most cases, the relative importance of steric and electronic effects on reactivity remains largely unknown. For example, $P(Ph)(CH_3)_2$-complexes are significantly more reactive than $PPh_3$-complexes. The reason for this is that $P(Ph)(CH_3)_2$ is both a better donor and sterically smaller than $PPh_3$.[159,168] In itself, steric hindrance does play a significant role in determining the rate of oxidative addition reactions and the phosphine ligands under discussion, as well as other non-labile ligands and the addendum contribute. According to Ugo[123] and associates, differences in the mechanistic detail of the transition state are to be expected with a change in the bulkiness of the phosphine ligand. Brown[172] investigated the effect of steric hindrance on the nucleophilic substitution in alkyl halides. The results he acquired from substituted pyridines can be compared to those of Hart-Davis and Graham,[145] who studied nucleophilic addition of methyl iodide to $[C_5H_5Co(CO)L]$. The relative reaction rates are as follows:

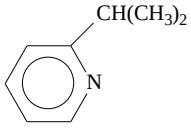


1,0

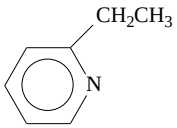


3,2

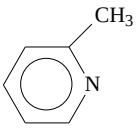


6,7

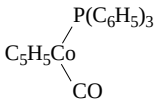


1,0

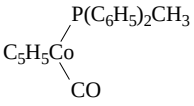


6,1

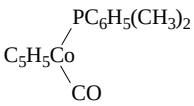


10,7

In both series of nucleophiles, an increase in bulkiness resulted in the decrease in rate constants. This tendency is the same as what is expected in terms of the Lewis basisity of the particular phosphines. However, the researchers found a clear indication of the steric effect of phosphine ligands with tricyclohexylphosphine. The latter is a very strong Lewis base and, as a result of its bulkiness, exhibits a slow reaction.

[172] Brown, H.C., *J. Chem. Soc.,* 1249 (1956).

In the systems discussed thus far, the electronic effect that a tertiary phosphine has on the reactivity of the metal, exerted this influence via the phosphorous atom. Miller and Shaw[169] came to the conclusion that, in the case of a ligand like orthomethoxyphenyl(dimethyl)phosphine, the ether-oxygen may interact directly with the metal and will decrease through electron donation the activation energy needed for oxidative addition (Figure 2.19).

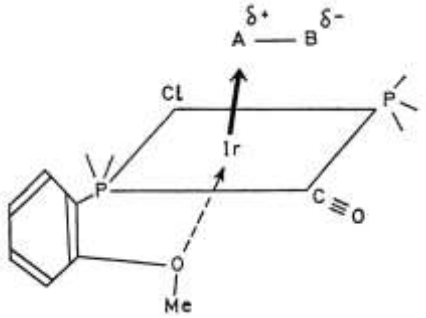


**Figure 2.19** Increase in the nucleophilicity of iridium by electron donation from the methoxy-oxygen.[169]

The interaction of the oxygen with the metal is probably weak, but increases in strength during the formation of highly polar transition states.[140] In the oxidative addition reactions of some platinum(II)- and rhodium(I)-complexes, participation of neighbouring groups causes an increase in reaction rates of between 100 to 250 times.[173]

(3) The addend

The mechanism,[99] stereochemistry and the nature of the products can be influenced by the electronic and steric aspects as well as addend orientation during oxidative addition. The addenda participating in oxidative addition reactions can be divided into three classes:[2] (a) polar electrophilic reactants; (b) molecules that remain bound in the adduct; and (c) non-polar addenda. Class A and C both fragment during addition.

Examples of the addenda of different classes are as follows: (R = alkyl)

[173] Constable, A.G., Langrick, C.R., Shabanzadeh, B. and Shaw, B.L., *Inorg. Chim. Acta*, **65**, L151 (1982).

Class A: $X_2$ (halogens), H-Y (Brönsted acids), R-X (alkylating reactants), RCOX (acylating reactants), $SnCl_4$, $HgX_2$, RSCl, etc.
Class B: $O_2$, $S_2$, $Se_2$, $RCON_3$, $RN_3$, RC≡CR, RN═NR, RCH═CHR, S═C═S, $H_2C$═O, etc.
Class C: $H_2$, $R_3SiH$, $R_3Ge$-H, $R_3Sn$-H, RSH, RCHO, RH, etc.

Addition of Class A addenda yields *cis*- or *trans*-products. The addenda of Class B maintain at least one bond in the adduct, as the two new bonds on the metal necessarily have to be *cis.* Class C-addenda almost always yield a stereospecific *cis*-addition. Here, the addition of C-H-bonds is restricted mainly to intramolecular oxidative additions of activated C-H-groups.

Various factors have to be considered when looking specifically at the role of alkyl halides, RX, in oxidative addition. For example, the reactivity of an alkyl halide depends upon the dissociation energy of the R-X-bond and the electron donating ability of the halogen. Douek and Wilkinson[100] found that methyl iodide reacted considerably faster than methyl bromide at room temperature. The order of reactivity for different halogens, bound to the same alkyl-group, is I > Br > Cl.[99,141,174] It also reflects the order of the leaving group effectivity in $S_N2$ reactions.[149]

For a nucleophilic attack by the metal complex on the α-carbon of an alkyl halide, the ease of the attack will depend a great deal upon the electrophilic nature of the α-carbon and thus, also on the inductive effect of X. Corresponding to this, is the inability of ethyl- and butyl iodide to add to $[RhCl(CO)(PPh_3)_2]$, while methyl iodide readily undergoes addition.[100] Although the dipole moments of ethyl- and butyl iodide are higher than that of methyl iodide, the central carbon atoms are less positive and thus less predisposed to nucleophilic attack. However, another factor also exerting an influence is the steric effect of the substituent methyl groups that obstructs access to the metal, for example, rhodium. Hart-Davis and Graham[145] found that ethyl iodide reacted about 400-1200 times slower than methyl iodide. By and large, the order of reactivity of alkyl halides for different alkyl-groups bound to the same halide can be regarded as $CH_3$ > $CH_3CH_2$ > secondary > cyclohexyl.[99,141,174]

[174] Collman, J.P., Murphy, D.W. and Dolcetti, G., *J. Am. Chem. Soc*., **95**, 2687 (1973).

Unless the mechanism is purely ionic, the alkyl halide (e.g. methyl iodide) has to be the reacting species. Moreover, during one of the stages, there is a nucleophilic attack of the rhodium electron pair on the methyl group, with corresponding transfer of the iodine atom to the metal. In such a case, the methyl iodide molecule can be free (A), coordinated to the attacking rhodium via iodine (B), or coordinated to a rhodium atom in another molecule (C), where A, B and C refer to the next structures.

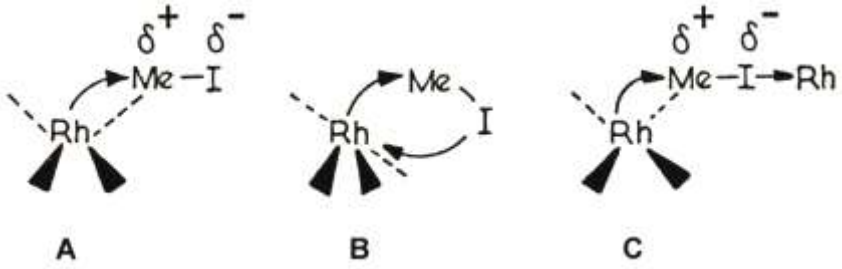


A theoretical study by Ortiz, Havlas and Hoffmann[148] investigated the possibilities of methyl iodide addition to a phenyl-Pt-complex. The three mechanisms that were under consideration required initial coordination of the metal to the iodine atom, or the carbon atom or oxidative addition over the C-I bond, respectively.

Coordination of iodine to the three-coordinated Pt-complex yields a four-coordinated transition state, with iodine in the same plane as the other ligands. According to MO-calculations, the overlapping population reaches a maximum if the Pt-I-C angle, α, is equal to 90° and the $C_\alpha$-Pt-I-angle, Φ, is equal to 180° (structure 13).

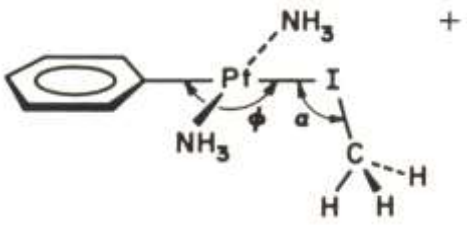


**13**

The entrance of $CH_3I$, next to the axis perpendicular to the plane of the complex (i.e., Φ = 90°), is repulsive as a result of destabilising interactions between the iodine lone pairs and the $d_{z^2}$-orbital of Pt.

The alternative is an oxidative addition in which the central point of the $H_3C$-I bond is under observation. The angle formed between the $C_\alpha$-Pt bond and the bond between

Pt and the central point of the C-I bond can be indicated as α', while the Pt-central point distance may be indicated as R' in structure 14. The minimum angle of α' is 150° for R' = 2.5Å.

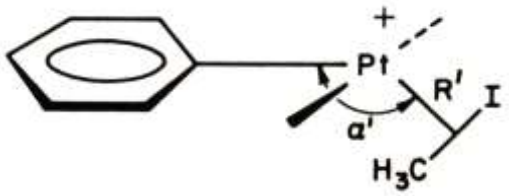


**14**

Already at the start of the reaction, the Pt-I bond has been well formed. A second stage of the reaction is the disintegration of the molecule to $[(C_6H_5)Pt(NH_3)_2I]$ and $CH_3^+$ (structure 15).

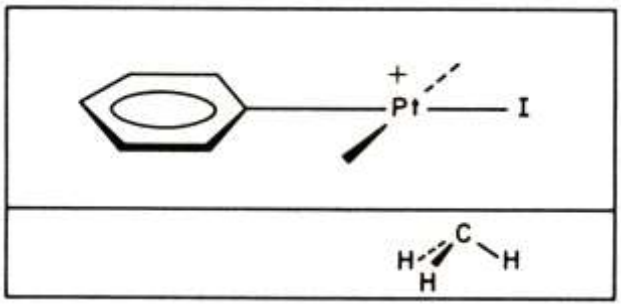


**15**

The $CH_3^+$ LUMO is a vacant $sp^3$-hybrid, rotating as the reaction proceeds. Initially, the most significant interaction is with the HOMO of the $[Ph(NH_3)_2PtI]$ fragment. This particular fragment is in fact a lone pair orbital on iodine. The interaction of the $CH_3^+$ LUMO with the $d_z^2$ type orbital of Pt has a slow start, but increases very rapidly thereafter. The nodal structure of the $d_z^2$ orbital prevents the possibility of a significant overlap until the $C_3$ axis of the methyl group is aligned with the $d_z^2$ lobe. The product of the reaction may be represented by structure 16.

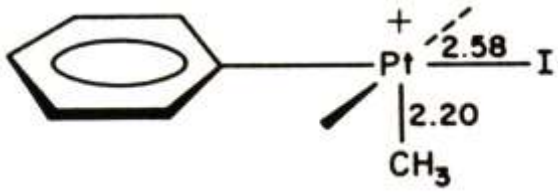


**16**

The mechanism that requires initial coordination of the carbon atom involves inversion of the methyl group. The approaching of MeI to the $d_{z^2}$ orbital of Pt is slightly less repulsive if the $CH_3$ group is aimed at the metal, as in structure 17.

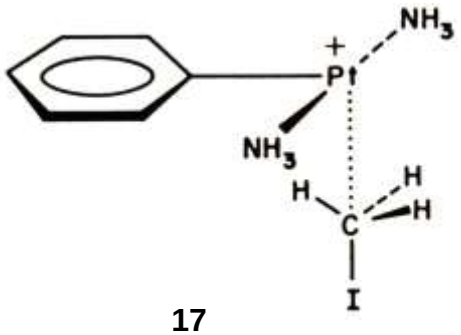


**17**

Transmission of the methyl, via inversion to Pt, represents a migration from the one donor, $I^-$, to the other, the $d_{z^2}$ orbital of Pt. However, an energy profile indicates an activation energy of about 1.3 eV due to the breaking of the C-I bond. This mechanism is a reasonable alternative to oxidative addition over the C-I bond, even if the initial entrance is repulsive.

(4) The solvent

The medium, in which the oxidative addition reaction is taking place, influences the total progress of the reaction. The reaction rate,[99,145,167] the mechanism of the reaction,[175] the stereochemistry of the intermediates and the products,[4,176] as well as the composition of the formed products,[141,177] are all dependent upon the reaction medium. However, distinguishing between effects is not self-evident because the choice of solvent may affect the progress of the reaction for example by differentially changing the rates of competing pathways. This comprehensive influence may be traced back to fundamental physical or chemical properties of solvents.

Protic solvents like water, methanol, formamide, hydrogen fluoride and ammonia, have the ability to form strong hydrogen bonds. Dipolar aprotic solvents are highly polar in nature, but can only be regarded as very weak hydrogen bond donors.

[175] Pearson, R.G. and Rajaram, *Inorg. Chem.*, **13**, 246 (1974).

[176] Blake, D.M. and Kubota, M., *Inorg. Chem.*, **9**, 989 (1970).

Dimethyl formamide (DMF), dimethyl sulphoxide (DMSO), acetone, acetonitrile and nitromethane are well-known examples of dipolar aprotic solvents. According to this classification,[178] the phenomenon of hydrogen bonding may be regarded as an important interaction in determining the protic/dipolar aprotic solvent effects on reaction rates. Although N-methyl formamide is a weak protic solvent, and nitromethane a weak dipolar aprotic solvent, many of the reactions occur more than a hundred times faster in nitromethane than in N-methylformamide.[179] Exceptional cases excluded, the macroscopic dielectric constants of the solvents do not indicate the protic/dipolar aprotic solvent effect on reaction rates. For example, some reactions proceed more rapidly with a factor of $10^6$ in dipolar aprotic solvents (e.g., DMF) than in protic solvents (e.g., methanol) with almost identical dielectric constants.[178,180]

As with internal pressure,[181] the dielectric constant of a solvent is also a measure of polarity. Kirkwood[182] suggested a theory for the influence of the dielectric constant of a medium on the free energy of a polar molecule. If only electrostatic forces are considered, the difference in free energy of a dipole in a medium with dielectric constant $\varepsilon_r$, versus a medium with unity dielectric constant $\varepsilon_0$ , is given by:

$$\Delta G_e = -L\frac{\mu^2(\varepsilon_r - 1)}{r^3(2\varepsilon_r + 1)4\pi\varepsilon_o}$$

where μ is the dipole moment and r, the radius of the molecule. Application of this equation on the transition state theory for the reaction A + B $\rightleftharpoons$ M*, where A, B and M* are polar species and $k = RTe^{-\Delta G^*/RT}/Lh$, leads to

[177] Collman, J.P., Kubota, M., Vastine, F.D., Sun, J.Y. and Wang, J.W., *J. Am. Chem. Soc.*, **90**, 5430 (1968).

[178] Parker, A.J., *Chem. Rev*., **69**, 1 (1969).

[179] Parker, A.J., *Adv. Phys. Org. Chem*., **5**, 173 (1967).

[180] Alexander, R., Ko, E.C.F., Parker, A.J. and Broxton, T.J., *J. Am. Chem. Soc*., **90**, 5049 (1968).

[181] Moore, J.W. and Pearson, R,G., *Kinetics and mechanism*, John Wiley & Sons, New York (1981).

[182] Kirkwood, J.G., *J. Chem., Phys*., **2**, 351 (1934).

$$\ln k = \ln k_o - \frac{L(\varepsilon_r - 1)}{4\pi\varepsilon_o RT(2\varepsilon_r + 1)}\left[\frac{\mu_A^2}{r_A^3} + \frac{\mu_B^2}{r_B^3} - \frac{\mu_M^2}{r_M^3}\right]$$

where k is the rate constant in a medium with dielectric constants $\varepsilon_r$ and $k_0$, the rate constant in a medium with unity dielectric constant $\varepsilon_0$ and non-electrostatic forces are the same for the activated complex and for the reactant. This equation predicts that the rate of the reaction will increase with increased dielectric constant of the medium if the activated complex is more polar than that of the reactants.[181]

Basson, Leipoldt and Nel[167] have found corresponding evidence that the rate for the oxidative reaction, [Rh(TFAA)(CO)($PPh_3$)] + $CH_3I$, increases with increased polarity of the solvent. The relative reaction rates of the different solvents are as follows: acetone (1.0) > 1,2-dichlorethane (0.66) >> chlorobenzene (0.05) > toluene (0.02). The formation of a polar transition complex, in which a moderate measure of charge separation is present, was postulated on this ground. This result also corresponded to the findings of Pearson and Rajaram[175] as well as those of Hart-Davis and Graham.[145] In both cases, polar transition states were suggested.

In contrast to the effect of stabilisation of a transition state, Flood[183] and associates had indicated that direct attack by the solvent on the metal centre might also explain the influence of polar donating solvents. Consequently, this leads to questioning the nature of solvent involvement.

The dependence of the dissociation of ion-associated complexes upon the dielectric constant of a solution does not necessarily imply that the dielectric constant is a measure of the ionising ability of the solvent.[184] Heterolysis of a covalent bond cannot occur solely as a result of a high dielectric constant. It is only coordination that can lead to ionisation. However, the degree of the ionisation depends on the interplay between the coordinatively dependent and dielectric dependent components. Calculations of three aprotic solvents, $D_1$, with ε = 10 and medium

[183] Flood, T.C., Jensen, J.E. and Statler, J.A., *J. Am. Chem. Soc*., **103**, 4410 (1981).

[184] Gutman, V., *Angew. Chem. Int. Ed. Engl.*, **9**, 843 (1970).

donor strength, $D_2$, with ε = 35 and medium donor strength and $D_3$ with ε = 10 and a high donor strength, lead to the results in Table 2.3:

**Table 2.3** Ionisation ability of three aprotic solvents.

| Solvent | ε | Donor strength | % Ionisation |
|---|---|---|---|
| $D_1$ | 10 | Medium | 53 |
| $D_2$ | 35 | Medium | 75 |
| $D_3$ | 10 | High | 77 |

According to the table, a compound can be ionised to a greater extent by a solvent with a low dielectric constant and high donor-strength ($D_3$) than by a solvent with a high dielectric constant that exerts only medium donor-strength ($D_2$). In a donor-solution, the anions have to compete with solvent molecules for coordination and thus, may be regarded as competitive ligands.

The importance of donor-strength in coordination chemistry has created the need to define donor-strength as a relative magnitude with regard to a reference acceptor. As a reference acceptor, Gutmann[184] has chosen antimony(V) chloride, as this forms 1:1 adducts with various donors.

$$D + SbCl_5 \rightleftharpoons D{\cdot}SbCl_5 \qquad -\Delta H_{D\cdot SbCl_5}$$

and $$K_{D\cdot SbCl_5} = \frac{a_{D\cdot SbCl_5}}{a_D \times a_{SbCl_5}}$$

In a diluted solution of 1,2-dichloroethane, it was found that log $K_{D\cdot SbCl_5}$ is directly proportional to $-\Delta H_{D\cdot SbCl_5}$. As a measure of donation properties of donor solutions, the negative $\Delta H_{D\cdot SbCl_5}$-value was identified as the donor number, $DN_{SbCl_5}$, or donocity, Dn. A donocity-value expresses the total interaction of a donor with $SbCl_5$, including electrostatic interactions, like Van der Waal-forces. Donocity-values,[185] together with dielectric constants of a number of known solvents, are given in Table 2.4.

[185] Mayer, U. and Gutmann, V., *Adv. Inorg. Chem. Radiochem*., **17**, 189 (1975).

**Table 2.4** Donocity-values and dielectric constants of a number of known solvents.

| Solvent | Dn | ε |
|---|---|---|
| 1,2-Dichloroethane | 0 | 10.1 |
| Benzene | 0.1 | 2.28 |
| Nitromethane | 2.7 | 35.9 |
| Acetonitrile | 14.1 | 38.0 |
| Ethyl acetate | 17.1 | 6.0 |
| Methanol | 19 | 32.6 |
| Dimethylformamide | 26.6 | 36.1 |
| Dimethylsulphoxide | 29.8 | 45.0 |

Donocity is also a measure of the kinetic concept nucleophilicity, which can be regarded as the ability of a Lewis base to act as an incoming ligand and to influence the rate of a nucleophilic substitution reaction. Because the ability to form a bond is dependent upon the attributes of the other reactant, donocity can, at best, be used as a semi-quantitative value. But, essentially, it can be used as a qualitative value, like electronegativity.

The increasing degree of ionisation of a covalent salt with increased solvent donocity was found, for example, in the behaviour of cobalt(II)iodide.[184] In nitromethane, NM, with Dn = 2.7, a tetrahedral adduct, $[CoI_2(NM)_2]$, is formed, while complete ionisation may be observed in a solvent with a high donocity, like DMSO (Dn = 29.8):

$$CoI_2 + 6DMSO \rightleftharpoons [Co(DMSO)_6]^{2+} + 2I^-$$

Generally speaking, the ionisation ability of a solvent increases with an increase in donocity and dielectric constant.

Separation of donor and polarity effects in reactions, which are influenced by solvents, is prevented largely by the relatively high nucleophilicity often revealed by polar solvents. In order to overcome this limitation, Wax and Bergman[186] undertook a study of solvent coordination during CO-insertion reactions (reaction scheme 3.18) in

[186] Wax, M.J. and Bergman, R.G., *J. Am. Chem. Soc.*, **103**, 7028 (1981).

which they utilised a series of methyl substituted tetrahydrofuranes that varied moderately with regard to their donocity values, but not their dielectric constants (structures 18 – 21).

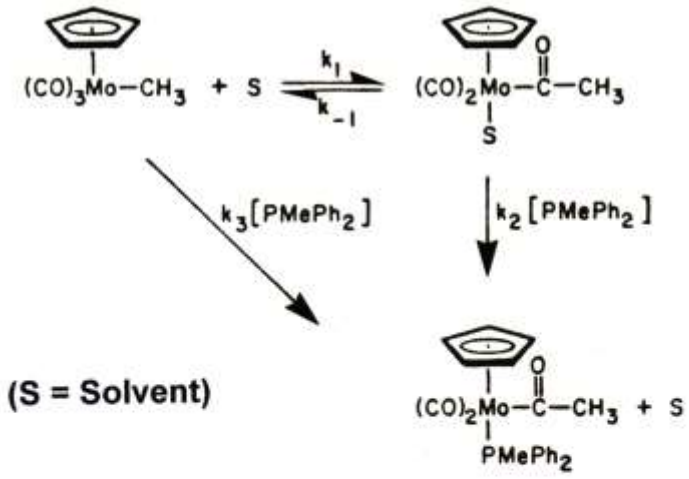


**3.18**

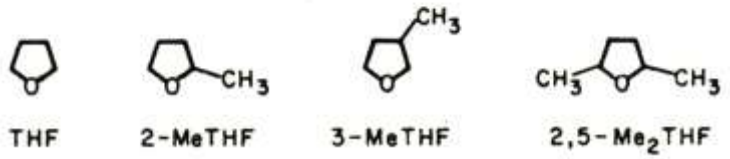


**18** **19** **20** **21**

These researchers have also succeeded in establishing clear evidence of solvent-coordination. In addition to the difference in nucleophilicity, the steric effect of the substituted tetrahydrofuranes was considered as an important factor in the coordination of THF to molybdenum. This could have had a significant influence on the value of $k_1$. As is evident from Table 2.5, the $k_1$-values decrease drastically from THF to 2,5-$Me_2$THF.

**Table 2.5** Rate of coordination of tetrahydrofuran and three methyl-substituted tetrahydrofuranes to molybdenum according to reaction scheme 3.18

| **Solvent** | **$10^4$ $k_1$ ($s^{-1}$)** | **$k_1/k_2$ (M)** | **$10^4$ $k_3$ ($M^{-1}s^{-1}$)** |
|---|---|---|---|
| THF | 7.78(7) | 0.0104(4) | 1.73(8) |
| 3-MeTHF | 6.46(5) | 0.0082(5) | 1.86(8) |

| | | | |
|---|---|---|---|
| 2-Me THF | 1.48(5) | | 1.95(12) |
| 2,5-Me2THF | 0.23(3) | | 1.67(7) |

Cotton and Dunstan[187] also suggested two competing pathways (in a mechanism similar to scheme 3.18) for the reaction of alkylisocyanides with [($\eta^5$-$C_5H_5$)$(CO)_3$Mo($CH_2$·$C_6H_5$)]. The one pathway, via a so-called solvent-stabilised intermediate, is preferably followed by solvents with high donocities and for low concentrations of inducing nucleophiles of moderate strength. Such a solvent-stabilised intermediate, in which the solvent is coordinated to the metal, is only observable directly in reactions of [($\eta^5$-$C_5H_5$)$(CO)_2$FeR] in the strong donor solvent, DMSO.[188,189] The pathway is completed through substitution of the solvent molecule by the nucleophile.[187] The competing reaction route that proceeds, by and large, in non-polar solvents and high concentrations of strong nucleophiles, comprises a direct attack from the nucleophile on the metal in order to yield the product. The observed rate constant of this reaction is given as $k_{obs} = k_1 + k_3[L]$ for a high concentration of L. As expected, an almost zero intercept was obtained for a non-coordinative solvent like cyclohexane, when $k_{obs}$ was plotted against [L], so that $k_{obs} \approx k_3[L]$. The rate constant, $k_1$ could also have been represented by $k'_1[S]$. In an attempt to represent this reaction route as a second-order process, values of $k_1$ were divided by the concentration of the solvent (in mol $dm^{-3}$) to obtain a more realistic comparison of the relative donor-ability of the solvent and isocyanide. The results are shown in Table 2.6.

**Table 2.6** Rate constants for the reaction of [($\eta^5$-$C_5H_5$)$(CO)_3$Mo($CH_2$·$C_6H_5$)] with t-butylisocyanide at 28°C.

| **Solvent** | **$10^4$ $k_1$ ($s^{-1}$)** | **$10^4$ $k_1'$ ($M^{-1}s^{-1}$)** | **$10^4$ $k_3$ ($M^{-1}s^{-1}$)** |
|---|---|---|---|
| Cyclohexane | 0 | 0 | 0.39 |
| Tetrahydrofurane | ≈1 | ≈0 | 0.4 |

[187] Cotton, J.D. and Dunstan, P.R., *Inorg. Chim. Acta*, **88**, 223 (1984).

[188] Cotton, J.D., Crisp, G.T. and Johari, L., *Inorg. Chim. Acta*, **47**, 171 (1981).

[189] Nicholas, K., Raghu, S. and Rosenblum, M., *J. Organomet. Chem.,* **78**, 133 (1974).

| | | | |
|---|---|---|---|
| Acetonitrile | 2.84 | 0.15 | 0.33 |
| Dimethylsulphoxide | 40 | 2.9 | - |

The significant variation in $k_1$ with the solvent, is regarded as an indication of solvent-metal interactions for the $k'_1$-value, rather than a simple account of the polarity of the medium. In contrast, the $k_3$-value is only a result of the normal solvolysis of such a complex.

For the oxidative addition of *trans*-[IrCl(CO){P($Et_nPh_{3-n}$)$_3$}$_2$] with alkyl halides, Ugo[123] and associates observed large ΔS*-values and solvent effects. It is not only attributed to the significant dipolar interaction between the addend and the metal ($S_N2$-type), but also to the large degree of transformation postulated for the three-centred transition state.

According to Haga, Kawakami and Tanaka,[190] the ΔH*- and ΔS*-values will indicate significant solvent dependency when the mechanism proceeds via a dipolar intermediate. In a polar solvent, like acetone or acetonitrile, the solvent molecule surrounding the cationic complex should be orientated strongly and the charge separation induced by the formation of a dipolar intermediate will cause a stronger orientation of the solvent molecule at the activated complex than at the reactants. A negative value for ΔS* and a small ΔH*-value should be observed under such conditions in a polar solvent, as the dipolar intermediate is stabilised through solvation.

The influence of the solvent on the formed product is clearly illustrated by Collman's study[177] of the reaction of Vaska's compound with acylazides (reaction 3.19).

[190] Haga, M., Kawakami, K. and Tanaka, T., *Inorg. Chim. Acta*, **12**, 93 (1975).

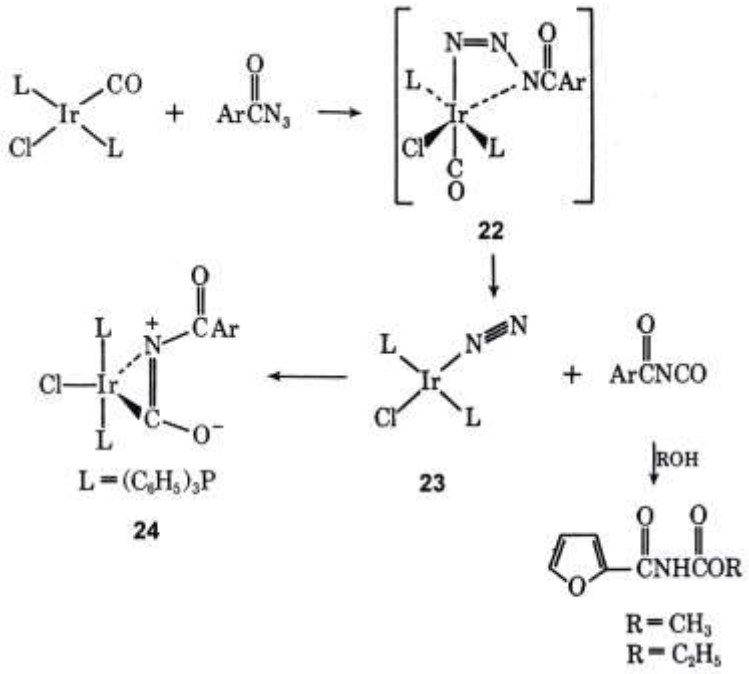


**3.19**

The course of the reaction in pure chloroform yields product 24, while a chloroform/ethanol blend yields product 23. As an explanation, the reaction of ethanol with the product of the first phase of the reaction, acylisocyanide, was presented. This prevented further reaction of acylisocyanide with the $N_2$-complex.

Often, reactions of solvents with a metal complex are the cause of the instability of the complex. A further effect that has implications regarding the suitability of a particular solvent for comparative kinetic determinations is, e.g., the reaction of DMF with $CH_3I$.[100] This particular reaction could result in oxidative addition taking place according to another mechanism in DMF.

(5) Catalysis

The catalysis by iodide ions plays an important role in oxidative addition. In the iodide-catalysed methyl iodide addition to $[RhI(CO)L_2]$[191] (L = $AsPh_3$ or $SbPh_3$, but not $PPh_3$), L is substituted by an iodide ion (reaction 3.20) and the formed anionic complex adds $CH_3I$ much more rapidly than the neutral starter-complex, as expected for an elecrophilic attack at the metal.

[191] Forster, D., *J. Am. Chem. Soc*., **97**, 951 (1975).

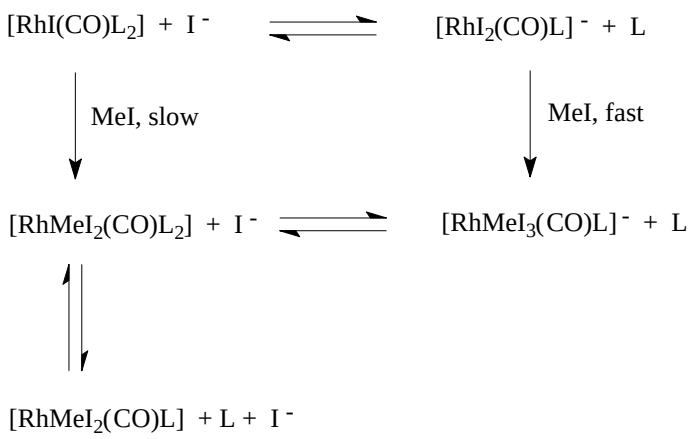


**3.20**

Although such a system is quite uncommon, the operation thereof can have profound outcomes. For example, dissociated triarylphosphine, resulting from $[RhI(CO)L_2]$ reacts with $CH_3I$ to form $[PAr_3Me]^+I^-$. This iodide ion coordinates, in turn, with rhodium to form $[RhClI(CO)L]^-$, that reacts more rapidly than the original complex.[192] An induction period, sometimes observed in such reactions, can be explained on the above grounds.[100,192]

Iodide ion catalysis of a different kind was found with $[Ir(COD)(phen)]^+$.[193] Instead of substituting another ligand, $I^-$ adds to $[Ir(COD)(phen)]^+$ and the five-coordinated [IrI(COD)(phen)] undergoes a more rapid addition with $CH_3I$ than the square-planar complex (reaction 3.21).

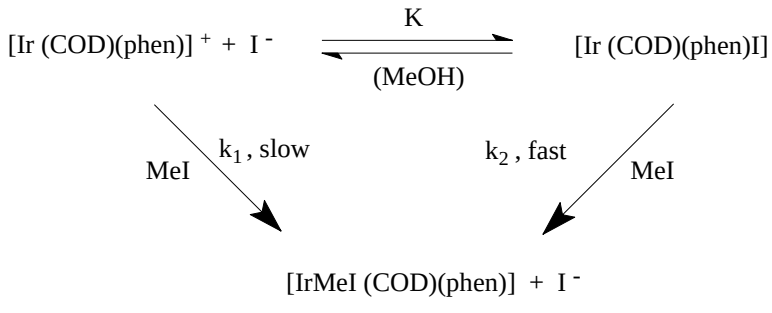


**3.21**

Activation parameters for the iodide-catalysed $k_2$-step, an expected $S_N2$-substitution of $I^-$, concur with the $k_1$-step value, pointing to the same configuration of the transition state.

[192] Franks, S., Hartley, F.R. and Chipperfield, J.R., *Inorg. Chem*., **20**, 3238 (1981).

[193] De Waal, D.J.A., Gerber, T.I.A. and Louw, W.J., *Inorg. Chem*., **21**, 1259 (1982).

The role of solvent coordination in nucleophilic catalysis has briefly been referred to in previous sections. Evidence of solvent coordination not being that exceptional, Bercaw[194] deliberately synthesised platinum solvento complexes with, for example, acetone and acetonitrile as ligands. In the study of the oxidative addition of [Rh(cupf)(CO)($PX_3$)][195] with $CH_3I$, a reaction mechanism was proposed where the reaction proceeds through two competing rate-determining steps. The $k_1$ path implies a nucleophilic attack on $CH_3I$, giving a 16-electron five-coordinate intermediate, whereas the solvent-assisted $k_2$ path proceeds via a solvent-stabilised *tbp* intermediate. The solvent-assisted $k_2$ path was viewed as an oxidative addition catalysis phenomenon similar to the solvent effects in the migratory insertion of CO into transition metal alkyl bonds. The fast dissociative trapping of the solvent-stabilised *tbp* intermediate by $CH_3I$ during its conversion to the ionic intermediate of the $k_1$ path was proposed. This solvent-stabilised intermediate, being still a Rh(I) complex, is also expected to be much more reactive towards $CH_3I$, since the stereochemical transformation, similar to that of the ionic intermediate, has already been taken care of during the $k_2$ step.

## 2.2.2 Insertion reactions

### *2.2.2.1 Introduction*

The concept of insertion is defined as a reaction in which any atom or group of atoms is inserted between two bonded atoms:[1,196]

$$L_nM—X + YZ \longrightarrow L_nM—(YZ)—X$$

The YZ species is, by definition, unsaturated. This makes it possible for the bonding electrons to be redistributed. Examples of this unsaturated species are $CO_2$, $CS_2$, $SO_2$, $SO_3$, carbenes and olefines. Insertion reactions can be regarded as being

[194] Wong-Foy, A.G., Henling, L.M., Day, M., Labinger, J.A. and Bercaw, J.E., *J. Mol. Catal. A Chem*., **189**, 3 (2002).

[195] Basson, S.S., Leipoldt, J.G., Roodt, A. and Venter, J.A., *Inorg. Chim. Acta*, **128**, 31 (1987).

[196] Ziegler,T., *J. Am. Chem. Soc*., **108**, 612 (1986).

either intra-[197] or inter-molecular[198] depending on whether or not the inserted group was coordinated beforehand.

#### *2.2.2.2 Carbonyl insertion reactions*

The most intensively studied insertion reactions are those where CO is inserted into metal-carbon alkyl bonds to form metal-acyl bonds. These reactions have important catalytic and industrial importance.

These reactions have been studied kinetically as a result of the direct link with the industrial hydroformylation of alkenes in the presence of a cobalt carbonyl catalyst.

Mechanistic studies were conducted by using mainly $[CH_3Mn(CO)_5]$, $[(\eta^5\text{-}C_5H_5)Fe(CO)_2Me]$ or related complexes. Using $^{14}CO$ as a tracer, the following became evident:[199,200] (a) the CO molecule that becomes the acyl carbonyl is not derived from external CO but it one already coordinated to the metal atom, (b) the incoming CO is added *cis* to the acyl group and the existing alkyl of the complex migrates to a *cis*-bound CO-group, that is,

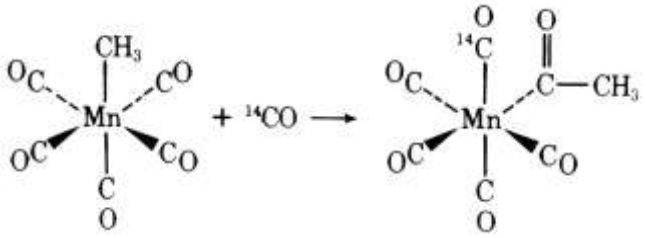

(c) The conversion of alkyl into acyl can be effected by the addition of nucleophilic ligands, other than CO,for example,

[197] Noack, K., Calderazzo, F., *J. Organomet. Chem.,* **10**, 101 (1967).

[198] Yamamoto, Y. and Yamazaki, H., *J. Organomet. Chem.,* **24**, 717 (1970).

[199] Erker, G., *Acc. Chem. Res*., **17**, 103 (1984).

[200] Andersen, G.K. and Cross, R.J., *Acc. Chem. Res*., **17**, 67 (1984).

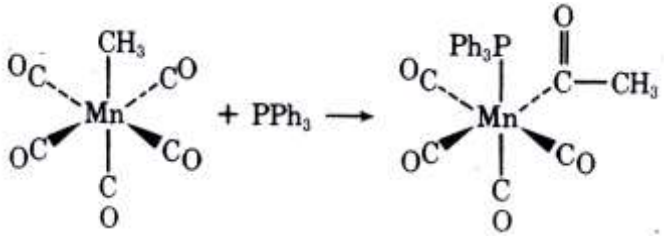

The first step involves an equilibrium between the octahedral alkyl and a square pyramidal five-coordinated acyl.[201] The coordinately unsaturated acyl then adds the incoming ligand L (CO, $PPh_3$, etc) with the reformation of an octahedral complex,

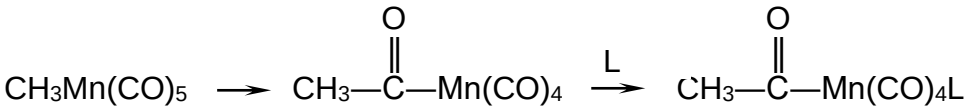

The activation energy for this insertion reaction[202] was determined as 70.2 kJ $mol^{-1}$ while the unsaturated intermediate is about 41.3 kJ $mol^{-1}$ less stable than $CH_3COMn(CO)_5$. In addition, it is important to note that there might be more than one isomer of the final product since five-coordinated intermediates can undergo stereochemical rearrangements.

The M(CO)R specie normally reacts with a wide range of ligands L, for example: phosphines, phosphites, arsines, stibines, organic amines, iodide and carbonyl, to form the corresponding acyl. The reverse of carbonyl insertion is known as decarbonylation, which causes the loss of a CO group. This process can occur either spontaneously, when heated or as a result of photolysis. For example, Booth and Chatt[203] discovered that the alkyl and aryl derivatives of Pd(II), Pt(II), Ni(II) and Co(II) undergo reversible insertion reactions as typified by the following reaction:

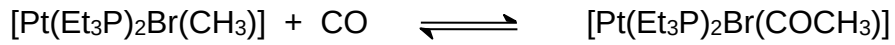

[201] Wright, S.C. and Baird, M.C., *J. Am. Chem. Soc*., **107**, 6899 (1985).

[202] Axe, F.V. and Marynick, D.S., *Organometallics*, **6**, 572 (1987).

[203] Booth, G. and Chatt, J., *Proc. Chem. Soc*., 67 (1961).

Although carbonyl insertion normally involves the transformation of an alkyl complex into an acyl complex, the rearrangement of acyl back to alkyl is also possible. These reactions involving the migration of an alkyl group to a metal are usually solvent catalysed[204] or are catalysed by the presence of an additional ligand.[205]

Carbonyl insertion reactions proceed intramolecular and the reaction will only take place if the CO and R are in a *cis*-orientation relative to each other in the reacting complex. This condition is illustrated in planar macrocyclic metal complexes where the macrocyclic ligand occupies the square planar plane so that no *cis*-migration can take place. For example, although both the alkyl and acyl derivatives of macrocyclical rhodium(III) complexes are stable compounds, conversion from one to the other by means of carbonylation or decarbonylation cannot take place. This is thus a clear illustration that the two active ligands must be *cis* to each other.

#### *2.2.2.3 The mechanism of carbonyl insertion reactions*

The carbonyl insertion reaction are a 1,2-migration of an alkyl group to a coordinated carbonyl ligand in a *cis*-position, proceeding through a three-centre transition state.

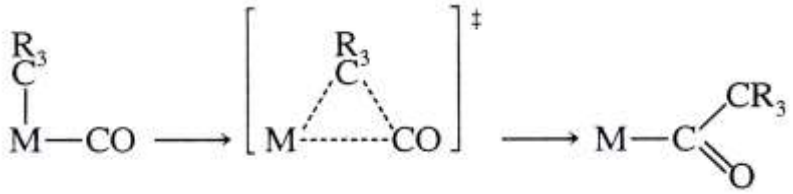

Heck and Garrou[206] proposed the following mechanism for the carbonylation of halo-bis(ligand) organoplatinum(II), -palladium(II) and -nickel(II) complexes:

[204] Kubota, M., Blake, D.M. and Smith, S.A., *Inorg. Chem*., **10**, 1430 (1971).

[205] Bennett, M.A., Jeffery, J.C. and Robertson, G.B., *Inorg. Chem*., **20**, 323 (1981).

[206] Garrou, P.E. and Heck, R.F., *J. Am. Chem. Soc*., **98**, 4115 (1976).

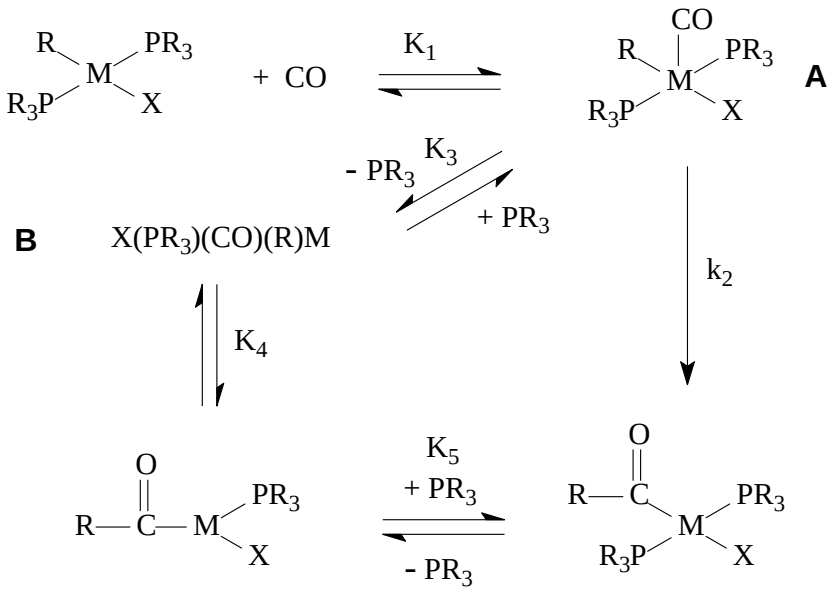


Intermediates A and B were characterized by IR and NMR data and, in some cases, have even been isolated to prove their existence. In view of the fact that the final products have also been isolated, the reaction scheme can be regarded as a true mechanistic representation of a carbonyl insertion reaction. In addition, it appeared that an increase in the $PR_3$ concentration resulted in a decrease in the quantity of B so that the reaction path $k_3$ was suppressed by $k_4$ and $k_5$. The direct migration route, $k_2$, is controlled experimentally by the equation, $-d[CO]/dt = k_2K_1[A][CO]$.

In all the examples studied, it has been found that the reaction proceeds more readily via the indirect dissociative route through $k_3$, $k_4$ and $k_5$ than through the direct migration route, $k_2$. This example demonstrates clearly that an excess (or even the mere presence) of an additional ligand exerts a definite influence on the insertion reaction.

The fact that the solvent also plays a role in the insertion reaction is clearly noticeable in the DMSO activated CO-insertion in $[(\eta^5\text{-}C_5H_5)Fe(CO)_2R]$:[207]

[207] Nicholas, K., Raghu, S. and Rosenblum, M., *J. Organomet. Chem.,* **78**, 133 (1974).

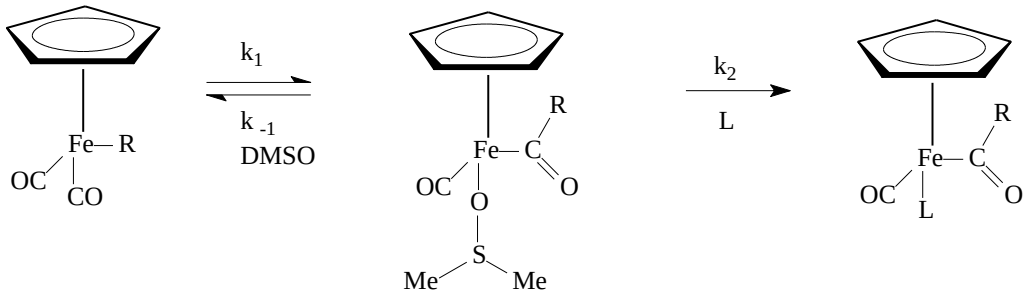


The DMSO-coordinated intermediate was identified with the aid of NMR and the rate constants could all be determined individually. Thus, it is clear that the carbonyl insertion mechanism do not only represent a direct route but that a solvent-supported route could also be present.

A more comprehensive mechanism for CO insertion can be described by the reaction scheme[4,208] in Figure 2.20.

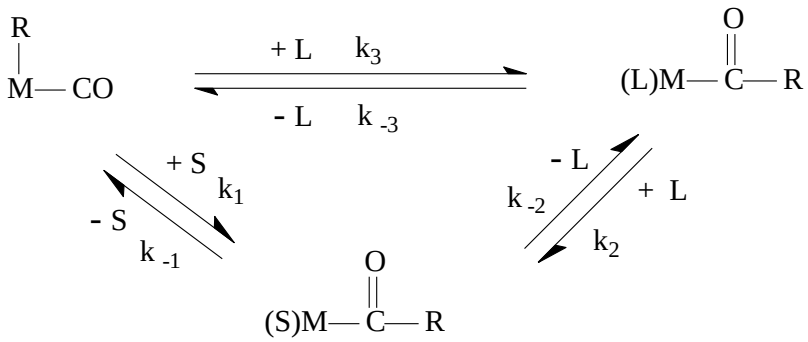


**Figure 2.20** Mechanism for CO insertion

If the steady state approximation is applied to the concentration of the intermediate, the following expression is obtained for the rate law:

$$\frac{d[M(COR)L]}{dt} = k_1[M(CO)R] - k_{-1}\left[\frac{k_1[M(CO)R] + k_{-2}[M(COR)L]}{k_{-1} + k_2[L]}\right] + k_3[M(CO)R][L] - k_{-3}[M(COR)L]$$

Based on the assumption that all insertion reactions run completely (which is, in fact, usually the case), $k_2$ and $k_3$ can be regarded as insignificantly small so that the rate law can be reduced to the following (3.22):

[208] Wojcicki, A., *Adv. Organomet. Chem.,* **11**, 87 (1973).

$$\frac{d[M(COR)L]}{dt} = \frac{k_1 k_2 [M(CO)R][L]}{k_{-1} + k_2[L]} + k_3[M(CO)R][L] \qquad \textbf{3.22}$$

This expression consists of two terms that are known as the $k_1$-(solvent) and $k_3$-(direct) paths respectively. The mechanistic options will be discussed briefly.

(1) $k_1$ path

If only the $k_1$ path is present, and there is no interaction between the acyl and L, expression 3.22 can be reduced to one of the following: (a) If $k_{-1} << k_2[L]$, the intermediate would react more readily with ligand L than to revert to the alkyl so that the $k_1$ term in 4.19 is reduced to: d[M(COR)L]dt = $k_1$[M(CO)R]. The rate law is thus first-order in the starting material, [M(CO)R], and independent of the concentration of the incoming ligand L so that $k_{obs} = k_1$. Thus, this first order behaviour indicates that the solvent is acting as a ligand. (b) If $k_{-1} >> k_2[L]$, a low concentration of the acyl-intermediate reacts with the external ligand at a rate much slower than the reversal to the alkyl so that the $k_1$-term in 3.22 is reduced to: d[M(COR)L]/dt = $K_1k_2$[M(CO)R][L], $K_1 = k_1/k_{-1}$. Second order kinetics are observed so that $k_{obs} = K_1k_2[L]$. The rate constant $k_2$ is sensitive to the nature of L so that more nucleophilic ligands give rise to an increase in $k_{obs}$. In these cases (where pure second-order behaviour is observed), the $k_1$-path cannot be distinguished from the $k_3$-path. (c) The condition when $k_{-1} \approx k_2[L]$ is reached by increasing the concentration of L or when the nucleophilicity of the ligand L increases. Then $k_{obs} = k_1k_2[L]/(k_{-1} + k_2[L])$ and reach a limit value at high [L].

(2) $k_3$ path

This route can occur alone or with the $k_1$-path. If the concentration of L is made relatively high, it diminishes the importance of $k_1$ so that 3.22 is reduced to:

$$d[M(COR)L]/dt = k_1[M(CO)R + k_3[M(CO)R][L] \text{ and}$$

$$k_{obs} = k_1 + k_3[L]$$

Further support for the MCOR intermediate comes from studies of a related pair of reactions. Rate constants were found to be identical for the substitution of CO in $CH_3$–CO–$Mn(CO)_5$ and for the decarbonylation of the acyl compound. This implies that the rate-determining step in both reactions is loss of CO to give the MCOR

intermediate, which can either be trapped by the nucleophile $PPh_3$ or rearrange to the alkylmanganese complex (reaction 3.23)

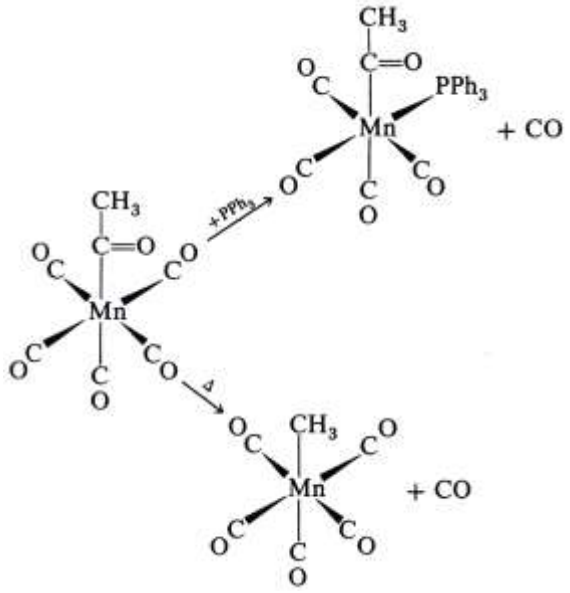


**3.23**

#### *2.2.2.4 Factors that influence the rate of carbonyl insertion reactions*

The mechanism according to which carbonyl insertion reactions proceed, can include either a coordinative unsaturated acyl complex or a $\pi$-acyl derivative[209] as intermediate. The steric and electronic nature of this intermediate will influence the rate of migration, and all factors that influence this intermediate will thus influence the rate of the reaction. For example, it is known that in some insertion reactions the solvent catalyses the formation of an acyl intermediate, while in others it stabilises the intermediate. In addition, some structures undergo molecular rearrangement in certain solvents while no rearrangement takes place in others. Bound ligands with a large steric parameter retard insertion, for example, while the nature of the migrating groups is also a determining factor. Thus it is clear that several factors can contribute to an increase or decrease in the reaction rate; or can even result in no insertion taking place.

(1) <u>The metal</u>

Carbonyl insertion reactions have been observed in several transition metal complexes. Consequently it seemed that the reactivity of transition metals in terms of

[209] Hitch, R.R., Gondal, S.K. and Sears, C.T., *Chem. Comm*., 777 (1971).

CO insertion was given as 3d > 4d > 5d. This tendency is illustrated in the reaction of $[MCl(CO)L_2] + CH_3I$, where in the case of Rh[100] (4d), the first step, oxidative addition, is reversible. Furthermore converts the alkyl product to the acyl end product in a final step. In the case of Ir[140] (5d) is the oxidative addition step irreversible and only lead to the alkyl product with no acyl formation. These tendencies can be attributed to the fact that 5d- transition metals form stronger metal-carbon bonds so that the rate of migration decreases.

(2) <u>The migrating groups</u>

As a model for the migration step in the rhodium-catalysed carbonylations, Maitlis[210] and associates studied the reaction of $[(C_5Me_5)RhR(CO)I]$ with $PPh_3$ to form the acyl product. In this reaction, the R-group was varied.

$$(C_5Me_5)RhR(CO)I + PPh_3 \longrightarrow (C_5Me_5)Rh(\overset{\overset{O}{\|}}{C})R(PPh_3)I$$

R = Me, Ph, *p*-$XC_6H_4$ with X = H, Me, Cl, CHO, CN, $NO_2$

Kinetic studies in different solvents showed that the general mechanism involves a direct bimolecular attack of the triphenylphosphine on the alkyl in both polar and non-polar solvents, that reactions were very fast and that the migration ability of phenyl (R) is larger than that of methyl. The aforementioned result is ascribed to entropy factors (ΔS* smaller if R = Ph compared to R = Me) despite the entropy preference of methyl to phenyl. However, a previous study showed that methyl migrates faster than phenyl with a factor of 8 in the case of $[MnR(CO)_5]$.[208,211] A fiftyfold thermodynamic preference of phenyl above methyl for the reverse migration from RCO-Re to R-Re(Co), and an approximate 28-fold kinetic preference of methyl migration of the five coordinated intermediate $[Re(CO)_3(COMe)(COPh)]^-$ has also been reported.[212]

The carbonylation reaction studied by Maitlis, was further varied in terms of *para*-substituted phenyl. Kinetic studies were conducted under pseudo-first-order

[210] Sunley, G.J., Fanizzi, F.P. and Maitlis, P.M., *J. Chem. Soc., Dalton Trans*., 1799 (1990).

[211] Wojcicki, A., *Adv. Organomet. Chem.,* **12**, 33 (1974).

[212] Casey, C.P. and Scheck, D.M., *J. Am. Chem. Soc*., **102**, 2723 (1980).

conditions with a large excess (> x 10) $PPh_3$ so that its concentration can be taken as constant. Second-order kinetics was observed, and since no equilibrium was observed ($k_3$ >> $k_{-3}$, Figure 2.20), the rate is given as $k_3$[alkyl][$PPh_3$] with $k_{obs}$ = $k_3$[$PPh_3$]. This results showed that the more electron donating *p*-substituted phenyls migrate faster so that the following tendency were obtained:

$$p\text{-}XC_6H_4, \qquad X = Me > H > Cl > CHO > NO_2 \approx CN$$

A Hammett plot of $k_3$ *vs* the corresponding σ is linear which indicates that there is no change in the migration mechanism from the most to the least reactive substrate. *Ab initio* calculations for the conversion of [$PdMe(H)(CO)PH_3$] to [$Pd(H)(COMe)PH_3$] were done by Koga and Morokuma.[213] They found that this conversion takes place via methyl migration and give reasons why CO insertion was not favoured. In addition, they found that the three-centred transition state was stabilised by the interaction between the methyl $sp^3$ , the CO-π* and the Pd (p and d) orbitals and that the methyl loses negative charge to CO in the course of the reaction. Substitution of methyl with ethyl lowers the calculated activation energy while substitution of methyl hydrogens with one or more electron withdrawing fluorine atoms caused a reasonable increase.

Although the metal, the oxidation state, d-electon number, CO-ligands and geometry are different from Maitlis's system, the general conclusion is in agreement with experimental data for several systems: that electron donating substituents on the organic group promotes its migration from the metal to CO. These *p*-phenyl substituent effects were observed for both the carbonylation of σ-aryls[214] and σ-benzyls.[215] Reverse migration (decarbonylation) should thus be favoured by electron withdrawing substituents on the organic group as was observed in the case of [$RhCl_2(PPh_3)_2(COR)$].[216]

[213] Koga, N. and Morokuma,K., *J. Am. Chem. Soc*., **108**, 6136 (1986).

[214] Saunders, D.R., Stephenson, M. and Mawby, R., *J. Chem. Soc., Dalton Trans*., 539 (1984).

[215] Cotton, J.D., Crisp, G.T. and Daly, V.A., *Inorg. Chim. Acta*, **47**, 165 (1981).

[216] Stille, J.K. and Regan, M.T., *J. Am. Chem. Soc*., **96**, 1508 (1974).

In an effort to evaluate the steric role of the migrating substituent, Cotton[217] studied the DMSO promoted carbonyl insertion of $[(\eta^5\text{-}C_5H_5)Fe(CO)_2R]$. He obtained a 600-fold difference for the $K_1$ values between the fastest measurable reaction ($Me_3CCH_2$) and the slowest (Me). The reactivity order of selected R-ligands can be given as follows: $(Me_3Si)_2CH > Me_3CCH_2 > Me_3SiCH_2 > CyCH_2 > Et > Me$. The interpretation of this order should include both steric and electronic factors. However, there are contradictions in the interpretation of these electronic effects[218] and so this result is explained more readily using steric effects. The reactivity order correlates with an intuitive feeling for the size of alkyl groups and explains, for example, the higher reactivity of $Me_3CCH_2$ compared with $Me_3SiCH_2$ in terms of the longer Si–C bond in comparison with the C–C bond. The above mentioned result suggests that the increase in reactivity can be associated with the relief of steric strain in the three-centred transition state as the metal-alkyl bond gets longer and partially breaks. With regard to the reactivity order, other researchers have also observed similar tendencies.[219]

(3) The incoming ligand and the solvent

The migration of a coordinated organic group R to a coordinated carbonyl of a metal, promoted by an incoming nucleophile, has been intensively studied. Craig and Green[220] investigated the reaction of $[(\eta^5\text{-}C_5H_5)(CO)_3MoR]$ with varying concentrations of phosphines and phosphites to form $[(\eta^5\text{-}C_5H_5)(CO)_2Mo(COR)L]$ (R = Me and Et, L = phosphines and phosphites). They found the rate of the reaction to be independent of both the type of L-ligand and the L-ligand concentration. With R = Et, a faster reaction was observed compared to when R = Me. The alkyl migration was promoted by the incoming phosphorous ligands but it is unlikely that a solvated intermediate was involved.

[217] Cotton, J.D., Crisp, G.T. and Latif, L., *Inorg. Chim. Acta*, **47**, 171 (1981).

[218] Charton, M., *J. Am. Chem. Soc*., **99**, 5687 (1977).

[219] Green, M. and Westlake, D.J., *J. Chem. Soc.,* **A***,* 367 (1971).

[220] Craig, P.J. and Green, M., *J. Chem. Soc.,* **A***,* 1978 (1968).

Cotton found, contradictory to the above result, that the steric influence of the incoming ligand does in fact influence the reaction rate.[221] He examined the DMSO-promoted reaction of $[(\eta^5\text{-}C_5H_5)(CO)_2Fe(CH_2Cy)]$ with phosphines (with varying steric parameters) to form the product $[(\eta^5\text{-}C_5H_5)(CO)(L)Fe(COCH_2Cy)]$. No correlation with the electronic parameter was observed, but a well-defined decrease in rate with increasing cone angle was evident. The decrease is gradual for angles from 120 to 130° but much steeper at larger cone angles. In phosphines with much larger cone angles, e.g. $PCy_3$ (170°) there is no marked reaction. These tendencies can be explained by the availability of space at the metal centre in which the entering nucleophile (L) has to fit (to be able to react) during the formation of the transition state. If the nucleophile is smaller than the space, the steric interactions are minimal and the rate constants vary very little with a varying cone angle. However, when the size of the nucleophile is comparable with the available space, the intermolecular interactions increase drastically with increasing cone angle so that the activation energy of the reaction increases accordingly. Very large nucleophiles cannot come close enough to the metal to establish a bonding interaction with the metal centre and consequently no detectable reaction occurs.

Butler, Basolo and Pearson[222] investigated the carbonyl insertion of several iron and molybdenum complexes. They found that the reactions of $[CH_3Mn(CO)_5]$ with phosphines and phosphites in tetrahydrofurane occur faster than the corresponding reactions of $[(\eta^5\text{-}C_5H_5)(CO)_2Fe(CH_3)]$ and $[(\eta^5\text{-}C_5H_5)(CO)_3Mo(CH_3)]$ that take place *via* the same mechanism. This difference in rates is ascribed to the strength of the methyl-metal bonds since the reaction mechanism includes methyl migration. $[(\eta^5\text{-}C_5H_5)(CO)_2Fe(CH_3)]$ reacts with L, that is, $PPh_3$, $P(C_4H_9)_3$ and $P(OC_4H_9)_3$ to form $[(\eta^5\text{-}C_5H_5)(CO)Fe(COCH_3)L]$. At lower concentrations, the reaction rate depends on the phosphorous-ligand concentration but a saturation rate is reached at higher concentrations. No reaction is observed with cyclohexylamine. Bibler and Wojcicki[223] obtained similar results with other nucleophiles and suggested that, considering that the nucleophiles that do not react are weaker $\pi$- bonding ligands than phosphines

[221] Cotton, J.D. and Markwell, R.D., *Inorg. Chim. Acta*, **63**, 13 (1982).

[222] Butler, I.S., Basolo, F. and Pearson, R.G., *Inorg. Chem*., **6**, 2074 (1967).

[223] Bibler, J.P. and Wojcicki, A., *Inorg. Chem*., **5**, 889 (1966).

and phosphites, their inability to react can be ascribed to insufficient π-bonding capacity of the donor atom. This reasoning is supported by the fact that [($\eta^5$-$C_5H_5$)$(CO)_2Fe(CH_3)$] undergoes insertion reactions with CO and $SO_2$, both of which are good π-bonding ligands. This also explains why cyclohexylamine, that cannot form π-bonds, does not react. The rate constants for the formation of the intermediate compare well with each other. This indicated the presence of a solvent-supported intermediate. An order of reactivity rate of $P(C_4H_9)_3 < P(OC_4H_9)_3 < PPh_3$ was obtained which is in accordance with its nucleophilic nature.

The incoming ligand and the solvent have a close relationship, and sometimes the solvent takes over the role of incoming ligand. Bibler and Wojcicki also observed the effect of the solvent in the reaction of [($\eta^5$-$C_5H_5$)$(CO)_2Fe(CH_3)$] with $PPh_3$. Under similar conditions, the above reaction runs completely in tetrahydrofurane to form [($\eta^5$-$C_5H_5$)$(CO)Fe(COCH_3)(PPh_3)$] while no reaction occurs in hexane. This result is in accordance with the proposed mechanism where the coordinated solvent can support a reaction route. The kinetic data of [($\eta^5$-$C_5H_5$)$(CO)_3Mo(CH_3)$] shows that the resulting mechanism is dependent on the interplay between the coordinating ability of the solvent and the nucleophilicity of the entering ligand. The insertion reactions of the above complex are extremely sensitive to changes, both in the solvent and in the nucleophile. The reaction rate is only dependent on the concentration of the nucleophile when the nucleophlity of the nucleophile is very high or the coordinated ability of the solvent is very low or both.

The study of Wax and Bergman[186] was already referred to during the discussion on the solvent as factor that influences oxidative addition. They gathered evidence of the coordinating effect of the solvent in the carbonyl insertion reaction of [($\eta^5$-$C_5H_5$)$(CO)_3Mo(CH_3)$] in methyl substituted tetrahydrofuranes as solvent. Because the electronic effect of this substituted tetrahydrofuranes is about the same, the steric hindrance with regard to the direct coordination of the solvent to the metal during the transition state is the only explanation for the observed α-methyl substitution effect. The steric blocking of the solvent thus leads to a delay in the formation of the solvent-bound intermediate so that it can be considered a solvent-catalysed migration.

The behaviour of carbonyl insertion reactions in different types of solvents can be summarised as follows: In more polar solvents the reactions proceed via two consecutive equilibria. The first of these equilibria determines the rate which leads to the formation of an intermediate which is either coordinatively unsaturated or stabilised by solvent molecules. The second step, during which the ligand L is added to the intermediate, takes place very fast. In non-polar solvents, relatively slow second-order kinetics are observed that include a direct bimolecular reaction with the incoming ligand to yield the acyl in one step. These mechanisms sometimes occur simultaneously and first-order, second-order as well as saturation kinetics are observed, depending on the nature of the solvent and/or the nucoleophile.

(4) The bound ligands

The orientation of the bound ligands in a complex has an influence on the possible outcome of carbonyl insertion reactions. Anderson and Cross[224] prepared the three geometric isomers of [PtCl(Ph)(CO)($PMePh_2$)] and found that only the isomer with the phenyl *trans* to $PMePh_2$ undergoes carbonyl insertion. In this isomer, the large bond-weakening *trans*-influence of the tertiary phosphine ligand favours the migration of the organic group. No bond weakening occurs in the isomer with the phenyl *trans* to the chlorine, and thus no migration is possible. The third isomer does not have the necessary *cis* arrangement of Ph and CO for insertion.

The influence of bound ligands with different electron withdrawing properties on carbonyl insertion is demonstrated by the work of Hart-Davis and Mawby.[225] They studied the carbonyl insertion of [$RMo(CO)_3CH_3$] in THF with a range of different R-groups, varying in their electron withdrawing properties. R is an already bound, non-migrating ligand. Carbonyl insertion occurs via a solvent supported route to form the corresponding [$RMo(CO)_2(COCH_3)$] complex. For the different R-groups, a twenty-fold difference in the rate of carbonyl insertion between the fastest and slowest reactions was observed. This change of rate can be attributed to the electronic character of R. If R is more electron withdrawing, the metal-methyl bond weakens

[224] Anderson, G.K. and Cross, R.J., *J. Chem. Soc., Dalton Trans*., 1246 (1979).

[225] Hart-Davis, A.J. and Mawby, R.J., *J. Chem. Soc.,* **A***,* 2403 (1969).

accordingly so that its migration is favoured. Haynes,[226] studying the rhodium/iodide catalysed methanol carbonylation, agrees that electron-donating ligands, while promoting oxidative addition, normally retard CO insertion. The formation of stronger rhodium-methyl bonds for the more nucleophilic precursors is given as part of the explanation. Higher electron density on the metal also leads to stronger M(d) → CO($\pi$*) back-bonding which is also thought to inhibit CO insertion.[227]

(5) Other factors

Migration can be initiated by electrochemical[228] or chemical oxidation with $Ag^+$ or Ce(IV),[229] where transfer takes place more readily in the oxidised state. Protonic acids can favour migration. $[(\eta^5\text{-}C_5H_5)(CO)_2Fe(CH_3)]$ is normally unreactive, but carbonyl insertion takes place with 1% $HBF_4$ in $CH_2Cl_2$.[230] An increase in rate can be obtained through the addition of Lewis acids like $BF_3$ and $AlCl_3$ that complex with the acyl group.[231]

Several catalytic reactions involving CO are favoured by halide ions,[232] particularly iodide. A study of osmium cluster compounds showed that the rate of insertion of $[Os_3(CO)_{10}(\mu\text{-}CH_2)(\mu\text{-}X)]^-$ was a hundred times faster than that of $[Os_3(CO)_{10}(\mu\text{-}CH_2)]$. This can be attributed to the fact that acyls are better electron accepters than alkyls or alkylidenes ($\mu\text{-}CH_2$) and are thus more able to stabilise the σ-donated electron density by $X^-$. The iridium/iodide-catalysed carbonylation of methanol[233] to acetic acid is promoted by carbonyl complexes of W, Re, Ru and Os and simple iodides of Zn, Cd, Hg, Ga and In. None of the promoters show any detectable activity in the absence of iridium catalyst. Mechanistic studies indicate that the promoters

[226] Gonsalvi, L., Adams, H., Sunley, G.J., Ditzel, E. and Haynes, A., *J. Am. Chem. Soc*., **121**, 11233 (1999).

[227] Margl, P., Ziegler, T. and Blöchl, P.E., *J. Am. Chem. Soc*., **118**, 5412 (1996).

[228] Therien, M.J. and Trogler, W.C., *J. Am. Chem. Soc*., **109**, 5127 (1987).

[229] Reger, D.L. and Mintz, E., *Organometallics*, **3**, 1759 (1984).

[230] Forschner, F.C. and Cutler, A.R., *Organometallics*, **4**, 1247 (1985).

[231] Cotton, J.D. and Markwell, R.D., *Organometallics*, **4**, 937 (1985).

[232] Earle, E. and Jablonski, C.R., *J. Chem. Soc., Dalton Trans*., 2137 (1986).

[233] Haynes, A, Maitlis, P.M., Morris, G.E., Sunley, G.J., Adams, H., Badger, P.W., Bowers, C.M., Cook, D.B., Elliot, P.I.P., Ghaffar, T., Green, H., Griffen, T.R., Payne, M., Pearson, J.M., Taylor, M.J., Vickers, P.W. and Watt, R.J., *J. Am. Chem. Soc*., **126**, 2847 (2004).

accelerate carbonylation of *fac,cis*-$[Ir(CO)_2I_3CH_3]^-$ by abstracting an iodide ligand from the Ir centre, allowing coordination of CO to give $[Ir(CO)_3I_2CH_3]$, identified by high-pressure IR and NMR spectroscopy. Migratory CO insertion is about 700 times faster for $[Ir(CO)_3I_2CH_3]$ than for *fac,cis*-$[Ir(CO)_2I_3CH_3]^-$, representing a lowering of $\Delta G^*$ by 20 kJ $mol^{-1}$. *Ab initio* calculations support a more facile methyl migration in $[Ir(CO)_3I_2CH_3]$, the principal factor being decreased $\pi$-back-donation to the carbonyl ligands compared to *fac,cis*-$[Ir(CO)_2I_3CH_3]^-$.

# 3 Synthesis of complexes

## 3.1 Introduction

The Rh(I) complexes involved in this study are of the type [Rh(LL′)(CO)($PX_3$)], with LL′ a β-diketone, cupferrate or neocupferrate, with the Rh(III) complexes the alkyl oxidative addition products thereof. These complexes were prepared for a crystallographic study (Chapter 4) and to act as starting complexes in the kinetic study (Chapter 5). Some of the complexes, those of acetylacetonato and thioacetylacetonato, were involved in previous studies in our group as well. The complexes of cupferrate and neocupferrate, however, are novel. In their synthesis a number of different phosphine (and one phosphite) ligands were selected to span a range of varying steric and electronic effects, the effect of which were to be investigated in kinetic studies.

The synthesis of all the mentioned rhodium complexes start with the reduction of $RhCl_3 \cdot 3H_2O$ by refluxing in dimethylformamide for approximately 30 minutes.[1] A generalised second step is the addition of an equivalent amount of bidentate ligand to the obtained yellow solution to form the dicarbonyl complex [Rh(LL′)$(CO)_2$],[2] which can be precipitated from solution by the addition of water. Details follow in section 3.2.

All chemicals were of reagent grade, and all preparations were carried out in air, except when indicated otherwise. $RhCl_3$ and $CH_3I$ were obtained from Merck and used without further purification. The phosphines, from Aldrich, were recrystallised from ethanol before use. The bicyclic phosphite ester, 4-methyl-2,6,7-trioxa-1-phosphabicyclo[2.2.2]octane was prepared in our laboratory. Cupferron and

[1] Varshavskii, Y.S. and Cherkasova, T.G., *Russ. J. Inorg. Chem*.., **12**, 1709 (1967).

[2] Goswami, K. and Singh, M.M., *Trans. Met. Chem.*, **5**, 83 (1980).

neocupferron (from Fluka) were recrystallised by precipitating with hexane from a 1:1 acetone/methanol solution to yield white (cupferron) and light brown (neocupferron) crystalline products.

Some of the complexes were subjected to element analyses, which were done by Mikroanalytisches Labor Pascher, in Remagen-Bandorf, Germany. A number of complexes were investigated by X-ray crystallography (Chapter 4) and the solved structures confirmed the outcome of the syntheses. Other techniques employed in the characterisation of the prepared complexes are IR spectrophotometry and NMR spectrometry. All IR measurements were done using KBr discs on a Hitachi model 270-50 spectrophotometer having a wavenumber accuracy of 2 $cm^{-1}$. NMR spectra were obtained on a Bruker 300-MHz spectrometer.

## 3.2 Synthesis of the complexes

### 3.2.1 The acac complexes

#### *3.2.1.1 Synthesis of [Rh(acac)(CO)($PX_3$)]*

A solution of $[Rh_2Cl_2(CO)_4]$ was prepared by refluxing a solution of $RhCl_3\ 3H_2O$ in dimethylformamide for approximately 30 minutes. An equivalent amount of acetylacetone was added to the resulting yellow solution. The solution was diluted with water, and the pink precipitate ($[Rh(acac)(CO)_2]$) was removed by centrifuging and washed with petroleum ether. $[Rh(acac)(CO)(PPh_3)]$ was prepared from $[Rh(acac)(CO)_2]$ as described by Bonati and Wilkinson,[3] and chromatographed on alumina using chloroform as eluant. $\upsilon_{CO}$ = 1986 $cm^{-1}$. Leipoldt and co-workers[4] solved the crystal structure of $[Rh(acac)(CO)(PPh_3)]$ earlier and confirmed the composition of the complex.

[3] Bonati, F. and Wilinson, G., *J. Chem. Soc.,* 3156 (1964).

Varying the phosphine ligand, employing P(*p*-$ClC_6H_4)_3$ and P(*p*-$MeOC_6H_4)_3$), the corresponding complexes, [Rh(acac)(CO)(P(*p*-$ClC_6H_4)_3$)] and [Rh(acac)(CO)(P(*p*-$MeOC_6H_4)_3$)] were prepared in a similar way, yielding IR spectra comparable to that of [Rh(acac)(CO)($PPh_3$)], with $\upsilon_{CO}$ = 1980 $cm^{-1}$ and 1972 $cm^{-1}$ respectively.

#### *3.2.1.2 Synthesis of [Rh(acac)(CO)($CH_3$)(I)($PX_3$)]*[5]

The alkyl oxidative addition product [Rh(acac)(CO)($CH_3$)(I)($PPh_3$)] was prepared by partly dissolving 0.632 g [Rh(acac)(CO)($PPh_3$)] in 25 $cm^3$ acetone, to which was added 0.5 $cm^3$ (five-fold excess) $CH_3I$. Stirring and heating (<35°C) for 10 minutes gave a clear yellow solution which gradually changed to a wine-red colour. The acetone was evaporated *in vacuo* after 3 h giving a viscous red oily residue. This was dissolved in 250 $cm^3$ diethylether followed by evaporation up to *ca*. 150 $cm^3$ with a strong air current. Addition of 50 $cm^3$ n-hexane gave a cloudy solution. Continued evaporation with an air-current up to *ca*. 150 $cm^3$ and storage at 0°C for 2 h gave a light brown precipitate, $\upsilon_{CO}$ = 2060 $cm^{-1}$. An element analysis yielded the following result, with the calculated value in parentheses: Rh, 16.30 (16.09); O, 7.40 (7.58); P, 4.78 (4.89) and I, 19.7 (20.04)%.

Varying the phosphine ligand, employing P(*p*-$ClC_6H_4)_3$ and P(*p*-$MeOC_6H_4)_3$), the corresponding complexes, [Rh(acac)(CO)($CH_3$)(I)(P(*p*-$ClC_6H_4)_3$)] and [Rh(acac)(CO)-($CH_3$)(I)(P(*p*-$MeOC_6H_4)_3$)] were prepared in a similar way, yielding IR spectra comparable to that of [Rh(acac)(CO)($CH_3$)(I)($PPh_3$)], with $\upsilon_{CO}$ = 2064 $cm^{-1}$ and 2056 $cm^{-1}$ respectively.

[4] Leipoldt, J.G., Basson, S.S., Bok, L.D.C., and Gerber, T.I.A., *Inorg. Chim. Acta*, **26**, L35 (1978).

[5] Basson, S.S., Leipoldt, J.G., Roodt, A., Venter, J.A. and Van der Walt, T.J., *Inorg. Chim. Acta*, **119**, 35 (1986).

## 3.2.2 The cupferrate and neocupferrate complexes

### *3.2.2.1 Synthesis of [Rh(cupf)(CO)(PPh$_3$)][6] and [Rh(neocupf)(CO)(PX$_3$)]*

A DMF refluxed solution of hydrated $RhCl_3$ produced [Rh(cupf)$(CO)_2$], which was isolated through precipitation with water. [Rh(cupf)(CO)$(PPh_3)$] was prepared in acetone solution by adding an equivalent amount of triphenylphosphine to [Rh(cupf)$(CO)_2$]. A yellow crystalline product was obtained, $\upsilon_{CO}$ = 1982 cm$^{-1}$. The structure of [Rh(cupf)(CO)$(PPh_3)$] was solved crystallographically,[6] which confirmed the composition of the complex.

Using neocupferrate instead of cupferrate, [Rh(neocupf)(CO)$(PPh_3)$] was prepared in a similar way, $\upsilon_{CO}$ = 1976 cm$^{-1}$. The structure of [Rh(neocupf)(CO)$(PPh_3)$] was solved crystallographically, which confirmed the composition of the complex (Chapter 4). Varying the phosphine ligand, employing P(*p*-$ClC_6H_4)_3$, P(*p*-$MeOC_6H_4)_3$), P(*o*-Tol)$_3$, $PPh_2C_6F_5$ and $PCy_3$, the corresponding complexes, [Rh(cupf)(CO)(P(*p*-$ClC_6H_4)_3$)] ($\upsilon_{CO}$ = 1971 cm$^{-1}$), [Rh(cupf)(CO)(P(*p*-$MeOC_6H_4)_3$)] ($\upsilon_{CO}$ = 1965 cm$^{-1}$), [Rh(cupf)(CO)(P(*o*-Tol)$_3$)] ($\upsilon_{CO}$ = 1965 cm$^{-1}$), [Rh(cupf)(CO)$(PPh_2C_6F_5)$] ($\upsilon_{CO}$ = 1978 cm$^{-1}$) and [Rh(cupf)(CO)$(PCy_3)$] ($\upsilon_{CO}$ = 1959 cm$^{-1}$) were prepared in a similar way.

### *3.2.2.2 Synthesis of [Rh(cupf)(CO)(CH$_3$)(I)(PX$_3$)][7] and [Rh(neocupf)(CO)(CH$_3$)(I)(PPh$_3$)]*

The alkyl oxidative addition product [Rh(cupf)(CO)$(CH_3)$(I)$(PPh_3)$] was prepared as follows: to 0.25 g [Rh(cupf)(CO)$(PPh_3)$], dissolved in 5 cm$^3$ acetone, was added 0.67 g $CH_3I$ (10x excess) and the solution covered with a plastic film for 20 minutes. Further slow evaporation of the orange solution gave yellow-brown needle-like single crystals, $\upsilon_{CO}$ = 2052 cm$^{-1}$. An element analysis yielded the following result, with the calculated value in parentheses: Rh, 15.8 (15.31); P, 4.61 (4.61); I, 19.2 (18.88); N, 4.3 (4.17) and O, 7.14 (7.14)%. The structure of [Rh(cupf)(CO)$(CH_3)$(I)$(PPh_3)$] was solved crystallographically,[7] which confirmed the composition of the complex (Chapter 4).

[6] Basson, S.S., Leipoldt, J.G., Roodt, A. and Venter, J.A., *Inorg. Chim. Acta*, **118**, L45 (1986).

[7] Basson, S.S., Leipoldt, J.G., Roodt, A. and Venter, J.A., *Inorg. Chim. Acta*, **128**, 31 (1987).

Varying the phosphine ligand, employing P(*p*-$ClC_6H_4)_3$, P(*p*-$MeOC_6H_4)_3$) and $PCy_3$, the corresponding complexes, [Rh(cupf)(CO)$(CH_3)$(I)(P(*p*-$ClC_6H_4)_3$)], [Rh(cupf)(CO)-$(CH_3)$(I)(P(*p*-$MeOC_6H_4)_3$)] and [Rh(cupf)(CO)$(CH_3)$(I)$(PCy_3)$] were prepared in a similar way, yielding IR spectra comparable to that of [Rh(cupf)(CO)$(CH_3)$(I)$(PPh_3)$], with $\upsilon_{CO}$ = 2052, 2045 and 2049 $cm^{-1}$ respectively.

Using neocupferrate instead of cupferrate, [Rh(neocupf)(CO)$(CH_3)$(I)$(PPh_3)$] was prepared in a similar way, $\upsilon_{CO}$ = 2048 $cm^{-1}$. The structure of [Rh(neocupf)(CO)$(CH_3)$-(I)$(PPh_3)$] was solved crystallographically, which confirmed the composition of the complex (Chapter 4).

#### *3.2.2.3 Synthesis of [Rh(cupf)(CO){P(OCH₂)₃CCH₃}]*

The bicyclic phosphite ester, 4-methyl-2,6,7-trioxa-1-phosphabicyclo[2.2.2]octane was prepared according to a general method described by Van Leeuwen and Roobeek.[8] A solution of 0.1 mol $PCl_3$ in 50 $cm^3$ dry ether was added in one hour to a stirred solution of 0.3 mol cyclohexanol and 0.3 mol pyridine in 250 $cm^3$ dry ether at −10°C. Subsequently the mixture was warmed and refluxed for one hour. After cooling down, the formed pyridine HCl salt formed was filtered off and washed twice with 50 $cm^3$ portions ether. From the combined washings and filtrate the ether was distilled off and the residue distilled in vacuo. All manipulations were done under nitrogen atmosphere and care was exercised in handling the product, since the bicyclic phosphites are highly toxic.[9]

[Rh(cupf)$(CO)_2$] was prepared in DMF and isolated as described. Equimolar amounts of the cyclic phosphite was mixed with [Rh(cupf)$(CO)_2$] in acetone, to form [Rh(cupf)(CO){$P(OCH_2)_3CCH_3$}], $\upsilon_{CO}$ = 2002 $cm^{-1}$. The structure of [Rh(cupf)(CO)-{$P(OCH_2)_3CCH_3$}] was solved crystallographically,[10] which confirmed the composition of the complex (Chapter 4).

[8] Van Leewen, P.W.N.M. and Roobeek, C.F., *Tetrahedron*, **37**, 1973 (1981).

[9] Bellet, E.M. and Casida, J.E., *Science*, **182**, 1135 (1973); *Toxicology and applied pharmacology*, **47**, 287 (1979).

[10] Basson, S.S., Leipoldt, J.G., Purcell, W. and Venter, J.A., *Acta Cryst*., **C48**, 171 (1992).

### 3.2.3 The Sacac complexes

#### *3.2.3.1 Synthesis of [Rh(Sacac)(CO)$_2$]*[11]

A solution of [$Rh_2Cl_2(CO)_4$] was prepared by refluxing a solution of 0.25 g of $RhCl_3 \cdot 3H_2O$ in 30 $cm^3$ dimethylformamide for approximately 30 minutes. An equivalent amount of thioacetylacetone (Hsacac) (synthesised as described in the literature[12]) was added to the resulting yellow solution. About 300 $cm^3$ cold water was added to this solution to precipitate the [Rh(Sacac)$(CO)_2$]. The red precipitate was removed by centrifuging and washed twice with cold water. [Rh(Sacac)$(CO)_2$] was recrystallised from methanol, $\upsilon_{CO}$ = 1966, 2064 $cm^{-1}$. $^1$H NMR (in $CDCl_3$): $\delta$ 2.25 ($CH_3C(O)$), $\delta$ 2.52 ($CH_3C(S)$) and $\delta$ 6.73 (–CH–). The infrared and $^1$H NMR values correspond to those of the literature.[11]

#### *3.2.3.2 Synthesis of [Rh(Sacac)(CO)(PPh$_3$)]*[11]

[Rh(Sacac)(CO)($PPh_3$)] was prepared by adding an equivalent amount of triphenylphosphine to a solution of 0.1 g of [Rh(Sacac)$(CO)_2$] in 20 $cm^3$ acetone. The solution was evaporated to give a fine yellow powder. The powder was dissolved in a minimum of cold acetone (about 5 $cm^3$) and 10 $cm^3$ n-hexane was added to this solution. The solution was allowed to evaporate at room temperature. A fine yellow crystalline precipitate was obtained, $\upsilon_{CO}$ = 1978 $cm^{-1}$. $^1$H NMR (in $CDCl_3$): $\delta$ 1.67 ($CH_3C(O)$), $\delta$ 2.52 ($CH_3C(S)$) and $\delta$ 6.56 (–CH–). The infrared and $^1$H NMR values correspond to those of the literature.[11] Earlier, the structure of [Rh(Sacac)(CO)-($PPh_3$)] was solved crystallographically,[13] which confirmed the composition of the complex.

[11] Leipoldt, J.G., Basson, S.S. and Botha, L.J., *Inorg. Chim. Acta*, **168**, 215 (1990).

[12] Duns, F. and Anthonsen, J.W., *Acta Chem. Scand., Ser. B*, **31**, 40 (1977).

[13] Botha, L.J., Basson, S.S. and Leipoldt, J.G., *Inorg. Chim. Acta*, **126**, 25 (1987).

# 4 X-ray crystallography

## 4.1 Introduction

The study as reported in this chapter was preceded by a crystallographic investigation of the struct ure of [Rh(cupf)(CO)($PPh_3$)][1] (Figure 4.1). The scope of this structural analysis was to determine the geometry of the specific isomer isolated from the reaction:

$$[Rh(cupf)(CO)_2] + PPh_3 \longrightarrow [Rh(cupf)(CO)(PPh_3)] + CO$$

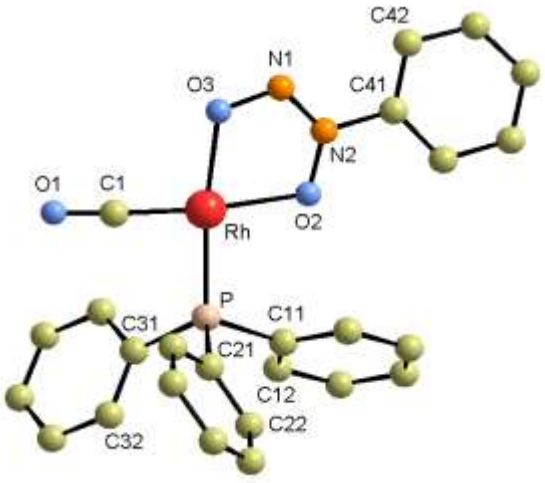


**Figure 4.1** Perspective view of [Rh(cupf)(CO)($PPh_3$)]

It is well known that neutral ligands, like the trivalent phosphine ligand $PPh_3$, only substitutes one CO ligand[2,3] in such a reaction, the CO ligand *trans* to the ligand atom with the largest *trans*-influence[4]. This phenomenon makes it possible to

---

[1] Basson, S.S., Leipoldt, J.G., Roodt, A. and Venter, J.A., *Inorg. Chim. Acta*, **118**, L45 (1986).

[2] Bonati, F.and Wilkinson, G., *J. Chem. Soc*., 3156 (1964).

[3] Varshavskii, Y.S., Knyazeva, N.N., Cherkasova, T.G., Cherkasova, N.V., Ivannikova, N.N. and Ionina, T.I., *Russ. J. Inorg. Chem*., **15**, 367 (1970).

[4] Botha, L.J., Basson, S.S. and Leipoldt, J.G., *Inorg. Chim. Acta*, **126**, 25 (1987).

determine the relative *trans*-influence of the two cupferrate bonding atoms with those of similar formulated complexes, [Rh(LL′-BID)(CO)($PPh_3$)] (LL′ = monoanionic bidentate ligands, such as β-diketones, thioacetylacetone, 8-hydroxyquinoline and 2-picolinic acid, having S, N or O atoms). In certain complexes unexpected substitution of the adjacent CO ligand takes place leading to the other isomer[5,6,7]. With β-aminovinylketonate as LL′, both isomers are formed, with well-pronounced dominance of one of them[8,9]. In most cases only one isomer crystallizes from solution[9,10], the one most abundant in solution. An exception was the case of [Rh(BA)(CO)($PPh_3$)][11] where both isomers crystallized in the same unit cell. Using $P(Oph)_3$ with a cone angle of 128º, complexes of the type [Rh(β-dik)($P(Oph)_3)_2$] could be prepared[12]. The reason for this phenomenon is not clear but both steric and electronic factors should operate since the σ-donor ability of $P(Oph)_3$ is one of the poorest for P(III) derivatives but this is being compensated for in its good π-acid behaviour[13].

As the oxidative addition of [Rh(cupf)(CO)($PPh_3$)] was studied as well, the structural analysis of the oxidative addition product, [Rh(cupf)(CO)($CH_3$)(I)($PPh_3$)] became increasingly important. The ground state stereochemistry of these complexes, although not specific for establishing the mechanistic pathway, could aid the interpretation of the kinetic data for the oxidative addition of $CH_3I$ to the Rh(I) complex. Previous crystallographic and kinetic studies concerning the oxidative addition of $CH_3I$ to [Rh(L,L'-BID)(CO)($PR_3$)] complexes have confirmed that both *cis*

[5] Leipoldt, J.G., Basson, S.S. and Potgieter, J.H., *Inorg. Chim. Acta*, **117**, L3 (1986).

[6] Steynberg, E.C., Lamprecht, G.J. and Leipoldt, J.G., *Inorg. Chim. Acta*, **133**, 33 (1987).

[7] Leipoldt, J.G., Basson, S.S. and Nel, J.T., *Inorg. Chim. Acta*, **74**, 85 (1983).

[8] Galding, M.R., Cherkasova, T.G., Osetrova, L.V. and Varshavsky, Y.S., *Rhodium Ex*., **1**, 14 (1993).

[9] Poletaeva, I.A., Cherkasova, T.G., Osetrova, L.V., Varshavsky, Y.S., Roodt, A. and Leipoldt, J.G., *Rhodium Ex*., **3**, 21 (1994).

[10] Graham, D.E., Lamprecht, G.J., Potgieter, I.M., Roodt, A. and Leipoldt, J.G., *Transition Met. Chem*., **16**, 193 (1991).

[11] Purcell, W., Basson, S.S., Leipoldt, J.G., Roodt, A. and Preston, H., *Inorg. Chim. Acta*, **234**, 153 (1995).

[12] Van Zyl, G.J., Lamprecht, G.J. and Leipoldt, J.G., *Inorg. Chim. Acta*, **102**, L1 (1985).

[13] Emsley, J. and Hall, D., *The Chemistry of Phosphorous*, Harper and Row, London (1976).

and *trans*-addition of $CH_3I$ to the Rh(I) centre can occur in forming the alkyl species.[14,15,16] The neocupferrate ligand, as derivative of cupferrate, was incorporated in the study to further understanding of the mechanistic outcome. By only slightly modifying the cupferrate complex as the neocupferrate complex, a similar result would act as confirmation to the results obtained with cupferrate.

The ability of the Rh(I) centre to accommodate additional ligands was investigated and the successful addition of the π-bonding ligand $PPh_3$ to [Rh(cupf)(CO)($PPh_3$)] could help to justify the proposed solvent stabilized intermediate in the oxidative addition mechanism. The structure determination of [Rh(cupf)(CO)($PPh_3$)$_2$] established the stereochemistry of this addition.

In an attempt to study the effect of a more drastic change to the Rh(I) centre, a bicyclic phosphite ester, 4-methyl-2,6,7-trioxa-1-phosphabicyclo[2.2.2]octane with a cone angle of only 101° was introduced instead of $PPh_3$ (with a cone angle of 145°) previously used. This caged phosphite ligand is also a strong π-acceptor ligand and would play a role to manipulate the Lewis basicity of the rhodium centre. The structures of [Rh(cupf)(CO){$P(OCH_2)_3CCH_3$}] as well as the oxidative addition product of this accessible Rh(I) complex was solved crystallographically.

Vaska's compound, *trans*-[Ir(CO)(Cl)( $PPh_3$)$_2$], was first prepared by Angolletta[17] in 1959 and was later correctly formulated by Vaska[18] in 1961. The analogous Rh(I) complexes were already known at that time and investigated to some extent.[19] These complexes were soon recognized as important model compounds in homogeneous catalysis and are widely known and used today.[20] This class of

[14] Leipoldt, J.G., Basson, S.S. and Botha, L.J., *Inorg. Chim. Acta*, **168**, 215 (1990).

[15] Van Aswegen, K.G., Leipoldt, J.G., Potgieter, I.M., Lamprecht, G.J., Roodt, A. and Van Zyl, G.J., *Transition Met. Chem*., **16**, 369 (1991).

[16] Cano, M., Heras, J.V., Lobo, M.A. and Pinilla, E., *Polyhedron*, **11**, 2679 (1992).

[17] Angoletta, M., *Gazz. Chim. Ital*., **89**, 2359 (1959).

[18] Vaska, L.and DiLuzio, J.W., *J. Am. Chem. Soc*., **83**, 2784 (1961).

[19] Chatt, J. and Shaw, B.L., *Chem. Ind*., 290 (1961).

[20] Roodt, A., Otto, S. and Steyl, G.J., *Coord. Chem. Rev*., **245**,121 (2003).

symmetrical square–planar complexes often crystallize with the metal atom on a crystallographic centre of symmetry, thus imposing a disordered packing arrangement. The structure of *trans*-[Rh(CO)(Cl)($PCy_3$)$_2$] forms part of an ongoing investigation[21,22,23,24,25] aimed at determining which factors govern a disordered packing mode in Vaska-type complexes.

A large number of metal complexes of the N-aryl-N-nitrosohydroxylamines have been investigated in solution for analytical purposes, but only a few crystallographic studies have been reported. The N-Nitroso compounds are known carcinogens and according to researchers from the Faculty of Pharmaceutical Sciences at the Kinki University in Osaka, Japan, it is important to accumulate structural data of metal complexes of N-nitroso compounds in order to clarify their cytotoxicity.[26] Totally unexpected, this study could possibly make a contribution from a biophysical point of view. The crystal structures of complexes derived from cupferrate, as well as neocupferrate, with metal ions are expected to serve as good models for the binding mode of the nitroso group to metal ions.

In this chapter we report the crystal structures that formed part of this study, namely:

[Rh(cupf)(CO)($CH_3$)(I)($PPh_3$)][27] (Par. 4.3.1),
[Rh(cupf)(CO)($PPh_3$)$_2$][28] (Par. 4.3.2),
[Rh(neocupf)(CO)($PPh_3$)]·$CH_3COCH_3$ (Par. 4.3.3),
[Rh(neocupf)(CO)($CH_3$)(I)($PPh_3$)]·$C_5H_{12}$ (Par. 4.3.4)
[Rh(cupf)(CO){$P(OCH_2)_3CCH_3$}][29] (Par. 4.3.5)

[21] Meijboom, R., Muller, A. and Roodt, A., *Acta Cryst*., **E61**, m1283 (2005).

[22] Meijboom, R., Muller, A. and Roodt, A., *Acta Cryst*., **E61**, m699 (2005).

[23] Meij, A.M.M., Muller, A. and Roodt, A., *Acta Cryst*., **E59**, m44 (2002).

[24] Muller, A., Roodt, A., Otto, S., Oskarsson, Å. and Yong, S., *Acta Cryst*., **C58**, m715 (2002).

[25] Meijboom, R., Muller, A. and Roodt, A., *Acta Cryst*., **E60**, m1071 (2004).

[26] Okabe, N. and Tamaki, K., *Acta Cryst*., **C51**, 2004 (1995).

[27] Basson, S.S., Leipoldt, J.G., Roodt, A. and Venter, J.A., *Inorg. Chim. Acta*, **128**, 31 (1987).

[28] Basson, S.S., Leipoldt, J.G., and Venter, J.A., *Acta Cryst*., **C46**, 1324 (1990).

[29] Basson, S.S., Leipoldt, J.G., Purcell, W. and Venter, J.A., *Acta Cryst*., **C48**, 171 (1992).

[Rh(cupf)($COCH_3$)(I){$P(OCH_2)_3CCH_3$}]$_2$ (Par. 4.3.6) and

*trans*-[Rh(CO)(Cl)($PCy_3$)$_2$] (Par. 4.3.7).

In each of the mentioned paragraphs a perspective view, stereoscopic view, a summary of the general crystal data and refinement parameters, the most relevant bond lengths and angles as well as possible hydrogen interaction is given. A more detailed account of the atomic coordinates and equivalent isotropic displacement parameters, a complete list of bond lengths and angles, anisotropic displacement parameters as well as the hydrogen coordinates can be found in Chapter 6 as supplementary data.

## 4.2 Experimental

Details of the preparation of the complexes were discussed in Chapter 3. Conditions for the preparation of single crystals will be described for each complex individually following the common procedures.

The densities of all the crystals were determined by flotation in aqueous NaI except for [Rh(neocupf)(CO)($CH_3$)(I)($PPh_3$)]·$C_5H_{12}$ where thallium formate with a higher density had to be used. Data collections were done on an Enraf-Nonius CAD-4F diffractometer with graphite-monochromated Mo Kα radiation. The intensity data were corrected for Lorentz, polarization effects and crystal decay. For [Rh(cupf)(CO)-{$P(OCH_2)_3CCH_3$}] an empirical absorption correction[30] was made with a minimum correction factor of 0.95 and a maximum of 0.99. All structures were solved by the heavy atom method and anisotropic refinement performed on all non-hydrogen atoms by full-matrix least-squares methods. The XRAY72 system of programs[31] was used for [Rh(cupf)(CO)($CH_3$)(I)($PPh_3$)] and [Rh(cupf)(CO)($PPh_3$)$_2$] while the rest of the structures was solved using SHELXS86[32] and SHELX76[33] used for refinement. Phenyl and methyl hydrogen positions were calculated riding on the adjacent carbon

[30] North, A.C.T., Phillips, D.C. and Mathews, F.S., *Acta Cryst*., **A24**, 351 (1968).

[31] Stewart, J.M., Kruger, G.J., Ammon, H.L., Dickinson, C. Hall, S.R., *The XRAY72 system*. Tech. Rep. TR-192. Computer Science Centre, University of Maryland, College Park, Maryland, USA (1972).

[32] Sheldrick, G.M., *Acta Cryst*., **A46**, 467 (1990).

[33] Sheldrick, G.M., *SHELX76*, Program for crystal structure determination, University of Cambridge, England (1976).

atoms assuming a C-H distance of 1.08 Å and refined with an overall isotropic temperature factor. Hydrogen interactions were calculated using the PLATON[34] program. Neutral-atom scattering factors were taken from Cromer & Mann[35] and anomalous-dispersion corrections for rhodium from *International Tables for X-ray Crystallography*[36]. Molecular graphics were obtained using DIAMOND[37]. Photographs taken from some of the single crystals (Figure 4.2, Figure 4.3, Figure 4.4 and Figure 4.5) were made possible using a JEOL WINSEM 6400 Scanning Electron Microscope. $^{31}P$ NMR spectra were recorded on samples of the [Rh(cupf)(CO)($PPh_3$)] and [Rh(neocupf)(CO)($PPh_3$)] complexes in $CDCl_3$ on a Bruker AM-500 spectrometer operating at 202.46 Hz with 85% phosphoric acid ($\delta^{31}P$ = 0.0 ppm) as external standard.

### 4.2.1 Preparation of crystals of [Rh(cupf)(CO)($CH_3$)(I)($PPh_3$)]

To 0.25 g [Rh(cupf)(CO)($PPh_3$)], dissolved in 5 $cm^3$ acetone, was added 0.67 g $CH_3I$ (10X excess) and the solution covered with a plastic film for 20 minutes. Further slow evaporation of the orange solution gave yellow-brown needle-like single crystals suitable for a structure analysis.

### 4.2.2 Preparation of crystals of [Rh(cupf)(CO)($PPh_3$)$_2$]

A 0.6 $cm^3$ acetone solution containing 23 mg (0.043 mmol) [Rh(cupf)(CO)($PPh_3$)] and 100 mg (0.38 mmol) $PPh_3$ was prepared by dissolving the complex and the phosphine in 0.2 and 0.4 $cm^3$ acetone respectively before combining. Gentle heating was required. The initial yellow colour changed gradually to yellow-orange. Yellow crystals of [Rh(cupf)(CO)($PPh_3$)$_2$] crystallized after 30 minutes.

---

**34** Spek, A.L., PLATON, A multipurpose crystallographic tool, Utrecht University, Utrecht, The Netherlands (2005); Spek, A.L. *J. Appl. Cryst*. **36**, 7 (2003).

**35** Cromer, D.T., and Mann, J., *Acta Cryst*., **A24**, 321 (1968).

**36** *International Tables for X-Ray Crystallography*, Vol III, p216 Birmingham: Kynoch Press.(1962).

**37** Brandenburg, K. and Brendt, M., *DIAMOND,* Release 2.1e. Crystal Impact GbR, Postfach 1251, D53002 Bonn, Germany. (2001).

### 4.2.3 Preparation of crystals of [Rh(neocupf)(CO)($PPh_3$)]·$CH_3COCH_3$

Single crystals of [Rh(neocupf)(CO)($PPh_3$)]·$CH_3COCH_3$ were obtained by placing a 5 $cm^3$ beaker containing a concentrated acetone solution of [Rh(neocupf)(CO)($PPh_3$)] in the draught of a fume hood. Well-shaped yellow crystals formed within 2 hours. Crystals had to be covered with Canada Balsam to prevent the evaporation of acetone from the crystal lattice, thus resulting in cracking of the crystals.

### 4.2.4 Preparation of crystals of [Rh(neocupf)(CO)($CH_3$)(I)($PPh_3$)]·$C_5H_{12}$

[Rh(neocupf)(CO)($PPh_3$)] was dissolved in neat $CH_3I$. The reaction mixture was covered and given 45 minutes to go to completion. The colour changed from light yellow to dark orange. Evaporation of the volatile contents left an oily residue, which was dissolved in a pentane/petroleum ether (80 –100°) mixture. Brown-red single crystals formed over a period of 12 hours after partially covering the container. The crystals tend to crack, as can be seen from Figure 4.2, and had to be covered with office glue since Canada Balsam proved to be insufficient in sealing in the evaporating pentane.

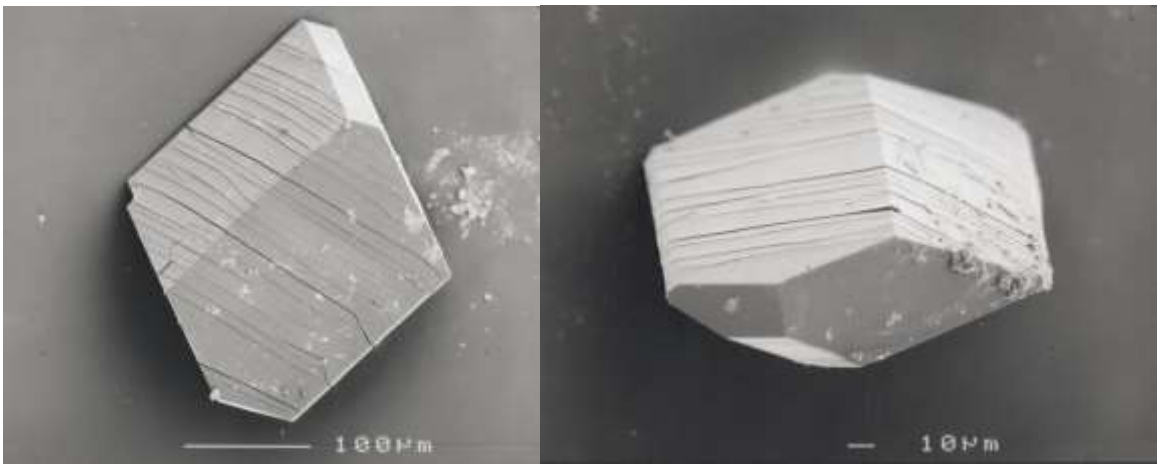


**Figure 4.2** Electron microscope photograph of crystals of [Rh(neocupf)(CO)($CH_3$)(I)-($PPh_3$)]·$C_5H_{12}$ showing the cracks that developed as the pentane evaporated from the crystal structure.

### 4.2.5 Preparation of crystals of [Rh(cupf)(CO){P(OCH$_2$)$_3$CCH$_3$}]

Single crystals of [Rh(cupf)(CO){P(OCH$_2$)$_3$CCH$_3$}] were obtained by recrystallization the complex from a 1:1 benzene/*n*-propanol mixture at room temperature. Yellow needles (Figure 4.3) crystallized within 6 hours.

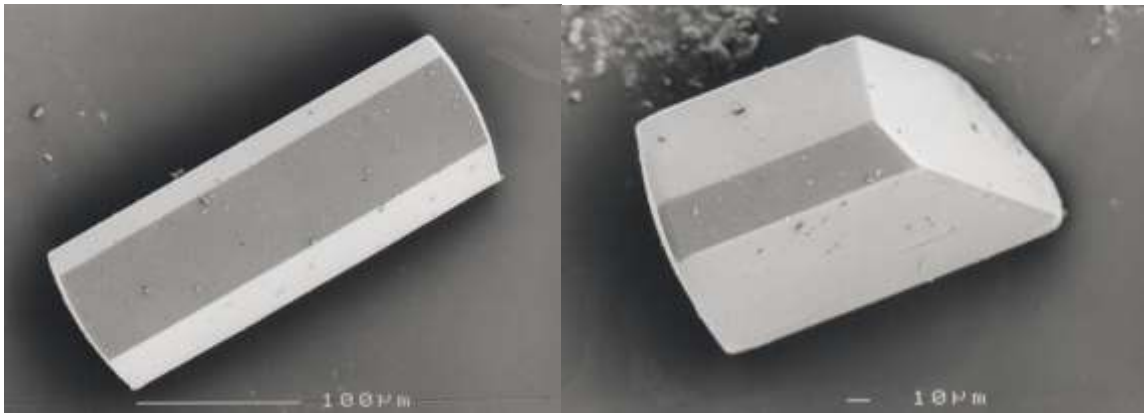

**Figure 4.3** Electron microscope photograph of crystals of [Rh(cupf)(CO){P(OCH$_2$)$_3$CCH$_3$}]

### 4.2.6 Preparation of crystals of [Rh(cupf)(COCH$_3$)(I){P(OCH$_2$)$_3$CCH$_3$}]$_2$

To a concentrated acetone solution of [Rh(cupf)(CO){P(OCH$_2$)$_3$CCH$_3$}] was added at least a tenfold excess of CH$_3$I. The container was sealed with plastic film and left in a dark cupboard for 90 minutes. Before transferring the container to a fridge at –2°C, the plastic film was perforated. Brown-red, boat like single crystals (Figure 4.4) formed within 2 days

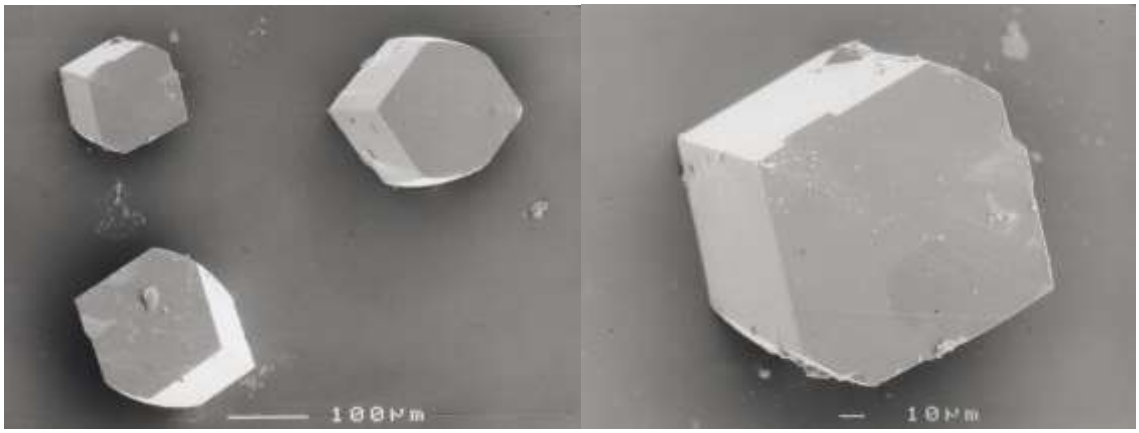

**Figure 4.4** Electron microscope photograph of crystals of [Rh(cupf)(COCH$_3$)(I)-{P(OCH$_2$)$_3$CCH$_3$}]$_2$.

### 4.2.7 Preparation of crystals of *trans*-[Rh(CO)(Cl)($PCy_3$)$_2$

Powdery *trans*-[Rh(CO)(Cl)($PCy_3$)$_2$ was recrystallized from acetone with addition of a small amount of petroleum ether (80 –100°). Suitable light yellow single crystals (Figure 4.5) formed after slow evaporation over a period of 2 to 3 days.

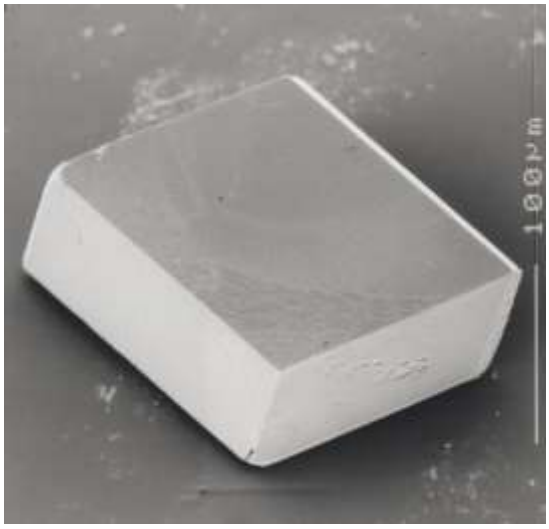


**Figure 4.5** Electron microscope photograph of a crystal of *trans*-[Rh(CO)(Cl)($PCy_3$)$_2$].

## 4.3 Crystal structure determinations

### 4.3.1 Crystal structure of [Rh(cupf)(CO)($CH_3$)(I)($PPh_3$)]

A perspective view of [Rh(cupf)(CO)($CH_3$)(I)($PPh_3$)] is presented in Figure 4.6 while Figure 4.7 portrays a stereoscopic view of the packing of molecules in the unit cell. A summary of the general crystal data and refinement parameters is given in Table 4.1. The most relevant bond lengths and angles are reported in Table 4.2 and Table 4.3.

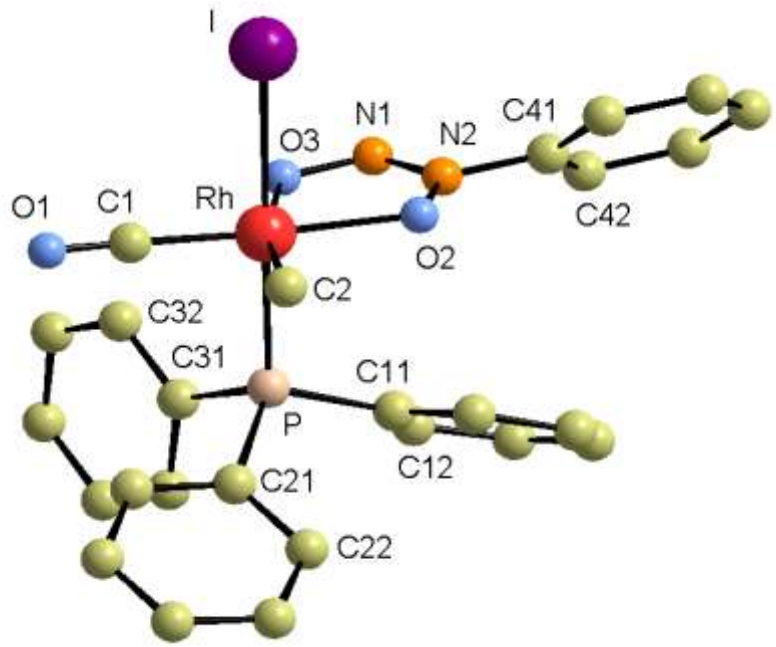


**Figure 4.6** The structure of [Rh(cupf)(CO)($CH_3$)(I)($PPh_3$)] showing the atom numbering scheme. Displacement ellipsoids are drawn at the 30% probability level. Hydrogen atoms are omitted for clarity. Only the first two carbon atoms of each phenyl ring are labeled. The first digit of the label indicates the ring number while the second digit indicates the position of the atom in the ring.

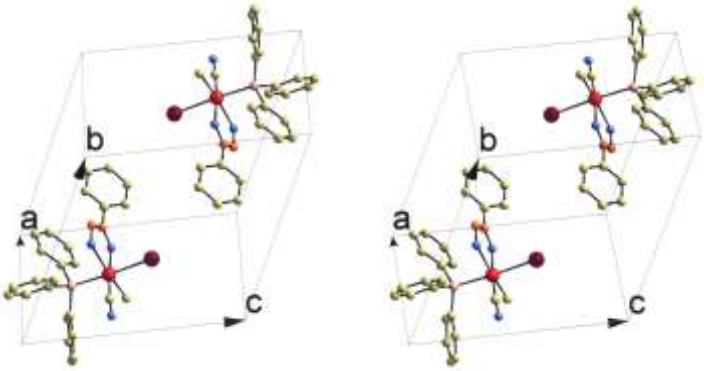


**Figure 4.7** Stereoscopic view of [Rh(cupf)(CO)($CH_3$)(I)($PPh_3$)] visualizing the packing of molecules in the unit cell.

**Table 4.1** Crystal data and structure refinement for [Rh(cupf)(CO)($CH_3$)(I)($PPh_3$)]

| | |
|---|---|
| Identification code | CUPOX |
| Empirical formula | $RhC_{26}H_{23}IN_2O_3P$ |
| Formula weight | 672.3 |
| Temperature (K) | 293(10) |
| Wavelength, Mo Kα (Å) | 0.71073 |
| Crystal system | Triclinic |
| Space group | Pī |
| Unit cell dimensions | a = 9.912(2)Å |
| | b = 11.534(1)Å |
| | c = 12.514(2)Å |
| | α = 67.84(2)° |
| | β = 84.41(2)° |
| | γ = 73.15(1)° |
| Volume ($Å^3$) | 1268.1(3) |
| Z | 2 |
| Density ,calculated ($mg/m^3$) | 1.73 |
| Absorption coefficient ($mm^{-1}$) | 1.95 |
| F(000) | * |
| Crystal size ($mm^3$) | 0.18 x 0.18 x 0.06 |
| Theta range for data collection (°) | 3.0 to 23.0 |
| Index ranges | $0 \le h \le 10$, $-12 \le k \le 12$, $-13 \le l \le 13$ |
| Reflections collected | 3492 |
| Independent reflections | 3492 [R(int) = 0.0000] |
| Refinement method | Full-matrix least-squares on $F^2$ |
| Data / restraints / parameters | 3492 / 0 / 308 |
| Goodness-of-fit on $F^2$ | * |
| Final R indices [I>3σ(I)] | $R_1$ = 0.058, $wR_2$ = 0.060 |
| R indices (all data) | * |
| Largest diff. peak and hole (e. $Å^{-3}$) | * |

* This is an older structure and these data are not available.

**Table 4.2** Selected bond lengths (Å) for [Rh(cupf)(CO)($CH_3$)(I)($PPh_3$)] with estimated standard deviations in parentheses.

| Bond | Length (Å) | Bond | Length (Å) |
|---|---|---|---|
| Rh–I | 2.708(2) | O(3)–N(1) | 1.27(2) |
| Rh–O(3) | 2.175(9) | O(2)–N(2) | 1.32(1) |
| Rh–O(2) | 2.04(1) | N(1)–N(2) | 1.33(2) |
| Rh–C(2) | 2.08(1) | N(2)–C(41) | 1.44(2) |
| Rh–C(1) | 1.81(2) | P–C(11) | 1.80(1) |
| Rh–P | 2.327(4) | P–C(21) | 1.79(1) |
| C(1)–O(1) | 1.14(2) | P–C(31) | 1.83(1) |

**Table 4.3** Selected bond angles (°) for [Rh(cupf)(CO)($CH_3$)(I)($PPh_3$)] with estimated standard deviations in parentheses.

| Bond | Angle (°) | Bond | Angle (°) |
|---|---|---|---|
| O(2)–Rh–O(3) | 74.9(4) | C(2)–Rh–O(3) | 167.3(6) |
| O(3)–Rh–C(1) | 108.1(5) | O(2)–Rh–C(1) | 174.8(6) |
| C(1)–Rh–C(2) | 84.6(7) | Rh–C(1)–O(1) | 174(1) |
| C(2)–Rh–O(2) | 92.4(6) | Rh–O(3)–N(1) | 115.3(8) |
| O(2)–Rh–P | 92.6(3) | Rh–O(2)–N(2) | 112.8(7) |
| O(3)–Rh–P | 87.0(4) | O(2)–N(2)–N(1) | 124(1) |
| C(1)–Rh–P | 91.8(6) | O(3)–N(1)–N(2) | 113(1) |
| C(2)–Rh–P | 92.5(5) | O(2)–N(2)–C(41) | 118(1) |
| O(2)–Rh–I | 86.7(3) | N(1)–N(2)–C(41) | 118(1) |
| O(3)–Rh–I | 89.5(4) | Rh–P–C(11) | 109.2(6) |
| C(1)–Rh–I | 89.1(6) | Rh–P–C(21) | 115.2(4) |
| C(2)–Rh–I | 90.8(5) | Rh–P–C(31) | 112.1(5) |
| I–Rh–P | 176.6(1) | | |

### 4.3.2 Crystal structure of [Rh(cupf)(CO)($PPh_3$)$_2$]

A perspective view of [Rh(cupf)(CO)($PPh_3$)$_2$] is presented in Figure 4.8 while Figure 4.9 portrays a stereoscopic view of the packing of molecules in the unit cell. A summary of the general crystal data and refinement parameters is given in Table 4.4. The most relevant bond lengths and angles are reported in Table 4.5 and Table 4.6.

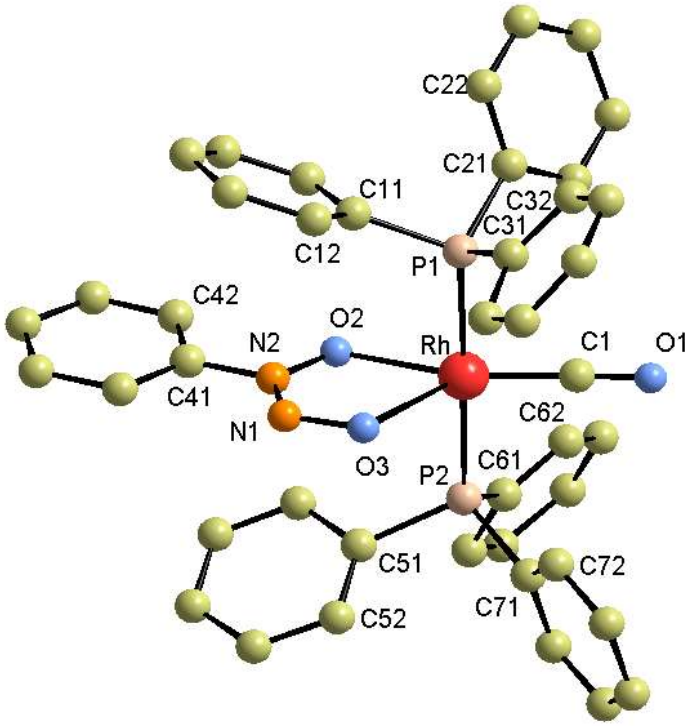


**Figure 4.8** The structure of [Rh(cupf)(CO)($PPh_3$)$_2$] showing the atom numbering scheme. Displacement ellipsoids are drawn at the 30% probability level. Hydrogen atoms are omitted for clarity. Only the first two carbon atoms of each phenyl ring are labeled. The first digit of the label indicates the ring number while the second digit indicates the position of the atom in the ring.

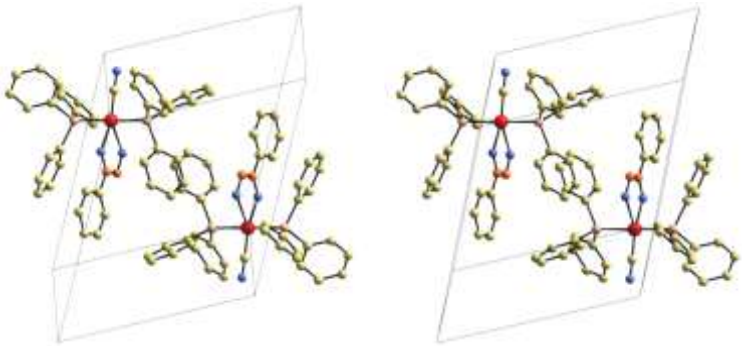

**Figure 4.9** Stereoscopic view of [Rh(cupf)(CO)($PPh_3$)$_2$] visualizing the packing of molecules in the unit cell.

**Table 4.4** Crystal data and structure refinement for [Rh(cupf)(CO)($PPh_3$)$_2$]

| | |
|---|---|
| Identification code | ROPPH5 |
| Empirical formula | $RhC_{43}H_{35}N_2O_3P_2$ |
| Formula weight | 792.6 |
| Temperature (K) | 293(2) |
| Wavelength, Mo Kα (Å) | 0.71073 |
| Crystal system | Triclinic |
| Space group | P$\bar{1}$ |
| Unit cell dimensions | a = 12.298(9)Å, |
| | b = 12.658(2)Å, |
| | c = 13.488(3)Å, |
| | α = 90.72(2)° |
| | β = 106.38(3)° |
| | γ = 112.76(3)° |
| Volume (Å$^3$) | 1840.1(2) |
| Z | 2 |
| Density ,calculated (mg/m$^3$) | 1.42 |
| Absorption coefficient (mm$^{-1}$) | 0.58 |
| F(000) | 812 |
| Crystal size (mm$^3$) | 0.09 x 0.15 x 0.20 |
| Theta range for data collection (°) | 3 to 25 |
| Index ranges | $0 \le h \le 14$, $-15 \le k \le 13$, $-16 \le l \le 15$ |
| Reflections collected | 6415 |
| Independent reflections | 6415 [R(int) = 0.0000] |
| Refinement method | Full-matrix least-squares on $F^2$ |
| Data / restraints / parameters | 6415 / 0 / 461 |
| Goodness-of-fit on $F^2$ | * |
| Final R indices [I>3σ(I)] | $R_1$ = 0.070, $wR_2$ = 0.076 |
| R indices (all data) | * |
| Largest diff. peak and hole (e. Å$^{-3}$) | * |

* This is an older structure and these data are not available.

**Table 4.5** Selected bond lengths (Å) for [Rh(cupf)(CO)($PPh_3$)$_2$] with estimated standard deviations in parentheses.

| Bond | Length (Å) | Bond | Length (Å) |
|---|---|---|---|
| Rh-C(1) | 1.77(1) | N(1)-N(2) | 1.30(1) |
| Rh-O(2) | 2.147(8) | N(1)-O(3) | 1.28(1) |
| Rh-O(3) | 2.339(9) | P(1)-C(11) | 1.82(1) |
| Rh-P(1) | 2.323(4) | P(1)-C(21) | 1.81(1) |
| Rh-P(2) | 2.342(4) | P(1)-C(31) | 1.83(1) |
| C(1)-O(1) | 1.16(2) | P(2)-C(51) | 1.83(1) |
| N(2)-O(2) | 1.33(1) | P(2)-C(61) | 1.82(1) |
| N(2)-C(41) | 1.43(2) | P(2)-C(71) | 1.80(1) |

**Table 4.6** Selected bond angles (°) for [Rh(cupf)(CO)($PPh_3$)$_2$] with estimated standard deviations in parentheses.

| Bond | Angle (°) | Bond | Angle (°) |
|---|---|---|---|
| Rh–C(1)–O(1) | 176(1) | Rh–P(1)–C(21) | 118.7(5) |
| Rh–O(2)–N(2) | 116.3(6) | Rh–P(1)–C(31) | 111.7(4) |
| Rh–O(3)–N(1) | 116.0(7) | Rh–P(2)–C(51) | 114.2(5) |
| O(2)–N(2)–N(1) | 124(1) | Rh–P(2)–C(61) | 116.3(4) |
| N(2)–N(1)–O(3) | 114(1) | Rh–P(2)–C(71) | 113.5(5) |
| O(2)–N(2)–C(41) | 117.4(9) | P(1)–Rh–O(2) | 87.7(3) |
| N(1)–N(2)–C(41) | 119(1) | P(1)–Rh–O(3) | 91.0(3) |
| C(1)–Rh–O(2) | 159.6(5) | P(1)–Rh–C(1) | 90.4(5) |
| C(1)–Rh–O(3) | 130.8(5) | P(2)–Rh–O(2) | 90.2(3) |
| O(2)–Rh–O(3) | 69.6(3) | P(2)–Rh–O(3) | 90.4(3) |
| P(1)–Rh–P(2) | 176.9(1) | P(2)–Rh–C(1) | 90.8(5) |
| Rh–P(1)–C(11) | 114.2(4) | | |

### 4.3.3 Crystal structure of [Rh(neocupf)(CO)($PPh_3$)]·$CH_3COCH_3$

A perspective view of [Rh(neocupf)(CO)($PPh_3$)]·$CH_3COCH_3$ is presented in Figure 4.10 while Figure 4.11 portrays a stereoscopic view of the packing of molecules in the unit cell. A summary of the general crystal data and refinement parameters is given in Table 4.7. The most relevant bond lengths and angles are reported in Table 4.8 and Table 4.9. Table 4.10 list the hydrogen interactions involved.

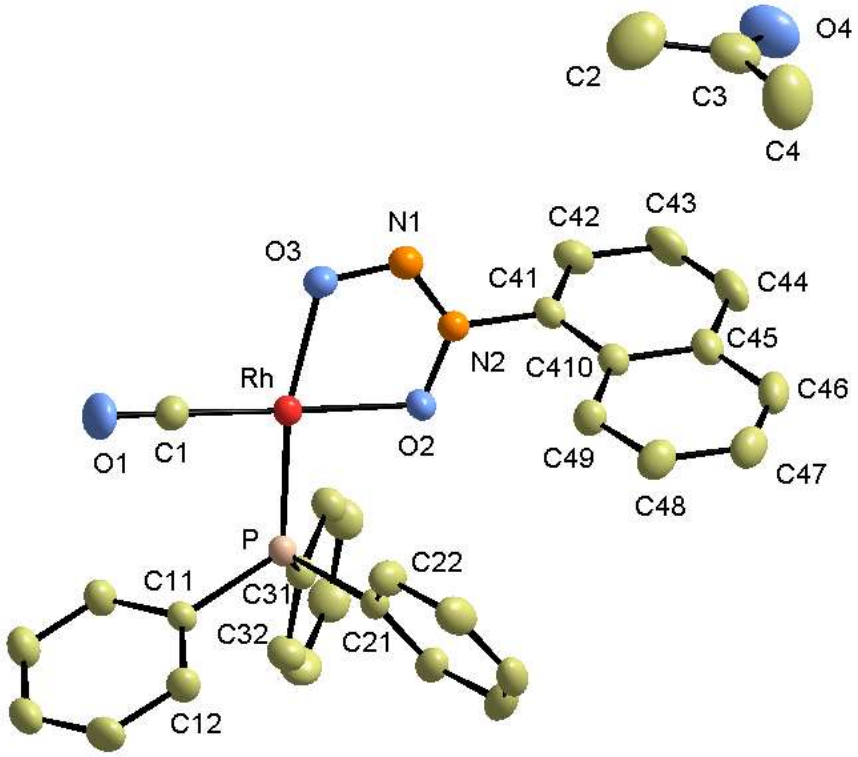


**Figure 4.10** The structure of [Rh(neocupf)(CO)($PPh_3$)]·$CH_3COCH_3$ showing the atom numbering scheme. Displacement ellipsoids are drawn at the 30% probability level. Hydrogen atoms are omitted for clarity. Only the first two atoms of each phenyl ring are labeled. The first digit on the label indicates the ring number while the second digit indicates the position of the atom in the ring.

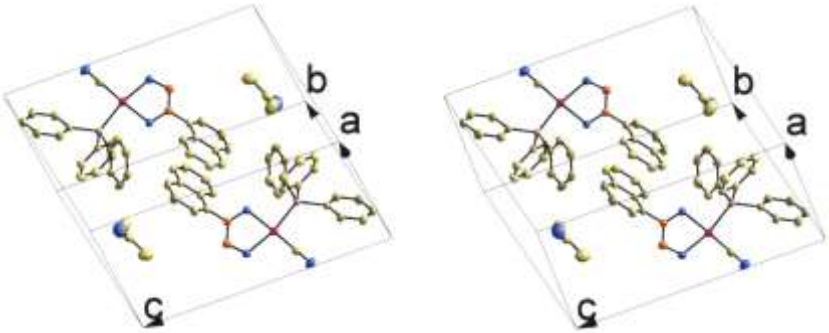


**Figure 4.11** Stereoscopic view of [Rh(neocupf)(CO)($PPh_3$)]·$CH_3COCH_3$ visualizing the packing of molecules in the unit cell.

**Table 4.7** Crystal data and structure refinement for $[Rh(neocupf)(CO)(PPh_3)]\cdot CH_3COCH_3$

| | |
|---|---|
| Identification code | RONEO |
| Empirical formula | $RhC_{32}H_{28}N_2O_4P$ |
| Formula weight | 637.94 |
| Temperature (K) | 293(2) |
| Wavelength, Mo Kα (Å) | 0.71073 |
| Crystal system | Triclinic |
| Space group | Pī |
| Unit cell dimensions | a = 9.8214(8)Å,<br>b = 10.2759(13)Å,<br>c = 15.638(2)Å,<br>α = 77.813(11)°<br>β = 85.575(8)°<br>γ = 70.285(9)° |
| Volume ($Å^3$) | 1452.2(3) |
| Z | 2 |
| Density ,calculated ($mg/m^3$) | 1.459 |
| Absorption coefficient ($mm^{-1}$) | 0.682 |
| F(000) | 651 |
| Crystal size ($mm^3$) | 0.15 x 0.30 x 0.13 |
| Theta range for data collection (°) | 3.05 to 29.96 |
| Index ranges | $0 \le h \le 13$, $-13 \le k \le 14$, $-21 \le l \le 21$ |
| Reflections collected | 7317 |
| Independent reflections | 7317 [R(int) = 0.0000] |
| Refinement method | Full-matrix least-squares on $F^2$ |
| Data / restraints / parameters | 7317 / 0 / 364 |
| Goodness-of-fit on $F^2$ | 1.041 |
| Final R indices [$I>2\sigma(I)$] | $R_1$ = 0.0545, $wR_2$ = 0.1330 |
| R indices (all data) | $R_1$ = 0.0644, $wR_2$ = 0.1400 |
| Largest diff. peak and hole (e. $Å^{-3}$) | 1.490 and -0.913 |

**Table 4.8** Selected bond lengths (Å) for [Rh(neocupf)(CO)($PPh_3$)]·$CH_3COCH_3$ with estimated standard deviations in parentheses.

| Bond | Length (Å) | Bond | Length (Å) |
|---|---|---|---|
| Rh-C(1) | 1.802(5) | P-C(11) | 1.827(4) |
| Rh-O(2) | 2.025(3) | O(2)-N(2) | 1.329(4) |
| Rh-O(3) | 2.081(3) | C(1)-O(1) | 1.139(5) |
| Rh-P | 2.2271(11) | N(2)-N(1) | 1.292(5) |
| P-C(21) | 1.822(4) | N(2)-C(41) | 1.447(5) |
| P-C(31) | 1.823(4) | O(3)-N(1) | 1.295(5) |

**Table 4.9** Selected bond angles (°) for [Rh(neocupf)(CO)($PPh_3$)]·$CH_3COCH_3$ with estimated standard deviations in parentheses.

| Bond | Angle (°) | Bond | Angle (°) |
|---|---|---|---|
| C(1)-Rh-O(2) | 175.8(2) | C(31)-P-Rh | 113.11(13) |
| C(1)-Rh-O(3) | 100.5(2) | C(11)-P-Rh | 121.61(13) |
| O(2)-Rh-O(3) | 77.23(11) | N(2)-O(2)-Rh | 109.7(2) |
| C(1)-Rh-P | 91.21(14) | O(1)-C(1)-Rh | 177.3(5) |
| O(2)-Rh-P | 90.95(8) | N(1)-N(2)-O(2) | 124.6(3) |
| O(3)-Rh-P | 168.16(9) | N(1)-N(2)-C(41) | 118.7(3) |
| C(21)-P-C(31) | 106.9(2) | O(2)-N(2)-C(41) | 116.6(3) |
| C(21)-P-C(11) | 104.3(2) | N(1)-O(3)-Rh | 114.7(2) |
| C(31)-P-C(11) | 102.2(2) | C(42)-C(41)-N(2) | 118.4(4) |
| C(21)-P-Rh | 107.56(13) | N(2)-N(1)-O(3) | 113.4(3) |

**Table 4.10** Hydrogen interactions in [Rh(neocupf)(CO)($PPh_3$)]·$CH_3COCH_3$.

| Donor - H...Acceptor | Type | D - H (Å) | H...A (Å) | D...A (Å) | D - H...A (°) |
|---|---|---|---|---|---|
| C(25) --H(25) ..O(4) | Inter | 0.93 | 2.55 | 3.2902 | 137 |
| C(49) --H(49) ..O(2) | Intra | 0.93 | 2.58 | 3.0714 | 113 |

### 4.3.4 Crystal structure of [Rh(neocupf)(CO)($CH_3$)(I)($PPh_3$)]·$C_5H_{12}$

A perspective view of [Rh(neocupf)(CO)($CH_3$)(I)($PPh_3$)]·$C_5H_{12}$ is presented in Figure 4.12 while Figure 4.13 portrays a stereoscopic view of the packing of molecules in the unit cell. A summary of the general crystal data and refinement parameters is

given in Table 4.11. The most relevant bond lengths and angles are reported in Table 4.12 and Table 4.13. Table 4.14 list the hydrogen interactions involved.

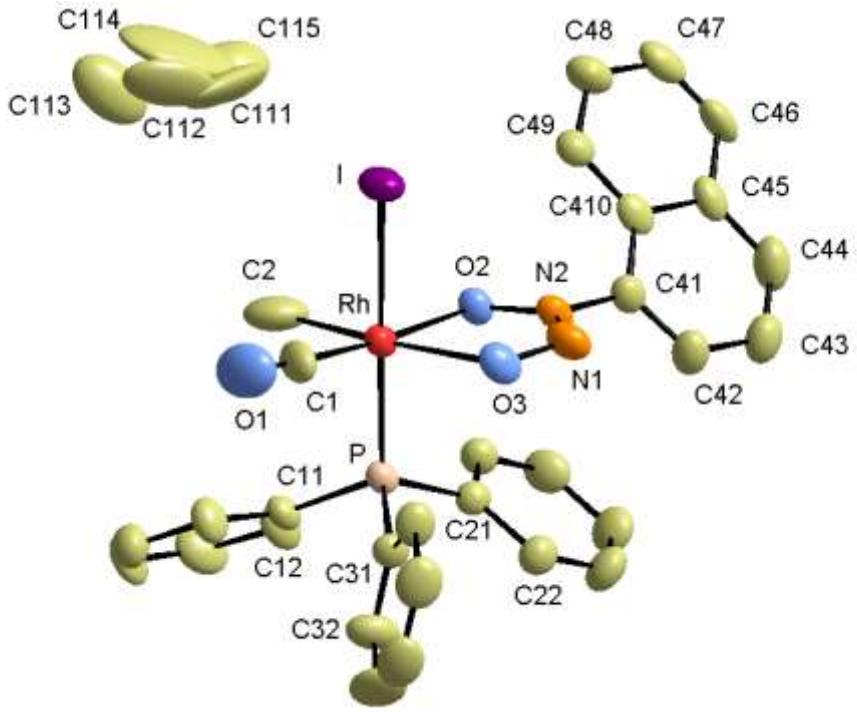


**Figure 4.12** The structure of [Rh(neocupf)(CO)($CH_3$)(I)($PPh_3$)]·$C_5H_{12}$ showing the atom numbering scheme. Displacement ellipsoids are drawn at the 30% probability level. Hydrogen atoms are omitted for clarity. Only the first two atoms of each phenyl ring are labeled. The first digit on the label indicates the ring number while the second digit indicates the position of the atom in the ring.

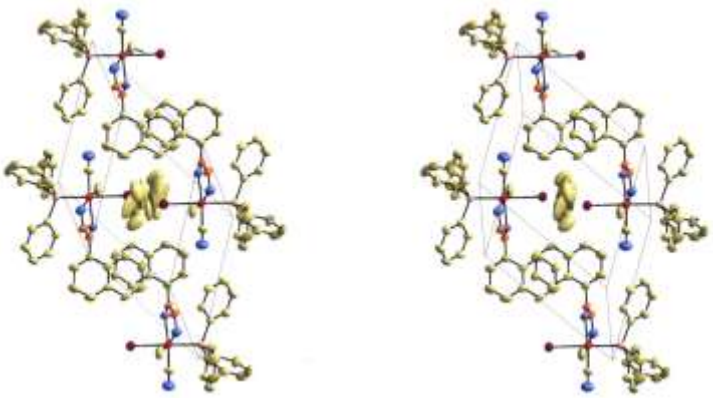

**Figure 4.13** Stereoscopic view of [Rh(neocupf)(CO)($CH_3$)(I)($PPh_3$)]·$C_5H_{12}$ visualizing the packing of molecules in the unit cell.

**Table 4.11** Crystal data and structure refinement for [Rh(neocupf)(CO)($CH_3$)(I)-($PPh_3$)]·$C_5H_{12}$

| | |
|---|---|
| Identification code | NEOOXA |
| Empirical formula | $RhC_{35}H_{37}IN_2O_3P$ |
| Formula weight | 794.45 |
| Temperature (K) | 293(2) |
| Wavelength, Mo Kα (Å) | 0.71073 |
| Crystal system | Triclinic |
| Space group | P$\bar{1}$ |
| Unit cell dimensions | a = 16.433(3)Å,<br>b = 10.474(2)Å,<br>c = 15.351(3)Å,<br>α = 95.456(14)°<br>β = 119.756(12)°<br>γ = 123.088(13)° |
| Volume ($Å^3$) | 1660.8(5) |
| Z | 2 |
| Density ,calculated ($mg/m^3$) | 1.589 |
| Absorption coefficient ($mm^{-1}$) | 1.528 |
| F(000) | 796 |
| Crystal size ($mm^3$) | 0.23 x 0.23 x 0.10 |
| Theta range for data collection (°) | 3.07 to 39.69 |
| Index ranges | -20 ≤ h ≤ 17, -13 ≤ k ≤ 13, 0 ≤ l ≤ 19 |
| Reflections collected | 4962 |
| Independent reflections | 4949 [R(int) = 0.0307] |
| Refinement method | Full-matrix least-squares on $F^2$ |
| Data / restraints / parameters | 4949 / 0 / 399 |
| Goodness-of-fit on $F^2$ | 1.025 |
| Final R indices [I>2σ(I)] | $R_1$ = 0.0638, $wR_2$ = 0.1741 |
| R indices (all data) | $R_1$ = 0.0664, $wR_2$ = 0.1763 |
| Largest diff. peak and hole (e. $Å^{-3}$) | 1.187 and -0.982 |

**Table 4.12** Selected bond lengths (Å) for $[Rh(neocupf)(CO)(CH_3)(I)(PPh_3)]\cdot C_5H_{12}$ with estimated standard deviations in parentheses.

| Bond | Length (Å) | Bond | Length (Å) |
|---|---|---|---|
| Rh-C(1) | 1.827(10) | P-C(11) | 1.818(8) |
| Rh-O(2) | 2.074(5) | P-C(31) | 1.819(6) |
| Rh-C(2) | 2.092(14) | O(1)-C(1) | 1.036(11) |
| Rh-O(3) | 2.128(6) | O(3)-N(1) | 1.265(9) |
| Rh-P | 2.307(2) | O(2)-N(2) | 1.344(8) |
| Rh-I | 2.7111(14) | N(1)-N(2) | 1.308(9) |
| P-C(21) | 1.807(7) | N(2)-C(41) | 1.422(9) |

**Table 4.13** Selected bond angles (°) for $[Rh(neocupf)(CO)(CH_3)(I)(PPh_3)]\cdot C_5H_{12}$ with estimated standard deviations in parentheses.

| Bond | Angle (°) | Bond | Angle (°) |
|---|---|---|---|
| C(1)-Rh-O(2) | 174.6(4) | C(21)-P-C(11) | 107.3(4) |
| C(1)-Rh-C(2) | 86.2(6) | C(21)-P-C(31) | 106.5(3) |
| O(2)-Rh-C(2) | 94.5(4) | C(11)-P-C(31) | 101.7(4) |
| C(1)-Rh-O(3) | 102.9(4) | C(21)-P-Rh | 111.0(3) |
| O(2)-Rh-O(3) | 76.3(2) | C(11)-P-Rh | 115.2(3) |
| C(2)-Rh-O(3) | 170.8(4) | C(31)-P-Rh | 114.3(3) |
| C(1)-Rh-P | 91.7(3) | N(1)-O(3)-Rh | 115.3(5) |
| O(2)-Rh-P | 93.7(2) | N(2)-O(2)-Rh | 108.9(3) |
| C(2)-Rh-P | 92.1(3) | N(1)-N(2)-O(2) | 124.7(6) |
| O(3)-Rh-P | 88.0(2) | N(1)-N(2)-C(41) | 118.4(7) |
| C(1)-Rh-I | 85.9(3) | O(2)-N(2)-C(41) | 116.6(5) |
| O(2)-Rh-I | 88.7(2) | O(3)-N(1)-N(2) | 114.4(8) |
| C(2)-Rh-I | 91.2(3) | O(1)-C(1)-Rh | 173.7(13) |
| O(3)-Rh-I | 89.1(2) | C(42)-C(41)-N(2) | 118.7(7) |
| P-Rh-I | 175.75(5) | | |

**Table 4.14** Hydrogen interactions in $[Rh(neocupf)(CO)(CH_3)(I)(PPh_3)]\cdot C_5H_{12}$.

| Donor - H...Acceptor | Type | D - H (Å) | H...A (Å) | D...A (Å) | D - H...A (°) |
|---|---|---|---|---|---|
| C(25) --H(25) ..O(1) | Inter | 0.93 | 2.49 | 3.2064 | 134 |
| C(35) --H(35) ..O(3) | Inter | 0.93 | 2.49 | 3.3682 | 157 |
| C(36) --H(36) ..O(3) | Intra | 0.93 | 2.33 | 3.0695 | 137 |
| C(49) --H(49) ..O(2) | Intra | 0.93 | 2.57 | 3.0391 | 112 |

### 4.3.5 Crystal structure of [Rh(cupf)(CO){P(OCH$_2$)$_3$CCH$_3$}]

A perspective view of [Rh(cupf)(CO){P(OCH$_2$)$_3$CCH$_3$}] is presented in Figure 4.14 while Figure 4.15 portrays a stereoscopic view of the packing of molecules in the unit cell. A summary of the general crystal data and refinement parameters is given in Table 4.15. The most relevant bond lengths and angles are reported in Table 4.16 and Table 4.17. Table 4.18 list the hydrogen interactions involved.

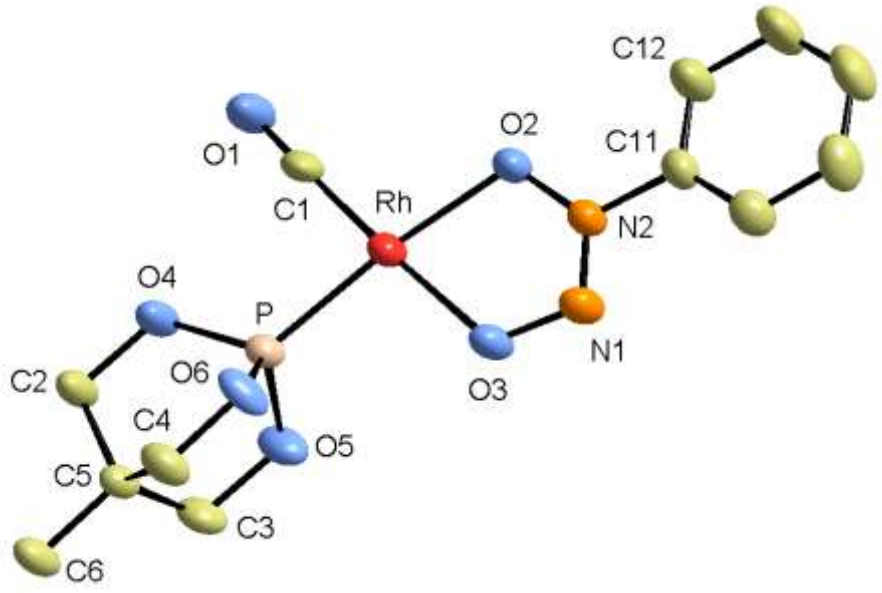


**Figure 4.14** The structure of [Rh(cupf)(CO){P(OCH$_2$)$_3$CCH$_3$}] showing the atom numbering scheme. Displacement ellipsoids are drawn at the 30% probability level. Hydrogen atoms are omitted for clarity. Only the first two atoms of each phenyl ring are labeled. The first digit on the label indicates the ring number while the second digit indicates the position of the atom in the ring.

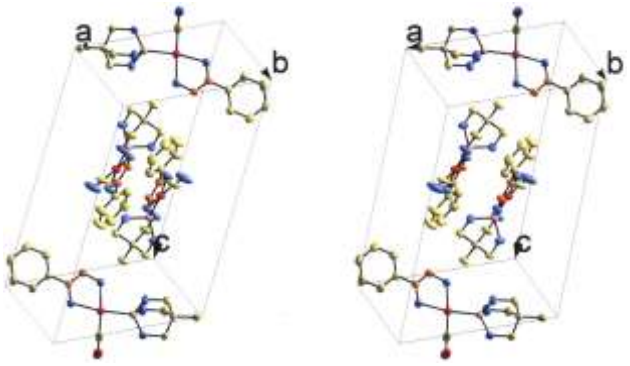


**Figure 4.15** Stereoscopic view of [Rh(cupf)(CO){P(OCH$_2$)$_3$CCH$_3$}] visualizing the packing of molecules in the unit cell..

**Table 4.15** Crystal data and structure refinement for [Rh(cupf)(CO){$P(OCH_2)_3CCH_3$}].

| | |
|---|---|
| Identification code | CUPFOS |
| Empirical formula | $RhC_{12}H_{14}N_2O_6P$ |
| Formula weight | 416.13 |
| Temperature (K) | 295(2) |
| Wavelength, Mo Kα (Å) | 0.71073 |
| Crystal system | Monoclinic |
| Space group | $P2_1/c$ |
| Unit cell dimensions | a = 11.990(1)Å, |
| | b = 6.195(1)Å, |
| | c = 20.906(3)Å, |
| | α = 90° |
| | β = 92.857(10)° |
| | γ = 90° |
| Volume ($Å^3$) | 1550.8(4) |
| Z | 4 |
| Density ,calculated ($mg/m^3$) | 1.78(1) |
| Absorption coefficient ($mm^{-1}$) | 1.212 |
| F(000) | 832 |
| Crystal size ($mm^3$) | 0.075 x 0.125 x 0.5 |
| Theta range for data collection (°) | 6 to 17 |
| Index ranges | $0 \le h \le 16$, $0 \le k \le 8$, $-29 \le l \le 29$ |
| Reflections collected | 3940 |
| Independent reflections | 3940 [R(int) = 0.0000] |
| Refinement method | Full-matrix least-squares on $F^2$ |
| Data / restraints / parameters | 3940 / 0 / 203 |
| Goodness-of-fit on $F^2$ | 1.041 |
| Final R indices [I>3σ(I)] | $R_1$ = 0.0525, $wR_2$ = 0.0541 |
| R indices (all data) | * |
| Largest diff. peak and hole (e. $Å^{-3}$) | * |

* This is an older structure and these data are not available.

**Table 4.16** Select bond lengths (Å) for [Rh(cupf)(CO){P(OCH$_2$)$_3$CCH$_3$}] with estimated standard deviations in parentheses.

| Bond | Length (Å) | Bond | Length (Å) |
|---|---|---|---|
| Rh-P | 2.156(2) | N(2)-C(11) | 1.448(8) |
| Rh-O(2) | 2.059(4) | C(1)-O(1) | 1.155(9) |
| Rh-O(3) | 2.026(5) | O(4)-C(2) | 1.460(8) |
| Rh-C(1) | 1.772(9) | O(5)-C(3) | 1.466(8) |
| P-O(4) | 1.574(5) | O(6)-C(4) | 1.458(7) |
| P-O(5) | 1.587(5) | C(2)-C(5) | 1.516(8) |
| P-O(6) | 1.579(5) | C(3)-C(5) | 1.497(10) |
| O(2)-N(2) | 1.325(6) | C(4)-C(5) | 1.546(9) |
| O(3)-N(1) | 1.325(7) | C(5)-C(6) | 1.535(8) |
| N(2)-N(1) | 1.264(7) | | |

**Table 4.17** Selected bond angles (°) for [Rh(cupf)(CO){P(OCH$_2$)$_3$CCH$_3$}] with estimated standard deviations in parentheses.

| Bond | Angle (°) | Bond | Angle (°) |
|---|---|---|---|
| P-Rh-O(2) | 170.8(1) | Rh-O(2)-N(2) | 108.9(3) |
| P-Rh-O(3) | 94.8(1) | Rh-O(3)-N(1) | 115.6(4) |
| O(2)-Rh-O(3) | 77.3(2) | O(2)-N(2)-N(1) | 124.7(5) |
| P-Rh-C(1) | 88.3(2) | O(2)-N(2)-C(11) | 116.7(5) |
| O(2)-Rh-C(1) | 99.9(3) | N(1)-N(2)-C(11) | 118.5(6) |
| O(3)-Rh-C(1) | 175.6(3) | O(3)-N(1)-N(2) | 113.5(5) |
| Rh-P-O(4) | 119.0(2) | Rh-C(1)-O(1) | 174.4(10) |
| Rh-P-O(5) | 115.8(2) | P-O(5)-C(3) | 115.7(4) |
| O(4)-P-O(5) | 102.8(3) | O(4)-C(2)-C(5) | 109.8(5) |
| Rh-P-O(6) | 113.2(2) | C(2)-C(5)-C(4) | 108.5(6) |
| O(4)-P-O(6) | 102.6(3) | C(3)-C(5)-C(6) | 110.5(6) |
| O(5)-P-O(6) | 101.1(3) | N(2)–C(11)–C(12) | 117.8(5) |

**Table 4.18** Hydrogen interactions in [Rh(cupf)(CO){P(OCH$_2$)$_3$CCH$_3$}].

| Donor - H...Acceptor | Type | D - H (Å) | H...A (Å) | D...A (Å) | D - H...A (°) |
|---|---|---|---|---|---|
| C(3)--H(31) ..O(3) | Inter | 1.08 | 2.54 | 3.3771 | 134 |
| C(4)--H(41) ..N(1) | Inter | 1.08 | 2.61 | 3.6514 | 162 |
| C(6)--H(63) ..O(3) | Inter | 1.08 | 2.54 | 3.5163 | 149 |

### 4.3.6 Crystal structure of [Rh(cupf)(COCH$_3$)(I){P(OCH$_2$)$_3$CCH$_3$}]$_2$

A perspective view of [Rh(cupf)(COCH$_3$)(I){P(OCH$_2$)$_3$CCH$_3$}]$_2$ is presented in Figure 4.16 while Figure 4.17 portrays a stereoscopic view of the packing of molecules in

the unit cell. A summary of the general crystal data and refinement parameters is given in Table 4.19. The most relevant bond lengths and angles are reported in Table 4.20 and Table 4.21. Table 4.22 list the hydrogen interactions involved.

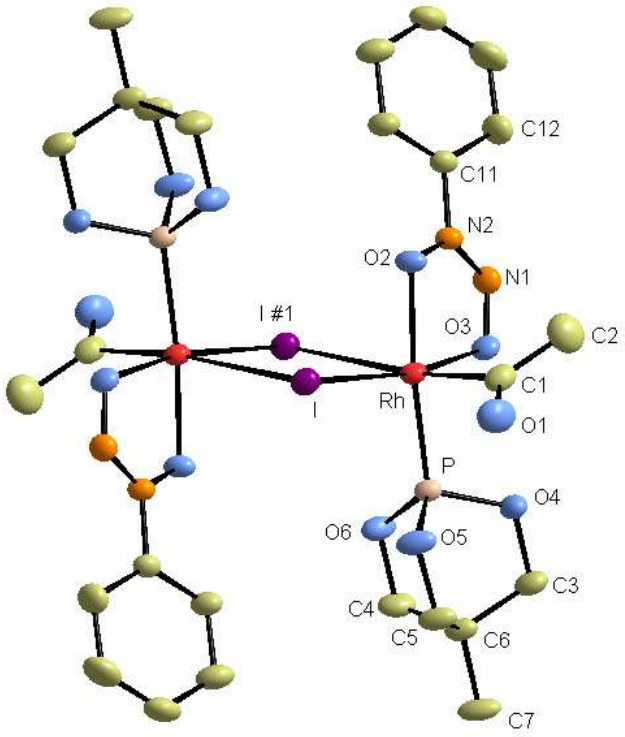


**Figure 4.16** The structure of $[Rh(cupf)(COCH_3)(I)\{P(OCH_2)_3CCH_3\}]_2$ showing the atom numbering scheme. Displacement ellipsoids are drawn at the 30% probability level. Hydrogen atoms are omitted for clarity. Only the first two atoms of each phenyl ring are labeled. The first digit on the label indicates the ring number while the second digit indicates the position of the atom in the ring.

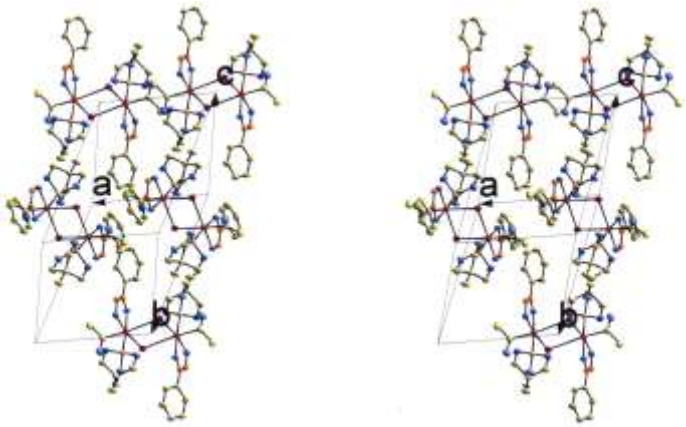


**Figure 4.17** Stereoscopic view of $[Rh(cupf)(COCH_3)(I)\{P(OCH_2)_3CCH_3\}]_2$ visualizing the packing of molecules in the unit cell.

**Table 4.19** Crystal data and structure refinement for [Rh(cupf)($COCH_3$)(I)-{$P(OCH_2)_3CCH_3$}]$_2$.

| | |
|---|---|
| Identification code | FOSOXA |
| Empirical formula | $RhC_{13}H_{17}IN_2O_6P$ |
| Formula weight | 558.06 |
| Temperature (K) | 293(2) |
| Wavelength, Mo Kα (Å) | 0.71073 |
| Crystal system | Monoclinic |
| Space group | $P2_1/c$ |
| Unit cell dimensions | a = 10.0620(12)Å,<br>b = 16.9290(11)Å,<br>c = 11.1480(12)Å,<br>α = 90°<br>β = 112.730(9)°<br>γ = 90° |
| Volume ($Å^3$) | 1751.5(3) |
| Z | 4 |
| Density ,calculated ($mg/m^3$) | 2.113 |
| Absorption coefficient ($mm^{-1}$) | 2.860 |
| F(000) | 1076 |
| Crystal size ($mm^3$) | 0.10 x 0.10 x 0.13 |
| Theta range for data collection (°) | 3.12 to 29.98 |
| Index ranges | $0 \le h \le 14$, $0 \le k \le 23$, $-15 \le l \le 14$ |
| Reflections collected | 4603 |
| Independent reflections | 4383 [R(int) = 0.0335] |
| Refinement method | Full-matrix least-squares on $F^2$ |
| Data / restraints / parameters | 4383 / 0 / 220 |
| Goodness-of-fit on $F^2$ | 1.061 |
| Final R indices [I>2σ(I)] | $R_1$ = 0.0424, $wR_2$ = 0.0927 |
| R indices (all data) | $R_1$ = 0.0506, $wR_2$ = 0.0966 |
| Largest diff. peak and hole (e. $Å^{-3}$) | 0.820 and -0.610 |

**Table 4.20** Selected bond lengths (Å) for $[Rh(cupf)(COCH_3)(I)\{P(OCH_2)_3CCH_3\}]_2$ with estimated standard deviations in parentheses.

| Bond | Length (Å) | Bond | Length (Å) |
|---|---|---|---|
| Rh-C(1) | 2.037(6) | O(5)-C(5) | 1.472(6) |
| Rh-O(3) | 2.040(4) | C(6)-C(5) | 1.511(7) |
| Rh-O(2) | 2.064(3) | O(4)-C(3) | 1.466(6) |
| Rh-P | 2.1876(13) | C(1)-O(1) | 1.205(7) |
| Rh-I | 2.6345(6) | C(1)-C(2) | 1.435(10) |
| Rh-I#1 | 3.0430(6) | C(6)-C(7) | 1.528(7) |
| P-O(6) | 1.585(4) | O(6)-C(4) | 1.469(6) |
| O(3)-N(1) | 1.281(5) | O(2)-N(2) | 1.329(5) |
| N(1)-N(2) | 1.301(6) | N(2)-C(11) | 1.448(6) |

Symmetry transformations used to generate equivalent atoms: #1 -x,-y,-z+2

**Table 4.21** Selected bond angles (°) for $[Rh(cupf)(COCH_3)(I)\{P(OCH_2)_3CCH_3\}]_2$ with estimated standard deviations in parentheses.

| Bond | Angle (°) | Bond | Angle (°) |
|---|---|---|---|
| C(1)-Rh-O(3) | 93.0(2) | O(5)-P-Rh | 119.52(15) |
| C(1)-Rh-O(2) | 92.3(2) | O(6)-P-Rh | 116.99(15) |
| O(3)-Rh-O(2) | 78.65(13) | O(4)-P-Rh | 109.54(15) |
| C(1)-Rh-P | 87.07(17) | N(1)-O(3)-Rh | 114.1(3) |
| O(3)-Rh-P | 93.77(10) | O(3)-N(1)-N(2) | 115.1(4) |
| O(2)-Rh-P | 172.36(10) | C(3)-O(4)-P | 115.9(4) |
| C(1)-Rh-I | 93.68(17) | O(1)-C(1)-C(2) | 123.4(6) |
| O(3)-Rh-I | 168.30(10) | O(1)-C(1)-Rh | 121.3(5) |
| O(2)-Rh-I | 91.47(9) | C(2)-C(1)-Rh | 115.3(5) |
| P-Rh-I | 96.17(4) | C(5)-C(6)-C(3) | 109.2(5) |
| C(1)-Rh-I#1 | 172.91(17) | C(5)-C(6)-C(7) | 110.3(4) |
| O(3)-Rh-I#1 | 85.46(11) | O(4)-C(3)-C(6) | 109.6(4) |
| O(2)-Rh-I#1 | 80.65(11) | N(2)-O(2)-Rh | 106.6(3) |
| P-Rh-I#1 | 99.93(4) | N(1)-N(2)-O(2) | 124.7(4) |
| I-Rh-I#1 | 86.767(17) | N(1)-N(2)-C(11) | 119.1(4) |
| Rh-I-Rh#1 | 93.233(17) | O(2)-N(2)-C(11) | 116.2(4) |
| O(6)-P-O(4) | 102.7(2) | | |

Symmetry transformations used to generate equivalent atoms: #1 -x,-y,-z+2

**Table 4.22** Hydrogen interactions in $[Rh(cupf)(COCH_3)(I)\{P(OCH_2)_3CCH_3\}]_2$.

| Donor - H...Acceptor | Type | D - H (Å) | H...A (Å) | D...A (Å) | D - H...A (°) |
|---|---|---|---|---|---|
| C(2) --H(2B) ..O(2) | Intra | 0.96 | 2.60 | 3.1665 | 118 |
| C(2) --H(2C) ..O(3) | Intra | 0.96 | 2.55 | 2.9599 | 106 |
| C(16) --H(16) ..O(2) | Intra | 0.93 | 2.38 | 2.7053 | 100 |
| C(13) --H(13) ..O(4) | Inter | 0.93 | 2.60 | 3.4580 | 154 |

### 4.3.7 Crystal structure of *trans*-[Rh(CO)(Cl)($PCy_3$)$_2$]

A perspective view of *trans*-[Rh(CO)(Cl)($PCy_3$)$_2$] is presented in Figure 4.18 with Figure 4.19 illustrating the disorder of the CO and Cl ligands in the structure. Figure 4.20 portrays a stereoscopic view of the packing of molecules in the unit cell. A summary of the general crystal data and refinement parameters is given in Table 4.23. The most relevant bond lengths and angles are reported in

Table 4.24 and Table 4.25. Table 4.26 list the hydrogen interactions involved.

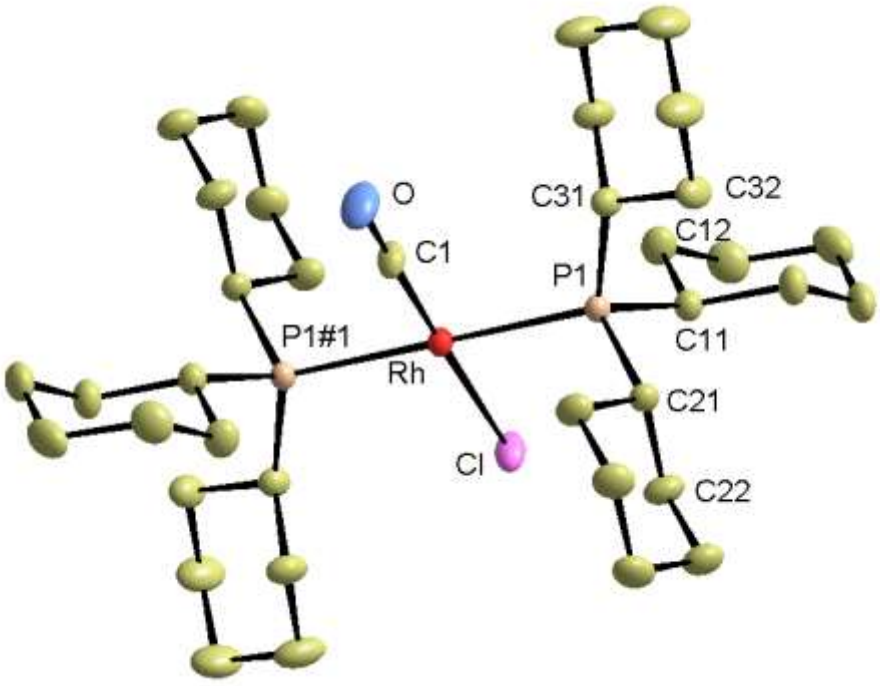


**Figure 4.18** The structure of *trans*-[Rh(CO)(Cl)($PCy_3$)$_2$] showing the atom numbering scheme. Displacement ellipsoids are drawn at the 30% probability level. Hydrogen atoms are omitted for clarity. Only the first two atoms of each cyclohexane ring are labeled. The first digit on the label indicates the ring number while the second digit indicates the position of the atom in the ring.

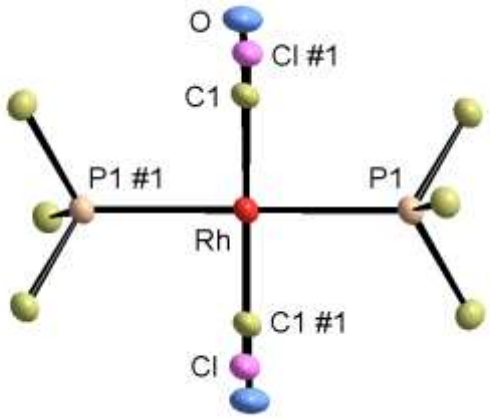


**Figure 4.19** Perspective view of the coordination polyhedron of *trans*-[Rh(CO)(Cl)($PCy_3$)$_2$] illustrating the 1:1 disorder of the CO and Cl ligands in the structure.

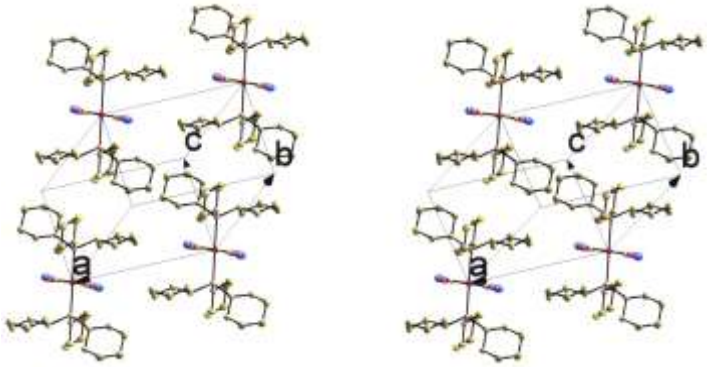


**Figure 4.20** Stereoscopic view of *trans*-[Rh(CO)(Cl)($PCy_3$)$_2$] visualizing the packing of molecules in the unit cell. Only four of the actual eight molecules involved with the unit cell is presented.

**Table 4.23** Crystal data and structure refinement for *trans*-[Rh(CO)(Cl)($PCy_3$)$_2$]

| | |
|---|---|
| Identification code | NEOBIS |
| Empirical formula | $RhC_{37}ClH_{66}OP_2$ |
| Formula weight | 727.20 |
| Temperature (K) | 293(2) |
| Wavelength, Mo Kα (Å) | 0.71073 |
| Crystal system | Triclinic |
| Space group | $P\bar{1}$ |
| Unit cell dimensions | a = 10.2390(14)Å, |
| | b = 10.7920(12)Å, |
| | c = 9.9450(11)Å, |
| | α = 109.260(10)° |
| | β = 90.660(10)° |

| | |
|---|---|
| | γ = 113.830(10)° |
| Volume (Å$^3$) | 935.5(2) |
| Z | 1 |
| Density ,calculated (mg/m$^3$) | 1.291 |
| Absorption coefficient (mm$^{-1}$) | 0.640 |
| F(000) | 388 |
| Crystal size (mm$^3$) | 0.14 x 0.14 x 0.23 |
| Theta range for data collection (°) | 3.37 to 29.97 |
| Index ranges | -14 ≤ h ≤ 14, -15 ≤ k ≤ 13, 0 ≤ l ≤ 13 |
| Reflections collected | 5103 |
| Independent reflections | 5096 [R(int) = 0.0123] |
| Refinement method | Full-matrix least-squares on F$^2$ |
| Data / restraints / parameters | 5096 / 0 / 206 |
| Goodness-of-fit on F$^2$ | 1.027 |
| Final R indices [I>2σ(I)] | $R_1$ = 0.0431, $wR_2$ = 0.1071 |
| R indices (all data) | $R_1$ = 0.0474, $wR_2$ = 0.1105 |
| Largest diff. peak and hole (e. Å$^{-3}$) | 0.948 and –0.489 |

**Table 4.24** Selected bond lengths (Å) for *trans*-[Rh(CO)(Cl)(PCy$_3$)$_2$] with estimated standard deviations in parentheses.

| Bond | Length (Å) | Bond | Length (Å) |
|---|---|---|---|
| Rh-C(1) | 1.748(8) | P(1)-C(31) | 1.864(3) |
| Rh-P(1) | 2.3491(7) | Cl-O#1 | 0.527(5) |
| Rh-Cl | 2.388(2) | Cl-C(1)#1 | 0.642(6) |
| P(1)-C(11) | 1.852(3) | O-C(1) | 1.163(7) |
| P(1)-C(21) | 1.852(2) | C(11)-C(12) | 1.529(4) |

Symmetry transformations used to generate equivalent atoms: #1 -x,-y,-z

**Table 4.25** Selected bond angles (°) for *trans*-[Rh(CO)(Cl)(PCy$_3$)$_2$] with estimated standard deviations in parentheses.

| Bond | Angle (°) | Bond | Angle (°) |
|---|---|---|---|
| C(1)-Rh-P(1) | 89.4(2) | C(11)-P(1)-Rh | 112.63(8) |
| C(1)-Rh-P(1)#1 | 90.6(2) | C(21)-P(1)-Rh | 112.14(8) |
| P(1)-Rh-P(1)#1 | 180.0 | C(31)-P(1)-Rh | 114.69(8) |
| C(1)-Rh-Cl | 178.6(2) | C(11)-P(1)-C(21) | 103.81(11) |
| P(1)-Rh-Cl | 91.41(5) | C(11)-P(1)-C(31) | 110.03(12) |
| P(1)#1-Rh-Cl | 88.59(5) | C(21)-P(1)-C(31) | 102.57(11) |
| O-C(1)-Rh | 178.3(9) | C(16)-C(11)-C(12) | 110.5(2) |

Symmetry transformations used to generate equivalent atoms: #1 -x,-y,-z

**Table 4.26** Hydrogen interactions in *trans*-[Rh(CO)(Cl)($PCy_3$)$_2$].

| Donor - H...Acceptor | Type | D - H (Å) | H...A (Å) | D...A (Å) | D - H...A (°) |
|---|---|---|---|---|---|
| C(11) --H(11) ..Cl(1) | Intra | 0.98 | 2.81 | 3.3738 | 117 |
| C(22) --H(22B) ..Cl(1) | Intra | 0.97 | 2.83 | 3.5082 | 128 |
| C(31) --H(31) ..Cl(1) | Intra | 0.98 | 2.66 | 3.2942 | 122 |

## 4.4 Discussion

### 4.4.1 The cupferrate and neocupferrate structures

These structures will be discussed according to a number of features common to them. As some of the features are interrelated to a large extent, a watertight division could not be achieved, but it nevertheless serves to systematise the observations and interpretations.

#### *4.4.1.1 The square planar coordination sphere*

The rhodium atoms in [Rh(neocupf)(CO)($PPh_3$)] and [Rh(cupf)(CO){$P(OCH_2)_3CCH_3$}], like in [Rh(cupf)(CO)($PPh_3$)], are square planar coordinated as can be expected from Rh(I) complexes. The rhodium atom is displaced by 0.01 Å from the O(2), O(3), C(1), P plane and the coordination polyhedrons are thus planar. The plane of the chelate ring atoms are tilted 5.2º from the latter plane.

The limited bite angle (76.6(3)º, 77.2(1)º and 77.3(2)º,Table 4.30) of the cupferrate and neocupferrate chelate rings is responsible for the angle distortion from the normal expected square planar array in Rh(I) complexes. As a result of this, the O(3)-Rh-P, O(2)-Rh-C(1), O(3)-Rh-C(1) and O(2)-Rh-P angles (Table 4.27) deviate significantly from the normal expected values. The significant longer Rh-O(3) bond, compared to Rh-O(2), as shown in Table 4.28, is due to the large *trans*-influence of the $PPh_3$ ligand compared to that of the carbonyl group. This tendency has been observed previously in [Rh(DBM)(CO)($PPh_3$)][38], in [Rh(acac)(CO)($PPh_3$)][39] as well as

[38] Lamprecht, D., Lamprecht, G.J., Botha, J.M., Umakoshi, K. and Sasaki, Y., *Acta Cryst*., **C53**, 1403 (1997).

in [Rh(Trop)(CO)($PPh_3$)].[40] In the case of [Rh(cupf)(CO){$P(OCH_2)_3CCH_3$}] with P *trans* to O(2), the difference between the two Rh-O bond lengths confirms the larger *trans*-influence of the phosphite ligand as well in comparison with the carbonyl ligand. Using the same phosphite ligand in [Rh(DBM)(CO){$P(OCH_2)_3CCH_3$}][41], corresponding Rh-O distances of 2.031(3) Å and 2.059(3) Å was observed. In general, the rhodium-ligand bond lengths compare very well with those found in similar complexes and will be discussed in more detail.

**Table 4.27** Bond angles about the rhodium centre in the square planar complexes (°).

| Complex | O(3)-Rh-P | O(2)-Rh-P | O(2)-Rh-C(1) | O(3)-Rh-C(1) |
|---|---|---|---|---|
| [Rh(neocupf)(CO)($PPh_3$)] | 168.16(9) | 90.95(8) | 175.8(2) | 100.5(2) |
| [Rh(cupf)(CO)($PPh_3$)] | 172.6(2) | 96.8(2) | 172.8(3) | 98.1(4) |
| [Rh(cupf)(CO){$P(OCH_2)_3CCH_3$}] | 94.8(1) | 170.8(1) | 99.9(3) | 175.6(3) |

**Table 4.28** Rh-O distances of the square planar coordination sphere.

| Complex | Rh-O3 (Å) | Rh-O2 (Å) |
|---|---|---|
| [Rh(neocupf)(CO)($PPh_3$)] | 2.081(3) | 2.025(3) |
| [Rh(cupf)(CO)($PPh_3$)] | 2.063(6) | 2.024(6) |
| [Rh(cupf)(CO){$P(OCH_2)_3CCH_3$}] | 2.026(5) | 2.059(4) |

The fact that only one CO group of the parent complexes, [Rh(cupf)$(CO)_2$] and [Rh(neocupf)$(CO)_2$] could be replaced by $PPh_3$, makes it possible to compare the relative *trans*-influence of the cupferrate and neocupferrate oxygen atoms with each other. Substitution of the CO group *trans* to the nitroso group, O(3), in [Rh(cupf)$(CO)_2$] and [Rh(neocupf)$(CO)_2$] by $PPh_3$ shows that the nitroso oxygen has the greater *trans*-influence. If the same parallelism exists with regard to β-diketone ligands,[42] it implies that O(2), compared to O(3), is more electron deficient (due to the electron withdrawing capacity of the phenyl or naphtyl group) resulting in a weaker

[39] Leipoldt, J.G., Basson, S.S., Bok, L.D.C. and Gerber, T.I.A., *Inorg. Chim. Acta*, **26**, L35 (1978).

[40] Leipoldt, J.G., Bok, L.D.C., Basson, S.S., and Meyer, H., *Inorg. Chim. Acta*, **42**, 105 (1980).

[41] Erasmus, J.J.C., Lamprecht, G.J., Kohzuma, T. and Nakano, Y., *Acta Cryst*., **C54**, 1085 (1998).

[42] Leipoldt, J.G., Bok, L.D.C., Basson, S.S. and Gerber, T.I.A., *Inorg. Chim. Acta*, **34**, L293 (1979).

Rh-O bond and thus exerting a smaller *trans*-influence. Exceptions to this substitution pattern have been found where bulky substituents and comparative electronegative substituent groups on the bidentate ligand alter the choice as illustrated by the structure determinations of [Rh(macsm)(CO)($PPh_3$)],[43] [Rh(tfdmaa)(CO)($PPh_3$)],[44] [Rh(tftmaa)(CO)($PPh_3$)],[45] and [Rh(tfhd)(CO)-($PPh_3$)].[46] [Rh(cupf)(CO){$P(OCH_2)_3CCH_3$}] with a much less bulky but stronger $\pi$-bonding P ligand (cone angle of 101° compared to the 145° of $PPh_3$) unexpectedly gave the other isomer compared to [Rh(neocupf)(CO)($PPh_3$)] and [Rh(cupf)(CO)($PPh_3$)]. Preston,[47] in a study of specific isomer formation of rhodium(I) thiolato complexes, proposed that in the case of phosphites, which are stronger $\pi$-acceptors compared to the phosphines, substitution takes place in a position *cis* to the donor atom with the largest *trans*-influence.

#### *4.4.1.2 The octahedral coordination sphere*

Both [Rh(cupf)(CO)($CH_3$)(I)($PPh_3$)] and [Rh(neocupf)(CO)($CH_3$)(I)($PPh_3$)] are products of a *cis* addition of iodomethane, with $d^2sp^3$ hybridisation of the $d^6$ Rh(III) centre displaying an octahedral geometry. The equatorial array formed by O(2), O(3), C(1) and C(2) is planar with no individual atom displaced by more than 0.044 Å from this plane. The Rh-I bond axis is slightly but significantly inclined by 3.3° towards O(2) and the Rh-P bond, in similar fashion, by 3° towards O(3). These result in a 3.4° deviation from linearity for the I-Rh-P bond axis. The chelate ring atoms are also planar and form an angle of 5.0° with the above-mentioned equatorial plane.

The most severe deviations from normal octahedral geometry are to be found in the O(2), O(3), C(1), C(2) equatorial plane, especially if the bond and angle data of [Rh(cupf)(CO)($CH_3$)(I)($PPh_3$)] are compared with those of [Rh(cupf)(CO)($PPh_3$)]. The latter complex contains $PPh_3$ *trans* to O(3) compared with the $CH_3$ group for [Rh(cupf)(CO)($CH_3$)(I)($PPh_3$)], making the two equatorial planes otherwise the same.

[43] Steyn,G.J.J., Roodt, A. and Leipoldt, J.G., *Inorg. Chem*., **31**, 3477 (1992).

[44] Leipoldt, J.G., Basson, S.S. and Nel, J.T., *Inorg. Chim. Acta*, **74**, 85 (1983).

[45] Leipoldt, J.G., Basson, S.S. and Potgieter, J.H., *Inorg. Chim. Acta*, **117**, L3 (1986).

[46] Steynberg, E.C., Lamprecht, G.J. and Leipoldt, J.G., *Inorg. Chim. Acta*, **133**, 33 (1987).

[47] Preston, H., Ph.D. Thesis, Free State University, Bloemfontein, South Africa (1993).

The Rh-O(3) bond is a significant 0.112 Å longer for [Rh(cupf)(CO)($CH_3$)(I)($PPh_3$)] due to the much larger *trans*-influence of the $CH_3$ group. With the Rh-O(2), O(2)-N(2), N(1)-N(2) and O(3)-N(1) distances (Table 4.29) as well as chelate ring and bite angles (Table 4.30) being the same within experimental error for the complexes under discussion, it is to be expected that the lengthening of the Rh-O(3) bond, together with different spatial requirements of the $PPh_3$ and $CH_3$ groups, will be mainly responsible for any differences between the two equatorial planes. In this respect we notice a formidable increase of 10° for the O(3)-Rh-C(1) angle in [Rh(cupf)(CO)($CH_3$)(I)($PPh_3$)] compared to that of [Rh(cupf)(CO)($PPh_3$)] (Table 4.31).

**Table 4.29** Chelate ring bond distances (Å)

| Complex | Rh-O3 | Rh-O2 | O2-N2 | O3-N1 | N1-N2 |
|---|---|---|---|---|---|
| [Rh(cupf)(CO)($PPh_3$)] | 2.063(6) | 2.024(6) | 1.329(8) | 1.30(1) | 1.28(1) |
| [Rh(cupf)(CO)($CH_3$)(I)($PPh_3$)] | 2.175(9) | 2.04(1) | 1.32(1) | 1.27(2) | 1.33(2) |
| [Rh(cupf)(CO)($PPh_3$)$_2$] | 2.339(9) | 2.147(8) | 1.33(1) | 1.28(1) | 1.30(1) |
| [Rh(neocupf)(CO)($PPh_3$)] | 2.081(3) | 2.025(3) | 1.329(4) | 1.295(5) | 1.292(5) |
| [Rh(neocupf)(CO)($CH_3$)(I)($PPh_3$)] | 2.128(6) | 2.074(5) | 1.344(8) | 1.265(9) | 1.308(9) |
| [Rh(cupf)(CO){$P(OCH_2)_3CCH_3$}] | 2.026(5) | 2.059(4) | 1.325(6) | 1.325(7) | 1.264(7) |
| [Rh(cupf)($COCH_3$)(I){$P(OCH_2)_3CCH_3$}]$_2$ | 2.040(4) | 2.064(3) | 1.329(5) | 1.281(5) | 1.301(6) |

**Table 4.30** Chelate ring backbone and bite angles (°)

| Complex | O3-Rh-O2 | O3-N1-N2 | N1-N2-O2 | Rh-O2-N2 | Rh-O3-N1 |
|---|---|---|---|---|---|
| [Rh(cupf)(CO)($PPh_3$)] | 76.6(3) | 113.6(7) | 123.5(7) | 110.7(5) | 115.4(6) |
| [Rh(cupf)(CO)($CH_3$)(I)($PPh_3$)] | 74.9(4) | 113(1) | 124(1) | 112.8(7) | 115.3(8) |
| [Rh(cupf)(CO)($PPh_3$)$_2$] | 69.6(3) | 114(1) | 124(1) | 116.3(6) | 116.0(7) |
| [Rh(neocupf)(CO)($PPh_3$)] | 77.2(1) | 113.4(3) | 124.6(3) | 109.7(2) | 114.7(2) |
| [Rh(neocupf)(CO)($CH_3$)(I)($PPh_3$)] | 76.3(2) | 114.4(8) | 124.7(6) | 108.9(3) | 115.3(5) |
| [Rh(cupf)(CO){$P(OCH_2)_3CCH_3$}] | 77.3(2) | 113.5(5) | 124.7(5) | 108.9(3) | 115.6(4) |
| [Rh(cupf)($COCH_3$)(I){$P(OCH_2)_3CCH_3$}]$_2$ | 78.7(1) | 115.1(4) | 124.7(4) | 106.6(3) | 114.1(3) |

Although the O(2)-Rh-C(1) angles of 174.8(6) and 172.8(3)° for the Rh(III) and Rh(I) complexes respectively do not differ very much, inspection of stereo models indicate that the Rh-O(2) and Rh-C(1) bond axes are mainly bent towards O(3) for [Rh(cupf)(CO)($PPh_3$)] in contrast to the opposite movement towards C(2) for

[Rh(cupf)(CO)($CH_3$)(I)($PPh_3$)]. Considering the 5-membered chelate ring as rather rigid, the conclusion can be made that the lengthening of the Rh-O(3) bond alone cannot be responsible for the clockwise turn of the chelate ring towards C(2), but that the bulkiness of the $CH_3$ and $PPh_3$ ligands also play a role. The ligand cone angles of 90° and 145° for $CH_3$ and $PPh_3$ respectively could implicate a greater steric demand for the $PPh_3$ group in the above-mentioned equatorial plane.

**Table 4.31** Angles of the coordination sphere (°)

| Complex | O3-Rh-C1 | O3-Rh-C2 | O2-Rh-C2 | C2-Rh-C1 | O2-Rh-C1 |
|---|---|---|---|---|---|
| [Rh(cupf)(CO)($PPh_3$)] | 98.1(4) | | | | 172.8(3) |
| [Rh(cupf)(CO)($CH_3$)(I)($PPh_3$)] | 108.1(5) | 167.3(6) | 92.4(6) | 84.6(7) | 174.8(6) |
| [Rh(neocupf)(CO)($PPh_3$)] | 100.5(2) | | | | 175.8(2) |
| [Rh(neocupf)(CO)($CH_3$)(I)($PPh_3$)] | 102.9(4) | 170.8(4) | 94.5(4) | 86.2(6) | 174.6(4) |

A conspicuous feature of the coordination spheres of [Rh(cupf)(CO)($CH_3$)(I)($PPh_3$)] and [Rh(neocupf)(CO)($CH_3$)(I)($PPh_3$)] as well as other known Rh(III) alkyl complexes of the form [Rh(LL′-BID)(CO)($PPh_3$)(I)($CH_3$)] (where LL′-BID is ox,[15] dmavk[48], quin[16] and fctfa[49]) is that in all these complexes the iodo ligand is bonded in the axial position of the octaheder, above or below the equatorial array formed by L, L′, CO and $CH_3$ or $PPh_3$. This is the case, irrespective of the mode of addition, since the cupf, neocupf, quin and fctfa complexes are examples of a *cis* addition of iodomethane, whereas the ox and dmavk complexes are *trans*-addition products. According to Cano,[16] the *trans* orientation of the iodide and phosphine ligands is consistent with the established behaviour of the bulky and electronegative ligands to occupy the apical positions. The carbonyl group is coordinated in the equatorial plane of the octaheder in all the complexes mentioned.

[Rh(cupf)($COCH_3$)(μ-I){$P(OCH_2)_3CCH_3$}]$_2$ is the product of the oxidative addition of iodomethane to [Rh(cupf)(CO){$P(OCH_2)_3CCH_3$}]. Apart from the fact that [Rh(cupf)($COCH_3$)(μ-I){$P(OCH_2)_3CCH_3$}]$_2$ is a bridged dimer complex, its octahedral coordination sphere differs considerably from that of [Rh(cupf)(CO)($CH_3$)(I)($PPh_3$)]

[48] Damoense, L.J., Ph.D. Thesis, Free State University, Bloemfontein, South Africa (2000).

[49] Conradie, J., Ph.D. Thesis, Free State University, Bloemfontein, South Africa (1999).

and [Rh(neocupf)(CO)($CH_3$)(I)($PPh_3$)]. In these two complexes the phosphine ligands moved out of the positions they occupied in the precursor square planar Rh(I) complexes to axial positions *trans* to iodide. In [Rh(cupf)($COCH_3$)(μ-I){$P(OCH_2)_3CCH_3$}]$_2$ the phosphorous ligand is still in the same plane as the chelate ring and still *trans* to O2 as in the precursor, [Rh(cupf)(CO){$P(OCH_2)_3CCH_3$}]. Instead, the CO group has moved out of this plane during oxidative addition and underwent insertion to form an acyl ligand. The P-Rh-*trans*-ligand configuration was also retained in the oxidative addition and CO insertion of [Rh(dmavk)(CO)($PPh_3$)].[50,51] The coordination geometry of a number of Rh(III)-acyl complexes was investigated (listed in par. 4.4.1.9, Table 4.37 and Table 4.38) and for all the complexes mentioned, the geometry was square pyramidal with the acyl group occupying the apical coordination site. That was also indicated in another study as the preferred arrangement for five-coordinate complexes of $d^6$ metal ions.[52] Taking all these into account, as well as the position of the chelate ring, the conclusion can be made that the two oxygen atoms of the chelate ring, and the atoms P and I define the equatorial plane of the octahedral coordination sphere. Perpendicular to the equatorial plane and tilted slightly towards the phosphorous ligand (C1-Rh-P = 87.1(2)°, whereas the other angles are 93.7(2)°, towards I, 93.0(2)° towards O3 and 92.3(2)° towards O2) is the coordination site of the acyl ligand. *Trans* to the acyl, occupying the sixth site (if it was assumed that this acyl complex was initially a five-coordinate square pyramidal complex like all the other acyl complexes) is I#1, which is actually the equatorial iodide of the other five-coordinate square pyramidal complex. Since the equatorial iodide ligands of both rhodium centres fulfil that role, the result is a centro-symmetrical iodo bridged Rh(III) dimer complex. The Rh-Rh distance is 4.14(2) Å and the I-I distance is 3.911(9) Å. Although other iodo bridged rhodium complexes such as [Rh($I_2$)(μ-I)($Ph_2PC_6H_4Sme$-2)]$_2$[53] and [Rh{$Ph_2P(CH_2)_3PPh_2$}(H)(I)(μ-I)]$_2$[54] are described in the literature, [Rh($I_2$)(μ-I)-

[50] Galding, M.R., Cherkasova, T.G., Varshavsky, Y.S., Osetrova, L.V. and Roodt, A., *Rhodium Ex.*, **9**, 36 (1995).

[51] Damoense, L.J., Purcell, W. and Roodt, A., *Rhodium Ex.*, **14**, 4 (1995).

[52] Hoffman, P.R. and Caulton, K.G., *J. Am. Chem. Soc*., **97**, 4221 (1975).

[53] Dilworth, J.R., Morales, D. and Zheng, Y., *J. Chem. Soc., Dalton Trans*., 3007 (2000).

[54] Moloy, K.G. and Petersen, J.L., *Organometallics*, **14**, 2931 (1995).

$(CO)(COCH_3)]_2^{2-}$[55] provided the most relevant comparison. Like $[Rh(cupf)(COCH_3)(\mu\text{-}I)\{P(OCH_2)_3CCH_3\}]_2$, $[Rh(I_2)(\mu\text{-}I)(CO)(COCH_3)]_2^{2-}$ is a Rh(III) dimer complex containing a double iodide bridge with an acyl ligand *trans* to one of the iodide ligands forming the bridge. Table 4.32 compares some of the bonding distances in the two complexes. The Rh-I#1 distance, the one *trans* to the acyl ligand, is significantly longer than the other Rh-I distance, demonstrating the large *trans*-influence of the acyl ligand. An acyl ligand is known to have a high *trans*-influence.[56] Anderson and Cross[57] studied the influence of different ligands on carbonyl insertion and found that phosphine ligands with better electron donating properties favoured the formation of a halogen bridged acyl dimer. With that condition not so much applicable to the bicyclic phosphite ligand, which is regarded a better π-acceptor and weaker σ-donor compared to phosphines, the formation of $[Rh(cupf)(COCH_3)(\mu\text{-}I)\{P(OCH_2)_3CCH_3\}]_2$ can most probably be attributed to the minor steric requirements of both the cupferrate ligand with its narrow bite angle and even more importantly the small cone angle of the phosphite.

**Table 4.32** Comparative bond distances in two iodo bridged dimers

| Complex | Rh-I (Å) | Rh-I#1 (Å) | Rh-C1 (Å) |
|---|---|---|---|
| $[Rh(cupf)(COCH_3)(\mu\text{-}I)\{P(OCH_2)_3CCH_3\}]_2$ | 2.6345(6) | 3.0430(6) | 2.037(6) |
| $[Rh(I_2)(\mu\text{-}I)(CO)(COCH_3)]_2^{2-}$ | 2.679(2) | 3.001(2) | 2.06(2) |

The octahedral coordination sphere of $[Rh(cupf)(COCH_3)(\mu\text{-}I)\{P(OCH_2)_3CCH_3\}]_2$ shows distortion from the ideal geometry and a number of angles deviate significantly as is reported in Table 4.21. The angles, P-Rh-O2 of 172.4(1)°, P-Rh-I of 96.17(4)°, P-Rh-I#1 of 99.93(4)° and P-Rh-C1 of 87.1(2)° clearly support the visual impression of Figure 4.16 showing the phosphite ligand bent outward to minimise steric interaction. For the same reason the acyl group is twisted 50.87(1)° with respect to

[55] Adamson, G.W., Daly, J.J. and Forster, D., *J. Organomet. Chem.* **71**, C17 (1974).

[56] Bennett, M.A., Jeffery, J.C. and Robertson, G.B., *Inorg. Chem*., **20**, 323 (1981).

[57] Anderson, G.K. and Cross, R.J., *Acc. Chem. Res.*, **17**, 67 (1984).

the Rh-O2 axis. Adams *et al*[58] report a torsion angle of 45.9° for the acyl group in [Rh(dppm)($COCH_3$)$I_2$]

#### *4.4.1.3 The trigonal bipyramidal coordination sphere*

[Rh(cupf)(CO)($PPh_3$)$_2$] is a five coordinate Rh(I) complex with the two phosphine ligands arranged *trans* (nearly linear at 176.9(1)) in the apical positions. This is a favoured arrangement for complexes of this type containing Group 15 ligands.[20] According to Emsley & Hall,[13] π-bonding has a secondary effect regarding this. While π-bonding may reinforce equatorial bonds more than apical bonds, it is not the guiding factor which determines whether a ligand prefers to be positioned equatorially or apically in the *tbp* structure. This is determined by the effect a ligand has on the σ-bonds, leading to more electron attracting ligands preferring the apical positions. The trigonal equatorial plane houses the cupferrate ligand and the carbonyl group. The small bite angle of the chelate ring causes severe angle distortion in this plane, compared to the ideal angles between $dsp^3$-hybridised orbitals. The angles in this plane are O(2)–Rh–O(3), 69.6(3)°; O(2)–Rh–C(1), 159.6(5)° and O(3)–Rh–C(1), 130.8(5)°. The Rh–O(2) and Rh–O(3) bonds are dramatically lengthened in comparison to distances in [Rh(cupf)(CO)($PPh_3$)] (Table 4.1), probably due to steric considerations. The consequence of that being the already small bite angle of cupferrate, 76.6(3)° in [Rh(cupf)(CO)($PPh_3$)], significantly narrowed further to 69.6(3)° since the chelate backbone, O(2)–N(2)–N(1)–O(3), is fairly stable (chelate angles and distances in Table 4.29 and Table 4.30). In a ring system with one set of angles fixed and one angle narrowing, some angle has to widen and in this case the Rh–O(2)–N(2) angle compensates from 110.7(5)° (in [Rh(cupf)(CO)($PPh_3$)]) to 116.3(6)°.

The R–P bond is treated more extensively in par. 4.4.1.4 and the discussion in this paragraph is only meant to place the phosphine as part of this coordination sphere into perspective with similar orientated phosphine ligands. The three rhodium(I) complexes of Table 4.33 have similar R–P bond distances, irrespective of

[58] Adams, H., Bailey, N.A., Mann, B.E. and Manuel, C.P., *Inorg. Chim. Acta*, **198**, 111 (1992).

coordination number. The observed increase in the R–P bond length in *trans*-[Rh(cupf)(CO)($PPh_3$)$_2$] compared to the 2.227(1) Å in [Rh(neocupf)(CO)($PPh_3$)] can be considered a result of competition of two phosphine ligands positioned trans to each other both for σ-acceptor and π-donor orbitals of the central rhodium atom. The significant lengthening of the Rh–P bond distance of [Rh(acac)($CH_3$)(I)($PPh_3$)$_2$],[59] compared to the Rh(I) complexes, also exhibiting *trans* $PPh_3$ moieties can be attributed to much less d–π* electron back-donation from the electron poor Rh(III) metal centre.

**Table 4.33** Comparative Rh–P bond distances for rhodium complexes comprising two *trans* orientated $PPh_3$ ligands

| Complex | Oxidation state | Coordination number | Rh-P1 | Rh-P2 |
|---|---|---|---|---|
| [Rh(cupf)(CO)($PPh_3$)$_2$] | Rh(I) | 5 | 2.323(4) | 2.342(4) |
| [Rh(trop$Br_3$)(CO)($PPh_3$)$_2$][20] | Rh(I) | 5 | 2.337(2) | 2.337(2) |
| [Rh(CO)(Cl)($PPh_3$)$_2$][60] | Rh(I) | 4 | 2.322(1) | 2.322(1) |
| [Rh(acac)($CH_3$)(I)($PPh_3$)$_2$][59] | Rh(III) | 6 | 2.394(3) | 2.377(3) |

The five coordinate *trans*-[Rh(cupf)(CO)($PPh_3$)$_2$] is an example of the ability of some Rh(I) complexes to enlarge their coordination number via an associative mechanism. Square planar substitution reactions proceed according to the same mechanism, which include a five-coordinated transition state. *Trans*-[Rh(cupf)(CO)($PPh_3$)$_2$] was stable enough to be isolated as an intermediate and can be seen as a model of a *tbp* transition state as suggested in the oxidative addition reaction mechanism of this study, where the proposed five-coordinated state has a solvento species coordinated to rhodium.

#### *4.4.1.4 The phosphorous ligand*

Rh-P bond distances of the complexes studied are presented in Table 4.34. The phosphorous ligands in *trans*-[Rh(cupf)(CO)($PPh_3$)$_2$] have already been discussed. T*rans*-[Rh(CO)(Cl)($PCy_3$)$_2$] is another example of two competing phosphine ligands *trans* to each other, resulting in significant lengthening of the Rh–P bond distance

[59] Roodt, A., Botha, J.M. and Otto,S., Rhodium Ex., 17, 4 (1996).

[60] Dunbar, K.R. and Haefner, S.C*., Inorg. Chem*., **31**, 3676 (1992).

compared to the other Rh(I) complexes. The Rh–P bond distances in [Rh(cupf)(CO)($PPh_3$)] and [Rh(neocupf)(CO)($PPh_3$)] are about the same and the difference in electron density on rhodium because of the change in bidentate ligand are not reflected this way in the Rh(I) complexes. Although not convincingly significant, the larger electron density on rhodium in the case of [Rh(neocupf)(CO)-($CH_3$)(I)($PPh_3$)], compared to [Rh(cupf)(CO)($CH_3$)(I)($PPh_3$)], tend to shorten the Rh-P bond because of the ability of increased back donation to phosphorous from a more electron rich rhodium centre. The sterically small cyclic phosphite ligand allows for a closer fit in the square-planar coordination sphere. An even better explanation for the really short Rh–P bond distance of 2.156(2) Å for [Rh(cupf)(CO){$P(OCH_2)_3CCH_3$}] stems from the nature of phosphites to be excellent π-acceptors, causing stronger back donation from rhodium resulting in a shorter Rh–P bond. The same trend is reflected in [Rh(cupf)($COCH_3$)(μ-I){$P(OCH_2)_3CCH_3$}]$_2$. To put these figures into perspective, a list of several other phosphine complexes and their Rh–P bond distances appear in Table 4.35.

**Table 4.34** Rh-P bond lengths of the complexes in this study.

| Complex | Rh-P (Å) |
|---|---|
| [Rh(cupf)(CO)($PPh_3$)] | 2.232(3) |
| [Rh(cupf)(CO)($CH_3$)(I)($PPh_3$)] | 2.327(4) |
| [Rh(cupf)(CO)($PPh_3$)$_2$], Rh-P1 | 2.323(4) |
| [Rh(cupf)(CO)($PPh_3$)$_2$], Rh-P2 | 2.342(4) |
| [Rh(neocupf)(CO)($PPh_3$)] | 2.227(1) |
| [Rh(neocupf)(CO)($CH_3$)(I)($PPh_3$)] | 2.307(2) |
| [Rh(cupf)(CO){$P(OCH_2)_3CCH_3$}] | 2.156(2) |
| [Rh(cupf)($COCH_3$)(I){$P(OCH_2)_3CCH_3$}]$_2$ | 2.188(1) |
| [Rh(CO)(Cl)($PCy_3$)$_2$] | 2.3491(7) |

The Rh–P bond may also be used to estimate the relative *trans*-influence of different donor atoms[10] especially since this distance is usually determined with great accuracy. The Rh–P bond distances for a number of [Rh(LL′-BID)(CO)($PPh_3$)] complexes (L,L′-BID = O,O-BID, O,N-BID O,S-BID, N,S-BID and S,S-BID) are listed in Table 4.35. These complexes can be divided into groups according to the nature of the coordinating atoms of the bidentate ligand. Each of these groups may be further divided into either complexes with a five membered or complexes with a six membered chelate ring.

**Table 4.35** Rh-P bond distances and NMR parameters of [Rh(LL′-BID)(CO)($PPh_3$)] square planar complexes containing LL′-BID bidentate ligands.

| L,L′-BID | L,L′ | Ring size | Bite angle (°) | Rh-P distance (Å) | δ($^{31}$P) (ppm) | $^{1}$J(PRh) (Hz) |
|---|---|---|---|---|---|---|
| cupf[1] | O,O | 5 | 76.6(3) | 2.232(2) | 48.85 | 171.1 |
| neocupf | | | 77.2(1) | 2.227(1) | 48.70 | 172.4 |
| bpha[61] | | | 78.4(1) | 2.232(1) | | |
| trop[62] | | | 77.8(3) | 2.232(2) | 48.66 | 176.2 |
| tfaa[6] | | 6 | 88.9(2) | 2.231(2) | 47.73 | 176.9 |
| ba[11] | | | 88.1(3) | 2.249(3) | | |
| tftma[7] | | | 88.1(3) | 2.238(3) | | |
| tfdmaa[7] | | | 87.5(2) | 2.239(2) | | |
| tfhd[6] | | | 87.5(4) | 2.252(3) | | |
| tta[63] | | | 87.5(3) | 2.245(3) | 47.86 | 177.8 |
| bzaa[64] | | | 86.9(1) | 2.243(1) | | |
| acac[39] | | | 87.9(2) | 2.244(4) | 48.84 | 175.7 |
| dbm[38] | | | 88.5(5) | 2.237(7) | | |
| pic[65] | N,O | 5 | 78.9(2) | 2.262(2) | 40.24 | 161.9 |
| quin[66] | | | 78.9(3) | 2.258(2) | | |
| ox[67] | | | 80.0(3) | 2.261(2) | 41.40 | 161.6 |
| dmavk[68] | | 6 | 87.4(2) | 2.275(1) | 41.47 | 148.0 |
| salnr[69] | | | 88.7(3) | 2.281(2) | | |
| anmetha[47] | S,O | 5 | 83.4(1) | 2.290(1) | 37.04 | 156.2 |
| hpt[70] | | | 83.9(1) | 2.278(1) | 37.77 | 157.1 |
| sacac[4] | | 6 | 91.7(1) | 2.300(2) | 35.36 | 144.5 |
| dbbtu[71] | | | 90.11(2) | 2.282(1) | | |
| pbtu[72] | | | 91.1(2) | 2.275(3) | 36.02 | 148.1 |

Table 4.35 continued.

[61] Leipoldt, J.G. and Grobler, E.C., *Inorg. Chim. Acta*, **60**, 141 (1982).

[62] Leipoldt, J.G., Bok, L.D.C., Basson, S.S. and Meyer, H., *Inorg. Chim. Acta*, **42**, 105 (1980).

[63] Leipoldt, J.G., Bok, L.D.C., Van Vollenhoven, J.S. and Pieterse, A.I., *J. Inorg. Nucl. Chem*., **40**, 61 (1978).

[64] Roodt, A., Leipoldt, J.G., Swarts, J.C. and Steyn, G.J.J., *Acta Cryst*., **C48**, 547 (1992).

[65] Leipoldt, J.G., Lamprecht, G.J. and Graham, D.E., *Inorg. Chim. Acta*, **101**, 123 (1985).

[66] Graham, D.E., Lamprecht, G.J., Potgieter, I.M., Roodt, A. and Leipoldt, J.G., *Trans. Met. Chem.*, **16**, 193 (1991).

[67] Leipoldt, J.G., Basson, S.S. and Dennis, C.R., *Inorg. Chim. Acta*, **50**, 121 (1981).

[68] Damoense, L.J., Purcell, W., Roodt, A. and Leipoldt, J.G., *Rhodium Ex.*, **5**, 10 (1994).

[69] Leipoldt, J.G., Basson, S.S., Grobler, E.C. and Roodt, A., *Inorg. Chim. Acta*, **99**, 13 (1985).

[70] Basson, S.S., Leipoldt, J.G., Roodt, A. and Preston, H., *Acta Cryst*., **C47**, 1961 (1991).

[71] Roodt, A., Leipoldt, J.G., Koch, K.R. and Matoetoe, M., *Rhodium Ex.*, **7-8**, 39 (1994).

[72] Kemp, G., Roodt, A., Purcell, W. and Koch, K.R., *J. Chem. Soc., Dalton Trans*., 4481 (1997).

| L,L′-BID | L,L′ | Ring size | Bite angle (°) | Rh-P distance (Å) | δ($^{31}$P) (ppm) | $^{1}$J(PRh) (Hz) |
|---|---|---|---|---|---|---|
| spymMe$_2$[73] | S,N | 4 | 69.03(7) | 2.2475(6) | | |
| macsm[74] | | 6 | 93.8(1) | 2.269(1) | | |
| hacsm[75] | | | 91.3(1) | 2.283(1) | 42.70 | 148.9 |
| Et$_2$dtc[76] | S,S | 4 | 74.2(1) | 2.259(2) | | |
| Etmt[77] | | 5 | 87.86(5) | 2.297(1) | | |

The average Rh–P bond distance *trans* to an oxygen atom is 2.239(7) Å, while the average Rh–P bond distance *trans* to a nitrogen atom is 2.266(10) Å and 2.300(2) Å *trans* to a sulfur atom.[10] These differences indicate that the order of the trans-influence of the donor atoms is sulfur > nitrogen > oxygen, in agreement with the π- and σ-*trans*-influence[78] since the sulphur atom is capable of forming a π-bond with the rhodium atom (it is expected that the π-*trans*-influence is greater than the σ-*trans*-influence[78]), while the nitrogen atom (being less electronegative than an oxygen atom) is the better σ-donor of the two and thus has a larger σ-*trans*-influence than the oxygen atom. The Rh-P distance for [Rh(cupf)(CO)(PPh$_3$)] and [Rh(neocupf)(CO)-(PPh$_3$)] indicates a *trans*-influence for the nitroso oxygen comparable to those of the β-diketone ligands.

The first order Rh–P coupling constants, $^{1}$J(PRh), in rhodium-phosphine complexes as determined by $^{31}$P NMR, enable good estimates of the Rh–P bond strength[79,80]. (Coupling constants between the $^{103}$Rh and $^{31}$P nuclei, $^{1}$J($^{31}$P–$^{103}$Rh) are denoted by $^{1}$J(PRh) for simplicity.) In this study the reported correlation was extended to include cupferrate and neocupferrate. Together with the Rh–P bond distances listed in Table

[73] Dahlenburg, L. and Kühnlein, M., *Eur. J. Inorg. Chem*., 2117 (2000).

[74] Steyn, G.J.J., Roodt, A. and Leipoldt, J.G., *Inorg. Chem*., **31**, 3477 (1992).

[75] Steyn, G.J.J., Ph.D. Thesis, Free State University, Bloemfontein, South Africa (1994).

[76] Cano, M., Heras, J.V., Lobo, A., Ovejero, P., Campo, J.A. and Pinilla, E., *Rhodium Ex.*, **9**, 8 (1995).

[77] Cheng, C.H. and Eisenberg, R., *Inorg. Chem*., **18**, 2438 (1979).

[78] Langford, C.H. and Gray, H.B., *Ligand Substitution Processes*, Benjamin, New York (1966).

[79] Steyn, G.J.J., Roodt, A., Poletaeva, I. And Varshavsky, Y., *J. Organomet. Chem*., **536**, 197 (1997).

[80] Roodt, A. and Steyn, G.J.J., *Recent Research Developments in Inorganic Chemistry*, Vol. 2, Edited by S.G. Pandalai, pp1-23. Trivandrum, India: Transworld Research Network (2000).

4.35 are $^{31}$P NMR data as measured for the different complexes, while the graphic relationships are illustrated in Figure 4.21 and Figure 4.22. Roodt, Varshavsky and co-workers[79] have done separate presentations of five- and six-membered chelates and obtained better individual relationships. However, the general trend showed in Figure 4.21 and Figure 4.1 is clear.

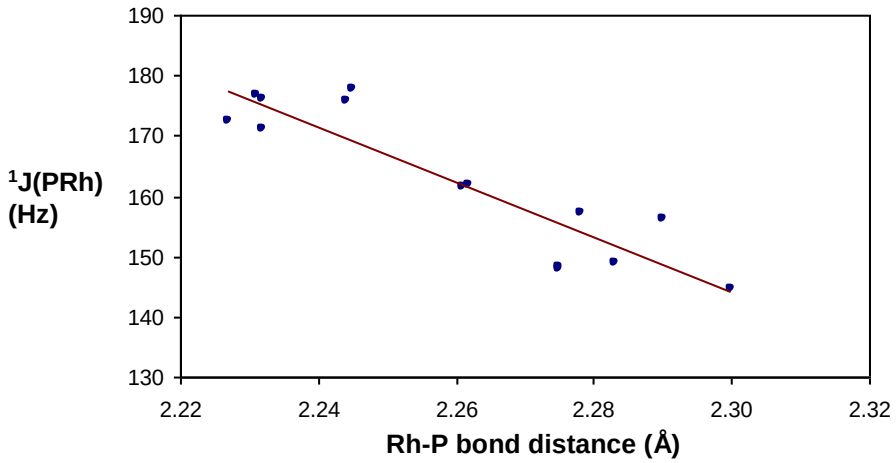


**Figure 4.21** Correlation between Rh-P bond distances and $^{1}$J(PRh)

The data demonstrates the increase in σ-donating ability of the L atom *trans* to the Rh–P bond (causing elongation of the Rh–P bond) and the corresponding decrease in the $^{1}$J(PRh) value as a result of changes in overlap between the 5s(Rh)-3s(P) orbitals. The values of 171.1 and 172.4 Hz obtained for [Rh(cupf)(CO)($PPh_3$)] and [Rh(neocupf)(CO)($PPh_3$)] respectively is lower than the values for [Rh(trop)(CO)($PPh_3$)] (176.2 Hz) and [Rh(tfaa)(CO)($PPh_3$)] (176.9 Hz) with identical Rh-P bond distances. It seems that the Rh-P bonds in the case of cupferrate and neocupferrate are lengthened in solution by solvent interaction, causing the lower $^{1}$J(PRh) values.

A similar correlation exists[80] between the δ($^{31}$P) and the Rh–P bond distances. Since the chemical shift is dependent on many factors, it is thus expected that this parameter, for the range of complexes studied, should not necessarily vary in parallel with the Rh–P bond distance. It is therefore remarkable that such a good correlation is obtained, which suggests that the electron density on the phosphorous atom does vary reasonably in conjunction with the Rh–P bond strength, and to a large extent

thus with the σ-donating ability of the phosphine ligand. The cupferrate and neocupferrate ligands fit convincingly well into the correlation.

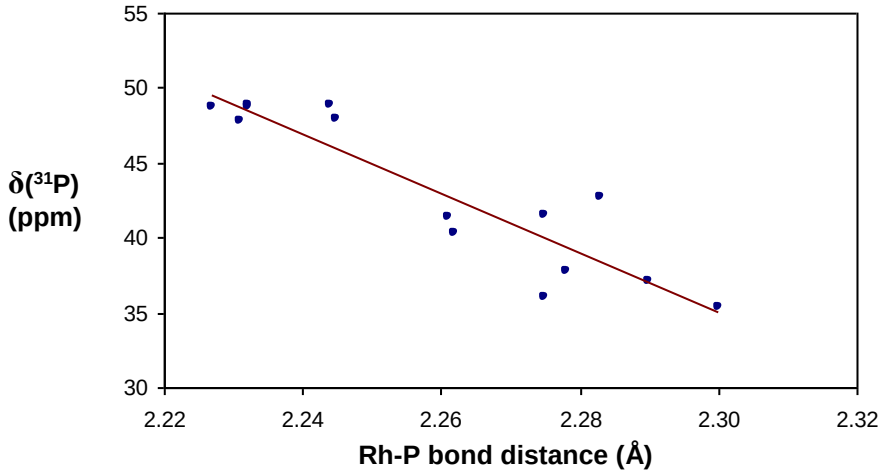


**Figure 4.22** Correlation between Rh-P bond distances and δ($^{31}$P), $CDCl_3$

A further tendency is perceptible from Rh–P bond distances. The Rh–P bond distances in the case of the five membered chelate rings are smaller than the corresponding value for the six membered chelate rings for both the O,O- and N,O-bonded bidentate ligands.[10] The average Rh–P bond distances for a five and six membered O,O-bonded chelate ring are 2.232(2) and 2.243(5) Å respectively while the average values for a five and six membered N,O-bonded chelate ring are respectively 2.260(2) and 2.281(2) Å. These results indicate that the *trans*-influence of a donor atom in a chelate ring may be explained in terms of orbital overlap. If the bite angle deviates significantly from 90° (the ideal angle for maximum overlap with the $dsp^2$-hybrid orbitals of the central metal atom) such as in the case of a planar five membered chelate ring, the overlap with the $dsp^2$ orbitals of the metal atom is less effective. The average bite angles for the five and six membered chelate rings listed in Table 4.35 are 78.4 and 88.2° respectively. Less effective overlap would lead to a weaker metal-ligand bond and thus a weaker *trans*-influence and accordingly a stronger Rh–P bond. Another example from Table 4.35 illustrating this principle is the case of the S,S donor bidentate ligands. The four-membered ring with a bite angle of 74.2(1)° has a Rh–P bond of 2.259(2) Å, while the value for the five-membered ring (87.86(5)°) is 2.297(1) Å.

The rhodium atom and three carbon atoms of the phenyl rings tetrahedrally surround the phosphorous atom. The phenyl rings are all planar and their C-C bond distances range from 1.37(1) to 1.42(1) Å with an average of 1.40(2) Å. The P–C bond distances are about the same as found in other $PPh_3$ complexes and are in excellent agreement with the accepted values for phenyl rings.

#### *4.4.1.5 The chelate ring*

The O–N, N–N and C–N bond distances of the cupferrate and neocupferrate ligands agree, within experimental error, very well with those of $[RhCl_2\{ONN(C_6H_4Me\text{-}p)O\}(H_2O)(PPh_3)]$,[81] $[Co(cupf)_2(OHCH_3)_2]$,[82] $[Al(cupf)_3]$,[83] $[Sn(cupf)_4]$,[84] $[Sn(cupf)_2(Ph)_2]$,[84] $[Zr(cupf)_4]$,[85], $[Fe(cupf)_3]$,[86] $[Cu(cupf)_2]$[87] and $[Cu(cupf)(PPh_3)_2]$[88]. The O–N and N–N bond distances, being roughly equalized within experimental error, show that delocalisation of $\pi$ electrons took place. The N–N distance using Pauling's criteria[89], as well as the linear relationship between N–N bond distances and bond order calculated by the HMO method[90], indicate an 80% double bond character. Taking the N-O single and double bond distances as 1.44 and 1.20 Å respectively[89], it is evident that the N(1)–O(3) and N(2)–O(2) bonds have 58 and 45% double bond character respectively. This is also in agreement with experimental bond distance to bond order relationships for nitroso compounds.[91]

---

[81] Ahmed, M., Edwards, A.J., Jones, C.J., McCleverty, J.A., Rothin, A.S. and Tate, J.P., *J. Chem. Soc., Dalton Trans*., 257 (1988).

[82] Deák, A., Párkányi, L., Kálmán, A., Venter, M. and Haiduc, I., *Acta Cryst*., **C54**, IUC9800036 (1998).

[83] Okabe, N., Tamaki, K., Suga, T. and Kohyama, Y., *Acta Cryst*., **C51**, 1295 (1995).

[84] Párkányi, L., Kálmán, A., Deák, A., Venter, M. and Haiduc, I., *Inorg. Chem*. *Commun*., **2**, 265 (1999).

[85] Mark, W., *Acta Chem. Scand.*, **24**, 1398 (1970).

[86] Van der Helm, D., Merritt, L.L., Degeilh, R. and MacGillavry, *Acta Chrystallogr*., **18**, 355 (1965).

[87] Shkol'nikova and Shugam, E.A., *J. Struct. Chem* (Engl. Transl.) **4**, 350 (1963).

[88] Charalambous, J., Haines, L.I.B., Harris, N.J., Henrick, K. and Taylor, F.B., *J. Chem. Res.*, **(M)**, 2101 (1984).

[89] Pauling, L., *The Nature of the Chemical Bond*, 3rd Ed., Cornell university Press, New York (1960).

[90] Sabesan, M.N. and Venkatesan, K., *Acta Cryst*., **B27**, 986 (1971).

[91] Linnett, J.W. Rosenberg, R.M., *Tetrahedron*, **20**, 53 (1964).

The N(2) bonded atoms form an average bond angle of 120(1)°, thus corresponding to a $sp^2$ hybridised state for this nitrogen atom. The C(41) and C(44) atoms, being displaced by 0.01 and 0.11 Å respectively from the chelate ring-atom plane, can also be considered as part of this plane. Calculations then show that the N-substituted phenyl ring of [Rh(cupf)(CO)($CH_3$)(I)($PPh_3$)] is twisted 39.5° along the N(2)–C(41)–C(44) axis relative to the chelate ring-atom plane. This is ascribed to packing considerations if compared with a similar ring-atom-to-equatorial plane angle of 5.2° but a quite different phenyl ring twist of 13.0° in [Rh(cupf)(CO)($PPh_3$)].

The structures of [Rh(neocupf)(CO)($PPh_3$)] and [Rh(neocupf)(CO)($CH_3$)(I)($PPh_3$)] comprising the neocupferrate ligand was preceded by only one published neocupferrate structure, that of [Co(neocupf)$_2$($H_2O$)$_2$],[92] according to the Cambridge Structural Database (CSD), Version 5.26, May 2005 update.[93] Angles and bond distances of the N-substituted naphtyl ring system are in good agreement with those of [Co(neocupf)$_2$($H_2O$)$_2$] and of a crystal structure of pure naphthalene.[94] The average C–C bond length is 1.392(6) Å, ranging from 1.359(8) to 1.419(7) Å. The naphtyl rings are flat (with a C(41)–C(410)–C(45)–C(46) torsion angle of 179.72(1)°) and twisted by 65.7(3)° in [Rh(neocupf)(CO)($PPh_3$)] and 57.0(3)° in [Rh(neocupf)(CO)($CH_3$)(I)($PPh_3$)] along the N(2)–C(41)–C(44) axis relative to the chelate ring-atom plane. As both neocupferrate complexes are involved in stacking interactions (to be discussed in par 4.4.1.10), this could be a contributing factor, along with packing considerations.

The electronic as well as steric effects which may be correlated with the ring size of the bidentate ligand may also have an effect on the coordination ability of the coordinatively unsaturated square planar rhodium complexes. It seems that the ability of the rhodium(I) complex to increase its coordination number increases with a decrease in the bite angle. The observed reaction of [Rh(cupf)(CO)($PPh_3$)] with $PPh_3$ resulting in the formation of the stable five- coordinated *trans*-[Rh(cupf)(CO)($PPh_3$)$_2$] complex supports this view. Addition of an excess $PPh_3$ to a solution of

[92] Tamaki, K. and Okabe, N., *Acta Cryst*., **C54**, 195 (1998).

[93] Allen, F.H., *Acta Cryst*., **B58**, 380 (2002).

[94] Cruickshank, D.W.J., *Acta Cryst*., **10**, 504 (1957).

[Rh(cupf)(CO)($PPh_3$)] did not lead to substitution of the remaining CO group, in line with similar observations on [Rh(β-dik)(CO)($PPh_3$)] (β-dik = β-diketones) complexes, but gave instead a trigonal-bipyramidal complex having the two $PPh_3$ groups *trans*-orientated in the apical positions. To date, the cupferrate ligand as contained in [Rh(cupf)(CO)($PPh_3$)] has the smallest bite angle (76.6°) of all the analogous complexes studied, followed closely by neocupferrate (77.2°) and tropolonato (77.6°). It is thus not a complete surprise to find that tropolonato fulfilled expectations with the forming of similar five-coordinated complexes in *trans*-[Rh(CO)(trop)($PPh_2Fc)_2$],[20] *trans*-[Rh(CO)(trop$Br_3$)($PPh_3)_2$][20] and *trans*-[Rh(CO)(trop$Br_3$)($AsPh_3)_2$][20]. Utilising their small cone angle of 78.9° in similar fashion, a related series of 2-quinaldinate (quin) complexes, [Rh(quin)(CO){P(*X*-$C_6H_4)_3\}_2$] (*X* = 4-$CH_3O$, 4-$CH_3$, 3-$CH_3$, 4-F and 4-Cl), crystallizing in two isomeric forms was also reported.[95] Corresponding structures of systems containing six-membered oxygen donor atoms have not been reported, possibly indicating that steric hindrance by the L,L'-BID ligand plays an important role in the formation of these five-coordinate complexes. An order-of-magnitude increase in the formation constant for the Htrop$Br_3$ complex compared to tropolonato relates the tendency to form a five-coordinate complex also directly with the electron density (or lack thereof) on the rhodium(I) as introduced by the bidentate ligand. Thus, when additional electron-withdrawing capacity was introduced on the L,L'-BID ligand, as in the case of 3,5,7-tribromotropolone (Htrop$Br_3$), the formation of both the $PPh_3$ and $AsPh_3$ five-coordinate complexes are favoured and could be isolated and crystallographically studied.[20] The conclusion can thus be reached that the combined effect of steric and electronic properties of the cupferrate ligand was necessary to enable the formation of *trans*-[Rh(cupf)(CO)($PPh_3)_2$]. *Trans*-[Rh(cupf)(CO)($PPh_3)_2$] is probably the first example of a five coordinated Rh(I) complex containing a bidentate ligand to be published.

#### *4.4.1.6 The carbonyl ligand*

The Rh–C–O chain is approximately linear (Table 4.36) with the Rh–CO bond distances in good agreement with those of similar complexes, for example,

[95] Heras, J.V., Cano, M., Lobo, M.A. and Pinilla, E., *Polyhedron*, **8**, 167 (1989).

[Rh(tfdmaa)(CO)($PPh_3$)],[7] [Rh(acac)(CO)($PPh_3$)],[39] [Rh(dmavk)(CO)($PPh_3$)],[96] [Rh(dmavk)(CO)($CH_3$)(I)($PPh_3$)],[48] [Rh(fctfa)(CO)($PPh_3$)][49] and [Rh(fctfa)(CO)($CH_3$)(I)-($PPh_3$)][49] (Table 4.36). Due to large errors, the Rh–CO bond distance is not a good indicator of electron density on the metal centre, with the Rh(I)–CO and Rh(IIII)–CO bond distances not significantly different. There is, however, a tendency for the Rh–CO bond to be longer and the C–O bond to be shorter for the Rh(III)-complexes, compared to the corresponding distances for the Rh(I)-complexes. This is in agreement with the fact that a lower electron density on the rhodium centre (as in the case of the Rh(III)-complexes) will result in a weaker Rh–CO bond due to less $\pi$ back-bonding of electron density into the carbon $\pi$*-orbitals. Consequently the bonding order in the CO moiety is increased and a stronger C≡O bond will characterise this conditions, measured as a shorter C–O bond distance and an increase in $\upsilon_{CO}$. The $\upsilon_{CO}$ values of 1982 and 2052 $cm^{-1}$ for [Rh(cupf)(CO)($PPh_3$)] and [Rh(cupf)(CO)($CH_3$)(I)($PPh_3$)] respectively, serves to illustrate this relationship. Back donation to the phosphite ligand tends to reduce electron density on the central metal atom to a larger extent compared with $PPh_3$, leading to a weakened ability to reduce the carbonyl bond order in the case of [Rh(cupf)(CO){$P(OCH_2)_3CCH_3$}]. This is demonstrated by comparing the carbonyl stretching frequency of the phosphite complex ($\upsilon_{CO}$ = 2004 $cm^{-1}$) with that of [Rh(cupf)(CO)($PPh_3$)] ($\upsilon_{CO}$ = 1982 $cm^{-1}$).

**Table 4.36** Particulars of the Rh-CO bond

| Complex | Rh-CO (Å) | C-O (Å) | Rh-C-O (°) |
|---|---|---|---|
| [Rh(cupf)(CO)($PPh_3$)] | 1.78(1) | 1.17(1) | 176.3(9) |
| [Rh(cupf)(CO)($CH_3$)(I)($PPh_3$)] | 1.81(2) | 1.14(2) | 174(1) |
| [Rh(cupf)(CO)($PPh_3$)$_2$] | 1.77(1) | 1.16(2) | 176(1) |
| [Rh(neocupf)(CO)($PPh_3$)] | 1.802(5) | 1.139(5) | 177.3(5) |
| [Rh(neocupf)(CO)($CH_3$)(I)($PPh_3$)] | 1.83(1) | 1.04(1) | 173.7(13) |
| [Rh(cupf)(CO){$P(OCH_2)_3CCH_3$}] | 1.772(9) | 1.155(9) | 174.4(10) |
| [Rh(TFDMAA)(CO)($PPh_3$)] | 1.781(9) | 1.159(12) | 178.2(7) |
| [Rh(acac)(CO)($PPh_3$)] | 1.801(8) | 1.153(11) | 176.8(9) |
| [Rh(dmavk)(CO)($PPh_3$)] | 1.784(5) | 1.142(6) | 177.9(5) |
| [Rh(dmavk)(CO)($CH_3$)(I)($PPh_3$)] | 1.85(1) | 1.116(15) | 177.0(14) |
| [Rh(fctfa)(CO)($PPh_3$)] | 1.801(5) | 1.147(5) | 178.1(4) |
| [Rh(fctfa)(CO)($CH_3$)(I)($PPh_3$)] | 1.834(9) | 1.118(10) | 175.6(8) |

[96] Damoense, L.J., Purcell, W., Roodt, A. and, Leipoldt, J.G., *Rhodium Ex.*, **5**, 10 (1994).

#### *4.4.1.7 The iodide ligand*

The Rh(III)-I bond length of 2.708(2) Å in [Rh(cupf)(CO)($CH_3$)(I)($PPh_3$)] and 2.711(1) Å in [Rh(neocupf)(CO)($CH_3$)(I)($PPh_3$)], being slightly longer than the range of 2.60-2.69 Å reported for complexes having a ligand with a small *trans*-influence opposite the Rh-I bond[97,98], is however still significantly shorter than the Rh-I distance found for complexes having $CH_3$ *trans* to the iodine atom. Examples of these are the 2.803(1) Å in [Rh(ox)(I)(CO)($CH_3$)($PPh_3$)][15], the 2.849(1) Å in [Rh(dmavk)(I)(CO)($CH_3$)($PPh_3$)][48] (average of two crystallographically independent molecules) and the 2.813(1) Å in [Rh(I)($CH_3$){$C_2$(DO)($DOBF_2$)}].[98] The Rh-I distance of 2.701(1) Å in [Rh(quin)(I)(CO)($CH_3$)($PPh_3$)][16] and the 2.716(1) Å in [Rh(fctfa)(I)(CO)($CH_3$)($PPh_3$)][49] compares very well with the 2.708(2) Å and 2.711(1) Å of the Rh(III) complexes of the present study. Like [Rh(cupf)(CO)($CH_3$)(I)($PPh_3$)] and [Rh(neocupf)(CO)($CH_3$)-(I)($PPh_3$)], [Rh(quin)(I)(CO)($CH_3$)($PPh_3$)] and [Rh(fctfa)(I)(CO)($CH_3$)($PPh_3$)] are the products of *cis* addition of iodomethane and contains *trans*-P-Rh-I moieties. The present distances thus comply with the concept of $PPh_3$ having a smaller *trans*-influence than an alkyl group. The methyl group is known for its strong *trans*-influence.[15,99] A shorter Rh-I bond can also be interpreted as stronger coordination of the iodo ligand due to less electron density on the metal centre.[20]

#### *4.4.1.8 The methyl ligand*

Taking a van der Waals radius of 2.0 Å for $CH_3$[100] and 1.6 Å for carbon in covalent cyanides[101] and CO further being isoelectronic with CN, we consider C(1)••••C(2) = 2.63(2) Å as indicative of a strong repulsive interaction between the CO and $CH_3$ groups. Similar neighbouring contacts of C(2)••••P = 3.19(2), C(2) ••••O(2) = 2.97(2) and I••••C(2) = 3.44(2) Å are also repulsive in character. The Rh-$CH_3$ bond distance

[97] Basson, S.S., Leipoldt, J.G., Potgieter, I.M., Roodt, A. and Van der Walt, T.J., *Inorg. Chim. Acta*, **119**, L9 (1986).

[98] Collman, J.P., Christian, P.A., Current, S., Denisevich, P., Halbert, T.R., Schmittou, E.C. and Hodgson, K.O., *Inorg. Chem*., **15**, 223 (1976).

[99] Appleton, P.C., Clark, H.C. and Manzer, L.E., *Coord. Chem. Rev*., **10**, 335 (1973).

[100] Cotton, F.A. and Wilkinson, G., *Basic Inorganic Chemistry*, Wiley, New York (1976).

[101] Britton, D. in Dunitz, J.D. and Ibers, J.A. (eds.), Perspectives in Structural Chemistry, Vol. 1, Wiley, New York (1967).

of 2.08(1) Å for [Rh(cupf)(CO)($CH_3$)(I)($PPh_3$)] and 2.092(14) Å for [Rh(neocupf)(CO)($CH_3$)(I)($PPh_3$)], compares well with other Rh(III) alkyl bonds (e.g. 2.11(1) Å in [Rh(quin)(I)(CO)($CH_3$)($PPh_3$)], 2.108(4) Å in [Rh(ox)(I)(CO)($CH_3$)($PPh_3$)], 2.078(8) Å in [Rh(fctfa)(I)(CO)($CH_3$)($PPh_3$)] and 2.069(12) Å in [Rh(dmavk)(I)-(CO)($CH_3$)($PPh_3$)]). With $CH_3$ as a strong σ-donor, all the above data point to a tight fit of the $CH_3$ group between neighbouring ligand atoms. The smaller stereochemical demand of $CH_3$ compared to $PPh_3$ seems to be the main responsible factor for the observed differences in the aforementioned equatorial planes of the Rh(III) and Rh(I) complexes.

#### *4.4.1.9 The acyl ligand.*

The acyl group in [Rh(cupf)($COCH_3$)(μ-I){$P(OCH_2)_3CCH_3$}]$_2$ compares well with other examples of Rh(III)-acyl complexes. Table 4.37 compares the bonding distances and Table 4.38 the bonding angles in a number of Rh(III)-acyl complexes.

**Table 4.37** Comparative bonding distances of the acyl group

| Complex | Rh-C1 (Å) | C1-C2 (Å) | C1-O1 (Å) |
|---|---|---|---|
| [Rh(cupf)($COCH_3$)(μ-I){$P(OCH_2)_3CCH_3$}]$_2$ | 2.037(6) | 1.44(1) | 1.205(7) |
| [Rh(dmavk)($COCH_3$)(I)($PPh_3$)][51] | 1.955(14) | 1.46(2) | 1.18(2) |
| [Rh(macsm)($COCH_3$)(I)($PPh_3$)][102] | 1.970(7) | 1.496(8) | 1.176(9) |
| [Rh(stsc)($COCH_3$)(I)($PCy_3$)][103] | 1.992(14) | 1.43(2) | 1.16(2) |
| [Rh(dppms)($COCH_3$)$I_2$][104] | 1.951(6) | 1.491(9) | 1.178(7) |
| [Rh(dppe)($COCH_3$)$I_2$][104] | 2.013(7) | 1.490(11) | 1.178(9) |
| [Rh($S_2PPh_2$)($COCH_3$)(I)($PPh_3$)][105] | 1.96(1) | 1.58(4) | 1.21(1) |
| [Rh(dppm)($COCH_3$)$I_2$][58] | 2.00(2) | 1.51(3) | 1.16(3) |
| [Rh($PMe_2Ph$)$_3$($COCH_3$)(Cl)]$^+$[56] | 1.971(5) | 1.528(8) | 1.184(6) |
| [Rh{$Ph_2P(CH_2)_3PPh_2$}($COCH_3$)$I_2$][54] | 1.981(6) | 1.513(9) | 1.182(7) |

**Table 4.38** Comparative bonding angles of the acyl group

[102] Steyn, G.J.J., Roodt, A. and Leipoldt, J.G., *Rhodium Ex.*, **0**, 11 (1993).

[103] Steyn, G.J.J., Ph.D. Thesis, Free State University, Bloemfontein, South Africa (1994).

[104] Gonsalvi, L., Adams, H., Sunley, G.J., Ditzel, E. and Haynes, A., *J. Am. Chem. Soc.*, **124**, 13597 (2002).

| Complex | C2-C1-O1 (°) | Rh-C1-C2 (°) | Rh-C1-O1 (°) |
|---|---|---|---|
| $[Rh(cupf)(COCH_3)(\mu\text{-}I)\{P(OCH_2)_3CCH_3\}]_2$ | 123.4(6) | 115.3(5) | 121.3(5) |
| $[Rh(dmavk)(COCH_3)(I)(PPh_3)]$ | 122(2) | 116.7(13) | 122.1(13) |
| $[Rh(macsm)(COCH_3)(I)(PPh_3)]$ | 123.0(7) | 118.6(7) | 118.2(6) |
| $[Rh(stsc)(COCH_3)(I)(PCy_3)]$ | 120(2) | 118.0(11) | 121.7(12) |
| $[Rh(dppms)(COCH_3)I_2]$ | 120.1(6) | 116.1(5) | 123.8(5) |
| $[Rh(dppe)(COCH_3)I_2]$ | 123.4(7) | 112.1(5) | 124.5(6) |
| $[Rh(S_2PPh_2)(COCH_3)(I)(PPh_3)]$ | 121.3(9) | 114.9(7) | 123.8(6) |
| $[Rh(dppm)(COCH_3)I_2]$ | 126(2) | 109(2) | 125(2) |
| $[Rh(PMe_2Ph)_3(COCH_3)(Cl)]^+$ | 122.2(5) | 112.2(4) | 125.5(4) |
| $[Rh\{Ph_2P(CH_2)_3PPh_2\}(COCH_3)I_2]$ | 121.1(6) | 113.1(4) | 125.7(5) |

Cheng *et al*[106,107] noticed a tendency for Rh(III)-acyl bonds to be shorter than nearly all reported Rh(III)-C σ-bonds, which could be explained in terms of the probability of back-bonding from the appropriate $d_\pi$ orbital of the Rh(III) centre to the $\pi^*$ orbital of the acyl ligand. It may also be attributed to the decrease of 0.04 Å in the covalent radius of carbon in going from the $sp^3$ hybridisation of alkyls to the $sp^2$ hybridisation of an acyl.[108] C-O bonds in the acyl ligands tend to be longer than rhodium bound carbonyl bonds (Table 4.36 and Table 4.37) which is also reflected in the $\upsilon_{CO}$ value of 1704 $cm^{-1}$ for $[Rh(cupf)(COCH_3)(\mu\text{-}I)\{P(OCH_2)_3CCH_3\}]_2$ compared to the 1985 $cm^{-1}$ for $[Rh(cupf)(CO)\{P(OCH_2)_3CCH_3\}]$. Angles about the $sp^2$ hybridised carbon deviate significantly from the expected 120°. In all the acyl structures the Rh-C1-C2 angle is smaller than 120° while the C1-C2-O1 and Rh-C1-O1 angles are on average roughly the same (122.5° and 123.3° respectively) and larger than 120°, due to the greater steric demand of the bonding orbitals of the multiple C-O bond compared to that of the other two single bonds.

[105] Cabeza, J.A., Riera, V., Villa-García, M.A., Ouahab, l. and Triki, S., *J. Organomet. Chem.,* **441**, 323 (1992).

[106] Cheng, C.H., Spivack, B.D. and Eisenberg, R., *J. Am. Chem. Soc*., **99**, 3003 (1977).

[107] Cheng, C.H. and Eisenberg, R., *Inorg. Chem*., **18**, 1418 (1979).

[108] Hoare, R.J. and Mills, O.S., *J. Chem. Soc., Dalton Trans*., 2138 (1972).

#### *4.4.1.10 Interactions*

No classical hydrogen bonds were observed. There were, however, several intermolecular and intramolecular hydrogen interactions with hydrogen-acceptor distances ranging from 2.33 to 2.83 Å for the intramolecular and from 2.49 to 2.61 Å for the intermolecular interactions, the latter due to efficient packing in the particular unit cells where the C–H•••acceptor interactions play a stabilising role.

A π-π interaction between the naphtyl rings is observed in the unit cell packing of [Rh(neocupf)(CO)($PPh_3$)]·$CH_3COCH_3$ and [Rh(neocupf)-(CO)($CH_3$)(I)($PPh_3$)]·$C_5H_{12}$, (Figure 4.23) with an interplanar distance of 3.48(1) Å. Similar π-π interactions were also observed between the aromatic rings of the oxinate ligand in [Rh($C_9H_6NO$)($C_{24}H_{27}O_3P$)(CO)],[109] with a stacking distance of 3.76(6) Å, and between the tropolone ring systems with an interplanar distance of 3.57(3) Å in [Rh(trop)(CO)($AsPh_3$)].[110] Figure 4.23 clearly shows a degree of offset between the two π systems, which is, according to Hunter and Sanders,[111] the favoured geometry in the case of parallel-orientated entities. Their model indicates that π-π interactions are not due to an attractive electronic interaction between the two π-systems but occur when the attractive interactions between π-electrons and the σ-framework outweigh unfavourable contributions such as π-electron repulsion. A face-to-face geometry, with zero offset, is dominated by π-π electronic repulsion while π-σ attraction dominates in an offset π-stacked geometry. The simple picture of a π-system as a sandwich of the positively charged σ-framework between two negatively charged π-electron clouds accounts well for the observed interactions between π-systems. Whereas these discussed electronic effects determine the geometry of interaction, Van der Waals interactions make the major contribution to the magnitude of the observed interaction.

[109] Janse van Rensburg, J.M., Roodt, A., Muller, A. and Meijboom, R., *Acta Cryst*., **E61**, m1741 (2005).

[110] Steyl, G. and Roodt, A., *Acta Cryst*., **E61**, m1212 (2005).

[111] Hunter, C.A. and Sanders, J.K.M., *J. Am. Chem. Soc*., **112**, 5526 (1990).

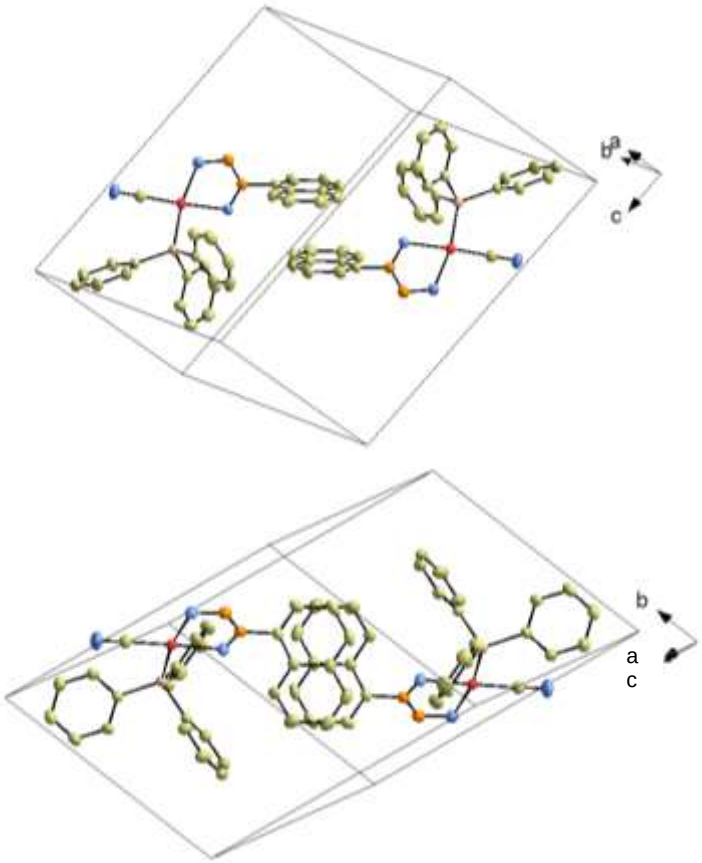


**Figure 4.23** Different orientations of the unit cell emphasizing the π-π stacking phenomenon observed in the structure of [Rh(neocupf)(CO)-($PPh_3$)]·$CH_3COCH_3$

### 4.4.2 The structure of *trans*-[Rh(CO)(Cl)($PCy_3$)$_2$]

The structure of *trans*- [Rh(CO)(Cl)($PCy_3$)$_2$] has already been determined in different studies, that of Wilson *et al*.[112] and that of Clarke *et al*.[113] The data collection for the structure determination of this study has already been done in 1991, but was never published. It gives on the other hand the opportunity to correlate this data with the published rhodium structures as well as with the structure of the iridium analogue[114]

[112] Wilson, M.R., Prock, A., Giering, W.P., Fernandez, A.L., Haar, C.M., Nolan, S.P. and Foxman, B.M., *Organometallics*, **21**, 2758 (2002).

[113] Clarke, M.L., Holliday, G.L., Slawin, A.M.Z. and Woollins, J.D., *J. Chem. Soc., Dalton Trans*., 1093 (2002).

[114] Kuwabara, E.and Bau, R., *Acta Cryst*., **C50**, 1409 (1994).

(Table 4.39). Wilson showed that the Rh complex crystallized in the triclinic P$\bar{1}$ system (Z = 1), and it to be *iso*-structural to the Ir complex.

The unit cell of *trans*-[Rh(CO)(Cl)($PCy_3$)$_2$] contains one molecule of the complex as the Rh atom is situated on the inversion centre at (0, 0, 0). The chloride and carbonyl ligands are necessarily disordered such that these ligands occupy mutually *trans* sites with 50% probability. Such a 1:1 disorder is a common form of disorder in [Rh(CO)(Cl)($PR_3$)$_2$] systems[115,116,117] and occurs in 14 [Rh(CO)(Cl)($PR_3$)$_2$] structures of this type[112]. This Cl/CO disorder is also present in the related crystal structures of *trans*-[Ir(CO)(Cl)($PCy_3$)$_2$][114] and *trans*-[Ir(CO)(Cl)($PPh_3$)$_2$].[118] Wilson also reported a two-fold disorder along the Cl–Rh–CO axis in his study of *trans*-[Rh(CO)(Cl)($PCy_3$)$_2$] while Clarke only speculated about the possibility of a disorder in the crystal packing but did not incorporate it in his refinement.

The complex of tri-*tert*-butylphosphine[119] of the type [Rh(L)$_2$(CO)(Cl)] has a tetrahedral structure, as was determined crystallographically. Tricyclohexyl-phosphine (Tolman cone angle of 170°) is thought to be nearly as bulky as tri-*tert*-butylphosphine (Tolman cone angle of 182°) and it was therefore of interest whether *trans*-[Rh(CO)(Cl)($PCy_3$)$_2$] would contain some distortion away from the expected square planar geometry. The rhodium atom is displaced by 0.008 Å from the equatorial array formed by P(1), P(1)#1, C(1) and Cl and the co-ordination polyhedron is thus planar. All angles within the Rh coordination sphere are close to those expected for an ideal square-planar environment with the phosphine ligands in a *trans*-orientation separated by 180° due to symmetry requirements. The angle between the disordered ligands *i.e*. C(1)–Rh–C(1)#1 or Cl(1)–Rh–Cl(1)#1 was determined as only 1.4(2)°.

[115] Cooper, M.K., Duckworth, P.A., Hambley, T.W., Organ, G.J., Henrick, K., McPartlin, M. and Parekh, A., *J. Chem. Soc., Dalton Trans*., 1067 (1989).

[116] Marsh, R.E., *Acta Cryst*., **B53**, 317 (1997).

[117] Dunbar, K.R. and Haefner, S.C., *Inorg. Chem*., **31**, 3676 (1992).

[118] Churchill, M.R., Fettinger, J.C., Buttrey, L.A., Barkan, M.D. and Thompson, J.S., *J. Organomet. Chem.* **340**, 257 (1988).

[119] Harlow, R.L., Westcott, S.A., Thorn, D.L. and Baker, R.T., *Inorg. Chem*., **31**, 323 (1992).

**Table 4.39** Comparison of crystal parameters for the different *trans*-[Rh(CO)(Cl)($PCy_3$)$_2$] studies as well as that of the Ir analogue.

| | **This Study** | **Wilson *et al.*[112]** | **Clarke *et al.*[113]** | **Kuwabara *et al.*[114]** |
|---|---|---|---|---|
| **Formula** | [Rh(CO)(Cl)($PCy_3$)$_2$] | [Rh(CO)(Cl)($PCy_3$)$_2$] | [Rh(CO)(Cl)($PCy_3$)$_2$] | [Ir(CO)(Cl)($PCy_3$)$_2$] |
| **$\upsilon_{CO}$ (cm$^{-1}$)** | 1943 | 1943 | 1943 | 1934 |
| **Crystal system** | Triclinic | Triclinic | Triclinic | Triclinic |
| **Space group** | P$\bar{1}$ | P$\bar{1}$ | P1 | P$\bar{1}$ |
| **a (Å)** | 10.2390(14) | 9.9412(6) | 9.9574(1) | 10.251(3) |
| **b (Å)** | 10.7920(12) | 10.2413(5) | 10.2575(1) | 10.789(4) |
| **c (Å)** | 9.9450(11) | 10.7881(5) | 10.8125(1) | 9.943(4) |
| **α (°)** | 109.260(10) | 113.774(4) | 113.782(1) | 109.25(3) |
| **β (°)** | 90.660(10) | 109.198(4) | 109.177(1) | 90.92(3) |
| **γ (°)** | 113.830(10) | 90.786(4) | 90.819(1) | 113.76(3) |
| **Rh-P** | 2.3491(7) | 2.3508(3) | 2.352(3) | 2.345(2) |
| **Rh-Cl** | 2.388(2) | 2.3880(13) | 2.422(4) | 2.398(7) |
| **Rh-C** | 1.748(8) | 1.745(5) | 1.93(1) | 1.78(2) |
| **C-O** | 1.163(7) | 1.153(4) | Not reported | 1.10(2) |
| **P-Rh-Cl** | 91.41(5) | 91.39(3) | 91.0(1) | 91.24(13) |
| **P1-Rh-P2** | 180.0 | 180.0 | 179.6(2) | 180.0 |
| **Rh-C-O** | 178.3(9) | 179.1(5) | Not reported | 178.3(15) |

The Rh–C and Rh–Cl distances are approximately 0.03 – 0.10 Å shorter and longer, respectively, compared to complexes where no disorder is involved[112]. This is a consequence of the inability to completely resolve the effects of the disorder. However, the Rh–P distances and related angles are unaffected by the disorder. The Rh–P distance of 2.3491(7) Å is slightly longer than that of 2.322(1) Å found in *trans*-[Rh(CO)(Cl)($PPh_3$)$_2$],[117] which can be attributed to the larger trans-influence of $PCy_3$. The strong electron-donating capability of $PCy_3$ is causing a mutual labilisation when occupying positions *trans* to each other. The same trend was observed with Ir where the Ir–P distances are 2.345(2) Å for $PCy_3$ and 2.330(1) Å for $PPh_3$. In general can it be noted that the Rh–P and Ir–P bonds are virtually identical in a number of Vaska-type complexes.[20]

The O–C–Rh moiety is close to linear with an angle of 178.3(9). Rh–C and C–O bond lengths are 1.748(8) and 1.163(7) respectively, reflecting most probably the relatively high elecron density on the rhodium centre due to the strong σ-donating $PCy_3$-ligand. In a comparative study of 11 *trans*-[Rh(CO)(Cl)($L)_2$] complexes Otto

and Roodt[120] report an average of 1.82(2) and 1.09(3) for the bond lengths of Rh–C and C–O respectively, but warn that it may be a risk to make conclusions based purely thereupon. The surprising Rh–C distance of 1.93(1) Å as reported by Clarke *et al.* should be interpreted, in their own words, with caution. Actually very little information can be obtained from the C–O bond lengths, because in the range of bond orders concerned, C–O bond length is relatively insensitive to bond order.[121] Looking at $\upsilon_{CO}$ values, the 1943 $cm^{-1}$ listed in Table 4.39 is significantly lower than the value of 1965 $cm^{-1}$ for *trans*-[Rh(CO)(Cl)($PPh_3$)$_2$].[117,122] As the electron-donating capability of the Group 15 donor ligand decreases, the electron density on the metal decreases accordingly and thus less electron density is available to the C≡O moiety via π-back-bonding into the carbon π*-orbitals. The result is a weaker M–CO bond (stronger C≡O bond) and an increase in $\upsilon_{CO}$.

In *trans*-[Rh(CO)(Cl)($PCy_3$)$_2$] one of the C–P–C angles is larger than the other two. The C–P–C angles are 102.6(1), 103.8(1) and 110.0(1)°, compared to the C–P–C angles of 103.0(3), 103.8(3) and 109.6(3)° found in the Ir analogue and angles of 103.4(2), 104.2(2) and 111.3(2)° found in [Rh($C_9H_{10}NO_2S$)(CO)($PCy_3$)].[123] The observation of one C–P–C angle being larger than the others is also observed, although to a lesser extent, in free $PCy_3$[124], where C–P–C angles of 103.1(3), 103.2(3) and 105.1(3)° were reported. All three of the cyclohexyl substituents of the phosphine ligands adopt the expected chair conformation for saturated six-membered rings and are exactly staggered with respect to the *trans* phosphine due to the inversion centre at the Rh position. Distances and angles within the cyclohexane groups are normal.

[120] Otto, S. and Roodt, A., *Inorg. Chim. Acta*, **357**, 1 (2004).

[121] Cotton, F.A. and Wing, R.M., *Inorg. Chem*., **4**, 314 (1965).

[122] Kemp, G., Roodt, A. and Purcell, W., *Rhodium Ex.*, **12**, 21 (1995).

[123] Basson, S.S., Leipoldt, J.G., Purcell, W., Lamprecht, G.J. and Preston, H., *Acta Cryst*., **C48**, 169 (1992).

[124] Davies, J.A., Dutremez, S. and Pinkerton, A.A., *Inorg. Chem*., **30**, 2380 (1991).

Otto[125] compared the *iso*-structural *trans*-[Pt(Cl)($CH_3$)($PCy_3$)$_2$] with other closely related $Ni^{II}$, $Pd^{II}$ and $Pt^{II}$ complexes from the literature, containing two bulky tricyclohexylphosphine ligands in a *trans*-orientation. It was found to be *iso*-structural with several of these complexes, showing that the crystal packing is predominantly determined by the tricyclohexylphosphine ligands and only when the metal core is drastically influenced as by the introduction of a phenyl or H ligand are the packing modes changed.

[125] Otto, S., *Acta Cryst*., **C57**, 793 (2001).

# 5 Reaction kinetics

## 5.1 Introduction

It is well-known that the oxidative addition of iodomethane to the rhodium(I) complex can be regarded as the key step in the industrial catalytic carbonylation of methanol to acetic acid. This process, developed in the late 60's by Monsanto, was for many years a topic of ongoing research by various groups.[1] Previous work in our group was also concerned with the study of oxidative addition and CO-insertion reactions of Rh(I) complexes.[2,3,4,5] The focus was in particular on the mechanistic behaviour of β-diketonato type ligands and analogues thereof on these reactions. Oxidative addition of iodomethane to such complexes showed results strongly in favour of an ionic $S_N2$ two-step operative mechanism. That implies a *trans*-geometry of addition for the alkyl halide, as was observed for example in the case of [Rh(ox)(CO)($CH_3$)(I)($PPh_3$)].[6] However, in the case of rhodium complexes containing the cupferrate ligand, an unusual *cis*-addition was obtained with [Rh(cupf)(CO)($CH_3$)(I)($PPh_3$)].[7] The latter product, an alkyl, is also in contrast to the acyl product formed as a result of the oxidative addition of iodomethane to [Rh(Sacac)(CO)($PX_3$)].[8] The different outcome of these and other oxidative addition reactions called for a closer look at such mechanisms.

---

[1] Haynes, A., Mann, B.E., Gulliver, D.J., Morris, G.E. and Maitlis, P.M., *J. Am. Chem. Soc*., **113**, 8567 (1991); Dekleva, T.W. and Forster, D., *Adv. Catal*., **34**, 81 (1986); Murphy, M., Smith, B., Torrence, G. and Aguilo, A., *Inorg. Chim. Acta*, **101**, 147 (1985); Schrod, M., Luft, G. and Grobe, J., *J. Mol. Catal*., **20**, 175 (1983).

[2] Roodt, A. and Steyn, G.J.J., *Resent Res. Devel. Inorg. Chem*., **2**, 1-23 (2000).

[3] Steyn, G.J.J., Roodt, A. and Leipoldt, J.G., *Inorg. Chem*., **31**, 3477 (1992).

[4] Smit, D.M.C., Basson, S.S. and Steynberg, E.C., *Rhodium Ex.*, **7-8**, 12 (1994).

[5] Basson,S.S., Leipoldt, J.G. and Nel, J.T., *Inorg. Chim. Acta*, **84**, 167 (1984).

[6] Van Aswegen, K.G., Leipoldt, J.G., Potgieter, I.M., Lamprecht, G.J., Roodt, A. and Van Zyl, G.J., *Trans. Met. Chem.*, **16**, 369 (1991).

[7] Basson, S.S., Leipoldt, J.G., Roodt, A. and Venter, J.A., *Inorg. Chim. Acta*, **128**, 31 (1987).

[8] Leipoldt, J.G., Basson, S.S and Botha, L.J., *Inorg. Chim. Acta*, **168**, 215 (1990).

Lack of appropriate spectrophotometers when the oxidative addition of [Rh(acac)(CO)($PX_3$)] was first studied,[5] prompted the re-opening of the case in order to establish the operative reaction pathways in this mechanism. The current study involved phosphine ligands with different *para*-substituents on their phenyl rings. These phosphines have the same cone angle, but influence the electron density on the rhodium atom differently due to the variation in electronegativity of the substituents.

In order to conclude the cupferrate study,[7] confirmation of the proposed oxidative addition mechanism was seek in a pressure dependence study. The cupferrate study was also extended to neocupferrate, to study the effect of a more bulky substituent on the same chelate backbone. The oxidative addition of $CH_3I$ to [Rh(neocupf)(CO)($PX_3$)] was studied with a number of different phosphine ligands, varying in terms of their steric and electronic properties. An effort was made to quantify the total effect of these variations. The role of the solvent, both during oxidative addition and in the subsequent CO-insertion reaction was also studied. Solvents having different polarities, coordinating abilities and bulkiness was employed.

The initial study of the oxidative addition of $CH_3I$ to [Rh(Sacac)(CO)($PX_3$)] were not able to come to a conclusion regarding the nature of the transition state.[8] A three-centered transition state and a linear transition state were under consideration. As part of the current study, a high-pressure investigation was conducted to study the intimate mechanism of oxidative addition in the Sacac system.

An effort was made, in the midst of the different reaction paths, different final products and stereochemistry thereof, to get to a better understanding regarding oxidative addition and CO-insertion. In al the systems investigated in this study, electron density on the rhodium atom, access to the metal centre, and thus reactivity of the complex, was manipulated by varying the phosphine ligands. The often-neglected study of the effect of solvents on the outcome and progress of reactions was conducted and gave significant evidence of solvent involvement.

## 5.2 Oxidative addition of $CH_3I$ to $[Rh(acac)(CO)(PX_3)]$[9]

### 5.2.1 Experimental

The starting complexes were prepared as described in Chapter 3. All IR measurements were done on a Hitachi model 270-50 spectrophotometer having a wavenumber accuracy of 2 $cm^{-1}$ in the region employed. Kinetic measurements were performed in a thermostated (0.1K) cell with 0.5 mm path length and NaCl optics. Visible spectrophotometry was performed on a Hitachi model 150-20 spectrophotometer within the same temperature control limits. All kinetic measurements were done in 1,2-dichloroethane as solvent at 25.0 °C. Typical complex concentrations were 5 x $10^{-3}$ M for the visible (383 nm) and 0.02 M for the IR kinetic measurements with [CH3I] ≥ 0.1 M. All kinetic data were fitted to the appropriate equation by using a non-linear least-squares program.[10]

### 5.2.2 Results and discussion

The general mechanistic pathway (Scheme 5.1) involves an initial dissociative equilibrium of the Rh(I) complex for which, in the case of $[Rh(acac)(CO)(PPh_3)]$, supporting evidence was obtained through rate acceleration[5] and changes in NMR spectra[11] with added free phosphine. The onset of the oxidative addition proceeds through the equilibrium step, $K_1$, resulting in the postulated ionic intermediate which reacts further by different pathways to produce the final presumably *trans*-addition product. Values for $K_1$, $k_2$ and $k_4$ in the case of $[Rh(acac)(CO)(PPh_3)]$ was previously reported.[5] Having used more sophisticated spectrophotometers, especially for IR measurements, there is now evidence to believe that the $k_2$-path is not operative (at least for the acac complexes) and that the previously determined $k_2$ value should be

[9] Basson,S.S., Leipoldt, J.G., Roodt, A., Venter, J.A. and Van der Walt, T.J. *Inorg. Chim. Acta*, **119**, 35 (1986).

[10] Moore, R.H., *Report No. LA 2367*, Los Alamos Scientific Laboratory, March 4, 1960, and addend, January 14, 1963.

[11] Trzeciak, A.M., Jon, M. and Ziolkowski, J.J., *React. Kinet. Catal. Lett.*, 20, 383 (1982).

considered as a $k_3$ constant, *i.e.*, the formation of the final oxidative addition product proceeds solely through the intermediate acyl complex C (Figure 5.1).

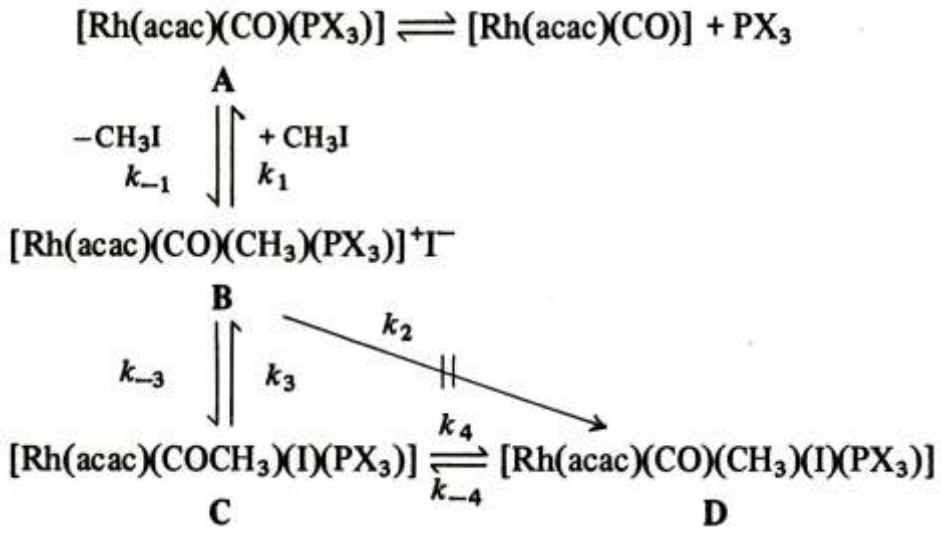


**Figure 5.1** Proposed reaction mechanism for the oxidative addition of $CH_3I$ to [Rh(acac)(CO)($PX_3$)].

Typical absorbance-time traces at 382 nm for the reaction progress of these acac complexes showed three distinctive phases: a short induction period (*ca*. 1-10 min), a slow increase in absorbance (up to *ca.* 30 min) and a still slower increase for the last phase. Since the induction period was less than *ca.* 3 min for [Rh(acac)(CO)($PPh_3$)], only a biphasic absorbance-time plot at 450 nm for this compound's reaction progress was previously reported. However, having used P(*p*-PhCl)$_3$ instead of $PPh_3$, the induction period could now retarded to the extent shown in Figure 5.2. All three acac complexes have an isosbestic point at 400 nm for this induction period. With an initial decrease in absorbance at 382 nm it was found that the observed pseudo-first-order rate constants (for [$CH_3I$] = 0.1 - 0.5 M) fitted equation 5.1,

$$k_{obs} = k_1[CH_3I] + k_{-1}, \qquad \textbf{5.1}$$

from which values for $k_1$, $k_{-1}$ and $K_1$ were obtained (Table 5.1).

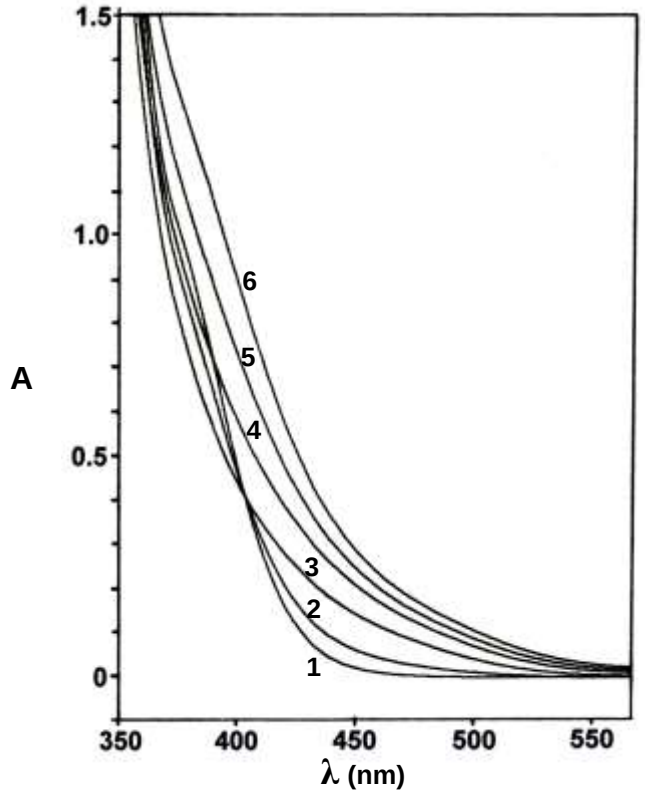


**Figure 5.2** Reaction progress between [Rh(acac)(CO)P(*p*-PhCl)$_3$] (6 x $10^{-3}$ M) and $CH_3I$ (1.0 M) in 1,2 dichloroethane at 25.0°C. Curves 1 to 3 correspond to the $K_1$ equilibrium (Scheme 5.1). Time scans: (1) 0; (2) 2; (3) 10; (4) 40; (5) 75; (6) 120 min.

**Table 5.1** Rates and equilibrium constants for the oxidative addition of $CH_3I$ to [Rh(acac)(CO)($PX_3$)] complexes.

| **X** | **$10^3k_1$** ($M^{-1}s^{-1}$) | **$10^4k_{-1}$** ($s^{-1}$) | **$K_1$** ($M^{-1}$) | **$10^3k_3$** ($s^{-1}$) | **$10^4k_4$** ($s^{-1}$) |
|---|---|---|---|---|---|
| *p*-chlorophenyl | 3.46(9) | 9(1) | 4.0(2) | | 0.98(3) |
| phenyl | 24(3) | 25(2) | 9(1) | 6.5(4) | 2.1(2) |
| p-methoxyphenyl | 138(3) | 88(12) | 16(2) | 9(3) | |

Repeated IR time scans showed that for the duration of the induction period this equilibrium involved a near complete disappearance of the Rh(I)-CO peak and the simultaneous appearance of a Rh(III)-CO peak ascribable to that of the ionic intermediate, **B** (Scheme 5.1). Observed rate constants obtained from the disappearance of the Rh(I)-CO peaks (Table 5.2) correspond well with $k_{obs}$ values

calculated (by means of eqn. 5.1) from the data in Table 5.1. The acyl peaks, observed at 1724 $cm^{-1}$ in all cases, formed at nearly the same (for X = *p*-PhCl) or at progressively slower rates (for the more basic phosphines) compared to that of the corresponding Rh(III)-CO peaks of **B**. When the latter started to disappear the acyl peak was still increasing to a near maximum absorbance value. The time required for the latter process coincided with the absorbance increase immediately following the induction period of the visible spectra. The $k_3$ values were determined from the earliest possible acyl peak formations in the IR, as well as from the linear reciprocal plots of equation 5.2 for the data obtained in the visible region.

$$k_{obs} = \frac{k_3 K_1 [CH_3I]}{1 + K_1 [CH_3I]} \qquad \textbf{5.2}$$

Equation 5.2 could not be applied for X = *p*-PhCl due to roughly equal $k_{obs}$ values in the **A**→**B** and **B**→**C** conversions (Table 5.2). The $k_{obs}$ values obtained from the visible spectra for the remaining complexes were found the most reliable at conversions of *ca.* 50% and more along the $k_3$ path. Absorbance-time data, collected at the isosbestic points (400 nm), also confirmed the latter as the most appropriate procedure.

**Table 5.2** Infrared carbonyl wavenumbers and rate constants for the oxidative addition of 0.5 M $CH_3I$ to [Rh(acac)(CO)($PX_3$)] complexes.

| **$PX_3$** | **CO wavenumbers** | | | **$10^3 k_{obs}$,** | **$10^3 k_3$,** | **$10^4 k_4$, $s^{-1}$** |
|---|---|---|---|---|---|---|
| | Complex A | Complex B | Complex D | Disappearance of A | Formation of C | Disappearance of C |
| P(*p*-$ClC_6H_4)_3$ | 1980 | 2076 | 2064 | 2.41(6) | 2.4(2) | 1.41(4) |
| $PPh_3$ | 1986 | 2072 | 2060 | 12(1) | 6.3(5) | 4.3(1) |
| P(*p*-$MeOC_6H_4)_3$ | 1972 | 2068 | 2056 | 36(2) | 9.2(1.7) | 4.0(2) |

The final and much slower disappearance of the acyl peak led to the formation of a second Rh(III)-CO peak to the order of 12 $cm^{-1}$ lower than the previous one (complex **B**) for each of the complexes (Table 5.2). This peak formation corresponds to the final oxidative addition product, **D**. The $k_4$ constants, determined from the acyl peak disappearance (Table 5.2), are in fair agreement with those in Table 5.1.

The equilibrium data in Table 5.1 show a forty-fold increase in $k_1$ values and a four-fold increase in the equilibrium constants, which is indirectly related to the σ-donor ordering of P(*p*-PhOMe)$_3$ > PPh$_3$ > P(*p*-PhCl)$_3$ and thus also to the relative basicity of the respective rhodium complexes toward oxidative addition. The carbonyl wavenumbers (Table 5.2), being also a function of the electron density on rhodium, display the same metal basicity trend. The constant lowering of 12 $cm^{-1}$ from the ionic intermediate to the final oxidative addition product in each case must be ascribed to a constant addition of electron density to the rhodium atom through coordination of the $I^-$ ligand. This effect is reconcilable with a lower coordination number five for the ionic intermediate **B**.

Both the $k_3$ and $k_4$ values show a very moderate increase with increasing Lewis basicity of the $PX_3$ ligand. The $k_3$ path, as mentioned before,[5] is assumed to comprise a rate-determining methyl group migration to CO followed by a fast nucleophilic attack $I^-$ on the resulting acetyl cation, since free added *N*-methylpyridinium iodide had no catalizing effect on the observed reaction rate. It is also known that added nucleophiles, like phosphines, enhance CO insertion rates.[12] Having a constant incoming nucleophile in the form of $I^-$ in the present case, it is only the different σ-donating properties of the coordinated phosphines which will fulfil the role of nucleophilic enhancement of $CH_3$ migration. The fact that the $k_3$ route is preferred over the more direct $k_2$ path can be attributed to the well-known strong *trans*-labilising effect of the $CH_3$ group. Bond formation of $I^-$ *trans* to the $CH_3$ group (implying the $k_2$ path) especially in a square pyramidal array of the ionic intermediate, **B**, should be more difficult in comparison with a solvated transient acetyl cation $[Rh(acac)(COCH_3)(PX_3)(solv)_x]^+$ for the $k_3$ path. Dielectric constant related solvent effects observed previously[5] emphasized the importance of stabilisation of these ionic species. The five-coordinate $[Rh(acac)(COCH_3)(PX_3)(I)]$ is similarly believed to contain a weakly coordinated solvent molecule since a nucleophilic substitution study of the $PPh_3$ derivative gave mechanistic evidence of a solvent-assisted equilibrium. The $k_4$ values listed should thus be strictly considered as $k_{obs}$ values in the process of attaining equilibrium proceeding from the acetyl to σ-methyl derivative. In this context

[12] Basolo, F. and Pearson, R.G., *Mechanisms of inorganic reactions*, 2nd ed., Wiley, New York (1967).

care was taken to obtain rate constants at the earliest possible stages of acyl→alkyl conversions. It was also noted previously[5] that both complexes exist in IR detectable quantities at infinite reaction times in neat $CH_3I$ as solvent, stressing the existence of the $K_4$ equilibrium. This equilibrium was probed further by IR monitoring of a 1,2-dichloroethane solution of [Rh(acac)(CO)($CH_3$)(I)($PPh_3$)]. It showed a gradual decrease of the Rh(III)-CO peak and a simultaneous growth in the acyl peak with time. When the latter tended to equilibrate, the Rh(I)-CO peak started to appear at the appropriate wavenumber. At longer reaction times (*ca.* 60 h) the solution spectrum showed an equilibrium mixture of complexes **A**, **C** and **D**. This as well as the noticeable upward shift of the Rh(III)-CO wavenumber, intermediate to those of **B** and **D**, confirmed the complete solvent-assisted reversibility of the system. A reaction run in 0.5 M $CH_3I$ retarded the formation of **A**, as was expected, and also yielded $k_{-4} = 2.7(1) \times 10^{-5}$ $s^{-1}$ based on the first *ca.* 10% conversion of the Rh(III)-CO peak. Thus $K_4 = 7.8(8)$ using the $k_4$ value in Table 5.1. This $k_4$ value (Table 5.1) is the average of twelve separate runs and is believed to be more reliable than the single estimate of Table 5.2. The $k_4$ constants increase roughly four-fold from the *p*-chlorophenyl to *p*-anisyl complexes whilst the reverse trend, based on the phosphine basicities[13] and as observed to a small extent in the decarbonylation of *trans*-[($\eta^5$-$C_5H_5$)Mo($CO$)$_2$(L)($COCH_3$)][14] (L = a tertiary phosphine), was expected.

Both the $k_3$ and $k_4$ pathways are retarded by making the 16-electron ionic intermediate (**B**) or acetyl complexes (**C**) more electron deficient by using weaker $\sigma$-donating phosphines. It would be interesting to observe this effect in more detail for the hexafluoroacetylacetonato complexes, since previous work has shown the absence of acetyl formation during reaction progress. It may be that a much slower $k_2$ route would operate under such circumstances.

[13] Streuli, C.A., *Anal. Chem*., **32**, 985 (1960).

[14] Barnett, K.W. and Pollmann, T.G., *J. Organomet. Chem.,* **69**, 413 (1974).

## 5.3 Oxidative addition of $CH_3I$ to [Rh(neocupf)(CO)($PX_3$)]

### 5.3.1 Experimental

The starting complexes were prepared as described in Chapter 3. All IR measurements were done on a Hitachi model 270-50 spectrophotometer having a wavenumber accuracy of 2 $cm^{-1}$ in the region employed. Kinetic measurements were performed in a thermostated (0.1K) cell with 0.5 mm path length and NaCl optics. Visible spectrophotometry was performed on a Hitachi model 150-20 spectrophotometer within the same temperature control limits. Typical complex concentrations were 1.7 X $10^{-4}$ M for the visible and 0.02 M for the IR kinetic measurements. [$CH_3I$] was varied between 0.17 and 1.02 M thus ensuring good pseudo-first-order plots of ln($A_t$ - $A\infty$) *versus* time. All kinetic data were fitted to the appropriate equation by using a non-linear least-squares program. All complexes gave a broad absorption maximum at *ca*. 385 nm in the 340-450 nm region. All kinetic measurements were done at this maximum.

### 5.3.2 Results and discussion

The [Rh(neocupf)(CO)($PX_3$)] complexes reported here are unstable in solutions of 1,2-dichloroethane (DCE), chloroform, and dimethylformamide. Distillation and drying of the solvents, together with exclusion of air ($N_2$ blanket), did not improve solution stability. In the case of DCE, IR time scans of [Rh(neocupf)(CO)($PPh_3$)] indicated the formation of a Rh(III)-CO peak at 2048 $cm^{-1}$, whilst monitoring at 365 nm in the visible region, gave an oxidative addition rate of 4.3(5) X $10^{-5}$ $s^{-1}$ at 25 ºC in absence of daylight. Normal room illumination gave a more complex reaction indicative of two consecutive rate-determining processes. The solvents employed in this study did not show any of the above effects.

All kinetic runs performed in the visible region gave a slow absorbance increase with time corresponding to the rate data reported here. At longer reaction times, the absorbance slowly decreased again indicating further reaction of the oxidative

addition product. IR monitoring showed a similar smooth decrease in the Rh(I)-CO peaks and corresponding simultaneous increase of the Rh(III)-CO peaks (2052-2060 $cm^{-1}$) thus confirming that the first slow process of the visible region is indeed the formation of the oxidative addition product, [Rh(neocupf)(CO)($CH_3$)(I)($PX_3$)]. To confirm the outcome of the second slow reaction, as well as to investigate any reversible trend in the first Rh(I)-Rh(III) conversion, the stability of [Rh(neocupf)(CO)($CH_3$)(I)($PPh_3$)] was investigated by IR in the absence and presence of $CH_3I$ in acetone and acetonitrile solutions respectively. Time scans indicated in all cases a decrease in the Rh(III)-CO peak and a simultaneous formation of an acyl peak at 1720 $cm^{-1}$. The second slow process is thus an alkyl→acyl conversion with rates at 25 °C as follows: visible region: acetone, neat, 1.3(1) x $10^{-3}$ $s^{-1}$; 1.0 M $CH_3I$, 1.0(2) x $10^{-3}$ $s^{-1}$; acetonitrile, neat, 7.6(6) x $10^{-4}$ $s^{-1}$; 1.0 M $CH_3I$, 1.3(1) x $10^{-3}$ $s^{-1}$, IR (2048 $cm^{-1}$): acetone, neat, 1.2(2) x $10^{-3}$ $s^{-1}$; 1.0 M $CH_3I$, 1.6(5) x $10^{-3}$ $s^{-1}$; acetonitrile, neat, 6.4(4) x $10^{-4}$ $s^{-1}$; 1.0 M $CH_3I$, 1.1(6) x $10^{-3}$ $s^{-1}$. These IR and corresponding visible data for a specific solvent are the same within experimental error as was also found in control experiments. The above solvent-assisted CO insertions agree with the general mechanistic concepts of this type of reaction.[15]

Plots of the pseudo-first-order rate constants, $k_{obs}$, for the oxidative addition reactions against [$CH_3I$] gave linear relationships with non-zero intercepts (except in MeOH medium being zero within experimental error) conforming to equation 5.3 where the constants are interpreted in terms of the reaction scheme (Figure 5.7). In this context it may be noted that the proposed rate-determining $k_2$ path is exactly the same as that for the solvent dependent path of square-planar substitution reactions. The same result was also obtained for the oxidative addition of $CH_3I$ to [Rh(cupf)(CO)($PX_3$)].[16]

$$k_{obs} = k_1[CH_3I] + k_2 \qquad \textbf{5.3}$$

The $k_1$ and $k_2$ values, determined in this way, are listed in Table 5.3 and Table 5.5 for the respective solvent and phosphine variations. In acetone, determined from data at

[15] Wojcicki, A., *Adv. Organomet. Chem.,* **11**, 87 (1973).

[16] Basson, S.S., Leipoldt, J.G., Roodt, A. and Venter, J.A., *Inorg. Chim. Acta*, **128**, 31 (1987).

four temperatures, the following activation parameters were obtained: $\Delta S^*_1$ = −190(25) and $\Delta S^*_2$ = −230(33) $JK^{-1}\,mol^{-1}$; $\Delta H^*_1$ = 33(6) and $\Delta H^*_2$ = 28(9) kJ $mol^{-1}$.

**Table 5.3** Solvent effects for the oxidative addition of $CH_3I$ to [Rh(neocupf)(CO)($PPh_3$)] at 25.0 °C

| **Solvent** | $\varepsilon^{17}$ | $D_n^{17}$ | $10^3k_1$ ($M^{-1}s^{-1}$) | $10^4k_2$ ($s^{-1}$) | $10^5k'_2$ ($M^{-1}s^{-1}$) | $k_1/k'_2$ |
|---|---|---|---|---|---|---|
| benzene | 2.3 | 0.1 | 0.0137(3) | 0.004(2) | 0.0036 | 381 |
| THF | 7.6 | 20.0 | 0.224(4) | 1.90(3) | 1.58 | 14 |
| 2-MeTHF | 7.6 | 20.0 | 0.229(3) | 1.61(4) | 1.63 | 14 |
| ethyl acetate | 6.0 | 17.1 | 0.31(4) | 0.12(3) | 0.12 | 258 |
| acetone | 20.7 | 17.0 | 1.41(2) | 1.4(1) | 1.03 | 137 |
| benzonitrile | 25.2 | 11.9 | 1.95(3) | 1.0(2) | 1.03 | 189 |
| methanol | 32.6 | 19.0 | 2.7(2) | 0.2(1) | – | – |
| nitromethane | 35.9 | 2.7 | 5.1(2) | 0.84(4) | 0.45 | 1133 |
| acetonitrile | 38.0 | 14.1 | 5.07(5) | 2.0(4) | 1.06 | 478 |
| dimethylsulphoxide | 45.0 | 29.8 | 8.4(1) | 9.5(7) | 6.75 | 124 |

Comparison of the rate constants in Table 5.3 with the dielectric constants and solvent donocities shows that, in general, the more polar and/or better donor solvent molecule accelerates the reaction. This can be taken as evidence that a function of the solvent is to ease the charge separation during the rearrangement and formation of the 5-coordinate intermediate ($k_1$ path) as is also evident from the large negative entropy of activation for acetone medium. The larger role of polarity compared to donocity in the case of the $k_1$ reaction can be seen from the dramatic increase in $k_1$ rate constants with increasing dielectric constants. The varying donocity values of the particular solvents do not seem to have a meaningful influence on this relationship. In order to make a more realistic comparison between $k_1$ and $k_2$ values, the latter was divided by the respective solvent concentrations (mol $dm^{-3}$) to obtain the second order rate constants, $k'_2$. ([S] = density x 1000/molar mass) The ratio $k_1/k'_2$ is thus a measure of competition between the $CH_3I$ and solvent dependent pathways. In the case of DMSO, which is known as a solvent having a good

[17] Mayer, U. and Gutman, V., *Adv. Inorg. Chem. Radiochem*., **17**, 189 (1975).

coordinating ability,[18] the $k_2$ path becomes more pronounced relative to $k_1$ if compared with for example benzene. In a similar sense it can be reasoned that the smaller ratio for acetone compared to acetonitrile reflects the trend in donor numbers but ethyl acetate, on the other hand, having near the same donocity gives a much greater ratio. Ethyl acetate has a lower dielectric constant probably playing a role in the slower $k_1$ reaction compared to $k_2$, with a consequent higher $k_1/k'_2$ ratio compared to acetone. The style of involvement for the solvent molecule, especially for the $k_2$ path, is thus not a clear-cut one. The smaller $\Delta H^*$-value for the $k_2$ path, compared to the $k_1$ path would have favoured the rate of reaction for the solvent path, though is counteracted by a more negative $\Delta S^*$-value. The large negative $\Delta S^*$-values for both reaction pathways, but especially the more negative value for the $k_2$ path, indicate a significant degree of increasing polarity and/or serious stereochemical limitations during the formation of the transition state. The dielectric constant dependency of $k_1$ values adds to the arguments in favour of a proposed polar transition state for the $k_1$ path, as well as similar observations from oxidative addition reactions with polar transition states. In the case of the postulated $k_2$ path, a direct attack of the solvent molecule on the metal centre with a consequent coordinated solvent molecule in the complex will be influenced to a large extent by the electron donating ability of the particular solvent and its tendency to coordinate. It is expected that the polarity of the solvent will play a role in such an action as well. It is therefore self evident that the rate constant for the $k_2$ path will not reflect a straightforward relationship with either the donocity aspect nor the solvent polarity.

Despite high polarity and donocity values, methanol, the only protic solvent in Table 5.3, makes an unexpectedly negligible contribution from the $k_2$ path to the overall rate. It is the only solvent in the range capable of hydrogen bond formation and being only a $\sigma$-donor, differs from ethyl acetate, acetone, acetonitrile and dimethyl sulfoxide containing multiple bonded functional groups. More specific $\pi$-bonding stabilisation of the transition state for the latter group of biphilic solvents, similarly proposed for $S_N2$ displacement reactions of Pt(II) complexes,[19] are thus expected.

[18] Baranovskii, V.I., Kukushkin, Y.N., Panina, N.S. and Panin, A.I., *Russ. J. Inorg. Chem*., **18**, 844 (1973).

[19] Pearson, R.G., Gray, H.B. and Basolo, F., *J. Am. Chem. Soc*., **82**, 787 (1960).

Such biphilic behaviour can be described by the ability of certain solvents to act as both an electron donor and electron acceptor towards the metal. Such solvents have available potentially vacant orbitals of a type capable of bonding with the filled $d_{yx}$ or $d_{xz}$ orbitals of the metal atom. These are the orbitals which project above and below the plane of the complex. Figure 5.3 shows how such $\pi$-bonding may permit these solvent molecules to approach so that their basic oxygen atoms are very close to the metal (Pt in this case) and in a good position to displace $Cl^-$ from the complex. Methanol, on the other hand, is a weaker solvating agent[20] but hydrogen-bonding is expected to occur in a transition state (different from those of the biphilic solvents) which will strongly favour the direct attack ($k_1$ path) of the nucleophilic Rh(I) centre on the polar $CH_3I$ molecule. The greater range (2.4 X $10^3$) for the $k_2$ rate constants, compared to those of $k_1$ (0.61 X $10^3$), is also suggestive, apart from polarity effects, of metal-solvent interactions of more specific nature as was also observed in the case of CO insertion reactions.[21,22]

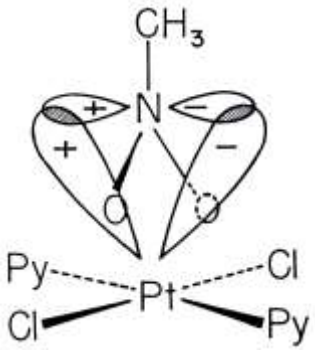


**Figure 5.3** Metal to ligand $\pi$-bonding in the interaction of a solvent molecule (nitromethane) with platinum(II)[19]

The electronic properties ($\upsilon$) of the different phosphine ligands used in Table 5.4 are that described by Tolman[23] and not the CO stretching frequencies of the [Rh(neocupf)(CO)($PX_3$)] complexes studied. The motivation for the decision is based on a study by Graham[24] on the influence of *cis*- and *trans*-ligands. According to his

[20] Belluco, U., Croatto, P., Uguagliati, P. and Pietropaolo, R., *Inorg. Chem*., **6**, 718 (1967).

[21] Mawby, R.J., Basolo, F. and Pearson, R.G., *J. Am. Chem. Soc*., **86**, 3994 (1964).

[22] Webb, S.L., Giandomenico, C.M. and Halpern, J., *J. Am. Chem. Soc*., **108**, 345 (1986).

[23] Tolman, C.A., *Chem.Rev*., **77**, 313 (1977).

[24] Graham, W.A., *Inorg. Chem*., **7**, 315 (1968).

study, the σ-donor ability of a ligand influences the stretching frequency of carbonyls *cis* and *trans* to it almost the same, while a π-bond between the ligand and the metal has twice the influence on the CO *trans* to the ligand, compared to *cis* CO groups. When π-bonding ligands like $PX_3$ are used, an interplay between the σ-donor and π-acceptor abilities of the different phosphine ligands cause CO stretching frequencies to be influenced more in some cases. The consequence is that the $\upsilon_{CO}$ order in complexes with CO and $PX_3$ *cis* to each other (as in [Rh(neocupf)(CO)($PX_3$)]) may differ from the order in *trans* complexes. Thompson and Sears[25] found the CO stretching frequencies in *trans* complexes to be a more accurate measure of the electronic influence of phosphine ligands than those of *cis* complexes. The conclusion was made that $\upsilon_{CO}$ values in complexes with $PX_3$ and CO *cis* are a less reliable measure of the electronic influence of phosphine ligands and thus of the nucleophilicity of the metal centre. The order of experimental $\upsilon_{CO}$-values of [Rh(neocupf)(CO)($PX_3$)] complexes differ indeed from the Tolman values, with a reversed order for $PPh_3$ and P(*p*-$ClC_6H_4)_3$ (Table 5.4).

**Table 5.4** Experimental $\upsilon_{CO}$-values of [Rh(neocupf)(CO)($PX_3$)] complexes (KBr), with the corresponding Tolman electronic parameter[23] values, $\upsilon$ ($cm^{-1}$)

| **$PX_3$** | **$\upsilon_{CO}$ ([Rh(neocupf)(CO)($PX_3$)])** | **$\upsilon$ (Tolman)** |
|---|---|---|
| P(*p*-$ClC_6H_4)_3$ | 1971 | 2072.8 |
| $PPh_3$ | 1976 | 2068.9 |
| P(*p*-$MeOC_6H_4)_3$ | 1965 | 2066.1 |
| $PPh_2C_6F_5$ | 1978 | 2074.8 |
| $PCy_3$ | 1959 | 2056.4 |
| P(*o*-Tol)$_3$ | 1965 | 2066.7 |

Observing the data for the neocupferrate complexes in Table 5.5 shows that the first three phosphine entries have the same stereochemical demand but should influence the Lewis basicity of the Rh(I) center differently due to the electronegativity differences[26] of the substituent groups. In accordance, the $k_1$ path shows a 18-fold

[25] Thompson, W.H. and Sears, C.T., *Inorg. Chem.*, **16**, 769 (1977).

[26] Huheey, J.E., *Inorganic chemistry*, 2nd Ed., Harper & Row, New York (1978).

increase from P(*p*-ClC$_6$H$_4$)$_3$ to P(*p*-MeOC$_6$H$_4$)$_3$ which is the expected trend for a nucleophilic attack at the (sp$^3$)C of iodomethane. To the contrary, the $k_2$ constants are all, except for P(*o*-Tol)$_3$ and PPh$_2$C$_6$F$_5$, the same within experimental error. This is also the expected result considering the solvent effects discussed above. If electronic effects[23] alone had been operative for the $k_1$ path, a rate trend of PCy$_3$>P(*o*-Tol)$_3$>>PPh$_2$C$_6$F$_5$ would have been expected with the three *p*-substituted derivates interspersed between the latter two.

**Table 5.5** Rate constants for the oxidative addition of $CH_3I$ to [Rh(neocupf)(CO)(PX$_3$)] and [Rh(cupf)(CO)(PX$_3$)] complexes in acetone at 25.0 °C. ($\theta$ = cone angle,[23] degrees; $\upsilon$ = Tolman electronic parameter[23], cm$^{-1}$)

| **PX$_3$** | **$\theta$** | **$\upsilon$** | **Neocupferrate** | | **Cupferrate[16]** | |
|---|---|---|---|---|---|---|
| | | | **$10^3k_1$** ($M^{-1}s^{-1}$) | **$10^4k_2$** ($s^{-1}$) | **$10^3k_1$** ($M^{-1}s^{-1}$) | **$10^4k_2$** ($s^{-1}$) |
| P(*p*-ClC$_6$H$_4$)$_3$ | 145 | 2072.8 | 0.29(1) | 0.63(8) | 0.193(8) | 1.4(6) |
| PPh$_3$ | 145 | 2068.9 | 1.41(2) | 1.4(1) | 1.22(2) | 3.1(1) |
| P(*p*-MeOC$_6$H$_4$)$_3$ | 145 | 2066.1 | 5.3(2) | 1.2(1) | 4.20(8) | 2.0(5) |
| PPh$_2$C$_6$F$_5$ | 158 | 2074.8 | 0.097(4) | 0.56(3) | 0.091(6) | 0.69(4) |
| PCy$_3$ | 170 | 2056.4 | 1.69(2) | 1.6(2) | 1.94(3) | 2.4(2) |
| P(*o*-Tol)$_3$ | 194 | 2066.7 | 0.049(2) | 0.05(1) | 0.21(2) | 1.9(2) |

According to Table 5.5, $k_1$(PCy$_3$) > $k_1$(P(*o*-Tol)$_3$) (in agreement with the electronic effect) but both values are smaller than those of the *p*-methoxy derivative which indicates that a steric influence is also operative. Similarly the $\upsilon_{CO}$ = 1955 cm$^{-1}$ for [Rh(neocupf)(CO)(PCy$_3$)] and the Tolman parameter of 2056.4 cm$^{-1}$ for PCy$_3$ is the lowest for these complexes indicating the good $\sigma$-donocity of PCy$_3$ resulting in the strongest potential Lewis base complex for oxidative addition. This order is also reflected in the higher p$K_a$-value of 9.7 for PCy$_3$, compared to the 2.7 of PPh$_3$.[27] For P(*o*-Tol)$_3$, comparable to P(*p*-MeOC$_6$H$_4$)$_3$ in $\sigma$-donocity and having the same $\upsilon_{CO}$-values in their respective Rh(I) complexes, we unexpectedly found $\upsilon_{CO}$ = 2027 cm$^{-1}$ (compared to the 2050-2060 cm$^{-1}$ range) for the oxidative addition product in acetone medium. This shows that the CO group, due to excessive bulkiness of the

[27] Rahman, M.M., Liu, H.Y., Eriks, K., Prock, A. and Giering, W.P., *Organometallics*, **8**, 1 (1989).

phosphine, is possibly shifted to a position implicating strong π-interaction with rhodium. The $k_1$ rate constant for $PPh_2C_6F_5$ is of the correct expected order indicating a small steric influence if any, but the smaller $k_2$ value is indicative of an electronic effect if compared with the more bulky phosphines' constants. In this respect we are tempted to ascribe this phenomenon to a neighbouring group participation effect since an *ortho*-substituted electronegative fluorine atom on the phosphine can interact with the metal $d_z^2$ orbital similar to the *o*-methoxy interaction in *trans*-[Ir(CI)(CO){$PMe_2$(*o*-$MeOC_6H_4$)}$_2$].[28] In such a case the decrease in electron density on the metal could place a restriction on the π-bonded transition state stabilisation of the solvent path.

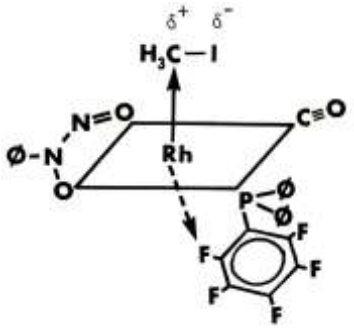


**Figure 5.4** Possible neighbouring group participation in the case of $PPh_2C_6F_5$

When the neocupferrate data is compared to that of cupferrate, the difference between the two bidentate ligands becomes evident. Neocupferrate, with a naphtyl group attached to a nitrogen of the chelate backbone, is expected to be a stronger Lewis base than cupferrate, with a phenyl group attached to the nitrogen mentioned.

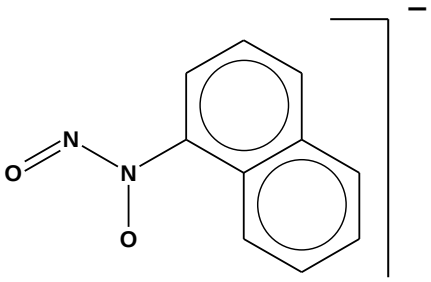


**Neocupferrate**

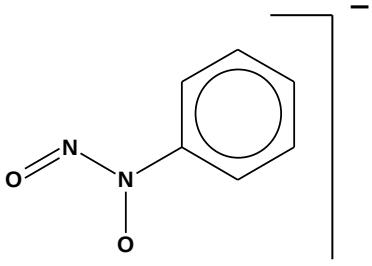


**Cupferrate**

[28] Miller, E.M. and Shaw, B.L., *J. Chem. Soc., Dalton Trans*., 480 (1974).

With neocupferrate coordinated to rhodium, more electron density will be available to the metal centre, as is observed from the slightly lower CO stretching frequencies. For [Rh(cupf)(CO)($PPh_3$)], $\upsilon_{CO}$ = 1982 $cm^{-1}$, whereas for [Rh(neocupf)(CO)($PPh_3$)], $\upsilon_{CO}$ = 1976 $cm^{-1}$ (Table 5.4). More electron density on the metal centre is associated with faster oxidative addition, as can be seen when the rate constants for the first four phoshines are compared. Moving to the more bulky phosphines, $PCy_3$ and P(*o*-Tol)$_3$, the size of the naphtyl group retards oxidative addition and smaller $k_1$ values are obtained for neocupferrate compared to cupferrate. The $k_2$ values of neocupferrate are smaller than that of cupferrate over the whole spectrum of phosphines, indicating the greater difficulty for a solvent molecule to enter the coordination sphere along the $k_2$ path in the case of neocupferrate.

As with most of the studies regarding the evaluation of the influence of phosphine ligands, that is, the relative contribution of steric and electronic effects, results presented in this way do not give a clear and quantifiable picture of the behaviour of a particular system under certain conditions. That is because conclusions are usually simply based upon the one-sided comparison of rate constants with either the steric or electronic effects. To illustrate, the rate constant for P(*p*-$MeOC_6H_4$)$_3$) is for example larger than that of $PCy_3$ because of the steric bulk of the latter, but the value for $PCy_3$ in turn is larger than the $k_1$ value for $PPh_3$, a much smaller ligand. By using Tolman's method to compare the rate constants with the steric and electronic effects simultaneously, the total effect of the phosphine ligands can be quantified. To do this, the $pk_1$ values was plotted as vertical heights on the two dimensional steric-electronic map as seen in Figure 5.5 Such a map was obtained by plotting the properties of the phosphine ligand, in terms of cone angle versus the Tolman electronic parameter.

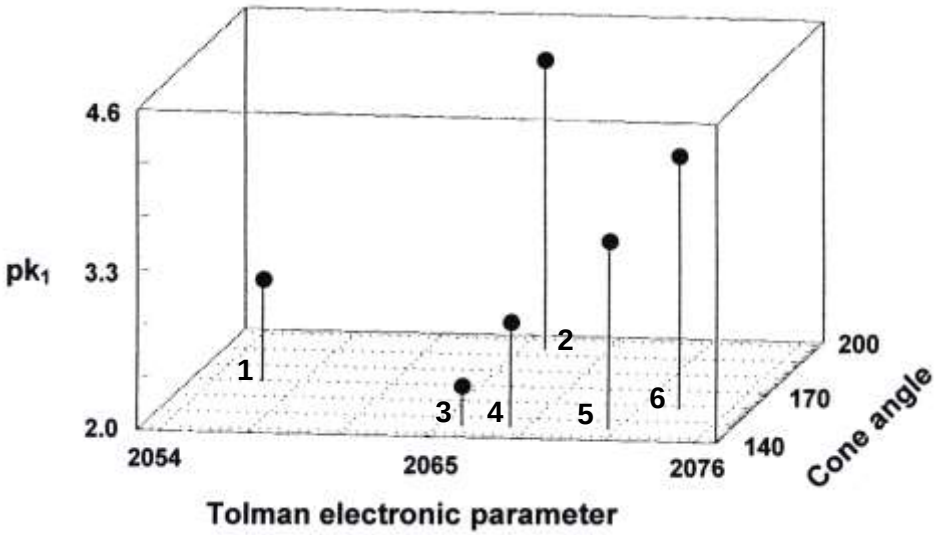


**Figure 5.5** Three dimensional representation of the relationship between $pk_1$, cone angle and Tolman electronic parameters for the oxidative addition of $CH_3I$ to [Rh(neocupf)(CO)($PX_3$)] at 25°C in acetone. The phosphine ligands are indicated as follows: (1) $PCy_3$, (2) P(*o*-Tol)$_3$, (3) P(*p*-$MeOC_6H_4$)$_3$, (4) $PPh_3$ (5) P(*p*-$ClC_6H_4$)$_3$ and (6) $PPh_2C_6F_5$

As can be seen from Figure 5.5, the data points as plotted already give the impression of defining a plane in three dimensions. Using least-squares methods, the equation defining the plane was calculated and Figure 5.6 obtained. For the oxidative addition of $CH_3I$ to [Rh(neocupf)(CO)($PX_3$)] at 25°C in acetone the variables a, b and c in the equation $pk_1 = a\theta + b\upsilon + c$ was calculated as a = 0.036(7), b = 0.10(2) and c = −206(45). With the mathematical equation as a measure of total phosphine involvement in this particular reaction, expected rate constants for other phosphines not involved in this study can be calculated for this system under the same solvent and temperature conditions. The only prerequisite being the availability of the cone angle and Tolman electronic parameter for the phoshine under consideration. According to Tolman, the percentage steric character is given by the equation: % steric influence = 100[a/(a+b)], giving in the case of neocupferrate at 25°C in acetone a value of 28(8)% steric influence. The relatively low steric involvement indicates a transition state for the oxidative addition where the phosphine ligand is positioned in a way not being crowded, like in the trigonal plane of a trigonal bipyramid, as presented in Figure 5.7 and Figure 5.8.

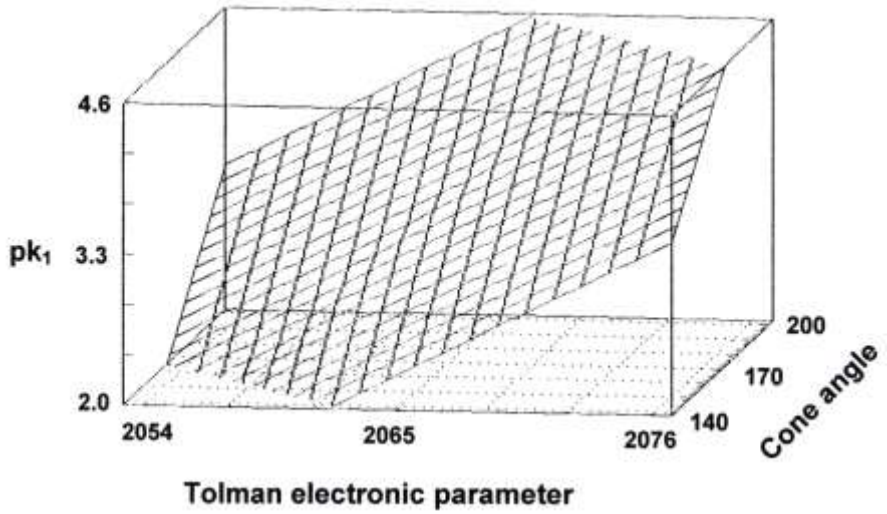


**Figure 5.6** Three dimensional representation of the plane fitted to the data points of Figure 5.6

Applying the calculation of steric involvement to the cupferrate system, the variables in the equation are obtained as a = 0.021(9), b = 0.09(3) and c = −192(59), with an overall steric influence of 19(9)%. Although the error limits are high, primarily because of too little data points involved in the calculations, an indication is given that the less substituted cupferrate ligand is sterically less demanding than the neocupferrate ligand. Considered carefully, the percentage sterical influence calculated this way, using the properties of the phosphine ligands as manipulator of the system, is actually an indication of the steric demand of the bidentate ligand, weighed against electronic influences. A unique result is thus obtained stretching much further than the simple comparison of bite angles of bidentate ligands. The different behaviour of the two systems, cupferrate and neocupferrate, having the same chelate backbone, proves this point. If this treatment of data could be extended to numerous other bidentate ligands involved in oxidative addition, an easier selection of the composition of a complex destined as a catalyst in a particular process would be possible.

A possible reaction mechanism consistent with the experimental results is shown in Figure 5.7. This mechanism also includes the ground-state stereochemistries of [Rh(neocupf)(CO)($PPh_3$)] and the *cis*-addition product, [Rh(neocupf)(CO)($CH_3$)(I)-($PPh_3$)]. Both complexes were characterised by X-ray crystallography (Chapter 4). Such a *cis* addition is contradictory to the general trend of alkyl halides to form *trans*-

addition products.[29,30,31] Addition of alkyl halides to $[Ir(Cl)(CO)(PMe_2Ph)_2]$[32] forms *cis* products similar to that obtained with the cupferrate/neocupferrate systems, and is described by Pearson and Poulos[33] as unique for the oxidative addition of alkyl halides to square planar metal complexes. Although rare, other examples of *cis*-addition, like the oxidative addition of $CH_3I$ to $[Rh(quin)(CO)\{P(R\text{-}C_6H_4)_3\}]$[34] are known as well.

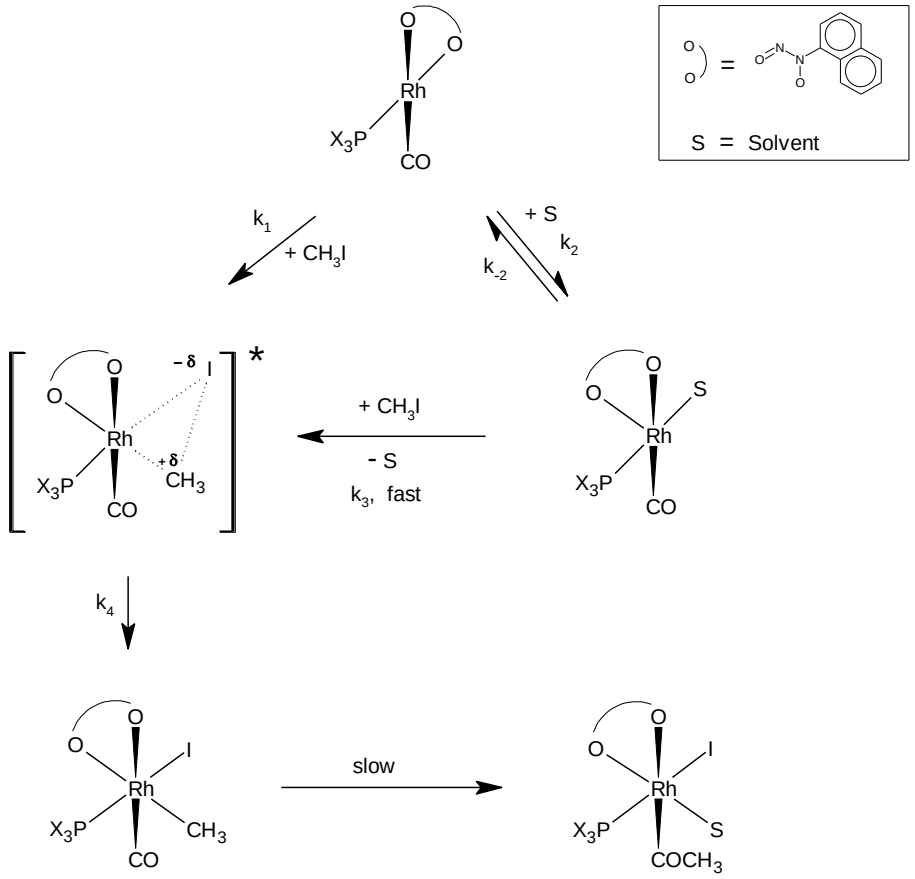


**Figure 5.7** Proposed reaction mechanism for the oxidative addition of $CH_3I$ to $[Rh(neocupf)(CO)(PX_3)]$.

The $k_1$ path implies a nucleophilic attack on $CH_3I$ giving the 16-electron 5-coordinate intermediate for which the degree of ion separation will be solvent-dependent. The

[29] Stille, J.K. and Lau, K.S.Y., *Acc. Chem. Res*., **10**, 434 (1977).

[30] Miller, E.M. and Shaw, B.L., *J. Chem. Soc., Dalton Trans*., 480 (1974).

[31] Terblans, Y.M., Basson, S.S., Purcell, W. and Lamprecht, G.J., *Acta Cryst*., **C51**, 1748 (1995).

[32] Deeming, A.J. and Shaw, B.L., *J. Chem. Soc.,* **A***,* 1562 (1969).

[33] Pearson, R.G. and Poulos, A.T., *Inorg. Chim. Acta*, **34**, 67 (1979).

[34] Cano, M., Heras, J.V., Lobo, M.A., Pinilla, E. and Monge, M.A., *Polyhedron*, **11**, 2679 (1992).

significant dependence of the reaction rates on the solvent is, according to Kubota and associates[35], typical of a transition state where the electron pair is associated more closely with the carbon atom than with the metal. This implies that the metal is already in the +3 oxidation state. Although such a transition state will have a strong dipole character, a certain degree of association between the carbon atom and the iodide ion can still be visualised, especially with the observed *cis*-addition product in mind. The postulate for the existence of the ionic intermediate, $[Rh(neocupf)(CO)(PX_3)(CH_3)]^+I^-$ is based upon studies that led to the isolation of the insoluble tetraphenylborate salts of, for example $[Rh(C_5H_5)(CO)(CH_3)\{P(CH_3)_2\text{-}C_6H_5\}]^+Br^-$. The charge separation of these complexes is solvent dependent as well. As the reaction proceeds from the ground state to the transition state, the increased dipole character causes an increasing degree of solvation, which is evident from the large negative values of the entropy of activation.

Although these trigonal-bipyramidal intermediates can give fast isomerisations, there is reason to believe that the constitution of the trigonal plane in the present case is related to the ground-state bond weakening effect of the phosphine ligand in $[Rh(neocupf)(CO)(PX_3)]$. During the Rh–$CH_3$ bond formation, the $CH_3$ ligand will tend, based on similar assumptions for square-planar substitution reactions,[36] to move towards the least strongly bound ligand (assumed to be the nitroso oxygen) and away from the most strongly bound ligand (assumed to be $PX_3$), *i.e.*, the folding leading to the formation of the trigonal plane takes place along the diagonal O–Rh–P axis of the Rh(I) complex (Figure 5.8). Once the Rh–C bond is firmly established, the phosphorous atom can facilitate the simultaneous C–I bond-breaking by $\pi$-bond stabilisation of the activated complex.[37,38] The same effect will also facilitate the fast nucleophilic attack of $I^-$ between the Rh–C and Rh–O bonds of the *tbp* intermediate thus leading, after minor rearrangement, to the *cis* addition product.

[35] Kubota, M., Kiefer, G.W., Ishikawa, R.M. and Bencala, K.E., *Inorg. Chim. Acta*, **7**, 195 (1973).

[36] Purcell, K.F. and Kotz, J.C., *Inorganic chemistry*, Saunders, Philadelphia (1977).

[37] Chatt, J., Duncanson, L.A. and Venanzi, L.M., *J. Chem. Soc.,* 4456 (1955).

[38] Orgel, L.E., *J. Inorg. Nucl. Chem.*, **2**, 137 (1956).

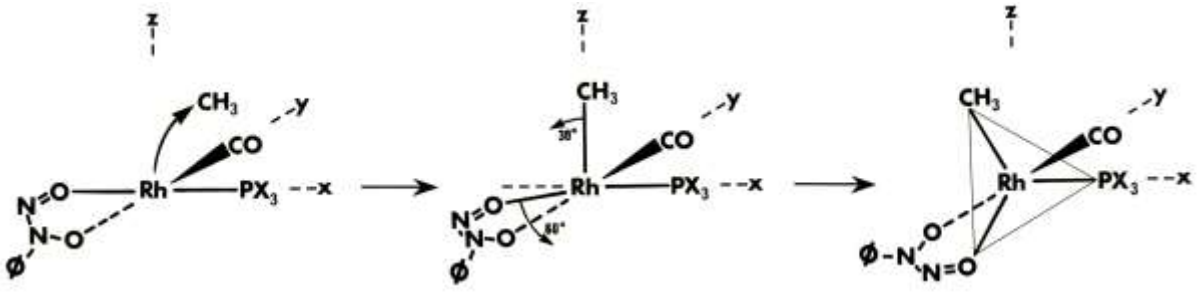


**Figure 5.8** Stereochemical change during $CH_3I$ addition. In order to obtain a separation of 120° between the incoming and weakest bound ligand, $CH_3$ moves through 30° in the xz-plane in the direction of the x-axis (and the weakest bound ligand) in the same time it takes O (nitroso) to move through 60° in the xz-plane in the direction of the z-axis, away from $CH_3$. As a result the trigonal plane, comprising $PX_3$, $CH_3$ and O (nitroso), is formed in the xz-plane.

The existence of a solvent-stabilised *tbp* intermediate for the $k_2$ path can be justified in terms of the propensity of [Rh(cupf)(CO)($PPh_3$)] to add on an extra nucleophilic π-bonding ligand[39] ($PPh_3$) as well as the reactivity of these complexes towards solvents alone. Secondly, the solvent-assisted $k_2$ path can be viewed as an oxidative addition catalysis phenomenon similar to the solvent effects in the migratory insertion of CO into transition-metal alkyl bonds. Halpern's research[40] indicates that the formation of the 5-coordinate intermediate acyl rather than its coordinative saturation and trapping is the key to the solvent's or nucleophile's role in these insertions. Similarly we could visualise a fast dissociative trapping of the solvent-stabilised *tbp* intermediate by $CH_3I$ during its conversion to the ionic intermediate of the $k_1$ path. This solvent-stabilised intermediate, being still a Rh(I) complex, is also expected to be much more reactive towards $CH_3I$, since the stereochemical transformation, similar to that of the ionic intermediate, has already been taken care of during the $k_2$ step.

The results of the solvent effects in this study show that it is an important factor responsible for enhancement of oxidation addition rates. The cupferrate system was claimed[7] to be probably the first example of a solvent catalysed pathway, and now the neocupferrate system has joined the ranks. In 2004, Bassetti and co-workers

[39] Basson, S.S., Leipoldt, J.G. and Venter, J.A., *Acta Cryst*., **C46**, 1324 (1990).

[40] Webb, S.L., Giandomenico, C.M. and Halpern, J., *J. Am. Chem. Soc*., **108**, 345 (1986).

proposed two parallel pathways[41] for the oxidative addition of iodomethane to the cationic rhodium(I) carbonyl complex $[Rh(L)(CO)]PF_6$ (L = 2,6-bis(benzylthiomethyl)-pyridine), with the iodomethane independent pathway due to reversible decoordination of one thiobenzyl arm from rhodium. They referred to cupferrate as the only case they could find, among the reactions of rhodium(I) complexes, in which a plot of $k_{obs}$ vs $[CH_3I]$ reveals a non-zero intercept on the y axis. With the reaction in the cupferrate system proceeding to completion, and thus eliminating the possibility that the intercept could represent a possible reverse reaction, the non-zero intercept was interpreted as indicative of a solvent pathway.

Apart from having a mutual ionic intermediate for the $k_1$ and $k_2$ pathways, as depicted in the reaction scheme, this solvent path could also possibly lead to oxidation addition products having for example different stereochemistries. In this respect, an additional product (which was not pursued further) was mentioned for the $CH_3I$ addition to *trans*-$[Ir(Cl)(CO)[PMe_2(p\text{-}MeOC_6H_4)\}_2]$[28] where an experimental rate law, similar to the present study, was operative. No evidence of an additional complex was found during the preparation of $[Rh(neocupf)(CO)(CH_3)(I)(PPh_3)]$, but small amounts of a second isomer could go undetected in this way.

A rate law as is discussed in the paragraph that follows, can be deduced from the proposed reaction mechanism. Although no reaction equilibria were observed experimentally, the following theoretically possible equilibrium reactions from the reaction scheme in Figure 5.7 can be used for the deduction.

$$[Rh(neocupf)(CO)(PX_3)] + CH_3I \underset{k_{-1}}{\overset{k_1}{\rightleftharpoons}} [Rh(neocupf)(CO)(PX_3)(CH_3)]^+I^-$$

$$[Rh(neocupf)(CO)(PX_3)] + S \underset{k_{-2}}{\overset{k_2}{\rightleftharpoons}} [Rh(neocupf)(CO)(PX_3)(S)]$$

$$[Rh(neocupf)(CO)(PX_3)(S)] + CH_3I \xrightarrow{k_3} [Rh(neocupf)(CO)(PX_3)(CH_3)]^+I^-$$

$$[Rh(neocupf)(CO)(PX_3)(CH_3)]^+I^- \xrightarrow{k_4} [Rh(neocupf)(CO)(CH_3)(I)(PX_3)]$$

[41] Bassetti, M., Capone, A. and Salamone, M., *Organometallics*, **23**, 247 (2004).

Strictly compared to Figure 5.7, the $k_1/k_{-1}$ equilibrium above implies an ionic intermediate as product using the transition state indicated in Figure 5.7. Rate constants $k_{-3}$ and $k_{-4}$ are not taken into consideration, since the reaction proceeds to completion. The steady state principle, based on the approximation that the change in concentration of the intermediates with time is zero, was used to obtain the rate law.

$$\begin{aligned} d[\{Rh(neocupf)(CO)(PX_3)(CH_3)\}^+I^-]/dt &= k_3[CH_3I][Rh(neocupf)(CO)(PX_3)(S)] \\ &+ k_1[Rh(neocupf)(CO)(PX_3)][CH_3I] \\ &- k_{-1}[\{Rh(neocupf)(CO)(PX_3)(CH_3)\}^+I^-] \\ &- k_4[\{Rh(neocupf)(CO)(PX_3)(CH_3)\}^+I^-] \\ &= 0 \end{aligned}$$

From this follows

$$\begin{aligned} [\{Rh(neocupf)(CO)(PX_3)(CH_3)\}^+I^-] &= k_3[CH_3I][Rh(neocupf)(CO)(PX_3)(S)] / (k_{-1} + k_4) \\ &+ k_1[Rh(neocupf)(CO)(PX_3)][CH_3I] / (k_{-1} + k_4) \end{aligned} \quad \textbf{5.4}$$

$$\begin{aligned} d[Rh(neocupf)(CO)(PX_3)(S)]/dt &= k_2[Rh(neocupf)(CO)(PX_3)][S] \\ &- k_{-2}[Rh(neocupf)(CO)(PX_3)(S)] \\ &- k_3[Rh(neocupf)(CO)(PX_3)(S)][CH_3I] \\ &= 0 \end{aligned}$$

From this follows

$$[Rh(neocupf)(CO)(PX_3)(S)] = k_2[Rh(neocupf)(CO)(PX_3)][S] / (k_{-2} + k_3[CH_3I])$$

Substitute into 5.4:

$$\begin{aligned} [\{Rh(neocupf)(CO)(PX_3)(CH_3)\}^+I^-] &= \frac{k_3[CH_3I]k_2[Rh(neocupf)(CO)(PX_3)][S]}{\frac{k_{-2} + k_3[CH_3I]}{k_{-1} + k_4}} \\ &= \frac{k_1[Rh(neocupf)(CO)(PX_3)][CH_3I]}{k_{-1} + k_4} \end{aligned} \quad \textbf{5.5}$$

$$R = d[Rh(neocupf)(CO)(CH_3)(I)(PX_3)]/dt = k_4[\{Rh(neocupf)(CO)(PX_3)(CH_3)\}^+I^-] \quad \textbf{5.6}$$

Substitute 5.5 into 5.6:

$$R = \frac{k_2 k_3 k_4 [CH_3I][Rh(neocupf)(CO)(PX_3)][S]}{(k_{-1} + k_4)(k_{-2} + k_3[CH_3I])} + \frac{k_1 k_4 [Rh(neocupf)(CO)(PX_3)][CH_3I]}{k_{-1} + k_4}$$

With $k_4 >> k_{-1}$, this changes to

$$R = \frac{k_2 k_3 [CH_3I][Rh(neocupf)(CO)(PX_3)][S]}{k_{-2} + k_3[CH_3I]} + k_1[Rh(neocupf)(CO)(PX_3)][CH_3I] \quad \textbf{5.7}$$

$k_3[CH_3I]$ is much larger than $k_{-2}$ for the concentration range of $CH_3I$ in which the reaction was investigated. Consequently, equation 5.7 reduces further to:

$$R = k_2[Rh(neocupf)(CO)(PX_3)][S] + k_1[Rh(neocupf)(CO)(PX_3)][CH_3I]$$

$$= [Rh(neocupf)(CO)(PX_3)](k_2[S] + k_1[CH_3I])$$

$$= [Rh(neocupf)(CO)(PX_3)](k'_2 + k_1[CH_3I])$$

Thus, $k_{obs} = k'_2 + k_1[CH_3I]$ **5.8**

If $k_3[CH_3I] < k_{-2}$ and $k_{-2} > k_2$, the solvent-assisted $k_2$ path is effectively blocked and the first term of equation 5.7 falls away, so that $k_{obs} = k_1[CH_3I]$. This expression applies to the case of methanol. Equation 5.8 is of the same form as equation 5.3, which was deduced directly from experimental results. It therefore shows that the proposed reaction mechanism is in accordance with experimental results.

# 5.4 Solvent, temperature and pressure dependence of the oxidative addition of $CH_3I$ to [Rh(Sacac)(CO)($PPh_3$)] and [Rh(cupf)(CO)($PPh_3$)][42]

## 5.4.1 Experimental

[Rh(Sacac)(CO)($PPh_3$)] and [Rh(cupf)(CO)($PPh_3$)] were synthesised as described in Chapter 3. Solvents and chemicals of analytical reagent grade were used throughout this study. The reactions at atmospheric pressure were followed on a Hitachi Model 150-20 spectrophotometer equipped with a thermostated cell holder (±0.1 ºC). The high pressure kinetic measurements were performed on a modified (double-beam) Zeiss PMQ II spectrophotometer equipped with a thermostated high-pressure cell.[43] The oxidative-addittion reactions were followed at 380 and 402 ± 3 nm for the cupferron and thioacetylacetone complexes, respectively. All reactions were studied under pseudo-first-order conditions with $CH_3I$ in at least a 10-fold excess. Typical experimental conditions were [Rh] = 2 X $10^{-4}$ M and [$CH_3I$] between 0.05 and 0.5 M. At least four concentrations of $CH_3I$ were selected to determine the second-order rate constant. The observed first-order rate constants were calculated from plots of ln ($A_t$ - $A_\infty$) versus time, where $A_t$ and $A_\infty$ are the absorbances at time *t* and infinity, respectively. These plots were linear for at least 2-3 half-lives of the reaction.

## 5.4.2 Results and discussion

The kinetics of the oxidative addition of iodomethane to complexes of the type [Rh(LL')(CO)($PX_3$)] and [Rh(LL)($PX_3$)]$_2$, where LL' = β-diketones and cupferron and X = phenyl, *p*-chlorophenyl and *p*-methoxyphenyl were studied before.[9,5,16,44] Solvent and pressure effects were studied[45,46,47] in order to obtain more information on the

[42] Venter, J.A., Leipoldt, J.G. and Van Eldik, R., *Inorg. Chem*., **30**, 2207 (1991).

[43] Fleischmann, F.K., Conze, E.G., Stranks, D.R. and Kelm, H., *Rev. Sci. Instrum*., **45**, 1427 (1974).

[44] Leipoldt, J.G., Basson, S.S and Botha, L.J., *Inorg. Chim. Acta*, **168**, 215 (1990).

[45] Leipoldt, J.G., Steynberg, E.C. and Van Eldik, R., *Inorg. Chem*., **26**, 3068 (1987).

nature of the transition state in terms of A (for a concerted three-centered mechanism) or B (for $S_N2$ mechanism).

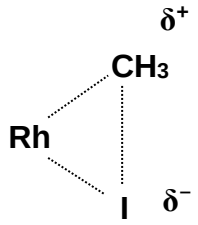


A

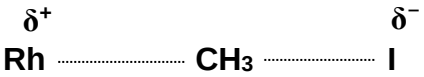


B

In these earlier studies, some solvent effects were observed, but data for a wide range of solvents in terms of ε and $q_p$[48] values were lacking and prevented a detailed interpretation. Thus, the necessity of this combined solvent/pressure dependence study, to be able to differentiate between these two possible transition states.

In this study the solvent, temperature and pressure dependence of reactions 5.9 and 5.10 have been investigated for a series of solvents. The product in the case of reaction 5.9 is the acyl complex, whereas the alkyl complex is the product in reaction 5.10. The solvents were selected in order to cover a wide as possible ε and $q_p$ range, so that it would be possible to separate $\Delta V^*$ into $\Delta V^*_{intr}$ and $\Delta V^*_{solv}$, the intrinsic and solvational volumes of activation, respectively.[49]

$[Rh(Sacac)(CO)(PPh_3)] + CH_3I \longrightarrow [Rh(Sacac)(COCH_3)(I)(PPh_3)]$ **5.9**

$[Rh(cupf)(CO)(PPh_3)] + CH_3I \longrightarrow [Rh(cupf)(CO)(CH_3)(I)(PPh_3)]$ **5.10**

[46] Van Zyl, G.J., Lamprecht, G.J., Leipoldt, J.G. and Swaddle, T.W., *Inorg. Chim. Acta*, **143**, 223 (1988).

[47] Stieger,H. and Kelm, H.J., *Phys.Chem*., **77**, 290 (1973).

[48] $q_p$ is the pressure derivative of the solvent parameter $q = (\varepsilon-1)/(2\varepsilon+1)$, i.e. $q_p = [3/(2\varepsilon+1)^2](\partial\varepsilon/\partial p)$, where ε is the dielectric constant of the solvent.

[49] Van Eldik, R., Asano,T. and Le Noble, W.J., *Chem. Rev*., **89**, 549 (1989).

A detailed study of reaction 5.9 indicated that the final acyl complex is formed via the alkyl intermediate, for which the formation of the latter species is the rate-determining step.[44] In reaction 5.10, the alkyl complex is formed without any evidence for the formation of a subsequent acyl complex on the time scale used for the kinetic runs.[16,44] The investigated reactions and selected conditions are such that the observed first-order rate constant, $k_{obs}$, depends linearly on the iodomethane concentration, i.e. $k_{obs} = k[CH_3I]$. The values of k as a function of solvent, temperature, and pressure are summarized in Table 5.6, Table 5.7, Table 5.8 and Table 5.9. The activation parameters $\Delta H^*$, $\Delta S^*$, and $\Delta V^*$ were calculated from these data by using a least-squares analysis and are summarised along with important solvent parameters in Table 5.10 and Table 5.11. Plots of ln k versus pressure were linear under all conditions, such that $\Delta V^*$ could be calculated directly from the slope ($=-\Delta V^*/RT$) of such plots. Both reactions 5.9 and 5.10 are characterised by significantly negative $\Delta S^*$ and $\Delta V^*$ values, which indicate that bond formation and/or charge creation (and consequently electrostriction) must play an important role on forming the transition state. The differentiation between the intrinsic and solvational contributions to the activation volumes should be possible on the basis of the solvent dependence of the kinetic parameters as employed and suggested before,[44,45] especially in terms of the data for $\Delta V^*$.

**Table 5.6** Rate constants ($10^4$k, $M^{-1}s^{-1}$) as a function of temperature for the oxidative addition of $CH_3I$ to [Rh(Sacac)(CO)($PPh_3$)] in various solvents

| Solvent | T = 288.0 K | T = 298.0 K | T = 308.0 K |
|---|---|---|---|
| chloroform | 58.3 | 108 | 177 |
| chlorobenzene | 4.70 | 9.25 | 16.5 |
| dichloromethane | 55.0 | 83.1 | 137 |
| 1,2-dichloroethane | 37.3 | 67.4 | 121 |
| acetone | 17.6 | 36.7 | 74.6 |
| nitromethane | 117 | 223 | 355 |
| acetonitrile | 56.4 | 123 | 221 |

**Table 5.7** Rate constants ($10^4$k, $M^{-1}s^{-1}$) as a function of temperature for the oxidative addition of $CH_3I$ to [Rh(cupf)(CO)($PPh_3$)] in various solvents

| Solvent | T = 288.0 K | T = 298.0 K | T = 308.0 K |
|---|---|---|---|
| chloroform | 28.5 | 50.4 | 76.6 |
| dichloromethane | 24.7 | 41.2 | 70.1 |
| 1,2 dichloroethane | 17.1 | 30.4 | 56.1 |
| acetone | 10.6 | 17.3 | 29.3 |
| acetonitrile | 43.9 | 84.6 | 150 |
| methanol | 15.6 | 32.8 | 57.5 |

**Table 5.8** Rate constants ($10^4$k, $M^{-1}s^{-1}$) as a function of pressure (p, bar) for the oxidative addition of $CH_3I$ to [Rh(Sacac)(CO)($PPh_3$)] in various solvents at 25°C

| Solvent | p = 50 | p = 250 | p = 500 | p = 750 | p = 1000 |
|---|---|---|---|---|---|
| chloroform | 108(2) | 127(1) | 156(4) | 182(4) | 207(2) |
| chlorobenzene | 9.3(3) | 10.5(4) | 12.0(2) | 13.6(2) | 15.9(3) |
| dichloromethane | 83.1(15) | 100(2) | 123(2) | 145(2) | 170(2) |
| 1,2-dichloroethane | 67.4(4) | 77.5(4) | 88.7(4) | 99(1) | 114(1) |
| acetone | 36.7(1) | 41.6(4) | 48.1(3) | 55.1(3) | 67.1(4) |
| nitromethane | 223(4) | 262(2) | 300(7) | 357(9) | 403(9) |
| acetonitrile | 124(3) | 138(2) | 155(2) | 179(2) | 215(3) |

**Table 5.9** Rate constants ($10^4$k, $M^{-1}s^{-1}$) as a function of pressure (p, bar) for the oxidative addition of $CH_3I$ to [Rh(cupf)(CO)($PPh_3$)] in various solvents at 25°C

| Solvent | p = 50 | p = 350 | p = 700 | p = 1000 |
|---|---|---|---|---|
| chloroform | 50.4(8) | 65(1) | 81.0(6) | 100(2) |
| dichloromethane | 41.2(5) | 53.0(4) | 67.4(9) | 81.2(15) |
| 1,2-dichloroethane | 30.4(8) | 37.6(6) | 48.2(15) | 56.8(18) |
| acetone | 17.3(3) | 21.2(6) | 25.6(2) | 32.2(3) |
| acetonitrile | 84.6(12) | 116(2) | 171(3) | 225(4) |

As pointed out, $\Delta V^*$ may be considered as the sum of two components: $\Delta V^*_{intr}$, which represents the change in volume due to changes in the coordination number, bond lengths, and angles, and $\Delta V^*_{solv}$, which represents the change in volume due to changes in solvation, i.e. electrostriction, on forming the transition state. During

oxidative addition, an overall volume decrease is expected because of bond formation with the metal centre ($\Delta V^*_{intr}$) and increasing electrostriction ($\Delta V^*_{solv}$) due to a polar transition state involving heterolytic cleavage of the $CH_3$–I bond as indicated in A and B. This volume decrease may be partially offset by a volume increase due to $CH_3$–I bond fission. The Kirkwood model can be adopted to account for the solvent dependence of $\Delta V^*_{solv}$ as shown in equation 5.11.[50,51]

$$\Delta V^* = \Delta V^*_{intr} + \Delta V^*_{solv}$$

$$= \Delta V^*_{intr} - (N_0 \Delta_\mu{}^2/r^3)q_p \qquad \textbf{5.11}$$

According to this equation, $\Delta V^*_{intr}$ can be estimated from a plot of $\Delta V^*$ versus $q_p$ for the investigated solvents as done before for the oxidative addition of $CH_3I$ to $[Ir(Cl)(CO)(PPh_3)_2]$.[47] The solvents selected in this study are such that the $\varepsilon$ and $q_p$ values vary by a factor of 10 (see Table 5.10 and Table 5.11), such that significant effects on $\Delta V^*$ are expected. The quoted $q_p$ values were calculated from the given expression[48] and the relationship $(1/\varepsilon_0{}^2)(\partial\varepsilon/\partial p) = A'/B'$, where A' and B' were taken from the literature.[51] It should be noted that the $q_p$ values obtained in this way were divided by 2.303 to take into account that the above equation was obtained by differentiation of the empirical equation $1/\varepsilon_0 - 1/\varepsilon_P = A'\log[(B'+P)/(B'+P_0)]$. This conversion of the log term to the ln term was not taken into account in the data reported in the literature.[51,52]

Although the data in Table 5.10 and Table 5.11 for the oxidative addition to the Sacac complex indicate some larger values for k at higher solvent polarity, both the $\Delta S^*$ and $\Delta V^*$ values are very constant. This trend indicates that the solvent can in some cases ease charge separation during the formation of the transition state[44] without affecting electrostriction.

[50] Kirkwood, J.G., *J Chem. Phys*., **2**, 351 (1934).

[51] Isaacs, N., *Liquid phase high pressure chemistry*, John Wiley, England, Chichester (1981).

[52] Hartmann, H., Neumann, A. and Schmidt, A.P., *Ber. Bunsen-Ges. Phys. Chem.*, **72**, 877 (1968).

**Table 5.10** Rate constants at 25°C and activation parameters for the oxidative addition of $CH_3I$ to [Rh(Sacac)(CO)($PPh_3$)] in various solvents

| **Solvent** | **$\varepsilon_0$** | **$10^6 q_p$** bar$^{-1}$ | **$10^4 k$** $M^{-1}s^{-1}$ | **ΔH*** kJ mol$^{-1}$ | **ΔS*** $JK^{-1}mol^{-1}$ | **ΔV*** cm$^3$ mol$^{-1}$ |
|---|---|---|---|---|---|---|
| chloroform | 4.64 | 16.7 | 108 | 37(2) | −160(6) | −17(1) |
| chlorobenzene | 5.44 | 10.2 | 9.25 | 43(1) | −160(4) | −13.6(3) |
| dichloromethane | 8.64 | 11.5 | 83.1 | 32(3) | −177(8) | −18.3(9) |
| 1,2-dichloroethane | 10.1 | 12.2 | 67.4 | 41(1) | −150(2) | −13.2(5) |
| acetone | 19.7 | 6.4 | 36.7 | 51(1) | −122(2) | −15.2(6) |
| nitromethane | 35.8 | 1.8 | 223 | 36(3) | −156(10) | −15.2(7) |
| acetonitrile | 36.1 | 1.5 | 123.5 | 45(3) | −128(10) | −13.9(7) |

**Table 5.11** Rate constants at 25°C and activation parameters for the oxidative addition of $CH_3I$ to [Rh(cupf)(CO)($PPh_3$)] in various solvents

| **Solvent** | **$\varepsilon_0$** | **$10^6 q_p$** bar$^{-1}$ | **$10^4 k$** $M^{-1}s^{-1}$ | **ΔH*** kJ mol$^{-1}$ | **ΔS*** $JK^{-1}mol^{-1}$ | **ΔV*** cm$^3$ mol$^{-1}$ |
|---|---|---|---|---|---|---|
| chloroform | 4.64 | 16.7 | 50.4 | 33(3) | −180(9) | −17.3(8) |
| dichloromethane | 8.64 | 11.5 | 41.2 | 37(1) | −168(4) | −17.4(8) |
| 1,2-dichloroethane | 10.1 | 12.2 | 30.4 | 42(2) | −151(5) | −16.1(3) |
| acetone | 19.7 | 6.4 | 17.3 | 36(2) | −180(5) | −15.7(7) |
| acetonitrile | 36.1 | 1.5 | 84.6 | 42(1) | −144(1) | −25.4(7) |
| methanol | 30.8 | 3.3 | 32.8 | 43(3) | −147(10) | −24.9(5) |

The ΔV* data are in excellent agreement with data reported for the oxidative addition of $CH_3I$ to [Rh(β-diketonate)($P(OPh)_3$)$_2$] in acetone, chloroform, and dichloromethane for β-diketone = acetylacetone, (trifluoroacetyl)acetone and (trifluorobenzoyl)-acetone.[45,46] The latter values also exhibit no significant dependence on $q_p$. It follows that the observed ΔV* for the present investigated reactions mainly represents $\Delta V^*_{intr}$ with an average value of −15.2 ± 1.5 cm$^3$ mol$^{-1}$ for the Sacac data in Table 5.10. This value is indeed very close to the $\Delta V^*_{intr}$ value of −17 cm$^3$ mol$^{-1}$ reported for the oxidative addition to [Ir(Cl)(CO)($PPh_3$)$_2$].[47] In the Sacac system, the final reaction product is the acyl complex, and two possible reaction routes via transition states A and B have been suggested.[44]

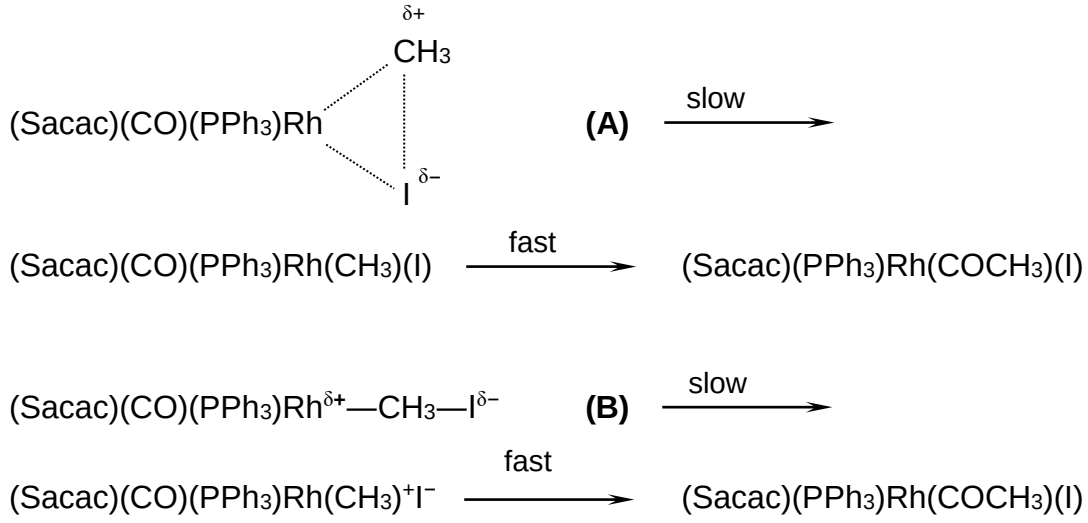


On the basis of the solvent-independent ΔV* data, we conclude that the reaction via transition state A is more likely, since a significant solvent dependence is expected for the reaction scheme (B) involving an ion-pair intermediate (see further discussion). The concerted three-centre reaction route (A) not only accounts for the solvent independence of ΔV* but can also quantitatively account for the magnitude of ΔV*. Substitution reactions of such Rh(I) complexes are typically associative and characterised by ΔV* values of *ca.* −6 $cm^3$ $mol^{-1}$. It should be noted that the volume decrease during the formation of a five-coordinate species is partially offset by the volume increase due to structural changes from tetragonal pyramidal to trigonal bipyramidal, generally observed in substitution reactions of square-planar complexes.[53] It thus follows that the average value of −15.2 ± 1.5 $cm^3$ $mol^{-1}$ is in line with the simultaneous formation of two bonds between the rhodium centre and $CH_3I$ in the concerted three-center mechanism (A).

The data for the cupferron system in Table 5.11 indicate no meaningful correlation between k and the polarity of the solvent. Furthermore, ΔV* has a value of −17 $cm^3$ $mol^{-1}$ for four solvents, but is significantly more negative, *ca.* −25 $cm^3$ $mol^{-1}$, for the more polar solvents acetonitrile and methanol. It follows that the more polar solvents may allow more charge creation, which is accompanied by a large change in dipole

[53] Kotowski, M. and Van Eldik, R., *Inorganic high pressure chemistry: Kinetics and mechanisms*; Van Eldik, R., Ed.; Elsevier: Amsterdam (1986).

moment ($\Delta\mu^2$, see eq 5.11) in the transition state. The more negative $\Delta V^*$ values do not correlate with the smaller $q_p$ values for these solvents, such that electrostriction effects cannot account for these observations. However, formation of an ion-pair intermediate will be more favoured in more polar solvents, indicating that this oxidative-addition reaction most probably proceeds via the linear transition state B in more polar solvents. In the case of the less polar solvents the $\Delta V^*$ value of −17 $cm^3$ $mol^{-1}$ can either be due to single-bond formation and partial charge creation in the linear transition state B or due to simultaneous formation of two bonds in the three-centre mechanism A. It was argued before[47] that such a $\Delta V^*$ value is not negative enough to suggest the simultaneous formation of two bonds between the rhodium centre and the $CH_3I$ moieties in a concerted three-centered mechanism. However, in the light of the substitution $\Delta V^*$ reported earlier,[45] a value of −17 $cm^3$ $mol^{-1}$ may be interpreted in terms of the formation of two bonds. It should also be kept in mind that at some stage during the process the formal oxidation state of rhodium changes from +1 to +3, which will be accompanied by a significant decrease in volume. This could also partly contribute toward the −17 $cm^3$ $mol^{-1}$ found in this study, which would then strengthen the argument in favour of a linear transition state.

To conclude, large variations in the nature of the solvent, in terms of parameters such as $\varepsilon_0$ and $q_p$, have a minor influence on oxidative addition reactions of most $Rh^I$(β-diketonate) complexes. So far only in the case of the cupferron complex could a meaningful effect be observed for highly polar solvents, which could indicate the participation of ion-pair intermediates. In all examples known, the inclusion of a sulphur donor atom in the bidentate chelate resulted in the formation of only the acyl complex. This trend could be related to a possible trans-labilisation effect of coordinated sulphur. Another property that can be used to determine the stereochemistry of the transition state is the configuration of optically active molecules like ethyl α-bromopropionate during oxidative addition.[54,55] It is however uncertain to what extent the oxidative addition of $CH_3I$ can be compared to the oxidative addition of such a bulky molecule. Since the radii of $CH_3$ and I are rather similar, the oxidative addition of $CH_3I$ can be rather compared with that of

[54] Pearson, R.G. and Muir, W.R., *J. Am. Chem. Soc*., **92**, 5519 (1970).

[55] Labinger, J.A. and Osborn, J.A., *Inorg. Chem*., **19**, 3230 (1980).

homonuclear molecules like $H_2$ and $I_2$, which are known to add in the *cis* configuration via a concerted three-centered transition state.

## 5.5 Migratory CO insertion of [Rh(cupf)(CO)($CH_3$)(I)($PX_3$)]

### 5.5.1 Experimental

[Rh(cupf)(CO)($CH_3$)(I)($PX_3$)] complexes, $PX_3$ = $PPh_3$, P(*p*-$ClC_6H_4$)$_3$, P(*p*-$MeOC_6H_4$)$_3$) and $PCy_3$ were prepared as described in Chapter 3. All IR measurements were done on a Hitachi model 270-50 spectrophotometer having a wavenumber accuracy of 2 $cm^{-1}$ in the region employed. Kinetic measurements were performed in a thermostated (0.1K) cell with 0.5 mm path length and NaCl optics. Visible spectrophotometry was performed on a Hitachi model 150-20 spectrophotometer within the same temperature control limits. Typical complex concentrations were 1.7 x $10^{-4}$ M for the visible and 0.02 M for the IR kinetic measurements. All kinetic data were fitted to the appropriate equation by using a non-linear least-squares program. All complexes gave a broad absorption maximum at *ca*. 392 nm in the 340-450 nm region. All kinetic measurements in the visible region were done at this maximum.

### 5.5.2 Results and discussion

The fact that the alkyl product of the oxidative addition reaction of $CH_3I$ with [Rh(cupf)(CO)($PPh_3$)] could be isolated, enabled the study of the subsequent CO insertion reaction without the complications associated with consecutive reactions. A further factor making things easier was that the alkyl product was formed as a result of an oxidative addition reaction which go to completion, without any signs of an equilibrium with reductive elimination as a backward reaction. When the crystalline Rh(III)-alkyl is dissolved in a suitable solvent, a CO insertion reaction proceeds spontaneously forming the Rh(III)-acyl as product.

With [Rh(cupf)(CO)($CH_3$)(I)($PPh_3$)] as starting complex, the reaction

$$[Rh(cupf)(CO)(CH_3)(I)(PPh_3)] + THF \underset{k_{-1}}{\overset{k_1}{\rightleftharpoons}} [Rh(cupf)(COCH_3)(I)(PPh_3)(THF)]$$

was studied at four temperatures (9, 15, 25 and 34°C) in an attempt to determine the equilibrium constant as well as the enthalpy and entropy. During the reaction the IR absorbance values of the Rh(III)-alkyl and Rh(III)-acyl peaks were monitored at appropriate time intervals till equilibrium was reached. The equilibrium constant, K, was calculated spectrophotometrically as $K = [acyl]_{Eq}/[alkyl]_{Eq}$ (concentrations at equilibrium). At the start of the reaction, $[alkyl]_0$ and its absorbance is known, and by measuring its absorbance at equilibrium, $[alkyl]_{Eq}$ could be calculated using Beer's law:[56] Absorbance = ϵ x c x $\ell$ (ϵ is the molar absorptivity, c the concentration and $\ell$ the path length of the radiation through the absorbing medium). Since the total rhodium concentration is known, equal to $[alkyl]_0$, $[acyl]_{Eq}$ could be calculated as the difference between $[alkyl]_0$ and $[alkyl]_{Eq}$ (The alkyl and acyl have the same molar mass). Utilising the relationships $K = k_1/k_{-1}$, as well as $k_{obs} = k_1 + k_{-1}$ [which leads to $k_1 = k_{obs}(K/(K + 1))$], values for $k_1$ and $k_{-1}$ could be calculated from the $k_{obs}$ values and K. The results are summarised in Table 5.12.

**Table 5.12** Rate and equilibrium constants for the reaction of [Rh(cupf)(CO)-$(CH_3)(I)(PPh_3)$] with THF, obtained from IR measurements.

| **T** (°C) | **K** | **$10^4k_1$** ($s^{-1}$) | **$10^5k_{-1}$** ($s^{-1}$) |
|---|---|---|---|
| 9.0 | 2.03 | 1.03 | 4.86 |
| 15.0 | 1.96 | 2.07 | 10.54 |
| 25.0 | 1.75 | 7.13 | 40.73 |
| 34.0 | 1.58 | 13.96 | 88.37 |

Noticeable is the phenomenon that higher temperatures favour the decarbonylation reaction ($k_{-1}$), causing a decrease in the equilibrium constant. Using the K values, ΔH° was calculated as −8.6(4) kJ $mol^{-1}$ and ΔS° as −24(1) $JK^{-1}$ $mol^{-1}$. The negative value of ΔS° could be interpreted as evidence in favour of a proposed product with a solvent molecule coordinated.

By varying the solvent (the proposed incoming ligand) the effect of the different electronic and steric properties of the solvents on the rate of insertion could be studied. The focus was first on the electronic properties by selecting a number of solvents with wide ranging dielectric constants and donocity values. The reactions were performed by dissolving [Rh(cupf)(CO)($CH_3$)(I)($PPh_3$)] in different solvents and monitoring the absorbance change with time using visible spectrophotometry. The results of Table 5.13 were obtained, showing an expected slow reaction for benzene, a weak coordinator, and a fast reaction for DMSO. However, the effect of both the polarity and the donocity is not dramatic at all. Cotton[57] studied the effect of the properties of phosphines as incoming ligands in the DMSO promoted reaction of [($\eta^5$-$C_5H_5$)$(CO)_2$Fe($CH_2$Cy)] and found no correlation with the electronic parameter of the phosphines.

**Table 5.13** Observed rate constants for the reaction of [Rh(cupf)(CO)($CH_3$)(I)($PPh_3$)] with solvents differing in electronic properties.

| **Solvent** | **Donocity[17]** | **Dielectric constant[17]** | **$10^4 k_{obs}$ ($s^{-1}$)** |
|---|---|---|---|
| Benzene | 0.1 | 2.3 | 9.96(1) |
| Nitromethane | 2.7 | 35.9 | 15.8(9) |
| Acetonitrile | 14.1 | 38.0 | 17.0(7) |
| Ethyl acetate | 17.1 | 6.0 | 12.5(2) |
| Acetone | 17.1 | 20.7 | 13.5(1) |
| THF | 20.0 | 7.6 | 11.2(2) |
| DMSO | 29.8 | 45.0 | 36.7(4) |

In order to evaluate the steric effect, the reaction of [Rh(cupf)(CO)($CH_3$)(I)($PPh_3$)] was performed with solvents of comparable electronic effects, but with differing sizes due to varying substituents. Two sets of such solvents were studied using visible spectrophotometry, THF and methyl substituted variants (A) as well as acetone and

**56** Skoog, D.A. and West, D.M., *Fundamentals of analytical chemistry*, 4th Ed, Holt-Saunders, Japan (1982).

**57** Cotton, J.D. and Markwell, R.D., *Inorg. Chim. Acta*, **128**, 31 (1987).

the structurally related methyl tertiary butyl ketone, MTBK (B). The results of Table 5.14 were obtained.

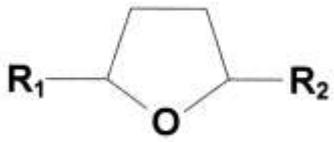


A

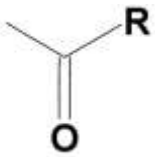


B

**Table 5.14** Observed rate constants for the reaction of [Rh(cupf)(CO)($CH_3$)(I)($PPh_3$)] with solvents of different steric properties.

| **Solvent** | **$10^4k_{obs}$** ($s^{-1}$) |
|---|---|
| THF (Structure **A**, $R_1$, $R_2$ = H) | 11.2(2) |
| 2-Me-THF (Structure **A**, $R_1$ = H, $R_2$ = $CH_3$) | 10.3(2) |
| 2,5-$Me_2$-THF (Structure **A**, $R_1$, $R_2$ = $CH_3$) | 9.12(1) |
| | |
| Acetone (Structure **B**, R = $CH_3$) | 13.5(1) |
| MTBK (Structure **B**, R = $C(CH_3)_3$) | 4.2(6) |

As expected, the more bulky solvents tend to slow down CO insertion. Because the electronic effect of the solvents within each set is about the same, the steric hindrance with regard to the direct coordination of the solvent to the metal during the transition state is the only explanation for the observed effect. A similar result was obtained by Wax and Bergman[58] in their study of the coordinating effect of the solvent in the CO insertion of [($\eta^5$-$C_5H_5$)$(CO)_3Mo(CH_3)$]. The steric blocking of the solvent leads to a delay in the formation of the solvent-bound intermediate. As can be seen from Table 5.14, the effect is very small for the THF set of solvents, probably because the range of sizes still fits in the available space around the metal centre. Evaluating the second set, acetone and MTBK, support comes from the study of Cotton[57] on the effect of incoming ligands with varying steric parameters. He found a well-defined decrease in rate with increasing cone angle of the entering phosphine ligands. The decrease is gradual for angles within a certain range, but much steeper at larger cone angles and no reaction with very large phosphines like $PCy_3$. He explained the tendency by the availability of space at the metal centre in which the entering ligand has to fit to be able to react during the formation of the transition

[58] Wax, M.J. and Bergman, R.G., *J. Am. Chem. Soc.*, **63**, 13 (1982).

state. If the entering ligand is smaller than the space, the steric interactions are minimal and the rate constants vary very little with varying size. However, when the size of the entering ligand is comparable with the available space, the intermolecular interactions increase drastically with increasing size so that the activation energy of the reaction increases accordingly. Very large ligands cannot come close enough to the metal to establish a bonding interaction with the metal centre. It seems that MTBK falls in a category much closer to the threshold for the particular metal centre.

The steric and electronic influence of the coordinated phosphine ligand in the [Rh(cupf)(CO)($CH_3$)(I)($PX_3$)] complexes was studied for $PX_3$ = P(*p*-$ClC_6H_4$)$_3$, $PPh_3$, P(*p*-$MeOC_6H_4$)$_3$) and $PCy_3$. The reaction was followed in THF as solvent (and entering ligand) at 25°C using IR spectrophotometry. The results of Table 5.15 were obtained.

$$[Rh(cupf)(CO)(CH_3)(I)(PX_3)] + THF \underset{k_{-1}}{\overset{k_1}{\rightleftharpoons}} [Rh(cupf)(COCH_3)(I)(PX_3)(THF)]$$

**Table 5.15** Rate constants for the reaction of [Rh(cupf)(CO)($CH_3$)(I)($PX_3$)] with THF showing the steric and electronic influence of the coordinated phosphine ligand. ($\theta$ = cone angle,[23] degrees; $\upsilon$ = Tolman electronic parameter[23], $cm^{-1}$)

| **$PX_3$** | $\theta$ | $\upsilon$ | **K** | **$10^4k_{obs}$** ($s^{-1}$) | **$10^4k_1$** ($s^{-1}$) | **$10^4k_{-1}$** ($s^{-1}$) |
|---|---|---|---|---|---|---|
| P(*p*-$ClC_6H_4$)$_3$ | 145 | 2072.8 | 2.44 | 7.32(6) | 5.19 | 2.13 |
| $PPh_3$ | 145 | 2068.9 | 1.75 | 11.2(2) | 7.13 | 4.07 |
| P(*p*-$MeOC_6H_4$)$_3$) | 145 | 2066.1 | 0.76 | 19.6(3) | 8.46 | 11.10 |
| $PCy_3$ | 170 | 2056.4 | 0.33 | 13.0(2) | 3.23 | 9.77 |

The first three entries of Table 5.15 have the same cone angle but an increasing donor ability from P(*p*-$ClC_6H_4$)$_3$ to P(*p*-$MeOC_6H_4$)$_3$). Rate constants increase in the same order. This observation is contradictory to the finding by Haynes[59], who studied the rhodium/iodide catalysed methanol carbonylation. According to him, electron-donating ligands, while promoting oxidative addition, normally retard CO insertion.

[59] Gonsalvi, L., Adams, H., Sunley, G.J., Ditzel, E. and Haynes, A., *J. Am. Chem. Soc*., **121**, 11233 (1999).

The reason given was that stronger rhodium-methyl bonds form and that higher electron density on the metal also leads to stronger M(d) → CO(π*) back-bonding which would inhibit CO insertion.[60] The trend in the present study can possibly be explained by a sovent-catalysed mechanism with the coordination of the solvent as the rate-determining step. Higher electron density on the metal centre could then facilitate faster solvent coordination, which would accelerate the overall process and account for the order of electronic effects found. Extrapolating the same trend the fastest rate would be expected for $PCy_3$, was it not for the large cone angle of 170°. The bulky $PCy_3$, thus blocks the way of entering THF molecules to a large extent and provide further proof to the postulate of coordinating solvent molecules.

The effect of competing solvents could gather more evidence confirming the model and was studied by dissolving [Rh(cupf)(CO)($CH_3$)(I)($PPh_3$)] in a range of DMSO/benzene mixtures and monitoring the reaction as CO insertion is taking place. The concentration of DMSO was varied from zero (reaction proceeds in pure benzene) to 14.1 mol $dm^{-3}$ (reaction proceeds in pure DMSO), with a number of intermediate combinations in between. Visible spectrophotometry was used at a temperature of 25°C. Plots of the pseudo-first-order constants, $k_{obs}$, for the CO insertion reactions against [DMSO] gave a linear relationship with a non-zero intercept, conforming to equation 5.12. The constants are interpreted in terms of the reaction scheme in Figure 5.9.

$$k_{obs} = k'_1 + k_3[L], \text{ with } L = DMSO \qquad \textbf{5.12}$$

The better coordinating DMSO acted as ligand while benzene fulfilled the role as solvent. The slope of the plot, $k_3$, was calculated as 1.89(2) x $10^{-4}$ $M^{-1}$ $s^{-1}$ with the intercept of 9.8(2) x $10^{-4}$ $s^{-1}$ close to the observed rate constant of 9.96(1) x $10^{-4}$ $s^{-1}$ for the reaction in pure benzene. The intercept value confirmed the intercept to be only the solvent contribution with no hint of a possible equilibrium for the $k_3$ path. The reaction scheme shows the proposed two competing reaction pathways with $k_3$ the direct or ligand route, favoured by strong nucleophiles, and $k_1$ the solvent assisted

[60] Margl, P., Ziegler, T. and Blöchl, P.E., *J. Am. Chem. Soc.*, **118**, 5412 (1996).

path. The intercept ($k'_1$), representing the solvent path is thus a combined $k_1$, $k_{-1}$ term ($k'_1 \approx k_{obs} = k_1 + k_{-1}$). Studying the reaction in neat benzene at 25°C using IR spectrophotometry, enabled the calculation of the equilibrium constant, K, as 1.54 and $k_1$ and $k_{-1}$ as 6.0 x $10^{-4}$ $s^{-1}$ and 3.9 x $10^{-4}$ $s^{-1}$ respectively. The $k_2$ step is believed to be very fast and was not determined.

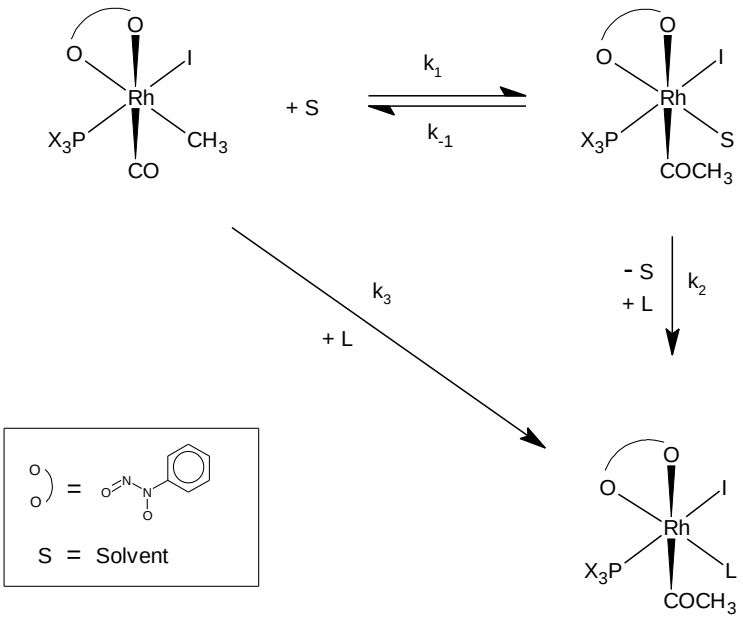


**Figure 5.9** Proposed reaction mechanism for the solvent assisted CO insertion of [Rh(cupf)(CO)($CH_3$)(I)($PX_3$)].

This type of mechanism as proposed in Figure 5.9 was also concluded by Cotton and Dunstan, [61] with the overall rate constant, $k_{obs}$, given by

$$k_{obs} = \frac{k_1 k_2 [L]}{k_{-1} + k_2 [L]} + k_3[L]$$

which, at high [L] or large $k_2$, reduces to $k_{obs} = k_1 + k_3[L]$.

The first-order relationship of DMSO, a solvent acting as ligand, confirms the proposal of coordinating solvents assisting the CO insertion, and the principle of a coordinated solvent which supports a reaction route. This competition of coordinating ability of solvents is further demonstrated when the same reaction was performed,

[61] Cotton, J.D. and Dunstan, R., *Inorg. Chim. Acta*, **88**, 223 (1984).

this time in a range of benzene/MTBK mixtures, where the concentration of benzene was varied from zero (reaction proceeds in pure MTBK) to 11.2 mol $dm^{-3}$ (reaction proceeds in pure benzene), with a number of intermediate combinations in between. The reaction was observed to be first-order in benzene, the better coordinating solvent of the two, following the direct or ligand path with MTBK following the solvent path.

From early days, the question of the style of solvent involvement in CO insertion has been widely debated.[58,62,63,64] Strengthening their case, Wax and Bergman[58], Cotton and Dunstan,[61] as well as Haynes[65] and co-workers provided definite evidence for direct solvent involvement. Haynes argued that migratory insertion in [Rh(dppmo)($I_2$)($CH_3$)(CO)] (dppmo = $Ph_2PCH_2POPh_2$) is promoted by coordination of acetonitrile to the five-coordinate acyl product, [Rh(dppmo)($I_2$)($COCH_3$)], to give isomers of the solvento species, [Rh(dppmo)($NCCH_3$)($I_2$)($COCH_3$)]. A crystal structure of this complex, with a molecule of acetonitrile coordinated to rhodium, supports his claims.

According to this discussion, regarding the cupferrate system, the conclusion can be made that solvents participate in a coordinative way, rather than just stabilising the migratory insertion transition state by solvation. Thus, both the oxidative addition of [Rh(cupf)(CO)($PX_3$)] and [Rh(neocupf)(CO)($PX_3$)] with iodomethane, as well as the subsequent carbonyl insertion reaction involves direct solvent interaction and can be regarded as solvent catalysed reactions.

[62] Cotton, J.D., Crisp, G.T. and Daly, V.A., *Inorg. Chim. Acta*, **47**, 165 (1981).

[63] Nicholas, K., Raghu, S. and Rosenblum, M., *J. Organomet. Chem.,* **78**, 133 (1974).

[64] Mawby, R.J., Basolo, F. and Pearson, R.G., *J. Am. Chem. Soc*., **86**, 3994 (1964).

[65] Gonsalvi, L., Adams, H., Sunley, G.J., Ditzel, E. and Haynes, A., *J. Am. Chem. Soc*., **124**, 13597 (2002).

# 6 Supplementary data

## Supplementary data for structure determinations

Supplementary data for the structures discussed in Chapter 4 are given in this chapter. For each of the structures (except for [Rh(cupf)(CO)($CH_3$)(I)($PPh_3$)] and *trans*-[Rh(cupf)(CO)($PPh_3$)$_2$]) five sets of data are given, containing tables with: (1) atomic coordinates and equivalent isotropic displacement parameters, (2) all bond distances, (3) all bond angles, (4) anisotropic thermal parameters and (5) hydrogen coordinates. For [Rh(cupf)(CO)($CH_3$)(I)($PPh_3$)] and *trans*-[Rh(cupf)(CO)($PPh_3$)$_2$], two of the older structures, no hydrogen coordinates were calculated.

## 6.1 [Rh(cupf)(CO)($CH_3$)(I)($PPh_3$)][1]

**Table 6.1** Atomic coordinates (x$10^4$) and equivalent isotropic displacement parameters (Å$^2$ x $10^3$) for [Rh(cupf)(CO)($CH_3$)(I)($PPh_3$)] with e.s.d.'s in parentheses. $U_{eq}$ is defined as one third of the trace of the orthogonalized $U_{ij}$ tensor, $U_{eq} = (⅓)\Sigma_i\Sigma_j[U_{ij}(a_i^* a_j^*)(a_i a_j)]$.

| Atom | x | y | z | $U_{eq}$ |
|---|---|---|---|---|
| Rh | 2395(1) | 1922(1) | 3385.2(9) | 37(1) |
| I | 1517(1) | 3082(1) | 4947(1) | 78(1) |
| N(1) | 3306(13) | 4256(12) | 1965(11) | 51(8) |
| N(2) | 4344(12) | 3427(11) | 2697(10) | 40(7) |
| O(1) | -322(12) | 1282(12) | 3632(11) | 70(8) |
| O(2) | 4288(10) | 2268(9) | 3432(9) | 44(6) |
| O(3) | 2244(12) | 3822(10) | 2042(10) | 57(7) |
| P | 3131(4) | 1049(3) | 1958(3) | 31(2) |
| C(1) | 700(15) | 1591(15) | 3481(14) | 48(9) |
| C(2) | 3000(18) | 103(15) | 4703(13) | 52(10) |
| C(11) | 4845(14) | 1260(13) | 1467(11) | 37(8) |
| C(12) | 5099(16) | 2025(15) | 350(12) | 47(9) |
| C(13) | 6448(18) | 2188(17) | 41(15) | 58(11) |
| C(14) | 7527(16) | 1533(16) | 882(16) | 57(11) |

[1] Basson, S.S., Leipoldt, J.G., Roodt, A. and Venter, J.A., *Inorg. Chim. Acta*, **128**, 31 (1987).

| | | | | |
|---|---|---|---|---|
| C(15) | 7303(17) | 743(16) | 1962(16) | 59(11) |
| C(16) | 5938(15) | 592(14) | 2288(13) | 45(9) |
| C(21) | 3204(13) | -635(12) | 2376(10) | 32(7) |
| C(22) | 4478(18) | -1610(14) | 2568(13) | 50(9) |
| C(23) | 4430(19) | -2937(17) | 3000(16) | 64(12) |
| C(24) | 3148(24) | -3242(16) | 3197(14) | 66(12) |
| C(25) | 1913(20) | -2264(19) | 2972(16) | 68(12) |
| C(26) | 1915(17) | -943(15) | 2551(14) | 55(10) |
| C(31) | 1959(15) | 1879(13) | 695(13) | 43(8) |
| C(32) | 807(15) | 2924(12) | 640(12) | 37(8) |
| C(33) | -62(15) | 3539(14) | -340(13) | 46(9) |
| C(34) | 229(18) | 3095(15) | -1249(14) | 54(10) |
| C(35) | 1385(17) | 2010(15) | -1155(14) | 54(10) |
| C(36) | 2237(17) | 1399(16) | -189(13) | 54(10) |
| C(41) | 5594(15) | 3821(12) | 2704(12) | 37(8) |
| C(42) | 6090(16) | 4493(14) | 1674(14) | 48(9) |
| C(43) | 7324(18) | 4865(16) | 1711(17) | 61(11) |
| C(44) | 7970(18) | 4547(16) | 2764(15) | 57(11) |
| C(45) | 7405(17) | 3853(15) | 3779(14) | 52(10) |
| C(46) | 6191(15) | 3480(14) | 3770(13) | 45(9) |

**Table 6.2** Bond lengths (Å) for [Rh(cupf)(CO)($CH_3$)(I)($PPh_3$)] with estimated standard deviations in parentheses.

| Bond | Length (Å) | Bond | Length (Å) |
|---|---|---|---|
| Rh–I | 2.708(2) | C(46)–C(41) | 1.38(3) |
| Rh–O(3) | 2.175(9) | C(11)–C(12) | 1.39(3) |
| Rh–O(2) | 2.04(1) | C(12)–C(13) | 1.40(3) |
| Rh–C(2) | 2.08(1) | C(13)–C(14) | 1.41(3) |
| Rh–C(1) | 1.81(2) | C(14)–C(15) | 1.36(3) |
| Rh–P | 2.327(4) | C(15)–C(16) | 1.42(2) |
| C(1)–O(1) | 1.14(2) | C(16)–C(11) | 1.40(3) |
| O(3)–N(1) | 1.27(2) | C(21)–C(22) | 1.40(2) |
| O(2)–N(2) | 1.32(1) | C(22)–C(23) | 1.43(3) |
| N(1)–N(2) | 1.33(2) | C(23)–C(24) | 1.39(3) |
| N(2)–C(41) | 1.44(2) | C(24)–C(25) | 1.37(3) |
| P–C(11) | 1.80(1) | C(25)–C(26) | 1.41(3) |
| P–C(21) | 1.79(1) | C(26)–C(21) | 1.40(2) |
| P–C(31) | 1.83(1) | C(31)–C(32) | 1.38(2) |
| C(41)–C(42) | 1.36(2) | C(32)–C(33) | 1.39(3) |
| C(42)–C(43) | 1.42(3) | C(33)–C(34) | 1.39(3) |
| C(43)–C(44) | 1.39(3) | C(34)–C(35) | 1.41(2) |
| C(44)–C(45) | 1.39(3) | C(35)–C(36) | 1.37(3) |
| C(45)–C(46) | 1.39(3) | C(36)–C(31) | 1.39(3) |

**Table 6.3** Bond angles (°) for [Rh(cupf)(CO)($CH_3$)(I)($PPh_3$)] with estimated standard deviations in parentheses.

| Bond | Angle (°) | Bond | Angle (°) |
|---|---|---|---|
| O(2)–Rh–O(3) | 74.9(4) | C(41)–C(42)–C(43) | 117(2) |
| O(3)–Rh–C(1) | 108.1(5) | C(42)–C(43)–C(44) | 120(2) |
| C(1)–Rh–C(2) | 84.6(7) | C(43)–C(44)–C(45) | 120(2) |
| C(2)–Rh–O(2) | 92.4(6) | C(44)–C(45)–C(46) | 121(2) |
| O(2)–Rh–P | 92.6(3) | C(45)–C(46)–C(41) | 117(1) |
| O(3)–Rh–P | 87.0(4) | C(46)–C(41)–C(42) | 125(1) |
| C(1)–Rh–P | 91.8(6) | C(11)–C(12)–C(13) | 120(1) |
| C(2)–Rh–P | 92.5(5) | C(12)–C(13)–C(14) | 118(2) |
| O(2)–Rh–I | 86.7(3) | C(13)–C(14)–C(15) | 122(2) |
| O(3)–Rh–I | 89.5(4) | C(14)–C(15)–C(16) | 120(2) |
| C(1)–Rh–I | 89.1(6) | C(15)–C(16)–C(11) | 118(1) |
| C(2)–Rh–I | 90.8(5) | C(16)–C(11)–C(12) | 121(1) |
| I–Rh–P | 176.6(1) | C(21)–C(22)–C(23) | 118(2) |
| C(2)–Rh–O(3) | 167.3(6) | C(22)–C(23)–C(24) | 121(2) |
| O(2)–Rh–C(1) | 174.8(6) | C(23)–C(24)–C(25) | 120(2) |
| Rh–C(1)–O(1) | 174(1) | C(24)–C(25)–C(26) | 121(2) |
| Rh–O(3)–N(1) | 115.3(8) | C(25)–C(26)–C(21) | 119(2) |
| Rh–O(2)–N(2) | 112.8(7) | C(26)–C(21)–C(22) | 121(1) |
| O(2)–N(2)–N(1) | 124(1) | C(31)–C(32)–C(33) | 120(1) |
| O(3)–N(1)–N(2) | 113(1) | C(32)–C(33)–C(34) | 120(1) |
| O(2)–N(2)–C(41) | 118(1) | C(33)–C(34)–C(35) | 119(2) |
| N(1)–N(2)–C(41) | 118(1) | C(34)–C(35)–C(36) | 121(2) |
| Rh–P–C(11) | 109.2(6) | C(35)–C(36)–C(31) | 119(1) |
| Rh–P–C(21) | 115.2(4) | C(36)–C(31)–C(32) | 121(1) |
| Rh–P–C(31) | 112.1(5) | | |

**Table 6.4** Anisotropic displacement parameters ($Å^2$ x $10^3$) for [Rh(cupf)(CO)($CH_3$)-(I)($PPh_3$)] with estimated standard deviations in parentheses. The anisotropic displacement factor exponent takes the form: $-2\pi^2(h^2a^{*2}U_{11} + k^2b^{*2}U_{22} + l^2c^{*2}U_{33} + 2klb^*c^*U_{23} + 2hla^*c^*U_{13} + 2\,h\,k\,a^*\,b^*\,U_{12}$.

| Atom | $U_{11}$ | $U_{22}$ | $U_{33}$ | $U_{23}$ | $U_{13}$ | $U_{12}$ |
|---|---|---|---|---|---|---|
| Rh | 35(1) | 43(1) | 40(1) | -16(1) | -2(1) | -12(1) |
| I | 65(1) | 107(1) | 84(1) | -68(1) | 15(1) | -27(1) |
| N(1) | 48(8) | 52(8) | 60(8) | -23(7) | -6(7) | -16(7) |
| N(2) | 47(7) | 34(7) | 47(7) | -13(6) | -8(6) | -16(6) |
| O(1) | 40(7) | 88(9) | 92(9) | -38(8) | 8(6) | -24(6) |
| O(2) | 38(5) | 37(6) | 61(6) | -12(5) | 4(5) | -17(4) |
| O(3) | 65(7) | 37(6) | 77(8) | -16(6) | -21(6) | -9(5) |
| P | 32(2) | 28(2) | 33(2) | -3(2) | -6(1) | -10(1) |
| C(1) | 29(8) | 57(10) | 66(10) | -35(8) | 2(7) | -5(7) |
| C(2) | 73(11) | 47(9) | 37(8) | 1(7) | 2(8) | -20(8) |
| C(11) | 44(8) | 35(7) | 35(8) | -12(6) | 3(6) | -11(6) |
| C(12) | 60(10) | 53(9) | 35(8) | -12(7) | 4(7) | -30(8) |
| C(13) | 57(10) | 66(11) | 62(11) | -19(9) | -5(8) | -33(9) |
| C(14) | 45(9) | 56(10) | 81(12) | -32(9) | 20(9) | -27(8) |
| C(15) | 59(10) | 52(10) | 78(12) | -34(9) | 11(9) | -26(8) |
| C(16) | 38(8) | 43(8) | 57(10) | -20(7) | 8(7) | -10(7) |
| C(21) | 36(7) | 36(7) | 27(7) | -7(6) | -8(6) | -12(6) |
| C(22) | 67(11) | 38(9) | 47(9) | -12(7) | -15(8) | 3(8) |
| C(23) | 66(12) | 52(10) | 80(13) | -29(10) | 10(10) | -10(9) |
| C(24) | 121(17) | 42(10) | 50(10) | -29(8) | 17(10) | -28(11) |
| C(25) | 76(13) | 80(13) | 71(12) | -45(10) | 24(10) | -50(11) |
| C(26) | 60(10) | 57(10) | 63(10) | -30(8) | 5(8) | -37(8) |
| C(31) | 45(8) | 34(8) | 58(9) | -17(7) | -1(7) | -19(7) |
| C(32) | 47(8) | 20(7) | 43(8) | -4(6) | -9(7) | -1(6) |
| C(33) | 45(9) | 36(8) | 57(9) | -3(7) | -17(7) | -7(7) |
| C(34) | 72(11) | 41(9) | 59(10) | -9(8) | -27(8) | -25(8) |
| C(35) | 57(10) | 51(10) | 62(10) | -20(8) | -12(8) | -18(8) |
| C(36) | 60(10) | 62(10) | 48(9) | -29(8) | -20(8) | -5(8) |
| C(41) | 46(8) | 22(7) | 49(9) | -10(6) | -12(7) | -10(6) |
| C(42) | 48(9) | 39(8) | 58(10) | -11(8) | 3(8) | -10(7) |
| C(43) | 59(11) | 46(9) | 86(13) | -22(9) | 22(10) | -26(8) |
| C(44) | 64(11) | 52(10) | 66(11) | -16(9) | -9(9) | -30(8) |
| C(45) | 58(10) | 50(9) | 52(10) | -7(8) | -11(8) | -16(8) |
| C(46) | 44(9) | 43(8) | 52(9) | -11(7) | -8(7) | -15(7) |

## 6.2 [Rh(cupf)(CO)($PPh_3$)$_2$][2]

**Table 6.5** Atomic coordinates (x$10^4$) and equivalent isotropic displacement parameters (Å$^2$ x $10^3$) for [Rh(cupf)(CO)($PPh_3$)$_2$] with estimated standard deviations in parentheses. $U_{eq}$ is defined as one third of the trace of the orthogonalized $U_{ij}$ tensor, $U_{eq} = (⅓)\Sigma_i\Sigma_j[U_{ij}(a_i^* a_j^*)(a_i a_j)]$.

| Atom | x | y | z | $U_{eq}$ |
|---|---|---|---|---|
| Rh | 977(1) | 2097(1) | 2624(1) | 34(1) |
| N(1) | 1774(9) | 3744(9) | 4682(8) | 51(4) |
| N(2) | 1310(9) | 2687(9) | 4869(7) | 42(4) |
| O(1) | 699(10) | 1720(11) | 402(8) | 84(5) |
| O(2) | 868(7) | 1764(7) | 4158(6) | 43(3) |
| O(3) | 1805(8) | 3835(7) | 3743(7) | 53(3) |
| P(1) | -1001(3) | 2068(3) | 2215(2) | 39(1) |
| P(2) | 2932(3) | 2033(3) | 3074(2) | 38(1) |
| C(1) | 788(11) | 1830(13) | 1278(11) | 58(6) |
| C(11) | -1431(10) | 2357(11) | 3344(9) | 44(4) |
| C(12) | -1378(12) | 3449(11) | 3656(10) | 55(5) |
| C(13) | -1675(14) | 3621(12) | 4563(11) | 70(6) |
| C(14) | -2091(14) | 2704(14) | 5105(11) | 75(7) |
| C(15) | -2091(13) | 1651(13) | 4836(11) | 66(6) |
| C(16) | -1797(11) | 1448(12) | 3938(10) | 57(5) |
| C(21) | -2315(11) | 754(10) | 1530(9) | 46(5) |
| C(22) | -3502(11) | 490(12) | 1601(12) | 63(6) |
| C(23) | -4482(13) | -561(14) | 1085(12) | 71(6) |
| C(24) | -4292(14) | -1344(14) | 509(12) | 74(7) |
| C(25) | -3117(13) | -1067(14) | 395(12) | 74(7) |
| C(26) | -2118(13) | -26(12) | 921(11) | 61(6) |
| C(31) | -1151(11) | 3195(10) | 1419(8) | 46(5) |
| C(32) | -2167(12) | 2946(13) | 504(9) | 62(6) |
| C(33) | -2271(16) | 3859(16) | -61(11) | 80(8) |
| C(34) | -1372(16) | 4982(15) | 301(12) | 80(7) |
| C(35) | -347(15) | 5207(13) | 1173(13) | 80(7) |
| C(36) | -226(12) | 4326(11) | 1758(12) | 62(6) |
| C(41) | 1214(10) | 249(1) | 5886(8) | 43(4) |
| C(42) | 650(13) | 1373(12) | 6065(10) | 61(6) |
| C(43) | 528(14) | 1149(12) | 7047(10) | 66(6) |
| C(44) | 985(13) | 2052(13) | 7843(10) | 65(6) |
| C(45) | 1584(14) | 3195(13) | 7657(10) | 70(6) |
| C(46) | 1690(12) | 3430(12) | 6657(10) | 61(6) |
| C(51) | 3828(10) | 2505(10) | 4453(8) | 43(4) |

[2] Basson, S.S., Leipoldt, J.G., and Venter, J.A., *Acta Cryst*., **C46**, 1324 (1990).

| | | | | |
|---|---|---|---|---|
| C(52) | 4903(12) | 3532(11) | 4806(10) | 58(5) |
| C(53) | 5493(13) | 3844(13) | 5881(11) | 64(6) |
| C(54) | 5034(13) | 3159(14) | 6598(10) | 63(6) |
| C(55) | 3961(14) | 2138(13) | 6233(10) | 63(6) |
| C(56) | 3348(10) | 1796(10) | 5168(9) | 46(4) |
| C(61) | 2951(10) | 627(10) | 2813(9) | 43(4) |
| C(62) | 2072(12) | -149(11) | 1989(10) | 54(5) |
| C(63) | 2061(14) | -1240(12) | 1740(13) | 69(6) |
| C(64) | 2995(15) | -1519(12) | 2382(12) | 70(6) |
| C(65) | 3911(14) | -719(14) | 3263(11) | 74(7 |
| C(66) | 3929(12) | 371(12) | 3484(11) | 64(6) |
| C(71) | 3940(11) | 2955(11) | 2408(9) | 43(4) |
| C(72) | 3625(11) | 3787(11) | 1884(9) | 50(5) |
| C(73) | 4388(14) | 4529(13) | 1350(11) | 68(6) |
| C(74) | 5474(13) | 4385(15) | 1323(11) | 71(7) |
| C(75) | 5782(13) | 3576(14) | 1837(12) | 68(6) |
| C(76) | 5035(12) | 2830(12) | 2378(10) | 59(6) |

**Table 6.6** Bond lengths (Å) for [Rh(cupf)(CO)($PPh_3$)$_2$] with estimated standard deviations in parentheses.

| Bond | Length (Å) | Bond | Length (Å) |
|---|---|---|---|
| Rh-C(1) | 1.77(1) | C(22)-C(23) | 1.40(4) |
| Rh-O(2) | 2.147(8) | C(23)-C(24) | 1.38(3) |
| Rh-O(3) | 2.339(9) | C(24)-C(25) | 1.40(3) |
| Rh-P(1) | 2.323(4) | C(25)-C(26) | 1.41(4) |
| Rh-P(2) | 2.342(4) | C(26)-C(21) | 1.41(3) |
| C(1)-O(1) | 1.16(2) | C(31)-C(32) | 1.41(4) |
| N(2)-O(2) | 1.33(1) | C(32)-C(33) | 1.42(3) |
| N(2)-C(41) | 1.43(2) | C(33)-C(34) | 1.39(4) |
| N(1)-N(2) | 1.30(1) | C(34)-C(35) | 1.39(4) |
| N(1)-O(3) | 1.28(1) | C(35)-C(36) | 1.41(3) |
| P(1)-C(11) | 1.82(1) | C(36)-C(31) | 1.41(4) |
| P(1)-C(21) | 1.81(1) | C(51)-C(52) | 1.40(4) |
| P(1)-C(31) | 1.83(1) | C(52)-C(53) | 1.40(3) |
| P(2)-C(51) | 1.83(1) | C(53)-C(54) | 1.40(3) |
| P(2)-C(61) | 1.82(1) | C(54)-C(55) | 1.40(4) |
| P(2)-C(71) | 1.80(1) | C(55)-C(56) | 1.39(3) |
| C(41)-C(42) | 1.37(4) | C(56)-C(51) | 1.42(3) |
| C(42)-C(43) | 1.40(2) | C(61)-C(62) | 1.36(4) |
| C(43)-C(44) | 1.38(3) | C(62)-C(63) | 1.41(2) |
| C(44)-C(45) | 1.41(3) | C(63)-C(64) | 1.40(3) |
| C(45)-C(46) | 1.42(2) | C(64)-C(65) | 1.43(4) |
| C(46)-C(41) | 1.39(3) | C(65)-C(66) | 1.40(3) |
| C(11)-C(12) | 1.41(2) | C(66)-C(61) | 1.44(3) |
| C(12)-C(13) | 1.41(3) | C(71)-C(72) | 1.39(3) |
| C(13)-C(14) | 1.38(3) | C(72)-C(73) | 1.41(3) |
| C(14)-C(15) | 1.38(3) | C(73)-C(74) | 1.43(3) |
| C(15)-C(16) | 1.41(3) | C(74)-C(75) | 1.36(3) |
| C(16)-C(11) | 1.41(3) | C(75)-C(76) | 1.41(3) |
| C(21)-C(22) | 1.40(2) | C(76)-C(71) | 1.43(2) |

**Table 6.7** Bond angles (°) for [Rh(cupf)(CO)($PPh_3$)$_2$] with estimated standard deviations in parentheses.

| Bond | Angle (°) | Bond | Angle (°) |
|---|---|---|---|
| Rh–C(1)–O(1) | 176(1) | C(15)–C(16)–C(11) | 119(1) |
| Rh–O(2)–N(2) | 116.3(6) | C(16)–C(11)–C(12) | 120(1) |
| Rh–O(3)–N(1) | 116.0(7) | C(21)–C(22)–C(23) | 120(1) |
| O(2)–N(2)–N(1) | 124(1) | C(22)–C(23)–C(24) | 121(1) |
| N(2)–N(1)–O(3) | 114(1) | C(23)–C(24)–C(25) | 120(2) |
| O(2)–N(2)–C(41) | 117.4(9) | C(24)–C(25)–C(26) | 120(2) |
| N(1)–N(2)–C(41) | 119(1) | C(25)–C(26)–C(21) | 120(1) |
| C(1)–Rh–O(2) | 159.6(5) | C(26)–C(21)–C(22) | 120(1) |
| C(1)–Rh–O(3) | 130.8(5) | C(31)–C(32)–C(33) | 119(1) |
| O(2)–Rh–O(3) | 69.6(3) | C(32)–C(33)–C(34) | 119(2) |
| P(1)–Rh–P(2) | 176.9(1) | C(33)–C(34)–C(35) | 121(2) |
| Rh–P(1)–C(11) | 114.2(4) | C(34)–C(35)–C(36) | 121(2) |
| Rh–P(1)–C(21) | 118.7(5) | C(35)–C(36)–C(31) | 118(1) |
| Rh–P(1)–C(31) | 111.7(4) | C(36)–C(31)–C(32) | 121(1) |
| Rh–P(2)–C(51) | 114.2(5) | C(51)–C(52)–C(53) | 118(1) |
| Rh–P(2)–C(61) | 116.3(4) | C(52)–C(53)–C(54) | 122(1) |
| Rh–P(2)–C(71) | 113.5(5) | C(53)–C(54)–C(55) | 119(1) |
| P(1)–Rh–O(2) | 87.7(3) | C(54)–C(55)–C(56) | 121(1) |
| P(1)–Rh–O(3) | 91.0(3) | C(55)–C(56)–C(51) | 119(1) |
| P(1)–Rh–C(1) | 90.4(5) | C(56)–C(51)–C(52) | 121(1) |
| P(2)–Rh–O(2) | 90.2(3) | C(61)–C(62)–C(63) | 123(1) |
| P(2)–Rh–O(3) | 90.4(3) | C(62)–C(63)–C(64) | 118(1) |
| P(2)–Rh–C(1) | 90.8(5) | C(63)–C(64)–C(65) | 120(1) |
| C(41)–C(42)–C(43) | 120(1) | C(64)–C(65)–C(66) | 121(1) |
| C(42)–C(43)–C(44) | 120(1) | C(65)–C(66)–C(61) | 117(1) |
| C(43)–C(44)–C(45) | 120(1) | C(66)–C(61)–C(62) | 121(1) |
| C(44)–C(45)–C(46) | 121(1) | C(71)–C(72)–C(73) | 121(1) |
| C(45)–C(46)–C(47) | 117(1) | C(72)–C(73)–C(74) | 119(2) |
| C(46)–C(41)–C(42) | 122(1) | C(73)–C(74)–C(75) | 120(2) |
| C(11)–C(12)–C(13) | 120(1) | C(74)–C(75)–C(76) | 122(1) |
| C(12)–C(13)–C(14) | 120(1) | C(75)–C(76)–C(71) | 119(1) |
| C(13)–C(14)–C(15) | 121(1) | C(76)–C(71)–C(72) | 119(1) |
| C(14)–C(15)–C(16) | 121(1) | | |

**Table 6.8** Anisotropic displacement parameters ($Å^2 \times 10^3$) for $[Rh(cupf)(CO)(PPh_3)_2]$ with estimated standard deviations in parentheses. The anisotropic displacement factor exponent takes the form: $-2\pi^2(h^2a^{*2}U_{11} + k^2b^{*2}U_{22} + l^2c^{*2}U_{33} + 2klb^*c^*U_{23} + 2hla^*c^*U_{13} + 2\,h\,k\,a^*\,b^*\,U_{12}$.

| Atom | $U_{11}$ | $U_{22}$ | $U_{33}$ | $U_{23}$ | $U_{13}$ | $U_{12}$ |
|---|---|---|---|---|---|---|
| Rh | 30(1) | 46(1) | 34(1) | 4(1) | 11(1) | 19(1) |
| N(1) | 53(7) | 54(7) | 56(7) | 3(6) | 18(5) | 25(6) |
| N(2) | 43(6) | 47(6) | 43(6) | 1(5) | 14(5) | 20(5) |
| O(1) | 82(8) | 131(10) | 46(6) | 4(6) | 26(5) | 40(7) |
| O(2) | 49(5) | 48(5) | 39(5) | -6(4) | 9(4) | 21(4) |
| O(3) | 59(6) | 53(6) | 54(6) | 7(4) | 18(5) | 19(5) |
| P(1) | 32(2) | 48(2) | 42(2) | 3(2) | 10(1) | 19(1) |
| P(2) | 37(2) | 44(2) | 42(2) | 4(1) | 13(1) | 21(2) |
| C(1) | 51(8) | 90(11) | 57(9) | 7(8) | 30(7) | 40(8) |
| C(11) | 30(6) | 64(8) | 49(7) | 4(6) | 6(5) | 26(6) |
| C(12) | 70(9) | 50(8) | 65(9) | 2(7) | 34(7) | 33(7) |
| C(13) | 94(11) | 64(9) | 64(9) | 7(7) | 36(8) | 43(9) |
| C(14) | 87(11) | 88(11) | 65(9) | 18(8) | 36(8) | 53(10) |
| C(15) | 62(9) | 83(11) | 63(9) | 17(8) | 33(7) | 33(8) |
| C(16) | 56(8) | 69(9) | 60(8) | 10(7) | 33(7) | 29(7) |
| C(21) | 40(7) | 49(7) | 47(7) | 5(6) | 10(5) | 18(6) |
| C(22) | 41(7) | 74(10) | 83(10) | 8(8) | 25(7) | 24(7) |
| C(23) | 45(8) | 88(12) | 79(11) | -12(9) | 1(7) | 17(8) |
| C(24) | 68(10) | 80(11) | 72(10) | -3(9) | 13(8) | 14(9) |
| C(25) | 56(9) | 72(11) | 94(12) | -17(9) | 15(9) | 16(8) |
| C(26) | 65(9) | 54(9) | 62(9) | -17(7) | 8(7) | 20(7) |
| C(31) | 48(7) | 55(7) | 39(6) | 11(6) | 16(5) | 36(6) |
| C(32) | 70(9) | 93(11) | 38(7) | 21(7) | 24(6) | 56(8) |
| C(33) | 94(12) | 117(15) | 57(9) | 21(10) | 35(9) | 75(12) |
| C(34) | 94(12) | 103(13) | 72(10) | 44(10) | 47(9) | 71(11) |
| C(35) | 97(12) | 75(11) | 99(12) | 29(9) | 55(10) | 54(10) |
| C(36) | 48(8) | 56(9) | 99(11) | 10(8) | 41(8) | 20(7) |
| C(41) | 41(6) | 47(7) | 39(6) | -6(5) | 18(5) | 13(6) |
| C(42) | 73(9) | 62(9) | 51(8) | 10(7) | 24(7) | 32(8) |
| C(43) | 88(11) | 67(9) | 42(7) | 4(7) | 29(7) | 26(8) |
| C(44) | 69(9) | 92(11) | 45(8) | 14(8) | 30(8) | 33(8) |
| C(45) | 96(11) | 71(10) | 44(8) | 4(7) | 30(8) | 25(9) |
| C(46) | 62(9) | 73(10) | 52(8) | -13(7) | 15(7) | 26(8) |
| C(51) | 44(7) | 50(7) | 41(6) | -2(5) | 13(5) | 27(6) |
| C(52) | 58(8) | 62(9) | 58(8) | -15(7) | -6(7) | 36(7) |
| C(53) | 57(9) | 73(10) | 60(9) | -13(8) | -3(7) | 29(8) |
| C(54) | 67(9) | 83(11) | 42(7) | -5(7) | 3(7) | 45(9) |
| C(55) | 81(10) | 81(11) | 47(8) | 6(7) | 12(7) | 51(9) |
| C(56) | 35(6) | 54(8) | 57(8) | 7(6) | 16(6) | 25(6) |
| C(61) | 46(7) | 44(7) | 47(7) | 1(6) | 20(6) | 21(6) |
| C(62) | 63(8) | 55(8) | 50(8) | -10(6) | 20(7) | 15(7) |
| C(63) | 79(10) | 47(8) | 99(12) | 24(8) | 51(9) | 35(8) |

| | | | | | | |
|---|---|---|---|---|---|---|
| C(64) | 88(11) | 61(9) | 71(10) | 9(8) | 42(9) | 37(9) |
| C(65) | 95(12) | 85(11) | 62(9) | 17(8) | 33(9) | 64(10) |
| C(66) | 69(9) | 68(9) | 80(10) | 18(8) | 31(8) | 52(8) |
| C(71) | 40(6) | 48(7) | 41(6) | 4(5) | 9(5) | 19(5) |
| C(72) | 51(7) | 52(8) | 47(7) | 10(6) | 13(6) | 21(6) |
| C(73) | 70(10) | 76(10) | 64(9) | 15(8) | 31(8) | 23(8) |
| C(74) | 63(10) | 98(13) | 58(9) | 12(9) | 22(8) | 19(9) |
| C(75) | 48(8) | 92(12) | 73(10) | 15(9) | 29(8) | 27(8) |
| C(76) | 46(7) | 81(10) | 55(8) | 4(7) | 21(6) | 32(7) |

## 6.3 [Rh(neocupf)(CO)($PPh_3$)]·$CH_3COCH_3$

**Table 6.9** Atomic coordinates (x$10^4$) and equivalent isotropic displacement parameters (Å$^2$ x $10^3$) for [Rh(neocupf)(CO)($PPh_3$)]·$CH_3COCH_3$ with estimated standard deviations in parentheses. $U_{eq}$ is defined as one third of the trace of the orthogonalized $U_{ij}$ tensor, $U_{eq} = (⅓)\Sigma_i\Sigma_j[U_{ij}(a_i^* a_j^*)(a_i a_j)]$.

| Atom | x | y | z | $U_{eq}$ |
|---|---|---|---|---|
| Rh | 7716(1) | 8618(1) | 6195(1) | 38(1) |
| P | 7482(1) | 7536(1) | 7563(1) | 38(1) |
| O(2) | 6759(3) | 7447(3) | 5728(2) | 48(1) |
| C(1) | 8683(5) | 9607(5) | 6562(3) | 53(1) |
| C(11) | 8285(4) | 7848(4) | 8483(2) | 40(1) |
| C(12) | 9355(5) | 6809(5) | 9000(3) | 51(1) |
| O(1) | 9341(5) | 10187(5) | 6798(3) | 84(1) |
| N(2) | 6778(4) | 7738(3) | 4859(2) | 42(1) |
| C(31) | 5602(4) | 7863(4) | 7912(2) | 42(1) |
| O(3) | 7749(4) | 9343(3) | 4848(2) | 54(1) |
| C(41) | 6207(4) | 6927(4) | 4422(2) | 41(1) |
| N(1) | 7279(4) | 8673(4) | 4389(2) | 52(1) |
| C(21) | 8284(4) | 5644(4) | 7609(2) | 42(1) |
| C(36) | 4520(4) | 8549(5) | 7288(3) | 48(1) |
| C(26) | 7669(5) | 4663(4) | 8032(3) | 52(1) |
| C(410) | 6933(4) | 5458(4) | 4531(2) | 41(1) |
| C(24) | 9663(6) | 2805(5) | 7605(3) | 64(1) |
| C(46) | 7025(6) | 3212(6) | 4206(3) | 65(1) |
| C(49) | 8214(4) | 4729(4) | 5021(3) | 47(1) |
| C(25) | 8368(6) | 3232(5) | 8022(4) | 67(1) |
| C(35) | 3074(5) | 8825(6) | 7528(3) | 61(1) |
| C(42) | 4974(5) | 7609(5) | 3945(3) | 55(1) |
| C(32) | 5209(5) | 7483(5) | 8772(3) | 59(1) |
| C(22) | 9600(5) | 5194(5) | 7171(3) | 56(1) |
| C(15) | 8306(6) | 9472(5) | 9388(3) | 63(1) |
| C(13) | 9896(5) | 7093(6) | 9705(3) | 62(1) |
| C(16) | 7775(5) | 9195(5) | 8684(3) | 53(1) |
| C(47) | 8264(6) | 2539(5) | 4676(3) | 64(1) |
| C(44) | 5026(5) | 5404(6) | 3635(3) | 65(1) |
| C(45) | 6322(5) | 4687(5) | 4114(3) | 50(1) |
| C(23) | 10292(6) | 3771(5) | 7178(3) | 68(1) |
| C(33) | 3749(6) | 7772(6) | 9002(3) | 66(1) |
| C(14) | 9382(5) | 8412(6) | 9904(3) | 59(1) |

| | | | | |
|---|---|---|---|---|
| C(43) | 4388(5) | 6823(6) | 3541(3) | 67(1) |
| C(48) | 8845(5) | 3309(5) | 5085(3) | 59(1) |
| C(34) | 2702(5) | 8425(6) | 8387(4) | 67(1) |
| O(4) | 4549(5) | 7415(7) | 1101(4) | 114(2) |
| C(3) | 5787(6) | 7154(8) | 1298(4) | 78(2) |
| C(2) | 6293(8) | 8247(9) | 1512(6) | 118(3) |
| C(4) | 6814(9) | 5733(9) | 1392(6) | 128(3) |

**Table 6.10** Bond lengths (Å) for $[Rh(neocupf)(CO)(PPh_3)]\cdot CH_3COCH_3$ with estimated standard deviations in parentheses.

| Bond | Length (Å) | Bond | Length (Å) |
|---|---|---|---|
| Rh-C(1) | 1.802(5) | C(26)-C(25) | 1.401(6) |
| Rh-O(2) | 2.025(3) | C(410)-C(49) | 1.415(5) |
| Rh-O(3) | 2.081(3) | C(410)-C(45) | 1.418(5) |
| Rh-P | 2.2271(11) | C(24)-C(25) | 1.360(8) |
| P-C(21) | 1.822(4) | C(24)-C(23) | 1.372(8) |
| P-C(31) | 1.823(4) | C(46)-C(47) | 1.362(8) |
| P-C(11) | 1.827(4) | C(46)-C(45) | 1.419(7) |
| O(2)-N(2) | 1.329(4) | C(49)-C(48) | 1.364(6) |
| C(1)-O(1) | 1.139(5) | C(35)-C(34) | 1.378(7) |
| C(11)-C(12) | 1.381(5) | C(42)-C(43) | 1.403(7) |
| C(11)-C(16) | 1.399(5) | C(32)-C(33) | 1.397(7) |
| C(12)-C(13) | 1.383(6) | C(22)-C(23) | 1.388(6) |
| N(2)-N(1) | 1.292(5) | C(15)-C(16) | 1.373(6) |
| N(2)-C(41) | 1.447(5) | C(15)-C(14) | 1.392(7) |
| C(31)-C(32) | 1.383(6) | C(13)-C(14) | 1.372(7) |
| C(31)-C(36) | 1.394(5) | C(47)-C(48) | 1.391(7) |
| O(3)-N(1) | 1.295(5) | C(44)-C(43) | 1.359(8) |
| C(41)-C(42) | 1.364(5) | C(44)-C(45) | 1.417(7) |
| C(41)-C(410) | 1.414(5) | C(33)-C(34) | 1.359(8) |
| C(21)-C(26) | 1.374(6) | O(4)-C(3) | 1.204(7) |
| C(21)-C(22) | 1.395(6) | C(3)-C(4) | 1.452(10) |
| C(36)-C(35) | 1.389(6) | C(3)-C(2) | 1.477(10) |

**Table 6.11** Bond angles (°) for [Rh(neocupf)(CO)($PPh_3$)]·$CH_3COCH_3$ with estimated standard deviations in parentheses.

| Bond | Angle (°) | Bond | Angle (°) |
|---|---|---|---|
| C(1)-Rh-O(2) | 175.8(2) | C(22)-C(21)-P | 116.5(3) |
| C(1)-Rh-O(3) | 100.5(2) | C(35)-C(36)-C(31) | 120.3(4) |
| O(2)-Rh-O(3) | 77.23(11) | C(21)-C(26)-C(25) | 119.8(5) |
| C(1)-Rh-P | 91.21(14) | C(49)-C(410)-C(41) | 124.2(3) |
| O(2)-Rh-P | 90.95(8) | C(49)-C(410)-C(45) | 118.9(4) |
| O(3)-Rh-P | 168.16(9) | C(41)-C(410)-C(45) | 116.9(4) |
| C(21)-P-C(31) | 106.9(2) | C(25)-C(24)-C(23) | 120.5(4) |
| C(21)-P-C(11) | 104.3(2) | C(47)-C(46)-C(45) | 121.4(4) |
| C(31)-P-C(11) | 102.2(2) | C(48)-C(49)-C(410) | 120.1(4) |
| C(21)-P-Rh | 107.56(13) | C(24)-C(25)-C(26) | 120.4(5) |
| C(31)-P-Rh | 113.11(13) | C(34)-C(35)-C(36) | 120.1(5) |
| C(11)-P-Rh | 121.61(13) | C(41)-C(42)-C(43) | 118.8(4) |
| N(2)-O(2)-Rh | 109.7(2) | C(31)-C(32)-C(33) | 120.0(5) |
| O(1)-C(1)-Rh | 177.3(5) | C(23)-C(22)-C(21) | 120.4(5) |
| C(12)-C(11)-C(16) | 118.4(4) | C(16)-C(15)-C(14) | 120.1(4) |
| C(12)-C(11)-P | 123.1(3) | C(14)-C(13)-C(12) | 120.6(4) |
| C(16)-C(11)-P | 118.5(3) | C(15)-C(16)-C(11) | 120.8(4) |
| C(11)-C(12)-C(13) | 120.7(4) | C(46)-C(47)-C(48) | 119.5(5) |
| N(1)-N(2)-O(2) | 124.6(3) | C(43)-C(44)-C(45) | 121.1(4) |
| N(1)-N(2)-C(41) | 118.7(3) | C(44)-C(45)-C(46) | 122.2(4) |
| O(2)-N(2)-C(41) | 116.6(3) | C(44)-C(45)-C(410) | 119.3(4) |
| C(32)-C(31)-C(36) | 118.8(4) | C(46)-C(45)-C(410) | 118.5(4) |
| C(32)-C(31)-P | 122.6(3) | C(24)-C(23)-C(22) | 119.7(5) |
| C(36)-C(31)-P | 118.6(3) | C(34)-C(33)-C(32) | 120.7(5) |
| N(1)-O(3)-Rh | 114.7(2) | C(13)-C(14)-C(15) | 119.4(4) |
| C(42)-C(41)-C(410) | 123.3(4) | C(44)-C(43)-C(42) | 120.6(4) |
| C(42)-C(41)-N(2) | 118.4(4) | C(49)-C(48)-C(47) | 121.7(5) |
| C(410)-C(41)-N(2) | 118.3(3) | C(33)-C(34)-C(35) | 120.0(4) |
| N(2)-N(1)-O(3) | 113.4(3) | O(4)-C(3)-C(4) | 121.3(8) |
| C(26)-C(21)-C(22) | 119.2(4) | O(4)-C(3)-C(2) | 121.1(7) |
| C(26)-C(21)-P | 124.3(3) | C(4)-C(3)-C(2) | 117.5(6) |

**Table 6.12** Anisotropic displacement parameters ($Å^2$ x $10^3$) for [Rh(neocupf)(CO)-($PPh_3$)]·$CH_3COCH_3$ with estimated standard deviations in parentheses. The anisotropic displacement factor exponent takes the form: $-2\pi^2(h^2a^{*2}U_{11} + k^2b^{*2}U_{22} + l^2c^{*2}U_{33} + 2klb^*c^*U_{23} + 2hla^*c^*U_{13} + 2\,h\,k\,a^*\,b^*\,U_{12}$.

| Atom | $U_{11}$ | $U_{22}$ | $U_{33}$ | $U_{23}$ | $U_{13}$ | $U_{12}$ |
|---|---|---|---|---|---|---|
| Rh | 39(1) | 33(1) | 41(1) | -9(1) | -6(1) | -9(1) |
| P | 39(1) | 35(1) | 41(1) | -9(1) | -7(1) | -10(1) |
| O(2) | 64(2) | 50(2) | 39(1) | -11(1) | -4(1) | -28(1) |
| C(1) | 60(3) | 48(2) | 54(2) | -9(2) | -4(2) | -20(2) |
| C(11) | 43(2) | 42(2) | 38(2) | -10(1) | -7(1) | -13(2) |
| C(12) | 49(2) | 44(2) | 57(2) | -8(2) | -16(2) | -11(2) |
| O(1) | 97(3) | 90(3) | 93(3) | -22(2) | -14(2) | -61(3) |
| N(2) | 46(2) | 39(2) | 42(2) | -7(1) | -6(1) | -13(1) |
| C(31) | 41(2) | 42(2) | 44(2) | -12(2) | -3(2) | -14(2) |
| O(3) | 69(2) | 50(2) | 49(2) | -4(1) | -6(1) | -28(2) |
| C(41) | 41(2) | 50(2) | 36(2) | -12(2) | -3(1) | -17(2) |
| N(1) | 58(2) | 47(2) | 49(2) | -8(2) | -7(2) | -16(2) |
| C(21) | 49(2) | 34(2) | 43(2) | -7(1) | -13(2) | -12(2) |
| C(36) | 42(2) | 55(2) | 50(2) | -14(2) | -5(2) | -16(2) |
| C(26) | 57(2) | 44(2) | 58(2) | -5(2) | -17(2) | -18(2) |
| C(410) | 37(2) | 45(2) | 42(2) | -13(2) | 0(1) | -14(2) |
| C(24) | 82(3) | 38(2) | 68(3) | -17(2) | -30(3) | -4(2) |
| C(46) | 83(4) | 66(3) | 65(3) | -32(2) | 12(3) | -42(3) |
| C(49) | 39(2) | 47(2) | 57(2) | -14(2) | -4(2) | -15(2) |
| C(25) | 78(3) | 43(2) | 83(3) | -1(2) | -31(3) | -24(2) |
| C(35) | 40(2) | 70(3) | 71(3) | -19(2) | -5(2) | -12(2) |
| C(42) | 48(2) | 60(3) | 49(2) | -9(2) | -11(2) | -7(2) |
| C(32) | 60(3) | 67(3) | 52(2) | -12(2) | -3(2) | -24(2) |
| C(22) | 62(3) | 44(2) | 57(2) | -13(2) | 0(2) | -7(2) |
| C(15) | 71(3) | 60(3) | 64(3) | -24(2) | -10(2) | -22(2) |
| C(13) | 64(3) | 67(3) | 57(3) | -1(2) | -25(2) | -24(2) |
| C(16) | 58(2) | 43(2) | 57(2) | -16(2) | -14(2) | -8(2) |
| C(47) | 68(3) | 49(3) | 76(3) | -23(2) | 12(3) | -18(2) |
| C(44) | 64(3) | 91(4) | 58(3) | -31(3) | -9(2) | -38(3) |
| C(45) | 52(2) | 61(3) | 48(2) | -21(2) | 3(2) | -26(2) |
| C(23) | 77(3) | 53(3) | 61(3) | -18(2) | -10(2) | 1(2) |
| C(33) | 71(3) | 78(3) | 56(3) | -21(2) | 20(2) | -32(3) |
| C(14) | 69(3) | 71(3) | 50(2) | -15(2) | -10(2) | -34(2) |
| C(43) | 53(3) | 94(4) | 57(3) | -19(3) | -20(2) | -20(3) |
| C(48) | 49(2) | 48(2) | 75(3) | -15(2) | 5(2) | -11(2) |
| C(34) | 48(2) | 78(3) | 78(3) | -26(3) | 11(2) | -21(2) |
| O(4) | 71(3) | 148(5) | 114(4) | -22(3) | -23(3) | -24(3) |
| C(3) | 61(3) | 99(5) | 65(3) | -15(3) | 5(3) | -17(3) |
| C(2) | 79(5) | 104(6) | 162(8) | -23(6) | 18(5) | -26(4) |
| C(4) | 102(6) | 112(7) | 174(9) | -64(6) | -6(6) | -18(5) |

**Table 6.13** Hydrogen coordinates ( x $10^4$) and isotropic displacement parameters (Å$^2$ x $10^3$) with estimated standard deviations in parentheses for [Rh(neocupf)(CO)($PPh_3$)]·$CH_3COCH_3$.

| Atom | x | y | z | $U_{eq}$ |
|---|---|---|---|---|
| H(12) | 9716(5) | 5910(5) | 8873(3) | 83(3) |
| H(36) | 4766(4) | 8824(5) | 6708(3) | 83(3) |
| H(26) | 6790(5) | 4948(4) | 8325(3) | 83(3) |
| H(24) | 10125(6) | 1851(5) | 7609(3) | 83(3) |
| H(46) | 6632(6) | 2693(6) | 3939(3) | 83(3) |
| H(49) | 8627(4) | 5219(4) | 5300(3) | 83(3) |
| H(25) | 7945(6) | 2569(5) | 8301(4) | 83(3) |
| H(35) | 2356(5) | 9279(6) | 7109(3) | 83(3) |
| H(42) | 4529(5) | 8577(5) | 3890(3) | 83(3) |
| H(32) | 5917(5) | 7034(5) | 9198(3) | 83(3) |
| H(22) | 10015(5) | 5853(5) | 6873(3) | 83(3) |
| H(15) | 7945(6) | 10368(5) | 9520(3) | 83(3) |
| H(13) | 10616(5) | 6382(6) | 10048(3) | 83(3) |
| H(16) | 7069(5) | 9912(5) | 8335(3) | 83(3) |
| H(47) | 8718(6) | 1573(5) | 4724(3) | 83(3) |
| H(44) | 4604(5) | 4895(6) | 3380(3) | 83(3) |
| H(23) | 11178(6) | 3473(5) | 6894(3) | 83(3) |
| H(33) | 3491(6) | 7514(6) | 9582(3) | 83(3) |
| H(14) | 9749(5) | 8598(6) | 10378(3) | 83(3) |
| H(43) | 3557(5) | 7277(6) | 3206(3) | 83(3) |
| H(48) | 9686(5) | 2843(5) | 5411(3) | 83(3) |
| H(34) | 1734(5) | 8602(6) | 8546(4) | 83(3) |
| H(2A) | 7329(9) | 7906(16) | 1545(23) | 83(3) |
| H(2B) | 5891(31) | 8463(28) | 2065(12) | 83(3) |
| H(2C) | 5987(32) | 9083(15) | 1065(13) | 83(3) |
| H(4A) | 7301(28) | 5479(16) | 1942(12) | 83(3) |
| H(4B) | 7510(24) | 5694(13) | 924(14) | 83(3) |
| H(4C) | 6309(10) | 5086(10) | 1372(24) | 83(3) |

## 6.4 [Rh(neocupf)(CO)($CH_3$)(I)($PPh_3$)]·$C_5H_{12}$

**Table 6.14** Atomic coordinates (x$10^4$) and equivalent isotropic displacement parameters (Å$^2$ x $10^3$) for [Rh(neocupf)(CO)($CH_3$)(I)($PPh_3$)]·$C_5H_{12}$ with estimated standard deviations in parentheses. $U_{eq}$ is defined as one third of the trace of the orthogonalized $U_{ij}$ tensor, $U_{eq} = (⅓)\Sigma_i\Sigma_j[U_{ij}(a_i^* a_j^*)(a_i a_j)]$.

| Atom | x | y | z | $U_{eq}$ |
|---|---|---|---|---|
| Rh | 3782(1) | 1806(1) | 1231(1) | 46(1) |
| I | 5360(1) | 4341(1) | 3446(1) | 79(1) |
| P | 2321(2) | -360(2) | -681(2) | 46(1) |
| O(1) | 3496(10) | 4095(13) | 583(10) | 140(4) |
| O(2) | 4155(5) | 371(7) | 1875(5) | 55(1) |
| O(3) | 2334(6) | 246(9) | 1333(6) | 73(2) |
| N(1) | 2423(7) | -667(11) | 1788(7) | 74(2) |
| N(2) | 3343(6) | -589(9) | 2050(6) | 53(2) |
| C(1) | 3539(11) | 3217(12) | 805(10) | 88(3) |
| C(2) | 5293(11) | 3125(17) | 1220(11) | 119(5) |
| C(11) | 2837(7) | 191(11) | -1503(7) | 54(2) |
| C(12) | 3207(9) | -534(14) | -1809(8) | 71(2) |
| C(13) | 3658(11) | 23(18) | -2386(10) | 96(3) |
| C(14) | 3700(11) | 1226(18) | -2671(10) | 94(3) |
| C(15) | 3323(10) | 1956(13) | -2381(10) | 84(3) |
| C(16) | 2917(10) | 1444(13) | -1762(9) | 73(2) |
| C(21) | 1921(7) | -2385(9) | -786(7) | 50(2) |
| C(22) | 666(8) | -3955(11) | -1365(8) | 66(2) |
| C(23) | 403(9) | -5461(11) | -1421(10) | 85(3) |
| C(24) | 1332(10) | -5520(12) | -954(10) | 84(3) |
| C(25) | 2607(10) | -3928(13) | -359(9) | 80(3) |
| C(26) | 2892(8) | -2407(11) | -282(7) | 59(2) |
| C(31) | 804(6) | -912(10) | -1564(7) | 53(2) |
| C(32) | -17(9) | -1859(15) | -2739(9) | 90(3) |
| C(33) | -1171(9) | -2240(17) | -3408(12) | 116(5) |
| C(34) | 1489(10) | -1685(16) | -2906(13) | 100(4) |
| C(35) | -693(10) | -782(15) | -1757(12) | 89(3) |
| C(36) | 476(8) | -358(12) | -1042(10) | 70(2) |
| C(41) | 3435(7) | -1708(11) | 2456(7) | 56(2) |
| C(42) | 2376(9) | -3457(12) | 1820(10) | 75(3) |
| C(43) | 2413(10) | -4642(14) | 2158(11) | 87(3) |
| C(44) | 3531(11) | -3978(15) | 3159(12) | 90(3) |
| C(45) | 4666(9) | -2141(13) | 3893(8) | 65(2) |
| C(46) | 5827(10) | -1447(16) | 4939(9) | 72(3) |
| C(47) | 6859(11) | 206(17) | 5588(9) | 81(3) |
| C(48) | 6838(10) | 1416(15) | 5277(9) | 80(3) |
| C(49) | 5747(8) | 874(12) | 4272(7) | 62(2) |

| | | | | |
|---|---|---|---|---|
| C(410) | 4624(8) | -958(12) | 3529(7) | 59(2) |
| C(111) | 9169(42) | 6196(76) | 4111(51) | 431(59) |
| C(112) | 9149(25) | 7465(61) | 4051(27) | 218(18) |
| C(113) | 9640(38) | 8004(52) | 3728(30) | 188(12) |
| C(114) | 9847(71) | 7458(126) | 4408(26) | 338(36) |
| C(115) | 9625(42) | 6158(65) | 4159(43) | 199(20) |

**Table 6.15** Bond lengths (Å) for $[Rh(neocupf)(CO)(CH_3)(I)(PPh_3)]\cdot C_5H_{12}$ with estimated standard deviations in parentheses.

| Bond | Length (Å) | Bond | Length (Å) |
|---|---|---|---|
| Rh-C(1) | 1.827(10) | C(31)-C(32) | 1.357(13) |
| Rh-O(2) | 2.074(5) | C(31)-C(36) | 1.397(12) |
| Rh-C(2) | 2.092(14) | C(32)-C(33) | 1.405(13) |
| Rh-O(3) | 2.128(6) | C(33)-C(34) | 1.36(2) |
| Rh-P | 2.307(2) | C(34)-C(35) | 1.33(2) |
| Rh-I | 2.7111(14) | C(35)-C(36) | 1.405(12) |
| P-C(21) | 1.807(7) | C(41)-C(42) | 1.353(12) |
| P-C(11) | 1.818(8) | C(41)-C(410) | 1.425(11) |
| P-C(31) | 1.819(6) | C(43)-C(44) | 1.35(2) |
| O(1)-C(1) | 1.036(11) | C(43)-C(42) | 1.409(13) |
| O(3)-N(1) | 1.265(9) | C(44)-C(45) | 1.426(14) |
| O(2)-N(2) | 1.344(8) | C(45)-C(46) | 1.404(12) |
| N(1)-N(2) | 1.308(9) | C(45)-C(410) | 1.428(11) |
| N(2)-C(41) | 1.422(9) | C(410)-C(49) | 1.420(12) |
| C(11)-C(16) | 1.364(12) | C(46)-C(47) | 1.287(14) |
| C(11)-C(12) | 1.374(11) | C(47)-C(48) | 1.408(14) |
| C(12)-C(13) | 1.397(14) | C(48)-C(49) | 1.376(12) |
| C(13)-C(14) | 1.35(2) | C(111)-C(115) | 0.74(10) |
| C(14)-C(15) | 1.38(2) | C(111)-C(113) | 1.90(10) |
| C(15)-C(16) | 1.405(14) | C(111)-C(112) | 1.36(11) |
| C(21)-C(22) | 1.395(10) | C(111)-C(114) | 0.98(13) |
| C(21)-C(26) | 1.400(9) | C(112)-C(114) | 1.00(7) |
| C(22)-C(23) | 1.369(12) | C(112)-C(115) | 1.90(7) |
| C(23)-C(24) | 1.369(13) | C(113)-C(114) | 1.23(8) |
| C(24)-C(25) | 1.415(14) | C(115)-C(114) | 1.16(9) |
| C(25)-C(26) | 1.367(11) | | |

**Table 6.16** Bond angles (°) for $[Rh(neocupf)(CO)(CH_3)(I)(PPh_3)]\cdot C_5H_{12}$ with estimated standard deviations in parentheses.

| Bond | Angle (°) | Bond | Angle (°) |
|---|---|---|---|
| C(1)-Rh-O(2) | 174.6(4) | C(23)-C(24)-C(25) | 117.2(8) |
| C(1)-Rh-C(2) | 86.2(6) | C(26)-C(25)-C(24) | 121.3(8) |
| O(2)-Rh-C(2) | 94.5(4) | C(25)-C(26)-C(21) | 120.5(8) |
| C(1)-Rh-O(3) | 102.9(4) | C(32)-C(31)-C(36) | 119.4(7) |
| O(2)-Rh-O(3) | 76.3(2) | C(32)-C(31)-P | 120.1(6) |
| C(2)-Rh-O(3) | 170.8(4) | C(36)-C(31)-P | 120.5(6) |
| C(1)-Rh-P | 91.7(3) | C(31)-C(32)-C(33) | 119.3(11) |
| O(2)-Rh-P | 93.7(2) | C(34)-C(33)-C(32) | 121.6(12) |
| C(2)-Rh-P | 92.1(3) | C(35)-C(34)-C(33) | 118.8(9) |
| O(3)-Rh-P | 88.0(2) | C(34)-C(35)-C(36) | 122.2(10) |
| C(1)-Rh-I | 85.9(3) | C(31)-C(36)-C(35) | 118.6(10) |
| O(2)-Rh-I | 88.7(2) | C(42)-C(41)-N(2) | 118.7(7) |
| C(2)-Rh-I | 91.2(3) | C(42)-C(41)-C(410) | 121.8(8) |
| O(3)-Rh-I | 89.1(2) | N(2)-C(41)-C(410) | 119.4(7) |
| P-Rh-I | 175.75(5) | C(44)-C(43)-C(42) | 118.1(9) |
| C(21)-P-C(11) | 107.3(4) | C(41)-C(42)-C(43) | 121.5(9) |
| C(21)-P-C(31) | 106.5(3) | C(43)-C(44)-C(45) | 123.1(9) |
| C(11)-P-C(31) | 101.7(4) | C(46)-C(45)-C(44) | 123.2(8) |
| C(21)-P-Rh | 111.0(3) | C(46)-C(45)-C(410) | 118.6(9) |
| C(11)-P-Rh | 115.2(3) | C(44)-C(45)-C(410) | 118.2(8) |
| C(31)-P-Rh | 114.3(3) | C(49)-C(410)-C(41) | 124.7(7) |
| N(1)-O(3)-Rh | 115.3(5) | C(49)-C(410)-C(45) | 118.1(8) |
| N(2)-O(2)-Rh | 108.9(3) | C(41)-C(410)-C(45) | 117.1(8) |
| N(1)-N(2)-O(2) | 124.7(6) | C(47)-C(46)-C(45) | 123.2(9) |
| N(1)-N(2)-C(41) | 118.4(7) | C(46)-C(47)-C(48) | 119.7(9) |
| O(2)-N(2)-C(41) | 116.6(5) | C(49)-C(48)-C(47) | 121.7(10) |
| O(3)-N(1)-N(2) | 114.4(8) | C(48)-C(49)-C(410) | 118.6(8) |
| O(1)-C(1)-Rh | 173.7(13) | C(115)-C(111)-C(114) | 84(7) |
| C(16)-C(11)-C(12) | 119.8(8) | C(114)-C(111)-C(112) | 47(7) |
| C(16)-C(11)-P | 117.6(6) | C(115)-C(111)-C(113) | 95(10) |
| C(12)-C(11)-P | 122.5(6) | C(114)-C(112)-C(113) | 72(5) |
| C(11)-C(12)-C(13) | 119.3(9) | C(114)-C(112)-C(111) | 46(7) |
| C(14)-C(13)-C(12) | 120.7(9) | C(113)-C(112)-C(111) | 101(4) |
| C(13)-C(14)-C(15) | 120.9(9) | C(113)-C(112)-C(115) | 85(3) |
| C(14)-C(15)-C(16) | 118.3(9) | C(111)-C(115)-C(116) | 57(8) |
| C(11)-C(16)-C(15) | 121.0(9) | C(111)-C(114)-C(112) | 86(10) |
| C(22)-C(21)-C(26) | 118.1(7) | C(112)-C(114)-C(115) | 122(10) |
| C(22)-C(21)-P | 122.3(5) | C(111)-C(114)-C(113) | 118(7) |
| C(26)-C(21)-P | 119.6(6) | C(112)-C(114)-C(113) | 57(5) |
| C(23)-C(22)-C(21) | 120.6(7) | C(115)-C(114)-C(113) | 122(5) |
| C(22)-C(23)-C(24) | 122.3(8) | | |

**Table 6.17** Anisotropic displacement parameters ($Å^2$ x $10^3$) for [Rh(neocupf)(CO)($CH_3$)-(I)($PPh_3$)]·$C_5H_{12}$ with estimated standard deviations in parentheses. The anisotropic displacement factor exponent takes the form: $-2\pi^2(h^2a^{*2}U_{11} + k^2b^{*2}U_{22} + l^2c^{*2}U_{33} + 2klb^*c^*U_{23} + 2hla^*c^*U_{13} + 2\,h\,k\,a^*\,b^*\,U_{12}$.

| Atom | $U_{11}$ | $U_{22}$ | $U_{33}$ | $U_{23}$ | $U_{13}$ | $U_{12}$ |
|---|---|---|---|---|---|---|
| Rh | 48(1) | 56(1) | 50(1) | 31(1) | 35(1) | 39(1) |
| I | 92(1) | 76(1) | 56(1) | 27(1) | 42(1) | 59(1) |
| P | 48(1) | 59(1) | 50(1) | 32(1) | 37(1) | 40(1) |
| O(1) | 151(8) | 130(7) | 147(9) | 79(7) | 80(7) | 115(7) |
| O(2) | 59(3) | 71(3) | 63(3) | 43(3) | 45(3) | 50(3) |
| O(3) | 80(4) | 105(4) | 76(4) | 54(4) | 61(4) | 71(4) |
| N(1) | 83(5) | 92(5) | 62(5) | 46(4) | 44(4) | 69(4) |
| N(2) | 54(3) | 80(4) | 55(4) | 43(3) | 40(3) | 54(3) |
| C(1) | 116(8) | 64(5) | 80(7) | 49(5) | 62(6) | 61(6) |
| C(2) | 89(8) | 120(9) | 64(7) | 8(7) | 28(6) | 63(7) |
| C(11) | 59(4) | 73(5) | 51(4) | 38(4) | 43(4) | 48(4) |
| C(12) | 81(6) | 115(7) | 82(6) | 65(6) | 70(5) | 79(6) |
| C(13) | 111(8) | 147(10) | 97(8) | 66(8) | 86(7) | 100(8) |
| C(14) | 104(8) | 149(10) | 100(8) | 92(8) | 93(7) | 89(8) |
| C(15) | 90(7) | 75(6) | 93(8) | 51(6) | 66(6) | 53(5) |
| C(16) | 99(7) | 93(6) | 90(7) | 61(6) | 81(6) | 72(6) |
| C(21) | 49(4) | 56(4) | 57(4) | 28(3) | 39(4) | 38(3) |
| C(22) | 60(4) | 69(5) | 76(6) | 36(5) | 48(5) | 44(4) |
| C(23) | 70(5) | 54(4) | 108(8) | 36(5) | 57(6) | 35(4) |
| C(24) | 93(7) | 64(5) | 108(8) | 47(6) | 69(7) | 57(5) |
| C(25) | 98(7) | 89(6) | 87(7) | 49(6) | 61(6) | 77(6) |
| C(26) | 56(4) | 69(4) | 65(5) | 37(4) | 42(4) | 45(4) |
| C(31) | 41(3) | 68(4) | 57(5) | 33(4) | 34(3) | 39(3) |
| C(32) | 66(5) | 120(8) | 61(6) | 31(6) | 35(5) | 62(6) |
| C(33) | 49(5) | 132(10) | 87(8) | 48(8) | 14(6) | 56(6) |
| C(34) | 65(6) | 117(9) | 133(12) | 79(9) | 60(8) | 70(7) |
| C(35) | 80(6) | 110(8) | 133(11) | 72(8) | 79(8) | 80(6) |
| C(36) | 67(5) | 87(6) | 100(7) | 57(6) | 63(5) | 62(5) |
| C(41) | 57(4) | 69(4) | 69(5) | 43(4) | 48(4) | 47(4) |
| C(42) | 69(5) | 81(6) | 99(7) | 59(6) | 59(5) | 55(5) |
| C(43) | 83(6) | 79(6) | 121(9) | 62(7) | 78(7) | 54(5) |
| C(44) | 109(8) | 102(7) | 136(10) | 90(8) | 99(8) | 86(7) |
| C(45) | 92(6) | 97(6) | 86(6) | 70(5) | 77(6) | 79(6) |
| C(46) | 82(6) | 126(8) | 77(6) | 80(6) | 63(6) | 87(6) |
| C(47) | 94(7) | 140(9) | 69(6) | 69(7) | 65(6) | 93(8) |
| C(48) | 77(6) | 108(7) | 64(6) | 45(6) | 45(5) | 67(6) |
| C(49) | 67(5) | 78(5) | 60(5) | 38(4) | 47(4) | 52(4) |
| C(410) | 72(5) | 95(6) | 72(5) | 57(5) | 62(5) | 69(5) |

| | | | | | | |
|---|---|---|---|---|---|---|
| C(111) | 121(26) | 269(47) | 177(37) | -126(37) | 84(26) | -123(27) |
| C(112) | 91(13) | 382(45) | 103(17) | 54(24) | 39(13) | 161(23) |
| C(113) | 216(25) | 337(37) | 184(28) | 168(27) | 161(25) | 230(29) |
| C(114) | 355(74) | 558(111) | 72(16) | 91(37) | 121(31) | 327(85) |
| C(115) | 177(32) | 177(37) | 207(35) | 38(28) | 146(29) | 98(33) |

**Table 6.18** Hydrogen coordinates ( x $10^4$) and isotropic displacement parameters (Å$^2$ x $10^3$) with estimated standard deviations in parentheses for [Rh(neocupf)(CO)($CH_3$)(I)($PPh_3$)]·$C_5H_{12}$.

| Atom | x | y | z | $U_{eq}$ |
|---|---|---|---|---|
| H(2A) | 5151(31) | 2284(18) | 702(40) | 97(7) |
| H(2B) | 6092(13) | 3754(65) | 1990(15) | 97(7) |
| H(2C) | 5330(37) | 3942(57) | 965(49) | 97(7) |
| H(12) | 3157(9) | -1388(14) | -1634(8) | 97(7) |
| H(13) | 3932(11) | -440(18) | -2576(10) | 97(7) |
| H(14) | 3987(11) | 1565(18) | -3068(10) | 97(7) |
| H(15) | 3337(10) | 2769(13) | -2590(10) | 97(7) |
| H(16) | 2699(10) | 1967(13) | -1525(9) | 97(7) |
| H(22) | 3(8) | -3978(11) | -1716(8) | 97(7) |
| H(23) | -437(9) | -6479(11) | -1790(10) | 97(7) |
| H(24) | 1133(10) | -6564(12) | -1024(10) | 97(7) |
| H(25) | 3265(10) | -3918(13) | -15(9) | 97(7) |
| H(26) | 3737(8) | -1378(11) | 108(7) | 97(7) |
| H(32) | 183(9) | -2253(15) | -3098(9) | 97(7) |
| H(33) | -1731(9) | -2888(17) | -4213(12) | 97(7) |
| H(34) | -2251(10) | -1933(16) | -3360(13) | 97(7) |
| H(35) | -915(10) | -418(15) | -1413(12) | 97(7) |
| H(36) | 1020(8) | 278(12) | -237(10) | 97(7) |
| H(43) | 1687(10) | -5846(14) | 1704(11) | 97(7) |
| H(42) | 1606(9) | -3887(12) | 1145(10) | 97(7) |
| H(44) | 3564(11) | -4756(15) | 3381(12) | 97(7) |
| H(46) | 5852(10) | -2220(16) | 5174(9) | 97(7) |
| H(47) | 7615(11) | 601(17) | 6260(9) | 97(7) |
| H(48) | 7580(10) | 2613(15) | 5764(9) | 97(7) |
| H(49) | 5745(8) | 1690(12) | 4083(7) | 97(7) |

## 6.5 [Rh(cupf)(CO){P(OCH$_2$)$_3$CCH$_3$}][3]

**Table 6.19** Atomic coordinates (x10$^4$) and equivalent isotropic displacement parameters (Å$^2$ x 10$^3$) for [Rh(cupf)(CO){P(OCH$_2$)$_3$CCH$_3$}] with estimated standard deviations in parentheses. $U_{eq}$ is defined as one third of the trace of the orthogonalized $U_{ij}$ tensor, $U_{eq} = (⅓)\Sigma_i\Sigma_j[U_{ij}(a_i^* a_j^*)(a_i a_j)]$.

| Atom | x | y | z | $U_{eq}$ |
|---|---|---|---|---|
| Rh | 2910.0(1) | 4480.3(1) | 5924.0(2) | 53.9(1) |
| P | 4282(2) | 6640(3) | 6153.6(8 | 49.9(4) |
| O(2) | 1727(4) | 2084(8) | 5808(2) | 66(1) |
| O(3) | 2945(4) | 3075(8) | 6800(2) | 65(1) |
| N(2) | 1673(4) | 1012(9) | 6355(3) | 54(1) |
| N(1) | 2242(5) | 1448(10) | 6863(3) | 65(1) |
| C(1) | 2765(8) | 5722(16) | 5161(4) | 93(3) |
| O(1) | 2596(7) | 6617(13) | 4681(3) | 134(2) |
| O(4) | 4661(5) | 8264(9) | 5627(2) | 81(1) |
| O(5) | 4145(4) | 8157(9) | 6756(2) | 75(1) |
| O(6) | 5404(4) | 5425(7) | 6354(3) | 70(1) |
| C(2) | 5632(7) | 9603(13) | 5799(3) | 78(2) |
| C(3) | 5098(6) | 9561(12) | 6926(3) | 66(2) |
| C(4) | 6364(6) | 6759(11) | 6546(4) | 67(2) |
| C(5) | 6026(6) | 9161(9) | 6488(3) | 51(1) |
| C(6) | 7048(7) | 10545(12) | 6686(4) | 72(2) |
| C(11) | 925(6) | -823(11) | 6354(3) | 58(2) |
| C(12) | 159(8) | -1024(16) | 5855(4) | 96(3) |
| C(13) | -538(9) | -2832(19) | 5835(5) | 118(3) |
| C(14) | -471(8) | -4296(16) | 6318(5) | 95(3) |
| C(15) | 291(7) | -4059(14) | 6819(5) | 86(2) |
| C(16) | 1012(7) | -2292(13) | 6846(4) | 73(2) |

[3] Basson, S.S., Leipoldt, J.G., Purcell, W. and Venter, J.A., *Acta Cryst*., **C48**, 171 (1992).

**Table 6.20** Bond lengths (Å) for [Rh(cupf)(CO){$P(OCH_2)_3CCH_3$}] with estimated standard deviations in parentheses.

| Bond | Length (Å) | Bond | Length (Å) |
|---|---|---|---|
| Rh-P | 2.156(2) | O(5)-C(3) | 1.466(8) |
| Rh-O(2) | 2.059(4) | O(6)-C(4) | 1.458(7) |
| Rh-O(3) | 2.026(5) | C(2)-C(5) | 1.516(8) |
| Rh-C(1) | 1.772(9) | C(3)-C(5) | 1.497(10) |
| P-O(4) | 1.574(5) | C(4)-C(5) | 1.546(9) |
| P-O(5) | 1.587(5) | C(5)-C(6) | 1.535(8) |
| P-O(6) | 1.579(5) | C(11)–C(12) | 1.36(3) |
| O(2)-N(2) | 1.325(6) | C(12)–C(13) | 1.40(3) |
| O(3)-N(1) | 1.325(7) | C(13)–C(14) | 1.36(2) |
| N(2)-N(1) | 1.264(7) | C(14)–C(15) | 1.36(2) |
| N(2)-C(11) | 1.448(8) | C(15)–C(16) | 1.39(2) |
| C(1)-O(1) | 1.155(9) | C(16)–C(11) | 1.37(3) |
| O(4)-C(2) | 1.460(8) | | |

**Table 6.21** Bond angles (°) for [Rh(cupf)(CO){$P(OCH_2)_3CCH_3$}] with estimated standard deviations in parentheses.

| Bond | Angle (°) | Bond | Angle (°) |
|---|---|---|---|
| P-Rh-O(2) | 170.8(1) | P-O(4)-C(2) | 116.4(4) |
| P-Rh-O(3) | 94.8(1) | P-O(5)-C(3) | 115.7(4) |
| O(2)-Rh-O(3) | 77.3(2) | P-O(6)-C(4) | 117.0(4) |
| P-Rh-C(1) | 88.3(2) | O(4)-C(2)-C(5) | 109.8(5) |
| O(2)-Rh-C(1) | 99.9(3) | O(5)-C(3)-C(5) | 110.4(5) |
| O(3)-Rh-C(1) | 175.6(3) | O(6)-C(4)-C(5) | 108.9(5) |
| Rh-P-O(4) | 119.0(2) | C(2)-C(5)-C(3) | 110.2(6) |
| Rh-P-O(5) | 115.8(2) | C(2)-C(5)-C(4) | 108.5(6) |
| O(4)-P-O(5) | 102.8(3) | C(3)-C(5)-C(4) | 108.1(6) |
| Rh-P-O(6) | 113.2(2) | C(2)-C(5)-C(6) | 111.2(5) |
| O(4)-P-O(6) | 102.6(3) | C(3)-C(5)-C(6) | 110.5(6) |
| O(5)-P-O(6) | 101.1(3) | C(4)-C(5)-C(6) | 108.3(6) |
| Rh-O(2)-N(2) | 108.9(3) | N(2)–C(11)–C(12) | 117.8(5) |
| Rh-O(3)-N(1) | 115.6(4) | N(2)–C(11)–C(16) | 119.7(4) |
| O(2)-N(2)-N(1) | 124.7(5) | C(11)–C(12)–C(13) | 118.4(4) |
| O(2)-N(2)-C(11) | 116.7(5) | C(12)–C(13)–C(14) | 120.0(4) |
| N(1)-N(2)-C(11) | 118.5(6) | C(13)–C(14)–C(15) | 120.8(4) |
| O(3)-N(1)-N(2) | 113.5(5) | C(14)–C(15)–C(16) | 120.4(3) |
| Rh-C(1)-O(1) | 174.4(10) | C(15)–C(16)–C(11) | 117.8(4) |

**Table 6.22** Anisotropic displacement parameters ($Å^2$ x $10^3$) for [Rh(cupf)(CO)-{$P(OCH_2)_3CCH_3$}] with estimated standard deviations in parentheses. The anisotropic displacement factor exponent takes the form: $-2\pi^2(h^2a^{*2}U_{11} + k^2b^{*2}U_{22} + l^2c^{*2}U_{33} + 2klb^*c^*U_{23} + 2hla^*c^*U_{13} + 2\,h\,k\,a^*\,b^*\,U_{12}$.

| Atom | $U_{11}$ | $U_{22}$ | $U_{33}$ | $U_{23}$ | $U_{13}$ | $U_{12}$ |
|---|---|---|---|---|---|---|
| Rh | 613(3) | 479(3) | 517(3) | -30(3) | -48(2) | -138(3) |
| P | 61(1) | 39(1) | 49(1) | -2(1) | -5(1) | -8(1) |
| O(2) | 74(3) | 73(3) | 51(2) | 4(2) | -9(2) | -31(3) |
| O(3) | 79(3) | 56(3) | 59(3) | 3(2) | -19(2) | -19(3) |
| N(2) | 58(3) | 48(3) | 56(3) | 2(2) | -6(2) | -11(3) |
| N(1) | 75(4) | 57(4) | 60(3) | 6(3) | -16(3) | -11(3) |
| C(1) | 118(7) | 108(7) | 52(4) | -8(5) | -11(4) | -68(6) |
| O(1) | 177(7) | 151(7) | 68(4) | 31(4) | -40(4) | -103(6) |
| O(4) | 105(4) | 77(4) | 58(3) | 22(3) | -31(3) | -45(3) |
| O(5) | 76(3) | 71(4) | 80(3) | -33(3) | 6(3) | -13(3) |
| O(6) | 63(3) | 31(2) | 115(4) | -7(3) | -17(3) | -7(2) |
| C(2) | 101(6) | 66(5) | 62(4) | 18(4) | -25(4) | -44(5) |
| C(3) | 78(5) | 45(4) | 73(4) | -17(4) | -14(4) | -8(4) |
| C(4) | 59(4) | 47(4) | 92(5) | -4(4) | -17(4) | -4(3) |
| C(5) | 66(4) | 33(3) | 51(3) | 3(3) | -13(3) | -11(3) |
| C(6) | 89(5) | 48(4) | 76(5) | 6(4) | -26(4) | -25(4) |
| C(11) | 55(4) | 53(4) | 66(4) | 1(3) | 3(3) | -14(3) |
| C(12) | 102(7) | 100(8) | 83(6) | 18(5) | -22(5) | -52(6) |
| C(16) | 75(5) | 56(4) | 87(5) | 6(4) | -6(4) | -6(4) |
| C(13) | 108(8) | 130(10) | 113(8) | 16(7) | -28(6) | -72(7) |
| C(14) | 81(6) | 70(6) | 135(8) | 1(6) | 4(6) | -30(5) |
| C(15) | 83(6) | 56(5) | 119(7) | 20(5) | 8(5) | -5(4) |

**Table 6.23** Hydrogen coordinates ( x $10^4$) and isotropic displacement parameters ($Å^2$ x $10^3$) with estimated standard deviations in parentheses for [Rh(cupf)(CO){$P(OCH_2)_3CCH_3$}].

| Atom | x | y | z | $U_{eq}$ |
|---|---|---|---|---|
| H(21) | 6295(7) | 9220(13) | 5487(3) | 102(8) |
| H(22) | 5410(7) | 11285(13) | 5745(3) | 102(8) |
| H(31) | 4838(6) | 11227(12) | 6887(3) | 102(8) |
| H(32) | 5390(6) | 9227(12) | 7413(3) | 102(8) |
| H(41) | 6630(6) | 6401(11) | 7036(4) | 102(8) |
| H(42) | 7041(6) | 6433(11) | 6238(4) | 102(8) |
| H(61) | 6802(7) | 12221(12) | 6655(4) | 102(8) |
| H(62) | 7720(7) | 10255(12) | 6371(4) | 102(8) |
| H(63) | 7325(7) | 10169(12) | 7172(4) | 102(8) |
| H(12) | 82(8) | 208(16) | 5490(4) | 102(8) |
| H(16) | 1625(7) | -2078(13) | 7237(4) | 102(8) |
| H(13) | -1121(9) | -3092(19) | 5432(5) | 102(8) |
| H(14) | -1025(8) | -5672(16) | 6305(5) | 102(8) |
| H(15) | 329(7) | -5233(14) | 7201(5) | 102(8) |

## 6.6 $[Rh(cupf)(COCH_3)(I)\{P(OCH_2)_3CCH_3\}]_2$

**Table 6.24** Atomic coordinates ($x10^4$) and equivalent isotropic displacement parameters ($Å^2 \times 10^3$) for $[Rh(cupf)(COCH_3)(I)\{P(OCH_2)_3CCH_3\}]_2$ with estimated standard deviations in parentheses. $U_{eq}$ is defined as one third of the trace of the orthogonalized $U_{ij}$ tensor, $U_{eq} = (⅓)\Sigma_i\Sigma_j[U_{ij}(a_i^* a_j^*)(a_i a_j)]$.

| Atom | x | y | z | $U_{eq}$ |
|---|---|---|---|---|
| Rh | 2046(1) | 447(1) | 10995(1) | 34(1) |
| I | 664(1) | -6(1) | 8567(1) | 42(1) |
| P | 1674(2) | 1713(1) | 10624(1) | 35(1) |
| O(3) | 2974(4) | 584(2) | 12964(3) | 44(1) |
| N(1) | 3232(5) | -67(3) | 13599(4) | 43(1) |
| O(4) | 2953(4) | 2196(2) | 11668(4) | 53(1) |
| C(1) | 3949(6) | 605(3) | 10779(6) | 48(1) |
| O(5) | 1589(5) | 2067(2) | 9284(4) | 54(1) |
| C(6) | 1462(6) | 3284(3) | 10436(5) | 42(1) |
| O(1) | 3984(5) | 866(3) | 9786(5) | 74(1) |
| O(6) | 292(4) | 2077(2) | 10768(4) | 53(1) |
| C(3) | 2817(7) | 3058(3) | 11585(6) | 53(1) |
| C(5) | 1522(7) | 2935(3) | 9210(5) | 50(1) |
| C(7) | 1329(9) | 4182(3) | 10322(6) | 62(2) |
| C(4) | 181(7) | 2941(3) | 10657(7) | 56(2) |
| C(2) | 5213(8) | 382(5) | 11879(7) | 78(2) |
| O(2) | 2550(4) | -706(2) | 11600(3) | 42(1) |
| N(2) | 3006(5) | -702(2) | 12889(4) | 38(1) |
| C(11) | 3188(6) | -1466(3) | 13514(5) | 40(1) |
| C(15) | 2591(8) | -2831(4) | 13367(7) | 64(2) |
| C(12) | 4049(7) | -1541(4) | 14805(6) | 60(2) |
| C(16) | 2481(7) | -2093(3) | 12781(6) | 51(1) |
| C(14) | 3428(7) | -2907(4) | 14665(7) | 63(2) |
| C(13) | 4144(8) | -2280(5) | 15379(7) | 75(2) |

**Table 6.25** Bond lengths (Å) for $[Rh(cupf)(COCH_3)(I)\{P(OCH_2)_3CCH_3\}]_2$ with estimated standard deviations in parentheses.

| Bond | Length (Å) | Bond | Length (Å) |
|---|---|---|---|
| Rh-C(1) | 2.037(6) | O(5)-C(5) | 1.472(6) |
| Rh-O(3) | 2.040(4) | C(6)-C(5) | 1.511(7) |
| Rh-O(2) | 2.064(3) | C(6)-C(3) | 1.516(8) |
| Rh-P | 2.1876(13) | C(6)-C(4) | 1.518(8) |
| Rh-I | 2.6345(6) | C(6)-C(7) | 1.528(7) |
| Rh-I#1 | 3.0430(6) | O(6)-C(4) | 1.469(6) |
| I-Rh#1 | 3.0430(6) | O(2)-N(2) | 1.329(5) |
| P-O(5) | 1.580(4) | N(2)-C(11) | 1.448(6) |
| P-O(6) | 1.585(4) | C(11)-C(16) | 1.360(7) |
| P-O(4) | 1.588(4) | C(11)-C(12) | 1.369(7) |
| O(3)-N(1) | 1.281(5) | C(15)-C(14) | 1.370(9) |
| N(1)-N(2) | 1.301(6) | C(15)-C(16) | 1.394(8) |
| O(4)-C(3) | 1.466(6) | C(12)-C(13) | 1.392(9) |
| C(1)-O(1) | 1.205(7) | C(14)-C(13) | 1.354(10) |
| C(1)-C(2) | 1.435(10) | | |

Symmetry transformations used to generate equivalent atoms: #1 -x,-y,-z+2

**Table 6.26** Bond angles (°) for $[Rh(cupf)(COCH_3)(I)\{P(OCH_2)_3CCH_3\}]_2$ with estimated standard deviations in parentheses.

| Bond | Angle (°) | Bond | Angle (°) |
|---|---|---|---|
| C(1)-Rh-O(3) | 93.0(2) | O(1)-C(1)-Rh | 121.3(5) |
| C(1)-Rh-O(2) | 92.3(2) | C(2)-C(1)-Rh | 115.3(5) |
| O(3)-Rh-O(2) | 78.65(13) | C(5)-O(5)-P | 114.6(3) |
| C(1)-Rh-P | 87.07(17) | C(5)-C(6)-C(3) | 109.2(5) |
| O(3)-Rh-P | 93.77(10) | C(5)-C(6)-C(4) | 109.3(5) |
| O(2)-Rh-P | 172.36(10) | C(3)-C(6)-C(4) | 108.0(5) |
| C(1)-Rh-I | 93.68(17) | C(5)-C(6)-C(7) | 110.3(4) |
| O(3)-Rh-I | 168.30(10) | C(3)-C(6)-C(7) | 110.0(5) |
| O(2)-Rh-I | 91.47(9) | C(4)-C(6)-C(7) | 110.0(5) |
| P-Rh-I | 96.17(4) | C(4)-O(6)-P | 114.8(3) |
| C(1)-Rh-I#1 | 172.91(17) | O(4)-C(3)-C(6) | 109.6(4) |
| O(3)-Rh-I#1 | 85.46(11) | O(5)-C(5)-C(6) | 110.9(4) |
| O(2)-Rh-I#1 | 80.65(11) | O(6)-C(4)-C(6) | 110.6(4) |
| P-Rh-I#1 | 99.93(4) | N(2)-O(2)-Rh | 106.6(3) |
| I-Rh-I#1 | 86.767(17) | N(1)-N(2)-O(2) | 124.7(4) |
| Rh-I-Rh#1 | 93.233(17) | N(1)-N(2)-C(11) | 119.1(4) |
| O(5)-P-O(6) | 102.7(2) | O(2)-N(2)-C(11) | 116.2(4) |
| O(5)-P-O(4) | 103.4(2) | C(16)-C(11)-C(12) | 122.0(5) |
| O(6)-P-O(4) | 102.7(2) | C(16)-C(11)-N(2) | 118.0(5) |
| O(5)-P-Rh | 119.52(15) | C(12)-C(11)-N(2) | 120.0(5) |
| O(6)-P-Rh | 116.99(15) | C(14)-C(15)-C(16) | 119.0(6) |
| O(4)-P-Rh | 109.54(15) | C(11)-C(12)-C(13) | 118.1(6) |
| N(1)-O(3)-Rh | 114.1(3) | C(11)-C(16)-C(15) | 119.3(6) |
| O(3)-N(1)-N(2) | 115.1(4) | C(13)-C(14)-C(15) | 121.2(6) |
| C(3)-O(4)-P | 115.9(4) | C(14)-C(13)-C(12) | 120.4(6) |
| O(1)-C(1)-C(2) | 123.4(6) | | |

Symmetry transformations used to generate equivalent atoms: #1 -x,-y,-z+2

**Table 6.27** Anisotropic displacement parameters ($Å^2$ x $10^3$) for $[Rh(cupf)(COCH_3)(I)\text{-}\{P(OCH_2)_3CCH_3\}]_2$ with estimated standard deviations in parentheses. The anisotropic displacement factor exponent takes the form: $-2\pi^2(h^2a^{*2}U_{11} + k^2b^{*2}U_{22} + l^2c^{*2}U_{33} + 2klb^*c^*U_{23} + 2hla^*c^*U_{13} + 2\,h\,k\,a^*\,b^*\,U_{12}$.

| Atom | $U_{11}$ | $U_{22}$ | $U_{33}$ | $U_{23}$ | $U_{13}$ | $U_{12}$ |
|---|---|---|---|---|---|---|
| Rh | 43(1) | 27(1) | 32(1) | -2(1) | 14(1) | -1(1) |
| I | 52(1) | 44(1) | 33(1) | -4(1) | 19(1) | -4(1) |
| P | 44(1) | 30(1) | 33(1) | -1(1) | 16(1) | 0(1) |
| O(3) | 54(2) | 32(2) | 40(2) | -8(2) | 14(2) | -3(2) |
| N(1) | 50(3) | 47(3) | 30(2) | -3(2) | 11(2) | -2(2) |
| O(4) | 55(2) | 35(2) | 52(2) | -2(2) | 1(2) | -5(2) |
| C(1) | 55(3) | 39(3) | 58(3) | -8(2) | 30(3) | -3(2) |
| O(5) | 99(3) | 34(2) | 38(2) | -1(2) | 37(2) | 2(2) |
| C(6) | 67(4) | 30(2) | 31(2) | 1(2) | 23(2) | 0(2) |
| O(1) | 71(3) | 77(3) | 86(4) | 13(3) | 45(3) | 0(3) |
| O(6) | 58(2) | 36(2) | 76(3) | 3(2) | 38(2) | 3(2) |
| C(3) | 72(4) | 33(3) | 50(3) | -3(2) | 19(3) | -7(3) |
| C(5) | 88(4) | 32(2) | 37(3) | 2(2) | 31(3) | 3(3) |
| C(7) | 110(6) | 29(3) | 54(3) | 2(2) | 41(4) | 8(3) |
| C(4) | 74(4) | 36(3) | 66(4) | 1(3) | 37(3) | 11(3) |
| C(2) | 63(4) | 102(6) | 77(5) | 2(5) | 35(4) | 7(4) |
| O(2) | 60(2) | 32(2) | 31(2) | 1(1) | 15(2) | 4(2) |
| N(2) | 45(2) | 33(2) | 34(2) | 2(2) | 13(2) | 2(2) |
| C(11) | 43(3) | 37(3) | 40(3) | 8(2) | 16(2) | 2(2) |
| C(15) | 85(5) | 38(3) | 70(4) | 9(3) | 33(4) | 2(3) |
| C(12) | 63(4) | 61(4) | 40(3) | 2(3) | 0(3) | -3(3) |
| C(16) | 64(4) | 36(3) | 45(3) | 2(2) | 11(3) | 0(3) |
| C(14) | 69(4) | 52(4) | 68(4) | 26(3) | 26(4) | 14(3) |
| C(13) | 76(5) | 81(5) | 55(4) | 30(4) | 12(4) | 15(4) |

**Table 6.28** Hydrogen coordinates ( x $10^4$) and isotropic displacement parameters ($Å^2$ x $10^3$) with estimated standard deviations in parentheses for $[Rh(cupf)(COCH_3)(I)\{P(OCH_2)_3CCH_3\}]_2$.

| Atom | x | y | z | U(eq) |
|---|---|---|---|---|
| H(3A) | 3652 | 3285 | 11483 | 85(6) |
| H(3B) | 2773 | 3265 | 12381 | 85(6) |
| H(5A) | 674 | 3095 | 8467 | 85(6) |
| H(5B) | 2363 | 3135 | 9087 | 85(6) |
| H(7A) | 2095 | 4390 | 10104 | 85(6) |
| H(7B) | 1389 | 4401 | 11136 | 85(6) |
| H(7C) | 418 | 4320 | 9653 | 85(6) |
| H(4A) | 144 | 3161 | 11447 | 85(6) |
| H(4B) | -702 | 3084 | 9938 | 85(6) |
| H(2A) | 6042 | 420 | 11657 | 85(6) |
| H(2B) | 5112 | -152 | 12121 | 85(6) |
| H(2C) | 5330 | 728 | 12595 | 85(6) |
| H(12) | 4556 | -1111 | 15284 | 85(6) |
| H(16) | 1930 | -2030 | 11898 | 85(6) |
| H(14) | 3506 | -3397 | 15062 | 85(6) |
| H(13) | 4703 | -2345 | 16260 | 85(6) |

## 6.7 *trans*-[Rh(CO)(Cl)(PCy$_3$)$_2$]

**Table 6.29** Atomic coordinates (x10$^4$) and equivalent isotropic displacement parameters (Å$^2$ x 10$^3$) for *trans*-[Rh(CO)(Cl)(PCy$_3$)$_2$] with estimated standard deviations in parentheses. $U_{eq}$ is defined as one third of the trace of the orthogonalized $U_{ij}$ tensor, $U_{eq} = (⅓)\Sigma_i\Sigma_j[U_{ij}(a_i^* a_j^*)(a_i a_j)]$.

| Atom | x | y | z | $U_{eq}$ |
|---|---|---|---|---|
| Rh(1) | 0 | 0 | 0 | 29(1) |
| P(1) | 296(1) | 2044(1) | 2020(1) | 29(1) |
| Cl(1) | 743(3) | -1020(3) | 1488(2) | 51(1) |
| O(1) | -951(11) | 1164(10) | -1869(8) | 68(2) |
| C(1) | -582(8) | 707(7) | -1107(8) | 40(1) |
| C(11) | 1103(3) | 3758(3) | 1667(3) | 35(1) |
| C(12) | 2481(3) | 3981(3) | 1000(4) | 47(1) |
| C(13) | 2893(4) | 5259(4) | 491(4) | 59(1) |
| C(14) | 3057(4) | 6635(3) | 1694(4) | 59(1) |
| C(15) | 1714(4) | 6398(3) | 2383(4) | 54(1) |
| C(16) | 1317(4) | 5148(3) | 2913(3) | 47(1) |
| C(21) | -1458(3) | 1956(3) | 2552(3) | 34(1) |
| C(22) | -2409(3) | 2085(4) | 1461(3) | 47(1) |
| C(23) | -3829(3) | 2015(4) | 1971(4) | 53(1) |
| C(24) | -4643(3) | 629(4) | 2255(4) | 56(1) |
| C(25) | -3717(3) | 485(4) | 3345(4) | 53(1) |
| C(26) | -2285(3) | 559(3) | 2853(4) | 46(1) |
| C(31) | 1309(3) | 2251(3) | 3710(3) | 35(1) |
| C(32) | 1099(3) | 3179(4) | 5143(3) | 49(1) |
| C(33) | 1802(4) | 3016(5) | 6397(3) | 63(1) |
| C(34) | 3387(4) | 3398(5) | 6367(4) | 71(1) |
| C(35) | 3628(4) | 2538(5) | 4935(4) | 66(1) |
| C(36) | 2919(3) | 2694(4) | 3674(3) | 46(1) |

**Table 6.30** Bond lengths (Å) for *trans*-[Rh(CO)(Cl)($PCy_3$)$_2$] with estimated standard deviations in parentheses.

| Bond | Length (Å) | Bond | Length (Å) |
|---|---|---|---|
| Rh-C(1)#1 | 1.748(8) | C(12)-C(13) | 1.527(4) |
| Rh-C(1) | 1.748(8) | C(13)-C(14) | 1.512(5) |
| Rh-P(1) | 2.3491(7) | C(14)-C(15) | 1.510(5) |
| Rh-P(1)#1 | 2.3491(7) | C(15)-C(16) | 1.514(4) |
| Rh-Cl(1)#1 | 2.388(2) | C(21)-C(22) | 1.527(4) |
| Rh-Cl(1) | 2.388(2) | C(21)-C(26) | 1.534(4) |
| P(1)-C(11) | 1.852(3) | C(22)-C(23) | 1.526(4) |
| P(1)-C(21) | 1.852(2) | C(23)-C(24) | 1.513(5) |
| P(1)-C(31) | 1.864(3) | C(24)-C(25) | 1.518(5) |
| Cl(1)-O(1)#1 | 0.527(5) | C(25)-C(26) | 1.531(4) |
| Cl(1)-C(1)#1 | 0.642(6) | C(31)-C(32) | 1.523(4) |
| O(1)-Cl(1)#1 | 0.527(5) | C(31)-C(36) | 1.524(4) |
| O(1)-C(1) | 1.163(7) | C(32)-C(33) | 1.525(4) |
| C(1)-Cl(1)#1 | 0.642(6) | C(33)-C(34) | 1.508(5) |
| C(11)-C(16) | 1.528(4) | C(34)-C(35) | 1.507(5) |
| C(11)-C(12) | 1.529(4) | C(35)-C(36) | 1.532(4) |

Symmetry transformations used to generate equivalent atoms: #1 -x,-y,-z

**Table 6.31** Bond angles (°) for *trans*-[Rh(CO)(Cl)($PCy_3$)$_2$] with estimated standard deviations in parentheses.

| Bond | Angle (°) | Bond | Angle (°) |
|---|---|---|---|
| C(1)#1-Rh-C(1) | 180.0 | Cl(1)#1-C(1)-Rh | 174.8(9) |
| C(1)#1-Rh-P(1) | 90.6(2) | O(1)-C(1)-Rh | 178.3(9) |
| C(1)-Rh-P(1) | 89.4(2) | C(16)-C(11)-C(12) | 110.5(2) |
| C(1)#1-Rh-P(1)#1 | 89.4(2) | C(16)-C(11)-P(1) | 116.48(19) |
| C(1)-Rh-P(1)#1 | 90.6(2) | C(12)-C(11)-P(1) | 114.04(18) |
| P(1)-Rh-P(1)#1 | 180.0 | C(13)-C(12)-C(11) | 109.7(3) |
| C(1)#1-Rh-Cl(1)#1 | 178.6(2) | C(14)-C(13)-C(12) | 112.0(3) |
| C(1)-Rh-Cl(1)#1 | 1.4(2) | C(13)-C(14)-C(15) | 111.5(3) |
| P(1)-Rh-Cl(1)#1 | 88.59(5) | C(14)-C(15)-C(16) | 111.4(3) |
| P(1)#1-Rh-Cl(1)#1 | 91.41(5) | C(15)-C(16)-C(11) | 110.2(2) |
| C(1)#1-Rh-Cl(1) | 1.4(2) | C(22)-C(21)-C(26) | 110.4(2) |
| C(1)-Rh-Cl(1) | 178.6(2) | C(22)-C(21)-P(1) | 113.99(18) |
| P(1)-Rh-Cl(1) | 91.41(5) | C(26)-C(21)-P(1) | 110.15(18) |
| P(1)#1-Rh-Cl(1) | 88.59(5) | C(23)-C(22)-C(21) | 111.2(2) |
| Cl(1)#1-Rh-Cl(1) | 180.0 | C(24)-C(23)-C(22) | 111.1(3) |
| C(11)-P(1)-C(21) | 103.81(11) | C(23)-C(24)-C(25) | 111.0(3) |
| C(11)-P(1)-C(31) | 110.03(12) | C(24)-C(25)-C(26) | 111.3(3) |
| C(21)-P(1)-C(31) | 102.57(11) | C(25)-C(26)-C(21) | 111.2(2) |
| C(11)-P(1)-Rh | 112.63(8) | C(32)-C(31)-C(36) | 109.9(2) |
| C(21)-P(1)-Rh | 112.14(8) | C(32)-C(31)-P(1) | 117.76(19) |
| C(31)-P(1)-Rh | 114.69(8) | C(36)-C(31)-P(1) | 113.07(18) |
| O(1)#1-Cl(1)-C(1)#1 | 168.0(13) | C(31)-C(32)-C(33) | 110.2(3) |
| O(1)#1-Cl(1)-Rh | 171.5(12) | C(34)-C(33)-C(32) | 112.0(3) |
| C(1)#1-Cl(1)-Rh | 3.8(7) | C(35)-C(34)-C(33) | 111.7(3) |
| Cl(1)#1-O(1)-C(1) | 6.6(7) | C(34)-C(35)-C(36) | 111.6(3) |
| Cl(1)#1-C(1)-O(1) | 5.4(6) | C(31)-C(36)-C(35) | 110.6(2) |

Symmetry transformations used to generate equivalent atoms: #1 -x,-y,-z

**Table 6.32** Anisotropic displacement parameters ($Å^2$ x $10^3$) for *trans*-[Rh(CO)(Cl)($PCy_3$)$_2$] with estimated standard deviations in parentheses. The anisotropic displacement factor exponent takes the form: $-2\pi^2(h^2a^{*2}U_{11} + k^2b^{*2}U_{22} + l^2c^{*2}U_{33} + 2klb^*c^*U_{23} + 2hla^*c^*U_{13} + 2\,h\,k\,a^*\,b^*\,U_{12}$.

| Atom | $U_{11}$ | $U_{22}$ | $U_{33}$ | $U_{23}$ | $U_{13}$ | $U_{12}$ |
|---|---|---|---|---|---|---|
| Rh | 34(1) | 24(1) | 29(1) | 8(1) | 6(1) | 15(1) |
| P(1) | 30(1) | 26(1) | 31(1) | 7(1) | 6(1) | 13(1) |
| Cl(1) | 85(1) | 41(1) | 35(1) | 13(1) | 1(1) | 36(1) |
| O(1) | 117(6) | 65(4) | 49(4) | 30(3) | 11(4) | 58(4) |
| C(1) | 64(4) | 30(3) | 34(3) | 13(2) | 7(3) | 25(3) |
| C(11) | 38(1) | 28(1) | 38(1) | 10(1) | 7(1) | 14(1) |
| C(12) | 44(2) | 41(1) | 58(2) | 22(1) | 20(1) | 17(1) |
| C(13) | 60(2) | 54(2) | 59(2) | 29(2) | 19(2) | 16(2) |
| C(14) | 60(2) | 36(1) | 66(2) | 25(1) | -3(2) | 3(1) |
| C(15) | 65(2) | 27(1) | 63(2) | 11(1) | 1(2) | 18(1) |
| C(16) | 57(2) | 31(1) | 50(2) | 11(1) | 13(1) | 19(1) |
| C(21) | 30(1) | 33(1) | 38(1) | 10(1) | 6(1) | 15(1) |
| C(22) | 39(1) | 61(2) | 54(2) | 27(1) | 9(1) | 28(1) |
| C(23) | 38(2) | 62(2) | 65(2) | 24(2) | 10(1) | 28(1) |
| C(24) | 31(1) | 62(2) | 63(2) | 14(2) | 9(1) | 16(1) |
| C(25) | 38(2) | 58(2) | 62(2) | 26(2) | 14(1) | 16(1) |
| C(26) | 35(1) | 44(2) | 62(2) | 25(1) | 10(1) | 15(1) |
| C(31) | 36(1) | 40(1) | 31(1) | 9(1) | 6(1) | 20(1) |
| C(32) | 51(2) | 58(2) | 35(1) | 4(1) | 4(1) | 31(2) |
| C(33) | 66(2) | 97(3) | 33(1) | 18(2) | 6(1) | 45(2) |
| C(34) | 64(2) | 106(3) | 47(2) | 21(2) | -3(2) | 44(2) |
| C(35) | 55(2) | 107(3) | 53(2) | 30(2) | 7(2) | 51(2) |
| C(36) | 37(1) | 66(2) | 42(1) | 19(1) | 9(1) | 28(1) |

**Table 6.33** Hydrogen coordinates ( x $10^4$) and isotropic displacement parameters (Å$^2$ x $10^3$) with estimated standard deviations in parentheses for *trans*-[Rh(CO)(Cl)($PCy_3$)$_2$].

| Atom | x | y | z | $U_{eq}$ |
|---|---|---|---|---|
| H(11) | 390 | 3645 | 916 | 60(2) |
| H(12A) | 3264 | 4173 | 1710 | 60(2) |
| H(12B) | 2320 | 3105 | 188 | 60(2) |
| H(13A) | 3798 | 5430 | 124 | 60(2) |
| H(13B) | 2153 | 5014 | -293 | 60(2) |
| H(14A) | 3243 | 7396 | 1309 | 60(2) |
| H(14B) | 3880 | 6954 | 2422 | 60(2) |
| H(15A) | 914 | 6192 | 1684 | 60(2) |
| H(15B) | 1878 | 7279 | 3190 | 60(2) |
| H(16A) | 432 | 4997 | 3317 | 60(2) |
| H(16B) | 2081 | 5383 | 3668 | 60(2) |
| H(21) | -1243 | 2779 | 3460 | 60(2) |
| H(22A) | -1892 | 3000 | 1325 | 60(2) |
| H(22B) | -2617 | 1302 | 538 | 60(2) |
| H(23A) | -3626 | 2847 | 2850 | 60(2) |
| H(23B) | -4427 | 2059 | 1241 | 60(2) |
| H(24A) | -4926 | -202 | 1357 | 60(2) |
| H(24B) | -5517 | 632 | 2619 | 60(2) |
| H(25A) | -4243 | -435 | 3468 | 60(2) |
| H(25B) | -3519 | 1261 | 4272 | 60(2) |
| H(26A) | -2478 | -279 | 1983 | 60(2) |
| H(26B) | -1692 | 527 | 3597 | 60(2) |
| H(31) | 928 | 1267 | 3732 | 60(2) |
| H(32A) | 73 | 2878 | 5170 | 60(2) |
| H(32B) | 1530 | 4192 | 5236 | 60(2) |
| H(33A) | 1697 | 3646 | 7302 | 60(2) |
| H(33B) | 1304 | 2020 | 6350 | 60(2) |
| H(34A) | 3908 | 4429 | 6549 | 60(2) |
| H(34B) | 3771 | 3203 | 7130 | 60(2) |
| H(35A) | 3229 | 1519 | 4817 | 60(2) |
| H(35B) | 4660 | 2875 | 4924 | 60(2) |
| H(36A) | 3386 | 3695 | 3732 | 60(2) |
| H(36B) | 3044 | 2084 | 2768 | 60(2) |

# 7 Summary

Oxidative addition, and in particular the addition of iodomethane to rhodium(I) phosphine complexes is of great importance in catalytic processes. The Monsanto process for the production of acetic acid serves as one of the better-known examples.[1,2] In the process of clearing up uncertainties in the mechanism of oxidative addition, our group has been interested in the manipulation of the reactivity of the Rh(I) centre in the [Rh(LL′)(CO)($PX_3$)] type of complexes, where LL′ represents monocharged bidentate ligands such as acetylacetonate,[3,4] and substituted acac ligands,[5] thioacetylacetonate,[6] 8-hydroxyquinolinate,[7] cupferrate,[8] etc. containing different donor atoms such as oxygen, nitrogen and sulphur. $PX_3$ represents different monodentate phosphine ligands, such as $PPh_3$, $PCy_3$, P(*o*-Tol)$_3$, $PPh_2C_6F_5$, P(*p*-$ClC_6H_4$)$_3$ and P(*p*-$MeOC_6H_4$)$_3$. The phosphine ligands in such studies are selected to provide a significant variation in their electronic and steric properties. These and other ligand variations usually have a marked effect on the Lewis basicity of the metal centre and thus on its reactivity as well as on the type of product formed.

The different outcome of the oxidative addition reactions of acetylacetonate, thioacetylacetonate and cupferrate showed the importance of in depth studies of such mechanisms, taking into account as much factors as possible. More sophisticated apparatus enabled the unravelling of the oxidative addition of the acac system in the present study, coming to the conclusion that the mechanism involves

---

[1] Paulik, F.E., *Catal. Rev*., **6**, 49 (1972).

[2] Lowry, R.P. and Aguilo, A., *Hydrocarbon Process*., **53**, 103 (1974).

[3] Leipoldt, J.G., Basson, S.S., Bok, L.D.C. and Gerber, T.I.A., *Inorg. Chim. Acta*, **26**, L35 (1978).

[4] Basson, S.S., Leipoldt, J.G., Roodt, A., Venter, J.A. and Van der Walt, T.J., *Inorg. Chim. Acta*, **119**, 35 (1986).

[5] Basson, S.S., Leipoldt, J.G. and Nel, J.T., *Inorg. Chim. Acta*, **84**, 167 (1984).

[6] Leipoldt, J.G., Basson, S.S. and Botha, L.J., *Inorg. Chim. Acta*, **168**, 215 (1990).

[7] Van Aswegen, K.G., Leipoldt, J.G., Potgieter, I.M., Lamprecht, G.J., and Van Zyl, G.J., *Trans. Met. Chem.*, **16**, 369 (1991).

[8] Basson, S.S., Leipoldt, J.G., Roodt, A. and Venter, J.A., *Inorg. Chim. Acta*, **128**, 31 (1987).·

an initial dissociative equilibrium of the Rh(I) complex. The equilibrium step is followed by oxidative addition leading to a postulated ionic intermediate, which reacts further by different pathways to produce the final, presumably *trans*-addition product (D).

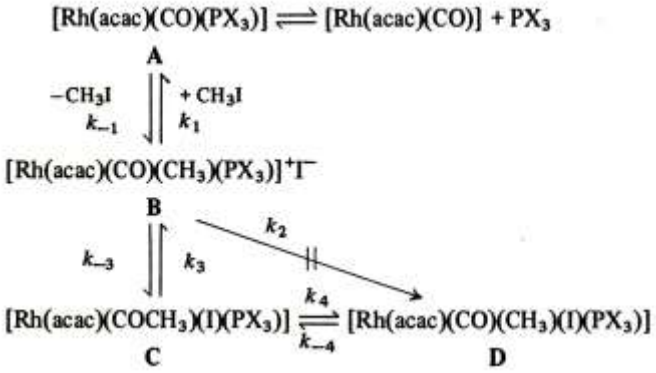


Uncertainty regarding the nature of the transition state in the oxidative addition of the Sacac system urged the high-pressure investigation undertaken in the present study. The final product is the acyl complex (similar to C in the acac system) and two possible reaction routes, via a three-centered transition state, or via a linear transition state ($S_N2$ mechanism) were under consideration. The high-pressure study concluded that, on the basis of the solvent-independent $\Delta V^*$ data, the reaction via the three-centered transition state is more likely, since a significant solvent dependence is expected for the linear transition state involving an ion-pair intermediate.

The high-pressure study was extended to incorporate the cupferrate system. It was concluded that the formation of an ion-pair intermediate would be more favoured in more polar solvents, indicating that this oxidative addition reaction most probably proceeds via a linear transition state in more polar solvents. In less polar solvents the observed $\Delta V^*$ value can either be due to single-bond formation and partial charge creation in the linear state, or due to simultaneous formation of two bonds in a three-centre mechanism.

Oxidative addition of the neocupferrate system resembles that of the cupferrate system. Similar to what was proposed for cupferrate, oxidative addition proceeds via two competitive pathways. The $k_1$ path implies a nucleophilic attack on $CH_3I$, giving a

16-electron 5-coordinate intermediate for which the degree of ion separation will be solvent dependent. The solvent assisted $k_2$ path can be viewed as a rare oxidative addition catalysis phenomenon, similar to the solvent effects in the migratory insertion of CO into transition metal alkyl bonds.

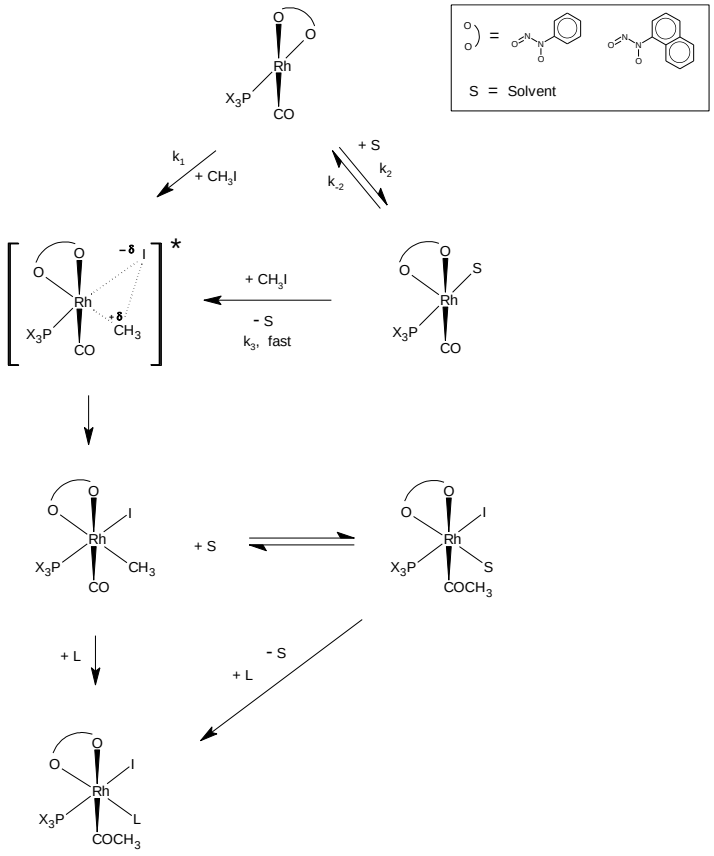


The migratory CO insertion as observed in the cupferrate and neocupferrate systems was studied in an effort to clarify the nature of solvent involvement. Using substituted THF and other steric manipulated solvents, solvents with different electronic properties as well as a variation of bound ligands, proof was given that solvents participate in a coordinative way, rather than just stabilising the migratory insertion transition state by solvation.

Studying the effect of the varying steric and electronic properties of the phosphine ligands on the oxidative addition of the neocupferrate system, a steric-electronic model, developed by Tolman, was applied to oxidative addition reactions to evaluate

the total effect of the phosphorous ligand in a particular system. This could lead to a better understanding and selection of the composition of catalysts.

A number of novel rhodium complexes were synthesised during the study, of which some were characterised by X-ray crystallography. This established the ground state stereochemistry of these complexes, and although not specific for determining the mechanistic pathway, aided the interpretation of kinetic data.

This study has already led to the following publications:

1. Basson, S.S., Leipoldt, J.G., Roodt, A., Venter, J.A. and Van der Walt, T.J., *Inorg. Chim. Acta,* **119**, 35 (1986).

2. Basson, S.S., Leipoldt, J.G., Roodt, A. and Venter, J.A., *Inorg. Chim. Acta*, **128**, 31 (1987).

3. Basson, S.S., Leipoldt, J.G. and Venter, J.A., *Acta Cryst*., **C46**, 1324 (1990).

4. Venter, J.A., Leipoldt, J.G. and Van Eldik, R., *Inorg. Chem*., **30**, 2207 (1991).

5. Basson, S.S., Leipoldt, J.G., Purcell, W. and Venter, J.A., *Acta Cryst*., **C48**, 171 (1992).

# 8 Opsomming

Oksidatiewe addisie, en spesifiek die addisie van jodometaan aan rodium(I) fosfienkomplekse is van groot belang in katalitiese prosesse. Die Monsantoproses vir die produksie van asynsuur is een van die bekendste voorbeelde hiervan.[1,2] In 'n poging om onsekerhede betreffende die meganisme van oksidatiewe addisie op te klaar, is ons groep geïnteresseerd in die manipulering van die reaktiwiteit van die Rh(I) senter van die [Rh(LL′)(CO)($PX_3$)] tipe komplekse, waar LL′ enkelgelaaide bidentate ligande soos asetielasetonaat,[3,4] gesubstitueerde acac-ligande,[5] tioasetielasetonaat,[6] 8-hidroksikinolinaat,[7] kupferraat,[8] ens., wat verskillende donoratome soos suurstof, stikstof en swawel bevat, verteenwoordig. $PX_3$ verteenwoordig verskillende monodentate fosfienligande soos $PPh_3$, $PCy_3$, P(*o*-Tol)$_3$, $PPh_2C_6F_5$, P(*p*-$ClC_6H_4$)$_3$ en P(*p*-$MeOC_6H_4$)$_3$. Die fosfienligande vir gebruik in sulke studies word geselekteer om betekenisvol te varieer wat betref hulle elektroniese en steriese eienskappe. Hierdie en ander ligandvariasies het gewoonlik 'n beduidende effek op die Lewisbasisiteit van die metaalsenter en dus ook op sy reaktiwiteit sowel as die tipe produk wat gevorm word.

Die noodsaaklikheid van 'n diepgaande studie van hierdie meganismes is beklemtoon deur die verskil in gedrag en produk van die oksidatiewe addisiereaksies van asetielasetonaat, tioasetielasetonaat en kupferraat. Sulke studies moet so veel faktore as moontlik in berekening bring. Meer gesofistikeerde apparaat het die

[1] Paulik, F.E., *Catal. Rev*., **6**, 49 (1972).

[2] Lowry, R.P. en Aguilo, A., *Hydrocarbon Process*., **53**, 103 (1974).

[3] Leipoldt, J.G., Basson, S.S., Bok, L.D.C. en Gerber, T.I.A., *Inorg. Chim. Acta*, **26**, L35 (1978).

[4] Basson, S.S., Leipoldt, J.G., Roodt, A., Venter, J.A. en Van der Walt, T.J., *Inorg. Chim. Acta*, **119**, 35 (1986).

[5] Basson, S.S., Leipoldt, J.G. en Nel, J.T., *Inorg. Chim. Acta*, **84**, 167 (1984).

[6] Leipoldt, J.G., Basson, S.S. en Botha, L.J., *Inorg. Chim. Acta*, **168**, 215 (1990).

[7] Van Aswegen, K.G., Leipoldt, J.G., Potgieter, I.M., Lamprecht, G.J., en Van Zyl, G.J., *Trans. Met. Chem.*, **16**, 369 (1991).

[8] Basson, S.S., Leipoldt, J.G., Roodt, A. en Venter, J.A., *Inorg. Chim. Acta*, **128**, 31 (1987).·

ontrafeling van die oksidatiewe addisie van die acac-sisteem in die huidige studie moontlik gemaak wat tot die gevolgtrekking gelei het dat die meganisme 'n aanvanklike dissosiatiewe ewewig van die Rh(I) kompleks behels. Die ewewigstap word deur oksidatiewe addisie gevolg, wat tot 'n gepostuleerde ioniese intermediêr lei, en verder langs verskillende reaksiepaaie reageer om die finale, waarskynlik *trans*-addisieproduk (D) te vorm.

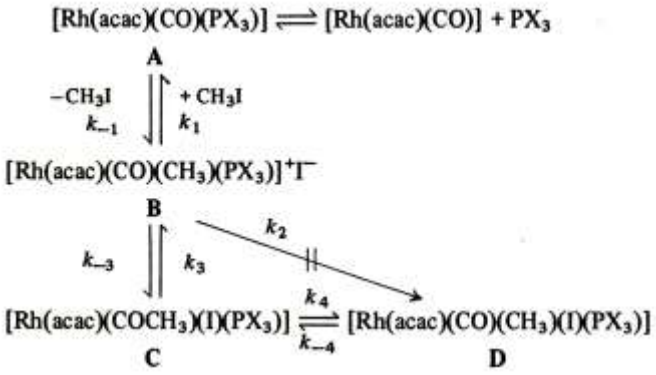


Onduidelikheid betreffende die aard van die oorgangstoestand in die oksidatiewe addisie van die Sacac-sisteem het die hoëdrukstudie soos in hierdie ondersoek onderneem is, genoodsaak. Die finale produk is die asielkompleks (soortgelyk aan C in die acac-sisteem) en twee moontlike reaksiepaaie, via 'n driesenter- of via 'n lineêre oorgangstoestand ($S_N2$ meganisme) het oorweging geniet. Die slotsom van die hoëdrukstudie, gebaseer op die oplosmiddel onafhanklike $\Delta V^*$-data, was dat die reaksie via die driesenteroorgangstoestand meer waarskynlik is, aangesien 'n betekenisvolle oplosmiddelafhanklikheid verwag sou kon word vir die lineêre oorgangstoestand waarby 'n ioonpaar-intermediêr betrokke is.

Die hoëdrukstudie is uitgebrei om ook die kupferraatsisteem in te sluit. Die resultaat het daarop gedui dat die vorming van 'n ioonpaar-intermediêr begunstig sou word in meer polêre oplosmiddels, wat impliseer dat hierdie oksidatiewe addisiereaksie heel waarskynlik via 'n lineêre oorgangstoestand in meer polêre oplosmiddels verloop. In minder polêre oplosmiddels kan die waargenome $\Delta V^*$-waarde die gevolg wees van enkelbindingsvorming en gedeeltelike ladingskepping in die lineêre toestand, of die gevolg van die gelyktydige vorming van twee bindings in 'n driesenter meganisme.

Oksidatiewe addisie van die neokupferraatsisteem stem ooreen met dié van die kupferraatsisteem. Soortgelyk aan wat vir kupferrat voorgestel is, verloop oksidatiewe addisie via twee kompeterende paaie. Die $k_1$-pad impliseer ’n nukleofiele aanval op $CH_3I$ wat tot ’n 16-elektron, vyfgekoördineerde intermediêr lei, waarvan die mate van ioonskeiding oplosmiddelafhanklik sal wees. Die oplosmiddelondersteunde $k_2$-pad kan as ’n uitsonderlike oksidatiewe addisie kataliseverskynsel beskou word, soortgelyk aan die oplosmiddeleffek soos aangetref by die migrerende CO-inlassing in oorgangsmetaal-alkielbindings.

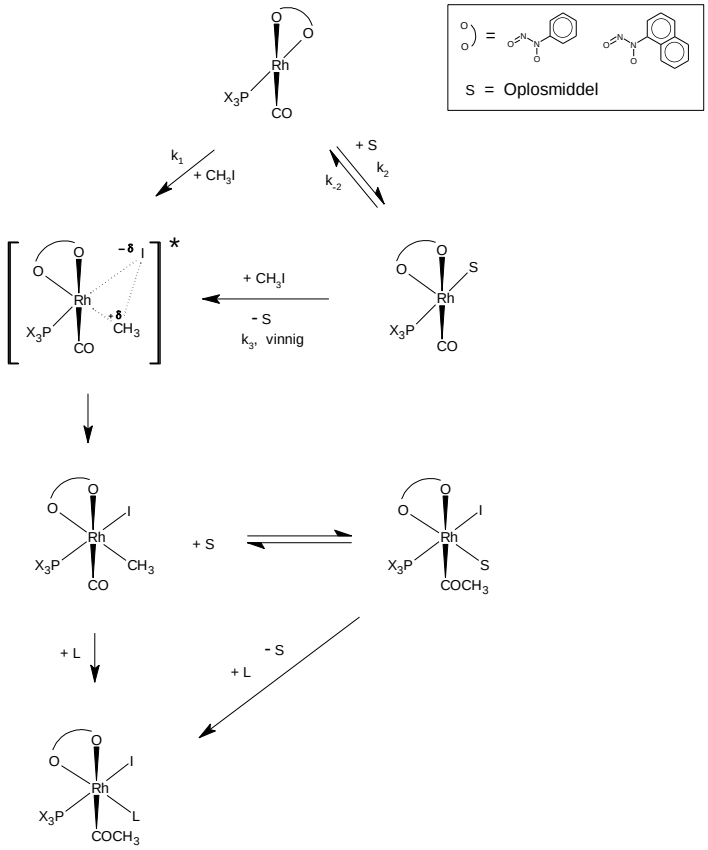


Die migrerende CO-inlassing soos waargeneem in die kupferraat- en neokupferraatsisteme is bestudeer in ’n poging om duidelikheid oor die aard van oplosmiddelbetrokkenheid te verkry. Deur van THF, ander steries-gemanipuleerde oplosmiddels en oplosmiddels met verskillende elektroniese eienskappe gebruik te maak, asook gebonde ligande te varieer, kon getuienis verkry word dat die oplosmiddels op ’n koördinatiewe manier aan die reaksie deelneem en nie slegs die oorgangstoestand van die inlassing deur solvering stabiliseer nie.

## Opsomming

Deur die effek van variërende steriese en elektroniese eienskappe van die fosfienligande op die oksidatiewe addisie van die neokupferraatsisteem te bestudeer, kon ’n steries-elektroniese model, ontwikkel deur Tolman, toegepas word op die oksidatiewe addisiereaksies om die totale effek van die fosforligand in ’n bepaalde sisteem te evalueer. Dit kan tot groter begrip rakende die samestelling van kataliste lei.

’n Aantal unieke rodiumkomplekse is gedurende hierdie studie berei, waarvan sommige deur X-straalkristallografie gekarakteriseer is. Dit het die grondtoestand stereochemie van hierdie komplekse vasgestel en hoewel dit nie opsigself voldoende is om die meganistiese verloop van reaksies te verklaar nie, het dit die interpretasie van die kinetiese data vergemaklik.

Hierdie studie het reeds tot die volgende publikasies gelei:

1. Basson, S.S., Leipoldt, J.G., Roodt, A., Venter, J.A. en Van der Walt, T.J., *Inorg. Chim. Acta,* **119**, 35 (1986).
2. Basson, S.S., Leipoldt, J.G., Roodt, A. en Venter, J.A., *Inorg. Chim. Acta*, **128**, 31 (1987).
3. Basson, S.S., Leipoldt, J.G. en Venter, J.A., *Acta Cryst*., **C46**, 1324 (1990).
4. Venter, J.A., Leipoldt, J.G. en Van Eldik, R., *Inorg. Chem*., **30**, 2207 (1991).
5. Basson, S.S., Leipoldt, J.G., Purcell, W. en Venter, J.A., *Acta Cryst*., **C48**, 171 (1992).